THE

LONDON, EDINBURGH, AND DUBLIN

PHILOSOPHICAL MAGAZINE

AND

JOURNAL OF SCIENCE.

[SEVENTH SERIES.]

JANUARY 1930.

I. *The Damping produced by Eddy Currents induced in Metal Spheres and Cylinders Oscillating in a Non-Uniform Magnetic Field, and its Application to the Determination of Resistivity.* *By* S. DAVIES, *B.Sc.*, *and* E. J. EVANS, *D.Sc.*, *University College of Swansea* *.

Introduction.

IT is well known that the resistivity of a conductor can be measured by swinging a magnetic needle over the conductor, or by oscillating the conductor about a vertical axis in a uniform magnetic field. Both methods were employed by F. Himstedt †, who also considered the problem from the theoretical standpoint. In the first method a magnetic system was set swinging near a fixed copper sphere, and the damping produced by the induced currents was measured. In the second method the damping was determined when the copper sphere was set oscillating about a vertical axis in a uniform magnetic field. Warburg ‡ emphasized the importance of considering the effect of hysteresis when a magnetic needle is set swinging over magnetic substances. When a needle swings over an iron plate the damping is greater than would be expected from its specific resistance. Weber § also employed the same two

* Communicated by Prof. E. J. Evans.
† Wied. *Ann.* ii. p. 812 (1880).
‡ Wied. *Ann.* xiii. p. 159 (1881).
§ Wied. *Ann.* lxviii. p. 705 (1899).

methods to determine the resistivities of copper-zinc alloys and zinc amalgams.

Strong damping is also produced when a metal plate is allowed to oscillate in a non-uniform field. Waltenhofen * has described a pendulum suitable for showing to a large audience the damping effect of Foucault currents, and Galitzin † has applied the damping produced by swinging a copper plate between the poles of a powerful magnet to his horizontal pendulum detector of earth disturbances.

In the present experiments, spheres and cylinders of metals and alloys are allowed to oscillate pendulum fashion between the pole-faces of a powerful electromagnet, which had been designed to give a uniform magnetic field over a large area. The pole-faces, which were of rectangular cross-section, were set at a small angle with one another, and thus a non-uniform field was produced along the line of swing of the pendulum.

The experimental results show that $\frac{d\mathrm{H}}{d\mathrm{S}}$, the rate of change of the magnetic field with distance along the line of swing, is constant for a given current passing through the magnet, and also that the retarding force acting on the pendulum bob, due to eddy currents, is proportional to the velocity of the bob at every point of its path.

It can be shown that the resistivities of the materials of the spheres or cylinders can be deduced from measurements of the change of logarithmic decrement produced by the field and the value of $\frac{d\mathrm{H}}{ds}$.

Theory of the Method.

Let m be the mass of the pendulum bob and l its length. The equation of motion is

$$m\frac{d^2s}{dt^2}+k_1m\frac{ds}{dt}+mg\frac{s}{l}=0 \quad . \quad . \quad . \quad . \quad (1)$$

where k_1 is the damping coefficient in the absence of the magnetic field.

Let it be assumed that the corresponding equation, when the magnetic field is acting, is given by

$$m\frac{d^2s}{dt^2}+(k_1+k_2)m\frac{ds}{at}+mg\frac{s}{l}=0, \quad . \quad . \quad . \quad (2)$$

* Wied. *Ann.* xix. p. 928 (1883).

† *Acad. Sci. St. Petersbourg*, ix. pp. 743–758 (1908).

where $k_2\, m\frac{ds}{dt}$ is the retarding force acting on the pendulum bob due to the action of the magnetic field on the eddy currents set up in the sphere.

If S_1 and S_2 are successive amplitudes, then the log dec with field ($\log \mathrm{dec}_1$) is given by

$$\log\frac{S_1}{S_2}=\tfrac{1}{4}(k_1+k_2)\mathrm{T}, \quad \text{where} \quad \mathrm{T}=2\pi\frac{l}{g}\text{approx.}$$

Similarly the log dec without field ($\log \mathrm{dec}_2$) is given by $\frac{1}{4}k_1\mathrm{T}$.

The difference of log dec or $\log \mathrm{dec}_1 - \log \mathrm{dec}_2 =$

$$\tfrac{1}{4}k_2\mathrm{T}. \quad . \quad . \quad . \quad . \quad . \quad . \quad . \quad (3)$$

Force acting on Pendulum Bob.

(a) *Spheres.*

The theory of dimensions can be applied to consider the force acting on the sphere. Assuming the permeability of the material of the sphere to be unity, and the force F acting on the sphere due to eddy currents to depend on (1) the diameter D, (2) the velocity $\frac{ds}{dt}$, (3) the conductivity σ, (4) the magnetic induction B, and (5) $\frac{d\mathrm{B}}{ds}$, it can be shown that

$$\mathrm{F}=\mathrm{K}\left(\frac{d\mathrm{B}}{ds}\right)^2.\mathrm{D}^5.\sigma.\frac{ds}{dt} \quad . \quad . \quad . \quad . \quad (4)$$

$$=\mathrm{K}\left(\frac{d\mathrm{H}}{ds}\right)^2.\frac{\mathrm{D}^5}{\rho}.\frac{ds}{dt}, \quad . \quad . \quad . \quad . \quad . \quad (5)$$

where ρ = resistivity and K is a constant.

The value of K, according to Keeping *, is $\frac{\pi}{240}$ when all quantities are expressed in C.G.S. units.

Now

$$k_2 m\frac{ds}{dt}=\mathrm{K}\left(\frac{d\mathrm{H}}{ds}\right)^2.\frac{\mathrm{D}^5}{\rho}.\frac{ds}{dt};$$

therefore

$$k_2=\frac{6\mathrm{K}}{\pi}\left(\frac{d\mathrm{H}}{ds}\right)^2.\frac{\mathrm{D}^2}{\rho}.\frac{1}{d},$$

where d = density of the material of the sphere.

* In the paper following the present one.

$$\log \mathrm{dec}_1 - \log \mathrm{dec}_2 = \tfrac{1}{4} k_2 \mathrm{T}$$

$$= \frac{3\mathrm{K}}{2\pi}\left(\frac{d\mathrm{H}}{ds}\right)^2 \cdot \frac{\mathrm{D}^2}{\rho} \cdot \frac{1}{d} \cdot \mathrm{T}$$

$$= \mathrm{C}\left(\frac{d\mathrm{H}}{ds}\right)^2 \cdot \frac{\mathrm{D}^2}{\rho} \cdot \frac{1}{d} \cdot \mathrm{T}, \quad . \quad . \quad (6)$$

where

$$\mathrm{C} = \frac{3}{2}\frac{\mathrm{K}}{\pi} = \frac{1}{160} = \cdot 00625.$$

(b) *Cylinders.*

(1) The pendulum bobs were cylinders of copper or brass swinging with their axes vertical in the horizontal magnetic field between the pole-pieces of the electromagnet. The lines of magnetic force were perpendicular to the axes of the cylinders.

In this case the experimental results in conjunction with the theory of dimensions show that

$$\log \mathrm{dec}_1 - \log \mathrm{dec}_2 = \mathrm{K}\left(\frac{d\mathrm{H}}{ds}\right)^2 \cdot \frac{f(\mathrm{D} \cdot l)}{\rho} \cdot \frac{1}{d} \cdot \mathrm{T}, \quad . \quad (7)$$

where K is a constant and $f(\mathrm{D} \cdot l)$ is of dimensions L^2.

(2) The pendulum bobs were cylinders supported by a bifilar suspension of fine silk, and swinging with their axes parallel to the lines of force.

The experimental results indicate that the difference of log dec is independent of the lengths of the cylinders, and it therefore follows from the theory of dimensions that

$$\log \mathrm{dec}_1 - \log \mathrm{dec}_2 = \mathrm{C}_1\left(\frac{d\mathrm{H}}{ds}\right)^2 \cdot \frac{\mathrm{D}^2}{\rho} \cdot \frac{1}{d} \cdot \mathrm{T}, \quad . \quad . \quad (8)$$

where C_1 is a constant.

According to Keeping* the value of $\mathrm{C}_1 = \frac{1}{128} = \cdot 00781.$

Experimental Work.

According to equation (6) deduced for a sphere, oscillating between the poles of the electromagnet, the difference of logarithmic decrement with and without the magnetic field is given by

$$\log \mathrm{dec}_1 - \log \mathrm{dec}_2 = \mathrm{C}\left(\frac{d\mathrm{H}}{ds}\right)^2 \cdot \frac{1}{\rho} \cdot \frac{1}{d} \cdot \mathrm{D}^2 \cdot \mathrm{T}.$$

* *Loc. cit.*

The experimental work therefore involves the measurement of $\frac{dH}{ds}$, the rate of variation of the magnetic field along the line of vibration of the pendulum, the resistivity ρ, the density d, the diameter D, and the period of swing T, together with the difference of logarithmic decrement with and without field. In order to test the various relationships involved in the above equation, spherical pendulum bobs were made of copper, aluminium, tin, zinc, lead, mercury, brass, and an alloy of tin and lead. In the case of copper, four spheres of diameters 2·48, 2·12, 1·715, and 1·263 cm. respectively were made. The smallest sphere of diameter 1·263 cm. was turned from a rod of very pure copper, and its resistivity was determined by measuring the resistance of the rod with the Kelvin bridge. This measured value of the resistivity was used in the application of the above equation to the measurement of resistivity.

The spheres of other materials were turned from rods or from cylinders of the materials specially cast for the purpose. With the exception of zinc and mercury, the actual resistivities of the materials employed in the preparation of the spheres were actually measured.

Resistivities.

The resistances of the various materials to be measured varied from about 0·0000670 ohm for the copper rod to ·00149 ohm for the lead rod. An accurate method for the determination of low resistances was therefore necessary, and for this reason the measurements were made with a Kelvin bridge constructed by the Cambridge Instrument Company. The method is well known, and no description is therefore necessary.

Logarithmic Decrement.

The metallic spheres were suspended by a fine silk thread, thus forming a simple pendulum. Behind the thread on the top of one of the pole-pieces, and parallel with the line of swing of the pendulum, was fixed a centimetre scale with its middle point opposite the centre of the magnetic field between the pole-pieces. The pendulum and scale were viewed by a telescope placed at a distance of about 4 feet from the magnet. The logarithmic decrement was then determined in the usual way.

Measurement of the Intensity of the Magnetic Field at the Centre of Swing and the Variation of the Field along the Line of Swing.

The electromagnet was designed to give a strong and uniform magnet field over a comparatively large area, and the pole-faces were of rectangular cross-section, having a length of 16·5 cm. and a breadth of 5·0 cm.

In the present experiments, measurements of H and $\frac{dH}{ds}$ were carried out with the distance between the pole-pieces tapering from 3·96 cm. at one end to 3·46 cm. at the other end, and also with the same distance tapering from 4·45 cm. at one end to 3·45 cm. at the other end. Three points, A, B, and C, were selected along the line of swing of the simple pendulum, and the intensities of the magnetic fields at B, the point of rest of the pendulum bob, were determined for 2, 3, 4, 5, and 6 amperes passing through the magnet coils by means of a search coil or fluxmeter. The values of $\frac{dH}{ds}$, corresponding to various values of the current passing through the magnet, could then be calculated from the deflexions observed when the search coil was placed at A and C respectively. The points A and C were situated on opposite sides of B, and at a distance of 2 cm. from it. The values of $\frac{dH}{ds}$ determined in this way were accurate to within about 4 per cent., and within the limits of experimental error the deflexions at A, B, and C indicated that $\frac{dH}{ds}$ was constant over the distance AC.

With the pole-faces adjusted for the larger taper a more accurate value of $\frac{dH}{ds}$ was obtained when a current of 5 amperes was passed through the electromagnet. Two small coils of equal mean area, and whose centres were at a distance apart of 4 cm., were connected up in series with the fluxmeter so that the E.M.F.'s induced were in opposition when the coils were simultaneously removed from the fields at A and C. The value of $\frac{dH}{ds}$ obtained in this way was about 3 per cent. higher than that obtained by the previous method, and will be used later in the determination of the values of the constants C and C_1 in equations (6) and (8).

Experimental Results for Spheres.

TABLE I.

Magnet pole-faces tapering from 3·46 cm. at one extremity to 3·96 cm at other extremity.

Nature of pendulum bob.	Diam. of bob in cm.	Current in amps. through magnet.	Field in gauss at B, the centre of swing.	Period of swing in secs.	Temperature in degrees centigrade of air between poles.	Log dec with field – log dec without field.
Copper	1·263	5·0	5660	1·0	23·0	·00158
,, ...	,,	,,	,,	1·5	22·5	·00238
,, ...	,,	,,	,,	2·0	23·8	·00312
,, ...	1·715	,,	,,	1·5	17·7	·00434
,, ...	2·120	,,	,,	,,	18·8	·00653
,, ...	2·480	,,	,,	,,	17·7	·00901
Brass.....	1·723	,,	,,	,,	23·8	·00125
Zinc	1·174	,,	,,	1·0	19·1	·00103
,, ...	,,	,,	,,	1·5	,,	·00154
,, ...	,,	,,	,,	2·0	,,	·00204
,, ...	2·485	,,	,,	1·5	21·2	·00310

TABLE II.

Magnet pole-faces tapering from 3·45 cm. at one extremity to 4·45 cm. at other extremity.

Nature of pendulum bob.	Diam. of bob in cm.	Current in amps. through magnet.	Field in gauss at B, the centre of swing.	Period of swing in secs.	Temperature in degrees centigrade of air between poles.	Log dec with field – log dec without field.
Copper	1·263	5·0	4993	1·5	21·2	·00712
Aluminium...	1·232	2·0	2152	,,	22·5	·00247
,, ...	,,	3·0	3207	,,	,,	·00525
,, ...	,,	4·0	4218	,,	,,	·00900
,, ...	,,	5·0	4993	,,	,,	·01290
,, ...	,,	6·0	5445	,,	,,	·01610
,, ...	2·19	5·0	4993	,,	22·0	·04110
Lead	1·26	5·0	4993	1·5	22·5	$\cdot 00046_2$
,, ...	2·48	,,	,,	,,	21·4	·00177
Tin	1·703	,,	,,	,,	23·7	·00229
Lead-Tin alloy. ...	1·713	,,	,,	,,	20·1	·00122
Mercury	2·16	,,	,,	,,	19·0	$\cdot 00024_7$

Discussion of Results.

According to equation (6) the difference between logarithmic decrement with the field and without the field is given by

$$C.\left(\frac{dH}{ds}\right)^2.\frac{D^2}{\rho}.\frac{T}{d}.$$

The variation of the difference of log dec with the various quantities concerned will now be considered.

TABLE III.

Variation with T. (Field at centre of swing = 5660 gauss.)

Nature of pendulum bob.	Period of swing in seconds.	Log dec with field − log dec without field.	$\frac{\text{Log dec}_1 - \text{log dec}_2}{T}$.
Copper, 1·263 cm.	1·0	·00158	·00158
,, ...	1·5	·00238	·00158
,, ...	2·0	·00312	·00156
Zinc, 1·714 cm.	1·0	·00103	·00103
,, ...	1·5	·00154	·00103
,, ...	2·0	·00204	·00102

The results show that for a given pendulum bob, keeping the field at each point constant, the value of $\log dec_1 - \log dec_2$ is directly proportional to the period of swing.

TABLE IV.

Variation with Diameter "D."

Period T = 1·5 seconds in all cases, 5 amperes passing through magnet and distance between pole-faces tapering from 3·46 cm. at one end to 3·96 cm. at other end.

Nature of pendulum bob.	Diameter "D" in cm.	Field in gauss at centre of swing.	$\frac{\text{Log dec}_1 - \text{log dec}_2}{D^2}$.
Copper	1·263	5660	·00149
,, ...	1·715	,,	·00148
,, ...	2·120	,,	·00145
,, ...	2·480	,,	·00147

The results given in Table IV. show, for spheres of the same material oscillating in the same magnetic field with the same period of swing, that $(\log dec_1 - \log dec_2)$ is proportional to the square of the diameter.

TABLE V.

Variation with $\frac{dH}{ds}$.

Aluminium sphere of diameter 1·23 cm., and the distance between pole-faces tapering from 3·45 cm. at one end to 4·45 cm. at other end.

Current through magnet in amperes.	Field in gauss at centre of swing.	$\frac{dH}{ds}$ in gauss per cm.	Relative values of $\left(\frac{dH}{ds}\right)^2$.	Relative values of $\log dec_1 - \log dec_2$.
2	2152	36·1	1	1
3	3207	54·0	2·24	2·13
4	4218	69·0	3·65	3·64
5	4993	83·4	5·34	5·22
6	5445	91·6	6·43	6·52

The above results show that the difference of logarithmic decrement with field and without field is proportional to $\left(\frac{dH}{ds}\right)^2$ when the current passing through the magnet is changed.

Measurements of the Resistivities of the various Conductors by comparison with the Resistivity of the Material from which the small Copper Sphere of Diameter 1·263 *cm. was turned.*

Let d_{Cu}, ρ_{Cu}, D_{Cu}, and $(\log dec_1 - \log dec_2)_{Cu}$ represent the values of the density, resistivity, diameter, and the difference of log dec with and without the magnet field in the case of copper, and d_m, ρ_m, D_m, $(\log dec_i - \log dec_2)_m$ the corresponding quantities in the case of the material examined.

It follows then, from equation (6) when $\frac{dH}{ds}$ and T are the same for both, that

$$\rho_M = \frac{D^2_m}{D^2_{Cu}} \cdot \frac{d_{Cu}}{d_m} \cdot \frac{(\log dec_1 - \log dec_2)_{Cu}}{(\log dec_1 - \log dec_2)_m} \cdot \rho_{Cu}.$$

The resistivities of the various substances calculated from the above equation are collected in Table IV. The values of the resistivities have been calulated from the results given for ($\log dec_1 - \log dec_2$) in Tables I. and II. when a current of 5 amperes passed through the magnet and T=1·5 seconds.

The resistivity of the copper from which the small sphere was turned equals 1·703 microhms per cm.^{3} at 16·7° C. The resistivities in all cases can be reduced to 18° C. from the known values of the temperature coefficients of resistance.

TABLE VI.

Nature of sphere.	Diameter of sphere in cm.	Density of material in grams per c.c.	Resistivity in michroms per cm.^{3} at 18° C. determined from pendulum experiments.	Resistivity in microhms per cm.^{3} at 18° C. determined directly.
Aluminium ...	1·23	2·71	2·95	2·91
	2·19		2·92	2·91
Zinc	1·714	7·18	6·15	6·10
	2·485		6·17	6·10
Brass	1·723	8·40	6·50	6·29
Lead	1·26	11·37	20·9	21·5
	2·48		21·20	21·5
Tin	1·703	7·22	11·92	12·0
Lead-Tin alloy ...	1·713	9·04	18·5	18·2
Mercury	2·16	13·6	96·6	95·6

The resistivities determined from the pendulum experiments agree within about 2 per cent. with those determined directly with the Kelvin bridge.

Determinations of the Constant "C."

The determination of the constant " C " in the equation

$$\log dec_1 - \log dec_2 = C\left(\frac{dH}{ds}\right)^2 . \frac{D^2}{\rho} . \frac{1}{d} . T$$

is rendered fairly difficult owing to the smallness of the quantity $\frac{dH}{ds}$. The value of $\frac{dH}{ds}$ was therefore re-determined when the distance between the pole-faces varied from 3·45 cm. at one end to 4·45 cm. at the other end, and a current of 5 amperes passed through the electromagnet. Two coils of equal mean area, whose centres were 4 cm. apart, were connected in series with the fluxmeter, so that the E.M.F.'s induced in the coils opposed one another when removed simultaneously from the field between the pole-pieces. The value of $\frac{dH}{ds}$ obtained in this way was 86 gauss per cm., and was about 3 per cent. higher than 83·4 gauss per cm. previously obtained.

Considering the results obtained with the small copper sphere of diameter 1·263 cm., we find :—

Difference of log dec = ·00712.

Density of copper = 8·92 gm. per c.c.

Resistivity of copper at 21·2° C. = $1{\cdot}733 \times 10^{-6}$ ohm per cm.^{3}

$= 1{\cdot}773 \times 10^3$ c.g.s. units.

T = 1·5 seconds and $\frac{dH}{ds} = 86$ gauss per cm.

Putting these values into the above equation, the constant "C" is found to be equal to ·00622.

The value obtained by Keeping *, from theoretical considerations, is ·00625.

Discussion of Results.

Variation with T.

An inspection of the results contained in Table VII. for the copper cylinder of length 2·57 cm. and diameter 1·270 cm., with a current of 5 amperes passing through the magnet, shows that the difference of log dec is approximately proportional to T.

Variation with $\left(\frac{dH}{ds}\right)^2$.

Taking the results for the copper cylinder 1·279 cm. long and 1·270 cm. diameter in conjunction with the values of

* *Loc. cit.*

Experiments with Cylinders.

(*a*) Cylinders oscillating in the horizontal magnetic field with their axes vertical, and the distance between the pole-faces varying from 3·45 cm. at one end to 4·45 cm. at the other.

TABLE VII.

Material of cylinder.	Length in cm.	Diameter in cm.	Current in amperes through magnet.	Field in gauss at centre of swing.	Period of swing in seconds.	Temperature in degrees centigrade between poles.	Log dec with field − log dec without field.
Copper...	1·279	1·270	2	2152	1·5	21·5	·00172
,, ...	,,	,,	3	3207	,,	,,	·00361
,, ...	,,	,,	4	4218	,,	,,	·00623
,, ...	,,	,,	5	4993	,,	,,	·00886
,, ...	,,	,,	6	5445	,,	,,	·01064
Copper...	2·57	1·270	5	4993	1·5	17·5	·01315
,, ...	,,	,,	6	5445	,,	,,	·01606
,, ...	,,	,,	5	4993	1·0	23·0	·00860
,, ...	,,	,,	5	4993	2·0	22·5	·01760
Copper...	1·29	1·907	5	4993	1·5	23·5	·01279
,, ...	,,	,,	6	5445	,,	,,	·01550
Copper...	2·57	1·910	5	4993	1·5	22·5	·02484
,, ...	,,	,,	6	5445	,,	,,	·03069
Brass ...	1·271	1·279	5	4993	1·5	18·5	·00269
,, ...	,,	,,	6	5445	,,	,,	·00331
Brass ...	2·57	1·27	5	4993	1·5	22·0	·00105
,, ...	,,	,,	6	5445	,,	,,	·00475
Brass ...	1·27	1·925	5	4993	1·5	20·5	·00395
,, ...	,,	,,	6	5445	,,	,,	·00482
Brass ...	2·57	1·925	5	4993	1·5	19·5	·00776
,, ...	,,	,,	6	5445	,,	,,	·00937

$\left(\frac{d\mathrm{H}}{ds}\right)^2$ contained in Table V., it can be shown that the difference of log dec is approximately proportional to $\left(\frac{d\mathrm{H}}{ds}\right)^2$.

Variation of Difference of log dec with Dimensions of Cylinders.

The experimental results given in Table VII. show that the difference of log dec for a cylinder with its axis perpendicular to the magnetic field depends upon both the length and diameter of the cylinder, but is not proportional to their product. The experimental results, coupled with the theory of dimensions, suggest the following equation :—

$$\log \mathrm{dec}_1 - \log \mathrm{dec}_2 = \text{constant} \left(\frac{d\mathrm{H}}{ds}\right)^2 \cdot \frac{f(l, \mathrm{D})}{\rho} \cdot \frac{1}{d} \cdot \mathrm{T},$$

where l and D represent the length and diameter of the cylinder, and $f(l, \mathrm{D})$ is of dimension L^2.

Determination of Resistivity.

The resistivities of brass and copper can be compared for cylinders of the same dimensions by means of the equation :

$$\frac{(\log \mathrm{dec}_1 - \log \mathrm{dec}_2)_{\mathrm{copper}}}{(\log \mathrm{dec}_1 - \log \mathrm{dec}_2)_{\mathrm{brass}}} \cdot \frac{d_{\mathrm{copper}}}{d_{\mathrm{brass}}} = \frac{\rho_{\mathrm{brass}}}{\rho_{\mathrm{copper}}}.$$

Experiments with Cylinders.

(*b*) Cylinders with bifilar suspension oscillating with their axes parallel to the lines of magnetic force.

TABLE VIII.

Material of cylinder.	Length in cm.	Diameter in cm.	Current in amperes through magnet.	Field in gauss at centre of swing.	Period of swing in seconds.	Temperature in degrees centigrade between poles.	log dec with field − log dec without field.
Brass ...	2·57	1·925	5	4993	1·5	15·2	·00625
„ ...	„	„	„	„	1·0	„	·00423
Copper...	2·57	1·910	2	2152	1·5	16·5	·00404
„ ...	„	„	3	3207	„	„	·00924
„ ...	„	„	4	4218	„	„	·01537
„ ...	„	„	5	4993	„	„	·02148
„ ...	„	„	6	5445	„	„	·0262
Copper...	1·29	1·907	5	4993	1·5	15·5	·0214
„ ...	„	„	„	„	1·0	16.0	·0142
„ ...	„	„	„	„	2·0	17·5	·0284
Copper...	1·279	1·27	5	4993	1·5	18·0	·00960

Using the results for cylinders of length 2·57 cm. and diameter 1·27 cm. in Table VII. and the resistivity of copper at 20° C. (1·73 microhms per cm.^{3}), the resistivity of brass calculated from the above equation is 6 microhms per cm.^{3} This result is in fair agreement with the value determined by the Kelvin bridge, viz. 6·3 microhms per cm.^{3}

Discussion of Results.

Variation with T.

Inspection of Table IX. shows that for a given substance and a given current passing through the magnet the difference of log dec is proportional to the period of swing T.

Variation with Dimensions of the Cylinders.

(i.) An examination of Table IX. also shows that for a given substance the difference of log dec is practically independent of the length of the cylinder when the latter is oscillating with its axis parallel to the lines of force.

(ii.) A comparison of the differences of log dec for copper cylinders of diameters 1·27 cm. and 1·907 cm. shows that the difference of log dec is directly proportional to D^2.

Variation with $\left(\frac{dH}{ds}\right)^2$.

If the differences of log dec for the copper cylinder of length 2·57 cm and diameter 1 910 cm. given in Table VIII. are examined in relation to the values of $\left(\frac{dH}{ds}\right)^2$ given in Table V., it can be shown that the difference of log dec is proportional to $\left(\frac{dH}{ds}\right)^2$.

Determination of Resistivity.

If the resistivity of copper be known, the resistivity of brass can be determined from the values of the difference of log dec for brass and copper cylinders of known dimensions and densities. Taking the values from Table VIII. for brass and copper cylin ers of diameters 1·925 and 1·910 cm. respectively, the resistivity of brass works out to be 6 4 microhms per cm.^{3} This value is in fair agreement with the experimental value 6·3 ohms per cm.^{3}

The experimental results for cylinders oscillating with their axes parallel to the lines of magnetic force show that

$$\log \mathrm{dec}_1 - \log \mathrm{dec}_2 = \mathrm{C}_1 \left(\frac{d\mathrm{H}}{ds}\right)^2 \cdot \frac{\mathrm{D}^2}{\rho} \cdot \frac{1}{d} \cdot \mathrm{T}.$$

Determination of the Constant C_1.

Considering the results for the copper cylinder of length 1·29 cm. and diameter 1·907 cm., it follows that

$\left(\frac{d\mathrm{H}}{ds}\right) = 86$ gauss per cm.,

$\log \mathrm{dec}_1 - \log \mathrm{dec}_2 = \cdot 0213_3$,

$d = 8{\cdot}92$ grams per c.c.,

$\mathrm{T} = 1{\cdot}5$ seconds,

$\rho = 1{\cdot}70 \times 10^{-6}$ ohm per cm.^{3} $= 1{\cdot}70 \times 10^3$ c.g.s. units.

The value of C_1 calculated from the above equation $= \cdot 00802$.

Taking the results for the copper cylinder of diameter 1·910 cm., the value of $\mathrm{C}_1 = \cdot 00804$.

The mean value of $\mathrm{C}_1 = \cdot 00803 = \frac{1}{125}$ approx.

The value of C_1 deduced theoretically by Keeping* is $\frac{1}{128}$.

Summary of Results.

1. The logarithmic decrements with and without the magnetic field have been measured for spheres and cylinders of conducting material swinging as pendulums between the pole-pieces of an electromagnet. The pole-pieces, which were of rectangular cross-section, were mounted with a slight taper, so that the spheres and cylinders were oscillating in a non-uniform field. Measurements showed that, for a given current passing through the magnetic coils, the value of $\frac{d\mathrm{H}}{ds}$ along the line of swing was constant.

2. It has been shown in the case of oscillating spheres that the difference of log dec with field and without field is given by

$$\mathrm{C}\left(\frac{d\mathrm{H}}{ds}\right)^2 \cdot \frac{\mathrm{D}^2}{\rho} \cdot \frac{1}{d} \cdot \mathrm{T},$$

* *Loc. cit.*

where D is the diameter of the sphere, ρ the specific resistance of the material composing the sphere, d the density, T the period of swing, and C a constant equal to ·00625.

3. For cylinders oscillating with their axes perpendicular to the magnetic field, the difference of log dec is given by

$$\text{constant}\left(\frac{d\mathrm{H}}{ds}\right)^2 \cdot \frac{f(l\mathrm{D})}{\rho} \cdot \frac{1}{d} \cdot \mathrm{T},$$

where l represents the length of the cylinder and $f(l\mathrm{D})$ is of dimensions L^2.

4. For cylinders oscillating with their axes parallel to the magnetic field, the difference of log dec is given by

$$\mathrm{C}_1\left(\frac{d\mathrm{H}}{ds}\right)^2 \cdot \frac{\mathrm{D}^2}{\rho} \cdot \frac{1}{d} \cdot \mathrm{T},$$

where the constant C_1 is equal to $\frac{1}{128}$ or ·00781.

5. The method can be used for comparing the resistances of conductors in the form of spheres and cylinders or for determining resistivities absolutely.

II. *On the Damped Oscillation of a Conductor in a Non-uniform Magnetic Field.* *By* E. S. Keeping, *B.Sc., D.I.C.* (*University College of Swansea*) *.

THIS note is intended as a supplement to the preceding paper by Mr. S. Davies and Prof. E. J. Evans [1] on the damping produced in metal spheres and cylinders oscillating in a non-uniform magnetic field and its application to the determination of resistivity. It gives a theoretical deduction of certain formulæ quoted in that paper.

There exists an extensive literature on the induction of eddy-currents in moving conductors, and the particular problems of the torsional oscillations of a suspended sphere and of a suspended cylinder with its axis vertical in a uniform

* Communicated by Prof. E. J. Evans.

field have been investigated by various writers[2]. The to-and-fro pendulum motion in a non-uniform field does not appear, however, to have been previously discussed. The only cases treated here are those of the sphere and the cylinder with its axis along the lines of force. The corresponding problem of the cylinder with axis perpendicular to the field presents great analytical difficulties.

Taking the origin of Cartesian coordinates at the centre of gravity of the pendulum bob when at rest, and the axis of x vertically upwards, the motion may, for small oscillations, be taken as simple harmonic along the y-axis. The magnetic lines of force are then practically parallel to the z-axis, and the strength of field increases uniformly along the y-axis, the gradient being produced in practice by slightly inclining the plane-poles of an electromagnet. The problem of the moving bob is then practically identical with that of the same bob at rest in a magnetic field fluctuating harmonically. If h is the amplitude of oscillation of the bob, the field at its centre fluctuates between the limits $\mathrm{H}_0 \pm h\ d\mathrm{H}/dy$. The magnetic field is not constant over the whole of the bob, but the extent of the fluctuation is the same at all points, and as the induced currents depend entirely on the variable part of the field, we can regard the eddy-currents actually produced as due to a uniform but harmonically oscillating field $h\,d\mathrm{H}/dy \cos pt$.

If E, M are the electric and magnetic field strengths in a medium of unit permeability and conductivity σ,

$$\left.\begin{aligned} \text{curl } \mathrm{M} &= 4\pi\sigma\mathrm{E}, \\ \text{curl } \mathrm{E} &= -d\mathrm{M}/dt, \\ \text{div } \mathrm{M} &= 0, \\ \text{div } \mathrm{E} &= 0, \end{aligned}\right\} \quad \ldots\ldots \quad (1)$$

the units being electromagnetic. These equations may be solved in particular cases by the method given by Bromwich[3]. The solutions must satisfy the boundary conditions that the tangential and normal components of magnetic field strength are continuous across the boundary. This type of solution has been used by Marcus[4] for the analogous problem of a rotating sphere.

Spherical Conductor.

Let a be the radius of the sphere. The axis of z is one of symmetry, and may be taken as the axis of spherical polar coordinates. A solution of (1) is

$$\left.\begin{aligned} M_r &= \frac{\partial^2 U}{\partial r^2} - 4\pi\sigma \frac{\partial U}{\partial t}, \\ M_\theta &= \frac{1}{r}\frac{\partial^2 U}{\partial r \partial \theta}, \\ M_\phi &= \frac{1}{r\sin\theta}\frac{\partial^2 U}{\partial r \partial \phi}, \\ E_r &= 0, \\ E_\theta &= \frac{1}{r\sin\theta}\frac{\partial}{\partial \phi}\left(\frac{\partial U}{\partial t}\right), \\ E_\phi &= -\frac{1}{r}\frac{\partial}{\partial \theta}\left(\frac{\partial U}{\partial t}\right), \end{aligned}\right\} \quad . \quad . \quad . \quad . \quad (2)$$

where V is any solution of the equation

$$\frac{\partial^2 U}{\partial r^2} + \frac{1}{r^2\sin\theta}\frac{\partial}{\partial\theta}\left(\sin\theta\frac{\partial U}{\partial\theta}\right) + \frac{1}{r^2\sin^2\theta}\frac{\partial^2 U}{\partial\phi^2} = 4\pi\sigma\frac{\partial U}{\partial t}. \quad (3)$$

If we write $U = V(r, \theta, \phi)e^{iqt}$, the equation becomes

$$(\nabla^2 + k^2)V = 0, \quad . \quad . \quad . \quad . \quad . \quad . \quad . \quad (4)$$

where $$k^2 = -4\pi i\sigma q. \quad . \quad . \quad . \quad . \quad . \quad . \quad . \quad (5)$$

A solution of (4) is

$$V = A\cos\theta[(\sin kr)/kr - \cos kr],$$

whence from (2)

$$\begin{aligned} M_r &= 2A\,.\cos\theta\,.\,e^{iqt}[(\sin kr)/kr^3 - (\cos kr)/r^2], \\ M_\theta &= -A/r\,.\sin\theta\,.\,e^{iqt}[\cos kr/r - \sin kr/kr^2 + k\sin kr], \\ M_\phi &= 0, \\ E_r &= 0, \\ E_\theta &= 0, \\ E_\phi &= A/r\,.\sin\theta\,iq\,e^{iqt}[(\sin kr)/kr - \cos kr]. \quad . \quad . \quad . \quad (6) \end{aligned}$$

Outside the sphere the part of the magnetic field arising from the induced currents is derivable from a potential χ, which satisfies the relation

$$\nabla^2\chi = 0. \quad . \quad . \quad . \quad . \quad . \quad . \quad . \quad . \quad (7)$$

The appropriate form of χ is Y_n/r^{n+1}, where Y_n is a spherical harmonic, and the particular solution corresponding to (6) is given by

$$\chi = B/r^2\,.\cos\theta. \quad . \quad . \quad . \quad . \quad . \quad . \quad . \quad (8)$$

The magnetic field arising from this is

$$\left.\begin{aligned} M_r' &= 2B/r^3 \,.\, \cos\theta \,.\, e^{iqt}, \\ M_\theta' &= B/r^3 \,.\, \sin\theta \,.\, e^{iqt}, \\ M_\phi' &= 0. \end{aligned}\right\} \quad . \quad . \quad . \quad . \quad (9)$$

The external inducing field is given by

$$\left.\begin{aligned} H_r &= h\, dH/dy \,.\, \cos pt \,.\, \cos\theta, \\ H\theta &= -h\, dH/dy \,.\, \cos pt \,.\, \sin\theta, \\ H_\phi &= 0, \end{aligned}\right\} \quad . \quad . \quad . \quad (10)$$

which may be written, in conformity with (6) and (9),

$$\left.\begin{aligned} H_r &= \Sigma \tfrac{1}{2} h\, dH/dy\, e^{iqt} \,.\, \cos\theta, \\ H\theta &= \Sigma -\tfrac{1}{2} h\, dH/dy\, e^{iqt} \,.\, \sin\theta, \\ H_\phi &= 0, \end{aligned}\right\} \quad . \quad . \quad . \quad (11)$$

the summation being over the two values of $q = \pm p$.

The boundary conditions at $r = a$ give

$$2A[(\sin ka)/ka^3 - (\cos ka)/a^2] = 2B/a^3 + \tfrac{1}{2} h\, dH/dy$$

$$A/a[(\cos ka)/a - (\sin ka)/ka^2 + k \sin ka] = -B/a^3 + \tfrac{1}{2} h\, dH/dy,$$

whence

$$A = \frac{3ha}{4k \sin ka}\, dH/dy \quad . \quad . \quad . \quad . \quad . \quad (12)$$

and

$$E_\phi = \Sigma \frac{3ha}{4k \sin ka} \cdot \frac{dH}{dy} \cdot \frac{\sin\theta}{r}\, iqe^{iqt}\left[\frac{\sin kr}{kr} - \cos kr\right]. \quad (13)$$

The two values of k in this summation are

$$\left.\begin{aligned} k_1 &= (1-i)\sqrt{2\pi\sigma p}, \\ k_2 &= (1+i)\sqrt{2\pi\sigma p}. \end{aligned}\right\} \quad . \quad . \quad . \quad . \quad (14)$$

Now in the experimental work $\sqrt{2\pi\sigma p}\, a$ is of the order of 1/10, so that it is permissible to the degree of approximation justified by the data to neglect terms of the third and higher orders in the expansion of $(\sin kr)/kr$ and $\cos kr$. We then obtain, on adding together the two expressions for E_ϕ,

$$E_\phi = \tfrac{1}{2} h \,.\, dH/dy \,.\, p \sin pt \,.\, r \sin\theta \,. \quad . \quad . \quad (15)$$

The work done per second by the eddy-currents in the sphere is given by

$$W = \iiint \sigma E_\phi^2 dt, \quad . \quad . \quad . \quad . \quad . \quad (16)$$

integrated throughout the volume of the sphere. This gives

$$W = 2/15 \, . \, \pi\sigma a^5 (dH/dy)^2 h^2 p^2 \sin^2 pt \, .$$
$$= 2/15 \, . \, \pi\sigma \, . \, a^5 \, . \, (dH/dy)^2 \, . \, \dot{y}^2, \quad . \quad . \quad . \quad (17)$$

$\dot{y}$ being the instantaneous velocity of the sphere.

If F is the instantaneous force per unit mass acting on the sphere due to eddy-currents,

$$W = 4/3 \, . \, \pi\rho a^3 \, . \, F\dot{y},$$

so that

$$F = 1/10 \, . \, \sigma/\rho \, . \, a^2 (dH/dy)^2 \dot{y} = 2x\dot{y},$$

where ρ is the density of the material of the bob.

The logarithmic decrement of the oscillations is, therefore,

$$\kappa T/2 = T/40 \, . \, \sigma/\rho a^2 \, . \, (dH/dy)^2, \quad . \quad . \quad . \quad (18)$$

where T is the period of swing of the pendulum.

It is clear from the discussion of results in the paper of Davies and Evans above that this formula is in satisfactory agreement with experiment.

Cylindrical Conductor, with Axis along Lines of Force.

Taking the axis of z as that of cylindrical coordinates, ρ, ϕ, z, with the origin at the centre of the cylinder, we find as solution of (1),

$$\left.\begin{aligned} M_\theta &= \frac{\partial^2 U}{\partial z \, \partial \rho}, \\ M_\phi &= \frac{1}{\rho} \frac{\partial^2 U}{\partial \phi \, \partial z}, \\ M_z &= \frac{\partial^2 U}{\partial z^2} - 4\pi\sigma \frac{\partial U}{\partial t}, \\ E_\rho &= -\frac{1}{\rho} \frac{\partial^2 U}{\partial \phi \, \partial t}, \\ E_\varphi &= \frac{\partial^2 U}{\partial \rho \, \partial t}, \\ E_z &= 0, \end{aligned}\right\} \quad . \quad . \quad . \quad . \quad . \quad (19)$$

where U is any solution of the equation,

$$\frac{\partial^2 U}{\partial \rho^2} + \frac{1}{\rho} \frac{\partial U}{\partial \rho} + \frac{1}{\rho^2} \frac{\partial^2 U}{\partial \phi^2} + \frac{\partial^2 U}{\partial z^2} - 4\pi\sigma \frac{\partial U}{\partial t} = 0. \quad (20)$$

Noting that there is symmetry about the z-axis, and putting $U=Ve^{iqt}$, we find for V the equation

$$\frac{\partial^2 V}{\partial \rho^2}+\frac{1}{\rho}\frac{\partial V}{\partial \rho}+\frac{\partial^2 V}{\partial z^2}+k^2 V=0, \quad . \quad . \quad . \quad (21)$$

where, as before,

$$k^2=-4\pi i\sigma q.$$

A solution of (21) is

$$V=AJ_0(\alpha\rho)e^{-\sqrt{a^2-k^2}\,.\,z}, \quad . \quad . \quad . \quad . \quad (22)$$

whence

$$\left.\begin{aligned} M_\rho &= -A\alpha\sqrt{\alpha^2-k^2}J_0'(\alpha\rho)e^{-\sqrt{a^2-k^2}\,.\,z}\,.\,e^{iqt},\\ M_z &= \alpha^2 AJ_0(\alpha\rho)e^{-\sqrt{a^2-k^2}\,.\,z}\,.\,e^{iqt},\\ E_\phi &= iq\alpha AJ_0'(\alpha\rho)e^{-\sqrt{a^2-k^2}\,.\,z}\,.\,e^{iqt},\\ M_\phi &= E_\rho = E_z - 0. \end{aligned}\right\} \quad . \quad (24)$$

The magnetic potential χ of the field in outside space arising from the induced currents may be written

$$\chi=BJ_0(\beta\rho)\,.\,e^{-\beta z}\,e^{iqt}, \quad . \quad . \quad . \quad . \quad (25)$$

whence

$$\left.\begin{aligned} M_\rho' &= -BJ_0'(\beta\rho)\beta\,.\,e^{-\beta z}\,e^{iqt},\\ M_z' &= B\beta J_0(\beta\rho)e^{-\beta z}\,e^{iqt},\\ M_\phi' &= 0. \end{aligned}\right\} \quad . \quad . \quad . \quad (26)$$

The external inducing field is

$$\left.\begin{aligned} H_\rho &= H_\phi = 0,\\ H_z &= \tfrac{1}{2}h\,dH/dy\Sigma e^{iqt}. \end{aligned}\right\} \quad . \quad . \quad . \quad . \quad . \quad (27)$$

The boundary conditions at the curved surface of the cylinder, $\rho=a$, are

$$\left.\begin{aligned} -A\alpha\sqrt{\alpha^2-k^2}\,.\,J_0'(\alpha a)e^{-\sqrt{a^2-k^2}\,.\,z} &= -BJ_0'(\beta a)\beta e^{-\beta z},\\ \alpha^2 AJ_0(\alpha a)e^{-\sqrt{a^2-k^2}\,.\,z} &= B\beta J_0(\beta a)\,.\,e^{-\beta z}+\tfrac{1}{2}h\;dH/dy, \end{aligned}\right\} \quad . \quad . \quad (28)$$

which are satisfied by putting

$$\beta=\sqrt{\alpha^2-k^2}=0.$$

Hence

$$E_\phi=\Sigma iq\,e^{iqt}A\,.\,kJ_0'(k\rho). \quad . \quad . \quad . \quad . \quad (29)$$

Expanding the Bessel functions in series, and retaining terms up to the third order, the expression for E reduces, after some manipulation, to

$$E_\phi = \tfrac{1}{4} ph\rho \, dH/dy \, . \, [2 \sin pt + \cos pt \, . \, \pi\sigma p(2a^2 + \rho^2)]. \quad (30)$$

The work W done per second is therefore given by

$$W = 2b\sigma \int_0^a \int_0^{2\pi} (\tfrac{1}{2} ph\rho \, dH/dy)^2 \, . \, [\sin pt + \tfrac{1}{2}\pi\sigma p(2a^2 + \rho^2) \cos pt]^2 \, d\rho \, . \, \rho \, d\phi$$

$= \tfrac{1}{4}\pi a^2 b\sigma \, p^2 h^2 \sin^2 pt \, (dH/dy)^2 +$ terms of higher order in σp which are negligible. (b denotes the half-length of the cylinder.)

The force per unit mass acting on the cylinder is therefore given by

$$F = 1/8 \, . \, \sigma/\rho a^2 \, . \, \dot{y} = 2\kappa\dot{y}, \quad . \quad . \quad . \quad . \quad (31)$$

and the logarithmic decrement of the oscillations is

$$\kappa T/2 = 1/32 \sigma/\rho a^2 (dH/dy)^2, \quad . \quad . \quad . \quad . \quad (32)$$

which again is in satisfactory agreement with experiment.

In the above working the boundary conditions at the flat ends of the cylinder have been ignored. Two of these are satisfied by the solution given, but the third appears to be incapable of being exactly satisfied by a solution of this type. It is clear, however, from the symmetry of the problem that the eddy-currents will flow in concentric circles in planes perpendicular to the axis, so that the effect of the finite length of the cylinder will be very small. That this is so is proved by the experimental work of Davies and Evans[5].

References.

(1) S. Davies and E. J. Evans, *suprà*, p. 1.
(2) *E. g.*, Lamb, Phil. Trans. clxxiv. p. 519 (1883); Lamb, Proc. Lond. Math. Soc. xv. pp. 139 & 270 (1884); Hertz, Inaug. Diss. ('Collected Works,' i. p. 37); Himstedt, *Gott. Nach.* p. 491 (1880). Himstedt, *Ann. der Phys.* xi. p. 812 (1880); Larmor, Phil. Mag. xvii. p. 1 (1884); J. J. Thomson, Mess. Math. xiv. p. 37 (1884); Kern, *Ann. der Phys.* xlii. p. 460 (1913); Gans, *Arch. für Elektrotechnik*, ix. p. 413 (1921); Marcus, Phys. Rev. xxiv. p. 68 (1924).
(3) T. J. I'a. Bromwich, Phil. Mag. xxxvii. p. 407 (1919).
(4) *Loc. cit.* note (2).
(5) *Loc. cit.* note (1).

III. *Determination of the End Correction and Conductance at the Mouth of a Stopped Organ (Flue) Pipe.* By A. E. Bate, *M.Sc., Northern Polytechnic, London* *.

§ 1. In a previous communication † an account was given of the effect of variation in the pressure of the air and of the dimensions of the mouth of a stopped organ-pipe on the frequency of the pipe. It was shown that, after the length of the pipe had been suitably adjusted, the most stable note was obtained when these factors were connected by the equation

$$\frac{V}{nh} = \frac{74}{3}(0{\cdot}3 - s), \quad . \quad . \quad . \quad . \quad . \quad (I.)$$

in which V stands for the velocity of the air in feet per second,

n „ „ frequency,

h „ „ height of the mouth in feet, and

s „ „ the width in inches of the slit from which the air issues.

The pipe referred to had its mouth in a plate which otherwise closed one end of the pipe, and in consequence the air had to be blown across the pipe instead of along it; this enabled the height of the mouth to be altered without altering the length of the air column.

The same pipe was used to obtain the results given in this paper, but in this case the slit width was ·05 inch throughout, so the formula becomes

$$\frac{V}{nh} = 6{\cdot}167, \quad . \quad . \quad . \quad . \quad . \quad (I.a)$$

and from this the air pressures were calculated which were required to make the pipe speak with maximum stability at frequencies of 128, 256, 288, 320, and 340 respectively, and with heights of mouth equal to 0·35, 0·5, 0·65, and 0·8 inch in each case.

§ 2. The correction was obtained by subtracting the length of the pipe (measured from the lip to the inner face of the plate closing the end) from one quarter of the corresponding wave-length. This correction was found for each frequency for each height of mouth, the air pressure having been

* Communicated by Reg. S. Clay, D.Sc.

† Phil. Mag. viii. p. 750 (1929).

adjusted to its appropriate value each time. The length of the pipe was found at which it gave four beats per second with the fork used as standard, *i.e.*, until the frequency of the pipe was $n-4$, where n is the frequency of the fork. The length of the pipe was then altered until it had a frequency of $n+4$, accurate counting of beats being assured by means of a metronome set at four ticks per second. Both lengths of pipe were measured and the arithmetic mean taken as the length of the pipe of frequency n. Actually the harmonic mean should be taken, but this is equal to the arithmetic mean to the degree of accuracy attained in the experiments. The method of beats was used, as it is practically impossible to obtain true agreement of frequencies directly.

§ 3. Lord Rayleigh * gives the equation

$$\tan\frac{2\pi L}{\lambda}=\frac{\lambda . c}{2\pi . A} \quad . \quad . \quad . \quad . \quad . \quad (II.)$$

for a cylindrical resonator without a neck, in which L is the length, A the cross-section, λ is the wave-length of the natural frequency, and c is the conductance of the orifice, which is assumed to be circular. He stated that c is of linear dimension, and equals the diameter of the orifice if circular, or $2\sqrt{\frac{\omega}{\pi}}$ if approximately circular, where ω stands for the area of the orifice. This quantity is referred to in the present paper as the equivalent diameter.

Another formula given by Lamb † for the same type of resonator is

$$\cot\frac{2\pi L}{\lambda}=\frac{2\pi}{\lambda}.\alpha, \quad . \quad . \quad . \quad . \quad . \quad (III.)$$

in which α is the end correction, *i.e.*, the amount by which L falls short of $\lambda/4$; the other symbols are as in (II.). It follows that, since (II.) may be written

$$\cot\frac{2\pi L}{\lambda}=\frac{2\pi}{\lambda}.\frac{A}{c},$$

that $$\alpha=\frac{A}{c}$$

or $$c=\frac{A}{\alpha}. \quad . \quad . \quad . \quad . \quad . \quad (IV.)$$

* Irons, Phil. Mag. p. 879 (May 1929).
† Lamb, 'Dynamical Theory of Sound,' Art. 86.

This indicates that, provided A remains unchanged, the product αc should be constant for all frequencies; hence, for a given area of mouth, *i.e.*, for a given value of c, α should also remain constant at all frequencies.

§ 4. Since the equation

$$\tan\frac{2\pi L}{\lambda} = \frac{\lambda}{2\pi}\,\frac{c}{A}$$

is satisfied by any one of a series of values of L increasing by $\lambda/2$, it follows that for each of these values the same frequency and mouth conditions should hold, as indicated in the previous paper.

§ 5. TABLE I.

Measured values of α corresponding to varying frequencies and heights of mouth. (All lengths in inches.)

Height of mouth.	Frequencies.				
	128	256	288	320	340
0·35	—	3·83	3·71	3·41	3·36
0·5	—	3·20	3·19	3·01	2·92
0·65	2·88	2·85	2·83	2·67	—
0·8	2·53	2·53	—	—	—

Table I. gives the values of the end correction obtained by direct measurement. The results missing from the second column were unobtainable, as the appropriate pressures were too low to cause the pipe to speak. The other missing values required pressures well above 4 ins. of water and are omitted, as such pressures increase the effect of the alteration of the density of the air in the jet beyond the limit taken in obtaining expression (I.).

It will be seen that the values are practically constant at the lower frequencies, and increase with decrease in the height of the mouth. As the frequencies increase, however, the correction gets smaller. This is attributed to the decrease in the volume of the pipe owing to the decrease in wave-length, which thereby invalidates the assumption that the orifice is small in comparison with the volume of the resonator.

§ 6. TABLE II.

Conductances calculated from the measurements given in Table I.

Height of mouth.	Frequencies.					Equivalent diameters.
	128	256	288	320	340	
0·35	—	0·86	0·88	0·95	0·95	0·83
0·5	—	1·05	1·04	1·10	1·13	0·98
0·65	1·21	1·19	1·19	1·26	—	1·11
0·8	1·39	1·36	—	—	—	1·24

The values of the conductances of the mouths given in Table II. were calculated from the results quoted in Table I. by Rayleigh's formula (II.). For the purposes of comparison the equivalent diameters are included; these were obtained as indicated in § 3, the width of the mouth being 1·5 ins. in each case. The table shows that the actual conductances with rectangular orifices are larger than the calculated equivalent diameters; other workers have shown that this is the case with circular orifices *.

§ 7. TABLE III.

Calculated values of α, the end correction.

Height of mouth.	Frequencies.				
	128	256	288	320	340
0·35	—	4·12	4·05	3·74	3·72
0·5	—	3·38	3·40	3·24	3·15
0·65	2·92	2·98	2·98	2·82	—
0·8	2·56	2·61	—	—	—

The end-corrections were calculated from equation (III.). It will be noticed that the discrepancies between the results in Tables I. and III. diminish with increase in height of mouth, and also with increase of wave-length. The latter variation is explained in § 5; the other effect appears to be due to alteration in the shape of the mouth.

* Irons, *ibid.* p. 886.

§ 8. TABLE IV.

Conductances calculated from equation (IV.), using the measured end-corrections.

Height of mouth.	Frequencies.				
	128	256	288	320	340
0·35	—	0·93	0·93	1·04	1·06
0·5	—	1·11	1·11	1·18	1·21
0·65	1·23	1·25	1·25	1·33	—
0·8	1·40	1·40	—	—	—

Since c is the only quantity in equation (IV.) which is not directly measured, the values of c were calculated from it, using the results in Table I. for α; the diameter of the pipe was $2\frac{1}{8}$ ins.

The results are given in Table IV. On comparing these with the values of c given in Table II., it will be seen that they agree more closely as the mouth is made larger, *i. e.*, as the mouth becomes more nearly square. This indicates that the approximation suggested by Rayleigh *—that any orifice may be treated as circular if it does not differ too much from a circle—is only valid in the case of a rectangle which is practically square. Even then the conductance is greater than the equivalent diameter. At first this was thought to be due to the shape of the orifice, but this cannot be the case in those instances in which the mouth is 0·8 inch in height, as the results in Tables II. and IV. agree so closely for this value.

§ 9. TABLE V.

End-corrections for different heights of mouth with added lengths of pipe equal to $\lambda/2$ and λ respectively, for a frequency of 256.

Height of mouth.	Normal length.	Normal+$\lambda/2$.	Normal+λ.
0·35	3·83	3·79	3·85
0·5	3·20	3·18	3·18
0·65	2·85	2·77	2·78
0·8	2·53	2·50	2·46

* Rayleigh, 'Scientific Papers,' i. Art. 5, p. 53, equation (26).

The theoretical conclusions of § 4 were tested for a frequency of 256 by lengthening the stopped pipe speaking with this frequency, by approximately one half-wave-length, and adjusting it by the method described in § 2. In this way the actual lengths of pipe required to produce a frequency of 256 with heights of mouth equal to the four values previously used were found. Within the limits of experimental error, the results indicate that the increase is one half-wave-length for each height of mouth. Repetition with a further addition of one half-wave-length gave similar results.

The end-corrections for each set of results are given in Table V., and were obtained by subtracting the actual lengths of pipe from three-quarters and five-fourths of the wave-length in each case respectively. The close agreement for each height of mouth shows that the conductances are unaltered.

§ 10. Conclusions.

A stopped organ-pipe behaves in exactly the same way as a cylindrical resonator without a neck, provided that the edge-tone set up by the vortex system in the air-stream at the mouth of the pipe synchronizes with the natural frequency of the air-column in the pipe. It follows that the usual resonator formulæ may be applied, and from these the equation $A = c.\alpha$ is deduced, and is shown to hold experimentally if c is regarded as being somewhat larger than the equivalent diameter of the orifice.

The author desires to acknowledge his indebtedness to Dr. Clay for the interest he has shown in this research, and for the facilities provided.

IV. *Temperature Distribution along a Heated Filament used as a Catalyst.* *By* Edward S. Lamar *and* W. Edwards Deming, *Bureau of Chemistry and Soils, Washington, D.C.**

Abstract.

An expression was found for the temperature gradient at any point along a heated molybdenum filament used

* Communicated by C. H. Kunsman. The basis of some of the work presented in this paper was used by E. S. Lamar to satisfy the dissertation requirements of George Washington University for the degree of M.A., 1928.

as a catalyst in the decomposition of ammonia. The temperature at any point along the length was obtained by graphical integration of this expression. The integrated resistance for the whole length of filament was compared with the measured resistance and found to agree within ·27 per cent. at four different temperatures. Knowing the distribution of temperature, it was possible to determine the equivalent length of the filament effective as a catalyst at the maximum temperature. From considerations of the thermal losses to the gas, a value of the heat of dissociation of ammonia was found that was in good agreement with that obtained by Lewis and Randall from Haber's data.

Introduction.

IN the course of some investigations made by C. H. Kunsman * on the catalytic decomposition of ammonia, it was feared that the equivalent length effective at the given maximum temperature of the heated filament used as a catalyst varied with the maximum temperature owing to the cooling at the ends. The present paper concerns an attempt to determine the distribution of temperature along a cylindrical molybdenum filament, to obtain its length effective as a catalyst, and to determine the heat of dissociation of ammonia.

Theory.

If the radial temperature gradient is zero, the steady thermal state of the filament can be represented by

$$\pi r^2\left[\mathrm{K(T)}\frac{d^2\mathrm{T}}{dx^2}+\frac{d\mathrm{K(T)}}{d\mathrm{T}}\left(\frac{d\mathrm{T}}{dx}\right)^2\right]dx+2\pi r\,\mathrm{S(T)}\,dx+\frac{\mathrm{R(T)}\,\mathrm{I}^2}{\pi r^2}dx=0. \quad (1)$$

The term in brackets represents the gain in heat by the element of length dx at x in unit time by metallic conduction along the axis. The second term represents the gain in heat through the surface of the element, and the third term is the gain in heat due to the flow of an electric current through the element. r is the radius of the

* C. H. Kunsman, J. Am. Chem. Soc. l. p. 2100 (1928); li. p. 688 (1929).

filament, T the temperature of the surface, and K(T) is the thermal conductivity of the metal, S(T) the heat gained by unit surface in unit time, R(T) the electrical resistivity, all at temperature T, and I the current. When the steady state is reached, the net gain in heat per unit time in the element of length dx is zero.

If $\left(\frac{dx}{d\mathrm{T}}\right)^2 [\mathrm{K(T)}]^2$ in equation (1) be replaced by U, the differential equation becomes

$$\frac{d\mathrm{U}}{d\mathrm{T}} + \frac{4\mathrm{K(T)\,S(T)}}{r} + \frac{2\mathrm{K(T)\,R(T)}}{\pi^2 r^4}\mathrm{I}^2 = 0, \quad . \quad . \quad (2)$$

from which

$$\mathrm{U} = -(4/r)\int \mathrm{K(T)\,S(T)}\,d\mathrm{T} - (2\mathrm{I}^2/\pi^2 r^4)\int \mathrm{K(T)\,R(T)}\,d\mathrm{T} + \mathrm{C} = 0. \quad . \quad . \quad . \quad (3)$$

Going back to the original variables,

$$\frac{dx}{d\mathrm{T}} = \mathrm{K(T)}\left\{-(4/r)\int \mathrm{K(T)\,S(T)}\,d\mathrm{T} - (2\mathrm{I}^2/\pi^2 r^4)\int \mathrm{K(T)\,R(T)}\,d\mathrm{T} + \mathrm{C}\right\}^{-\frac{1}{2}}. \quad . \quad (4)$$

The second integration can be performed graphically. If T is the temperature on an element at x and $\mathrm{T} + \Delta\mathrm{T}$ is the temperature on an element at $x + \Delta x$, then

$$x + \Delta x = x + \left.\frac{dx}{d\mathrm{T}}\right|_{\mathrm{T}+\frac{1}{2}\Delta\mathrm{T}} \cdot \Delta\mathrm{T}, \quad . \quad . \quad . \quad . \quad (5)$$

closely if $\Delta\mathrm{T}$ is small. The derivative $dx/d\mathrm{T}$ is to be evaluated at $\mathrm{T} + \frac{1}{2}\Delta\mathrm{T}$, as indicated.

Values of the Necessary Constants and Functions.

The only measurements on the thermal conductivity of molybdenum seem to be those of Barratt* at 0° and 100° C. The equation $\mathrm{K(T)} = 3{\cdot}455 \cdot 10^7\ \mathrm{T}^{-1{\cdot}533}$ satisfies his two values when expressed in C.G.S. units, and is used for K(T). From the data of A. G. Worthing † it was found that the heat lost by radiation could be represented quite accurately as $\mathrm{AT}^n = 12{\cdot}4\ \mathrm{T}^{4{\cdot}9} \times 10^{-16}$ watt per cm.^{2} Worthing found that the temperature coefficient of resistance was the same for two specimens of the same

* T. Barratt, Proc. Phys. Soc. xxvi. p. 347, August 1914.
† A. G. Worthing, Phys. Rev. xxviii. p. 190, July 1926.

purity. His measurements on the resistivity of molybdenum, over the temperature range used in our experiment, fit the equation $\rho = R_0 T^{1\cdot17}$ ohm cm. This also fits accurately the temperature variation of the resistivity of our filament from 0° to 100° C., so we feel justified in using 1·17 as the exponent of T. Our values of resistivity give $R_0 = 7\cdot893 \times 10^{-9}$; so we used $\rho = 7\cdot893 \times 10^{-9}\ T^{1\cdot17}$ ohm cm.

Along a short length in the middle of the filament, where the temperature gradient is zero, the heat delivered to the surrounding gas is equal to that generated by the current less that lost by radiation. By plotting the logarithm of the heat delivered to the gas against log $(T - T_0)$ a straight line of slope 2 is obtained (T_0 is the temperature of the water surrounding the tube), so we used $B(T - T_0)^2$ to represent the heat delivered per second to the gas. Thus

$$S(T) = -\{12\cdot4 \times 10^{-16} T^{4\cdot9} + B(T - T_0)^2\}.$$

Substituting the functions and constants thus far determined into equation (4) and performing the two simple integrations inside the brace, we have

$$\frac{dx}{dT} = \{1\cdot6211 \times 10^{-14} T^{6\cdot0533} + B(26\cdot392\, T^{3\cdot1533} - 81\cdot366\, T_0 T^{2\cdot1533} + 88\cdot732\, T_0^2 T^{1\cdot1533}) - \cdot0040493\, I^2 T^{2\cdot3233} + C T^{\cdot3066}\}^{-\frac{1}{2}}. \quad . \quad . \quad . \quad (6)$$

This is used in equation (5) for the graphical integration to get T as a function of x.

The constant B was determined in each case by assuming the first term of equation (1) to be zero at the maximum temperature and solving for B in S(T). The assumption made seems justifiable because the filament was of uniform temperature for quite a distance along its length. The constant C for each case was obtained by setting $\frac{dT}{dx}$ equal to zero, that is to say, by setting the quantity in the brace in equation (4) equal to zero for the maximum temperature and solving for C, the only unknown left.

Apparatus.

The experimental set-up was that described by Kunsman* with the exception that the filament was made

* C. H. Kunsman, J. Am. Chem. Soc. l. p. 2100 (1928); li. p. 688 (1929).

one arm of a Kelvin double bridge rather than of a Wheatstone bridge, as the absolute value of the filament resistance was desired.

The principal use of the tube was to measure the rate of decomposition of ammonia as a function of temperature. The temperature distribution along the filament was to be measured under the conditions of the experiment as a means of determining the equivalent length effective at the given maximum temperature. The maximum temperature was obtained by means of a rare metal thermocouple spot welded to the centre of the filament. These wires were two mils in diameter, and there was apparently no cooling at the junction. It was found that wires of such small diameter could be sealed successfully through pyrex glass. Cooling fins were attached to each end of the filament, and the assumption was made that the temperature of the ends was that of the water bath surrounding the tube. Preliminary investigations in air seemed to justify this assumption when the fins were made sufficiently large.

Experimental Procedure.

The tube was first pumped out, and the pumping system was then closed off from the tube by means of a mercury trap. Ammonia to a pressure of 26·6 cm. Hg was then admitted to the tube. Before starting a run, the ratio was set on the Kelvin bridge to produce the desired temperature. During the run simultaneous observations were made on the increase in pressure as the reaction progressed, on the current flowing in the filament, on the thermocouple E.M.F., and on the time.

The change in the maximum temperature of the filament from the beginning to the end of a decomposition run was less than five degrees. From this fact, and the fact that the resistance was kept constant, it is reasonable to assume that the distribution of temperature, and thus the effective length of the filament, did not vary appreciably during a single decomposition run.

The results of the graphical integration, giving the temperature as a function of the distance from one end of the filament, are shown in the figure for four different maximum temperatures. As a check on the accuracy of the work, the integrated resistance was compared with

the measured resistance and the results are shown in Table I.

The effective length of filament was determined by means of the expression

$$l = \Sigma k \Delta x / \bar{k},$$

where k is the rate of reaction for the temperature of the element Δx, and k is the rate at the maximum temperature.

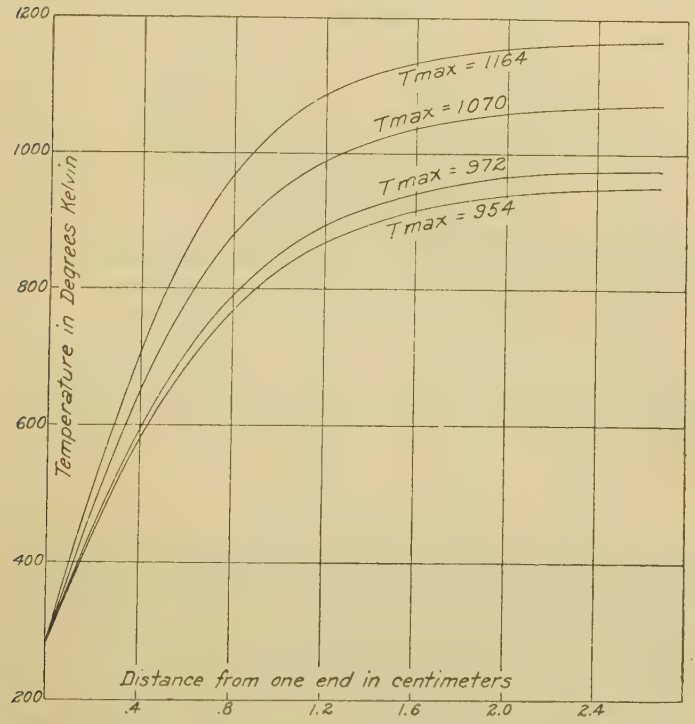

Results of the Graphical Integration. Temperature along the Filament as a Function of the Distance from one End

The rates of reaction for each of the temperatures used in the integration were obtained from a log k against T^{-1} plot of the experimental data.

Table I. gives the measured resistance, the computed resistance, the resistance that the filament would have if its entire length had been at the maximum temperature, and the effective length.

TABLE I.

T. °K.	Measured resistance.	Computed resistance.	Computed resistance. uncorrected.	Effective length $=\Sigma k\Delta x/\bar{k}$.
1164	·6969	·6988	·7398	15·23
1070	·6324	·6330	·6642	14·85
972	·5661	·5652	·5933	14·37
954	·5533	·5518	·5804	14·21

Heat of Dissociation of Ammonia.

As has been shown above, over the temperature range investigated the thermal losses to the gas in the tube could be represented as $W \equiv B(T - T_0)^2$. Lorenz * found empirically that the thermal losses from a filament to a gas could be represented by $B(T - T_0)^{5/4}$ over quite a wide range of temperatures. In the present work, it was thought that the discrepancy between the two empirical laws could be accounted for on the basis of the fact that the gas was reacting chemically. Irving Langmuir †, in his work on the thermal conductivity of hydrogen, expressed the losses to the gas as $S(\phi_2 - \phi_1)$, where S is a constant known as the shape factor, and

$$\phi_2 - \phi_1 = \int_{T_1}^{T_2} K \, dT,$$

where K is the thermal conductivity of the gas at the temperature T. T_1 and T_2 are the temperatures of the water-bath and of the surface of the metal. The function of convection, as postulated by Langmuir, is to maintain the boundary of an enveloping layer of gas practically at the temperature T_1. Langmuir's results are in agreement with the empirical law given by Lorenz. In the present work, the losses to the gas can be expressed as the sum of two terms, the first the conduction and convection loss, and the second the loss due to the chemical reaction. This second term should be proportional to the rate of reaction, so

$$W = S(\phi_2 - \phi_1) + \dot{q} k_0, \quad . \quad . \quad . \quad . \quad . \quad (7)$$

where k_0 is the rate of reaction at the beginning of the run,

* L. Lorenz, *Ann. Phys.* xiii. p. 582 (1881).

† Irving Langmuir, Phys. Rev. xxxiv. p. 401, June 1912.

and q is the heat of dissociation of ammonia. The experimental values of B were plotted against total pressure in the tube, and the smoothed curves were extended back to the beginnings of the decomposition runs to determine the values of W when the concentration of the products of the reaction were zero. The values of k at the beginnings of the runs were determined by plotting $1/k$ against p_1/p_0 and extending the straight lines back to the $1/k$ axis, where $p_1/p_0=0$, as described by Kunsman, Lamar, and Deming*. p_1 is the partial pressure of hydrogen, and p_0 is that of ammonia.

The formula $K=a\eta c_v$ was used for the thermal conductivity of ammonia in the calculation of $\phi_2-\phi_1$. a is a constant, η is the viscosity, and c_v the specific heat at constant volume. Sutherland's formula,

$$\eta=\eta_0 T^{\frac{1}{2}}/(1+c/T),$$

was used with $c=370$, as given in the International Critical Tables. c_p is given in these tables by the formula

$$c_p=8{\cdot}62+{\cdot}002\,(T-273)+7{\cdot}2\times10^{-9}(T-273)^2$$

calories per mol per degree. The last term was neglected. The pressure of the ammonia was 26·6 cm. Hg at the beginning of each run and its temperature next to the filament was in the neighbourhood of 1000°K, so we think the assumption that $c_p-c_v=$constant is justifiable. The ratio c_p/c_v at 15° C. is given in the tables as 1·31. This allows c_v to be calculated at 15° C., and assuming $c_p-c_v=$constant to be true for all temperatures, c_v is known at all temperatures. The constant a was computed using K as given for 100° C. in the Critical Tables, and η and c_v as given by the above formulas (remembering to reduce them all to the same units), whence $K=a\eta c_v$ becomes

$$K=35{\cdot}05\times10^{-6}T^{\frac{1}{2}}\{1+{\cdot}000304\,(T-273)\}/(1+370/T)$$

joules/cm. deg. . . . . (8)

Table II. furnishes eight observations on equation (7). The values of q and S that render

$$\sum_{i=1}^{8}\{(\phi_2-\phi_1)_i-W_i(1/S)+k_{0i}(q/S)\}^2$$

* Kunsman, Lamar, and Deming, "Rates and Temperature Coefficients of the Catalytic Decomposition of Ammonia over Molybdenum, Tungsten, and Promoted Iron," to be published soon.

a minimum were found. Thus the entire adjustment is thrown on to $\phi_2 - \phi_1$ for each temperature, which is fair enough because the experimental values of k and W are much more reliable than the determinations of $\phi_2 - \phi_1$. The least-square computation yields $q = 50{,}513$ joules per mol $= 12{,}067$ calories per mol, and $S = 32{\cdot}83$.

TABLE II.

W is the power in watts supplied to a length of filament that has an area of one square centimetre, as computed from the observed current and the calculated resistance, minus the calculated loss by radiation. $\phi_2 - \phi_1$ is calculated using K given in eq. (7). The values of k are smoothed values of the observed reaction rate, in mols per second per square centimetre.

T °K.	W(watts/cm.^{2}),	$(\phi_2 - \phi_1) \times 10^2$.	$k \times 10^6 - \frac{\text{mols}}{\text{sec. cm.}^2}$.
1164	26·08	63·22	121·20
1121	22·93	57·52	79·10
1081	20·27	53·17	52·80
1070	19·47	51·82	46·22
1043	17·90	49·17	31·48
1007	15·85	45·49	14·00
972	14·16	42·27	6·59
954	12·92	40·27	3·50

Thus 12,067 calories per mol is found to be the average heat of dissociation of ammonia for the temperature interval 954° to 1164° K. Lewis and Randall * give a formula, based on Haber's data, that yields $q = 13{,}375$ calories per mol over this temperature range. The agreement justifies the assumption that the discrepancy in the empirical law for the thermal loss to the gas was due to the progress of the chemical reaction.

The authors desire to thank Professor T. B. Brown of the George Washington University and Dr. C. H. Kunsman of this laboratory for several helpful suggestions made during the progress of this work.

* Lewis and Randall, 'Thermodynamics,' Chapt. XXXIX.

V. *New Bands in the Secondary Spectrum of Hydrogen.*—Part II. *By* D. B. Deodhar, *M.Sc., Ph.D., Physics Department, Lucknow University, India* *.

THE investigation of the secondary spectrum of hydrogen has been continued in the Physics Department of the Lucknow University, and it has brought to light a large number of new band-groups in the blue and the violet region of the spectrum similar to those in the yellow region, which were dealt with in detail in my last paper †. In the present paper I propose to set forth a system of seven new bands in the blue region which I have been able to examine thoroughly.

The band-groups in the yellow, blue, etc. region start respectively on the short-wave length side of H_α, H_β, etc., and extend further towards the violet end of the spectrum. In picking up band-lines use is made of the microphotograph of a typical first-type discharge spectrogram of hydrogen taken by Moll's self-registering photometer.

There is a large mass of lines in the blue and the violet region of the first-type spectrum whose intensity gradation on the photograph indicates the presence of regularities in a very conspicuous way. Many of these lines appear to be extensions of the systems developed by Professor O. W. Richardson ‡. There are some lines which have been grouped by Allen and Sandeman § as belonging to triatomic hydrogen. However, there are several lines which are not yet ordered, and which show regularities according to the microphotograph.

The leading lines have been picked up from the first-type spectrogram. The accurate picking of relevant lines has been further facilitated by the wave-length tables of hydrogen lines recently published by Gale, Monk, and Lee ‖. These authors have resolved several strong lines into their components with the help of a 21-foot concave grating, and the measurement of standard lines was made by them by means of a Fabry-Perot interferometer giving a high accuracy to the values of the interpolated lines.

* Communicated by the Author.
† Phil. Mag. vii. pp. 466–479 (1928).
‡ Roy. Soc. Proc. A, cxiii. pp. 368–419 (1926).
§ Roy. Soc. Proc. A, cxiv. pp. 293–313 (1927).
‖ Astro. Phys. Journ. lxvii. pp. 89–113 (1928).

The P(2)-lines of all the blue bands are about 150 wave-numbers apart, as in the case of P(2)-lines of the yellow bands, and the vertical differences of the various P, Q, and R branches are approximately of the same order as those of the yellow ones. These bands are named as D'_1, D'_2, D'_3, D'_4, D'_5, D'_6, and D'_7, the D's representing their similarity to the yellow bands. The signifying letter D is dashed to distinguish the blue group from the yellow group. The frequencies, properties, and other details of these bands are given in Table I. The band-lines are represented by their frequencies. The values of frequencies are taken from the tables of Gale, Monk, and Lee in general, and from the tables of Merton and Barratt *, Tanaka †, or Deodhar ‡ in the case of those lines which do not occur in the list of Gale, Monk, and Lee. The frequency of the line is followed by (1) the intensity estimate according to Gale, Monk, and Lee, and (2) the intensity estimate made by the author on the first-type spectrogram. It may be pointed out that the estimate of intensity in the list of Gale, Monk, and Lee is much higher than the intensity estimate in the lists of Merton and Barratt, Tanaka, or Deodhar.

Many (*r*) and (*rd*) lines in Tanaka's and Deodhar's lists appear as (0) and (1) lines in G., M., and L.'s tables. However, in this paper I have used G., M., and L.'s estimates for the sake of quick reference. Underneath the frequency value of the line are given the H.P., L.P., C.D., He, Z, and S properties according to Merton and Barratt's tables, where the letters have their usual meaning. These properties are followed in the same line by other claims, if any, made by other systems. The first and second differences are given in the next two columns. The horizontal and the vertical differences are given in Tables II. and III. respectively.

It will be seen from Table I. that the first-type property is exhibited by a majority of the band-lines in the blue region. There are also very few important claims by other systems. The line $D_3P(2)$ appears as Richardson's § 111 P(6) and 11 R(5), but Richardson considers it to be too strong for either of these two series. $D'_3R(2)$ figures as $3\gamma_4Q(4)$, but here Richardson ‖ appears to be in doubt about the proper assignment of the line as $3\gamma_4Q(4)$; $D'_1R(1)$ is claimed as $D'_3Q(4)$, and $D'_1R(3)$ appears as $D'_3Q(3)$. Nothing definite

* Phil. Trans. Roy. Soc. A, ccxxii. pp. 369–400 (1922).
† Roy. Soc. Proc. A, cviii. pp. 592, 606 (1925).
‡ Roy. Soc. Proc. A, cxiii. pp. 420–432 (1926).
§ Roy. Soc. Proc. A, cix. pp. 43, 44 (1925).
‖ Roy. Soc. Proc. A, cxiii. p. 388 (1926).

Table I.

$D'_1P(m)$.

m.		Δ_1.	Δ_2.
2.	21112·28 (0*h*) (*o*)		
		> 98·34	
3.	21013·94 (1) (2)		>15·98
		>114·32	
4.	20899 62 (Q′, *a*) (0)		>16·61
	2050 (Q)(3)		
		>130·93	
5.	20768·69 (7) (2)		
	L.P.+		

$D'_2P(m)$.

m.		Δ_1	Δ_2.
2.	21262·87 (2) (1)		
		>103·95	
3.	21158·92 (4) (2)		>15·18
	L.P.+		
		>119·13	
4.	21039·79 (4) (1)		>16·67
	H.P.+, S.		
		>135·80	
5.	20903·99(1, *a*) (*ab*)		

$D'_1Q(m)$.

m.		Δ_1.	Δ_2.
1.	21298·72 (1) (*ab*)		
		>29·01	
2.	21269·71 (0) (*ab*)		>11·24
		>40·25	
3.	21229·46 (1) (1)		>15·60
		>55·85	
4.	21173·61 (3) (0)		>15·22
		>71·07	
5.	21102·54 (0) (<0)		

$D'_2Q(m)$.

m.		Δ_1.	Δ_2.
1.	21424·74 (0) (*ab*)		
		>26·97	
2.	21397·77 (1) (0)		>11·21
		>38·18	
3.	21359·59 (5) (1)		>10·64
	L.P.+, 3,33 Q(1)		
		> 48·82	
4.	21310·77 (1) (0)		>14·07
		>62·89	
5.	21247·88 (3) (1)		

$D'_1R(m)$.

m.		Δ_1.	Δ_2.
1.	21456·53 (0) (0)		
	$D'_3Q)4$)		
		>28·99	
2.	21485·52 (6) (2)		>11·75
	Z		
		>17·24	
3.	21502·76 (0) (0)		>12·30
		>4·94	
4.	21507·70 (0, *a*) (0)		

$D'_2(Rm)$.

m.		Δ_1.	Δ_2.
1.	21559·99 (1) (<0)		
		>38·28	
2.	21598·27 (1) (prob. *ab*)		>6·03
		>32·25	
3.	21630·52 (0) (*ab*)		>7·33
		>24·92	
4.	21655·44 (00) (*ab*)		
	He++		

TABLE I. (*cont.*).

$D'_3P(m)$.

m.		Δ_1.	Δ_2.
2.	21410·61 (3) (1) H.P+, 111 P (6)		
		>110·15	
3.	21300·46 (0) (0)		>12·01
		>122·16	
4.	21178·30 (1,*a*) (<0)		>20·68
		>142·84	
5.	21035·46 (0) (*ab*)		

$D'_4P(m)$.

m.		Δ_1.	Δ_2.
2.	21557·79 (0*h*) (0)		
		>117·41	
3.	21440·31 (8) (3)		>7·66
	L.P.+		
		>125·14	
4.	21315·17 (7) (1)		>16·42
	H.P.+, 0δ2 Q(2)		
		>141·56	
5.	21173·61 (3) (0)		

$D'_3Q(m)$.

m.		Δ_1.	Δ_2.
1.	21562·97 (*r*) (*ab*) D.		
		>25·04	
2.	21537·93 (*r*) (*ab*) D.		>10·13
		>35·17	
3.	21502·76 (0) (0) $D'_1R(3)$		>11·06
		>46·23	
4.	21456·53 (0) (0)		>10·83
		>57·06	
5.	21399·47 (1) (1)		

$D'_4Q(m)$.

m.		Δ_1.	Δ_2.
1.	21709·81 (0) (*ab*)		
		>23·53	
2.	21686·28 (*r*) (*ab*) D.		>7·31
		>30·84	
3.	21655·44 (00) (<0) He++		>7·76
		>38·59	
4.	21616·85 (0) (*ab*) 4γ5 Q(1)		>14·99
		>53·58	
5.	21562·97 (*r*) (*ab*) $D'_3Q(1)$		

$D'_3R(m)$.

m.		Δ_1.	Δ_2.
1.	21690·06 (00) (<0) 5*a*2 Q(1)		
		>50·13	
2.	21740·19 (3) (0) H.P.++, He++ 3γ4 Q(4) ?		>9·52
		>40·61	
3.	21780·80 (1) (<0)		>0·77
		>39·84	
4.	21820·64 (4) (2) H.P.++, He++		

$D'_4R(m)$.

m.		Δ_1.	Δ_2.
1.	21837·43 (6) (0)		
		>63·74	
2.	21901·17 (1) (*ab*) 2γ3 Q(4) ?		>8·40
		>55·34	
3.	21956·51 (0) (*ab*)		>5·89
		>49·45	
4.	22005·96 (1) (*ab*)		

TABLE I. (*cont.*).

$D'_5P(m)$.

m.		Δ_1.	Δ_2.
2.	21702·52 (*r*) (? D.		
		>123·08	
3.	21579·44 (*q*) (?)		>6·48
	D.	>129·56	
4.	21449·88 (00*b*) (*ab*)		>13·56
		>143·12	
5.	21306·76 (5) (1) 0∂2 Q(3), 56R (4)		

$D'_6P(m)$.

m.		Δ_1.	Δ_2.
2.	21844·49 (1) (1)		
		>124·86	
3.	21719·63 (*r*) (0)		>11·15
	T.	>136·01	
4.	21583·62 (9) (6)		>15·68
	He+, Z.	>151·69	
5.	21431·93 (1) (<0)		

$D'_5Q(m)$.

m.		Δ_1.	Δ_2.
1.	21869·77 (0) (*ab*)		
		>22·63	
2.	21847·14 (0) (1)		>8·90
		>31·53	
3.	21815·61 (10 (3)		>7·98
		>39·51	
4.	21776·10 (*r*) (*ab*) D.		>7·58
		>47·09	
5.	21729·01 (1) (0)		

$D'_6Q(m)$.

m.		Δ_1.	Δ_2.
1.	22047·14 (1) (0)		
		>22·31	
2.	22024·93 (5) (2) H.P.++, Z.		>8·79
3.	21993·73 ( ) (*ab*) D.	>31·10	>6·12
		>37·22	
4.	21956·51 (0) (*ab*)		>7·38
		>44·60	
5.	21911·91 (1) (0)		

$D'_5R(m)$.

m.		Δ_1.	Δ_2.
1.	22014·85 (2) (1) H.P.+		
		>68·68	
2.	22083·53 (0) (0)		>10·90
		>57·78	
3.	22141·31 (2) (0)		> 0·55
		>57·23	
4.	22198·54 (00) (*ab*)		

$D'_6R(m)$.

m.		Δ_1.	Δ_2.
1.	22227·98 (3) (0) He+		
		>71·82	
2.	22299·80 (00) (<9)		>42·3
		>67·59	
3.	22367·39 (0) (0)		>−0·61
		>68·20	
4.	22435·59 (2) (1)		

$D'_7P(m)$.

m.		Δ_1.	Δ_2.
2.	21985·24 (1) (1)		
		>132·14	
3.	21853·10 (0) (0)		>13·21
		>145·35	
4.	21707·75 (2) (1) H.P.+, He+		> 7·46
		>152·81	
5.	21554·94 (00) (*ab*)		

$D'_7Q(m)$.

m.		Δ_1.	Δ_2.
1.	22241·08 (1) (<0)		
		>21·14	
2.	22219·94 (00) (0)		>7·02
		>28·16	
3.	22191·78 (1) (0) L.P.+, He++, $0\beta_0Q(4)$		> 3·41
		>31·57	
4.	22160·21 (1) (0)		>10·73
		>42·30	
5.	22117·91 (3) (prob. *ab*.) He++, Z, S		

$D'_7R(m)$.

m.		Δ_1.	Δ_2.
1.	22476·06 (6) (2)		
		>83·38	
2.	22559·44 (1) (0)		>−0·93
		>84·31	
3.	22643·75 (3) (*ab*) He++, Z, S		> 5·41
		>78·90	
4.	22722·65 (1) (*ab*)		

Table II.

Horizontal Differences of P(m)'s, Q(m)'s, and R(m)'s.

	$D'_2-D'_1$.	$D'_3-D'_2$.	$D'_4-D'_3$.	$D'_5-D'_4$.	$D'_6-D'_5$.	$D'_7-D'_6$.
P(2).....	150·59	147·74	147·18	144·73	141·97	140·75
P(3).....	144·98	141·54	139·85	139·13	140·19	133·47
P(4).....	140·17	138·51	136·87	134·71	133·74	124·13
P(5).....	135·30	131·47	138·15	133·15	125·17	123·01
Q(1).....	126·02	138·23	146·84	159·96	177·37	193·94
Q(2).....	128·06	140·16	148·35	160·86	177·79	195·01
Q(3).....	130·13	143·17	152·68	160·17	178·12	198·05
Q(4).....	137·16	145·76	160·32	159·25	180·41	203·70
Q(5).....	145·34	151·59	163·50	166·04	182·90	206·00
R(1).....	103·46	130·07	147·37	177·42	213·13	248·08
R(2).....	112·75	141·92	160·98	182·36	216·27	259·64
R(3).....	127·76	150·28	175·71	184·80	226·08	276·36
R(4).....	147·74	165·20	185·32	192·58	237·05	287·06

Table III.

Vertical Differences of P(m), Q(m), and R(m) lines.

Band.	P(2)−P(3).	P(3)−P(4).	P(4)−P(5).	
D'_1	98·34	114·32	130·93	
D'_2	103·95	119·13	135·80	
D'_3	110·15	122·16	142·84	
D'_4	117·48	125·14	141·56	
D'_5	123·03	129·56	143·12	
D'_6	124·86	136·01	151·69	
D'_7	132·14	145·35	152·81	
	Q(1)−Q(2).	Q(2)−Q(3).	Q(3)−Q(4).	Q(4)−Q(5).
D'_1	29·01	40·25	55·85	71·07
D'_2	26·97	38·18	48·82	62·89
D'_3	24·04	35·17	46·23	57·06
D'_4	23·53	30·84	38·59	53·58
D'_5	22·63	31·53	39·51	47·09
D'_6	22·31	31·10	37·22	44·60
D'_7	21·14	28·16	31·57	42·30
	R(2)−R(1).	R(3)−R(2).	R(4)−R(3).	
D'_1	28·99	17·24	4·94	
D'_2	38·38	32·25	24·92	
D'_3	50·13	40·61	39·84	
D'_4	63·74	55·34	49·45	
D'_5	68·68	57·78	57·23	
D'_6	71·82	67·59	68·20	
D'_7	83·38	84·31	78·90	

can be said about this double claim ; but these lines do not so far appear to be claimed by any other published series. $D'_4R(2)$ figures as Richardson's $2\gamma_3Q(4)$, but here also Richardson seems to be uncertain about the correctness of the line belonging there. The line 21306·76, which is $D'_5P(5)$ in the present paper, has been claimed as $0\delta2Q(3)$ and 56R(4) by Richardson. The line is rather strong for its place as $D'_5P(5)$; it also appears to be strong for 56R(4). $D'_6Q(2)$ figures as Allen and Sandeman's * $II_A.C.Q(2)$. Its first-type property is certainly favourable for its place as $D'_6Q(2)$, and its high-pressure nature may demand its position in Allen and Sandeman's series as well. $D'_7Q(5)$ is given as Allen and Sandeman's $II_A.d.Q(2)$. Its intensity is a bit strong for its assignment as $D'_7Q(5)$; but it shows helium effect, which favours its place there. Its probable absence, that is to say its extreme weakening in the first-type spectrum, speaks favourably for its place in Allen and Sandeman's series. The intensities of $D'_5P(2)$ and $D'_5P(3)$ cannot be exactly given on the judgment of the first-type plate, and this is indicated by making a query in the bracket for intensity; $D'_5P(2)$ is 21702·52(*r*)D, and it is very close to 21699·61, which is broad, and possesses intensity (1). $D'_5P_{(3)}$ is 21579·44(*q*)D, and is quite close to 21583·62, which is (7) in intensity on the first-type plate.

The horizontal and vertical differences of $P(m)$, $Q(m)$, and $R(m)$ lines are arranged in Tables II. and III. It will be seen from Table II. that the successive horizontal differences have a fairly systematic run. The value in wave-numbers of these differences for P's, Q's, and R's are roughly of the same order as for those in the case of the yellow bands. The run of the vertical differences in Table III. is very systematic. It is also interesting to compare the vertical differences of P's, Q's, and R's of all the bands of the blue with those in the yellow. For instance, the $P(2)-P(3)$ difference in the yellow gradually rises from 99 for the first band to 130 for the last band; and in the case of the blue bands it gradually rises from 98 for the first to 132 for the seventh band. $Q(1)-Q(2)$ for the yellow gradually decreases from 30 to 21, and for the blue it is 29 for the first band and then gradually goes down to 21 for the last band. The $R(2)-R(1)$ value of the yellow bands steadily rises from 26 to 82 approximately, while that of the blue bands also shows a gradual increase from 29 to 83.

* Roy. Soc. Proc. A, cxiv. p. 301 (1927).

The usual combination principle, such as $Q(m+1)+Q(m)=P(m+1)+R(m)$ is obeyed throughout by the P, Q, and R branches of all the seven bands. The accuracy with which the combination principle is satisfied can also be easily seen by looking to the initial and the final term differences which are tabulated in Tables IV. and V. respectively. The frequencies of the null lines, the moments of inertia, and other band-constants are given in Table VI. The properties of lines involved in all these bands and the systematic variation of the successive differences from band to band show that these bands are related to each other. The run of the null-line frequencies and the gradual variation of values of the initial and the final moments of inertia from D'_1 to D'_7 lend further support to this view.

As usual, the emission of the $R(m)$ line is the result of a quantum jump $m+1\rightarrow m$; the $P(m)$ line is due to a $m-1\rightarrow m$ jump, and the $Q(m)$ line is due to a $m\rightarrow m$ jump.

Thus
$$R(m)=\nu_0+(Fm1)-f(m),$$
$$Q(m)=\nu_0+F(m)-f(m),$$
$$P(m)=\nu_0+F(m-1)-f(m).$$

Here ν_0 is the frequency of the null lines and F and f represent the initial and the final states respectively of the molecule. From these equations the initial and the final differences can be easily calculated. The differences obtained in the above manner are tabulated in Tables IV. and V. With the help of the term-differences we can calculate the initial and the final moments of inertia of the emitters of the bands. We can also calculate Kratzer's correction terms P and ρ, representing the effect of the angular momentum due to electrons in the initial and the final state from relations of the form $F(m)=B(m-P)^2$ and $f(m)=b(m-\rho)^2$, where B and b can be easily shown to be equal to $\frac{1}{2}\{(F(3)-F(2))-(F(2)-F(1))\}$ and $\frac{1}{2}\{(f(3)-(f(2))-(f(2)-f(1))\}$ respectively. The evaluation of P and ρ gives a clue to the determination of the terms from which we can directly calculate the frequencies of the null lines of the various bands. The details of the process of these calculations have been already worked out in the paper on the yellow bands, and to avoid repetition it is assumed that that paper is available for reference. The values of ν_0's calculated for each band from Q(1), P(2), and R(1), and the values of the final and the initial terms, etc.,

TABLE IV.

Initial Terms.

Band.	m.	R(m) Q(m+1).	Q(m+1) −P(m+1).	Means.	Term diff.	2nd diff.
D'_1	1 ...	157·81	157·43	157·62	F(2)−F(1)	
						> 58·04
	2 ...	215·81	215·52	215·66	F(3)−F(2)	
						> 57·98
	3 ...	273·30	273·99	273·64	F(4)−F(3)	
						> 60·33
	4 ...	334·09	333·85	333·97	F(5)—F(4)	
D_2	1 ...	135·25	134·90	135·08	F(2)−F(1)	
						> 65·50
	2 ...	200·50	200·67	200·58	F(3)−F(2)	
						> 70·37
	3 ...	270·93	270·98	270·95	F(4)−F(3)	
						> 73·33
	4 ...	344·67	343·89	344·28	F(5)−F(4)	
D'_3	1 ...	127·09	127·32	127·20	F(2)−F(1)	
						> 75·08
	2 ...	202·26	202·30	202·28	F(3)−F(2)	
						> 75·86
	3 ...	278·04	278·23	278·14	F(4)−F(3)	
						> 85·92
	4 ...	364·11	364·01	364·06	F(5)−F(4)	
D'_4	1 ...	127·62	128·49	128·05	F(2)−F(1)	
						> 86·96
	2 ...	214·89	215·13	215·01	F(3)−F(2)	
						> 88·37
	3 ...	301·07	301·68	301·38	F(4)−F(3)	
						> 87·86
	4 ...	389·11	389·36	389·24	F(5)−F(4)	
D'_5	1 ...	145·08	144·62	144·85	F(2)−F(1)	
						> 91·43
	2 ...	236·39	236·17	236·28	F(3)−F(2)	
						> 89·68
	3 ...	325·70	326·22	325·96	F(4)−F(3)	
						> 96·39
	4 ...	422·44	422·25	422·35	F(5)−F(4)	
D'_6	1 ...	180·84	180·44	180·64	F(2)−F(1)	
						> 93·85
	2 ...	274·87	274·10	274·49	F(3)−F(2)	
						> 98·78
	3 ...	373·66	372·89	373·27	F(4)−F(3)	
						>106·26
	4 ...	479·08	479·98	479·53	F(5)−F(4)	
D'_7	1 ...	234·98	234·70	234·84	F(2)−F(1)	
						>104·25
	2 ...	339·50	338·68	339·09	F(3)−F(2)	
						>113·12
	3 ...	451·97	452·46	452·21	F(4)−F(3)	
						>110·50
	4 ...	562·45	562·97	562·71	F(5)−F(4)	

TABLE V.

Final Terms.

Band.	m.	R(m) $-$(Q(m+1).	Q(m) $-$P(m+1)	Means.	Term diff.	2nd diff.
D'_1	1 ...	186·82	186·44	186·61	$f(2)-f(1)$	
						> 69·30
	2 ...	256·06	255·77	255·91	$f(3)-f(2)$	
						> 73·59
	3 ...	329·15	329·84	329·50	$f(4)-f(3)$	
						> 75·54
	4 ...	405·16	404·92	405·04	$f(5)-f(4)$	
D'_2	1 ...	162·22	161·87	162·05	$f(2)-f(1)$	
						> 76·71
	2 ...	238·68	238·85	238·76	$f(3)-f(2)$	
						> 81·01
	3 ...	319·75	319·80	319·77	$f(4)-f(3)$	
						> 87·40
	4 ...	407·56	406·78	407·17	$f(5)-f(4)$	
D'_3	1 ...	152·13	152·36	152·25	$f(2)-f(1)$	
						> 85·20
	2 ...	237·43	237·47	237·45	$f(3)-f(2)$	
						> 86·92
	3 ...	324·27	324·46	324·37	$f(4)-f(3)$	
						> 96·75
	4 ...	421·17	421·07	421·12	$f(5)-f(4)$	
D'_4	1 ...	151·15	152·02	151·59	$f(2)-f(1)$	
						> 94·26
	2 ...	245·73	245·97	245·85	$f(3)-f(2)$	
						> 94·11
	3 ...	339·66	340·27	339·96	$f(4)-f(3)$	
						>103·15
	4 ...	442·99	443·24	443·11	$f(5)-f(4)$	
D'_5	1 ...	167·71	167·25	167·48	$f(2)-f(1)$	
						>100·33
	2 ...	267·92	267·70	267·81	$f(3)-f(2)$	
						> 97·66
	3 ...	365·21	365·73	365·47	$f(4)-f(3)$	
						>103·97
	4 ...	469·53	469·34	469·44	$f(5)-f(4)$	
D'_6	1 ...	203·05	202·65	202·85	$f(2)-f(1)$	
						>102·83
	2 ...	306·07	305·30	305·68	$f(3)-f(2)$	
						>104·82
	3 ...	410·88	410·11	410·50	$f(4)-f(3)$	
						>113·63
	4 ...	523·68	524·58	524·13	$f(5)-f(4)$	
D'_7	1 ...	256·12	255·84	255·98	$f(2)-f(1)$	
						>111·27
	2 ...	367·66	366·84	367·25	$f(3)-f(2)$	
						>116·53
	3 ...	483·54	484·03	483·78	$f(4)-f(3)$	
						>121·22
	4 ...	604·74	605·27	605·00	$f(5)-f(4)$	

TABLE VI.—Band Constants.

Band.	From Q(1).	From P(2).	From R(1).	F(2).	F(1).	$f(2)$.	$f(1)$.	P.	ρ.	Initial Moment of Inertia.	Final Moment of Inertia.
D'_1 ...	21323·17	21323·14	21323·69	299·02	141·74	352·60	166·18	−1·21	−1·06	$9{\cdot}41\times10^{-41}$ gm. cm.^{2}	$7{\cdot}60\times10^{-41}$ gm. cm.^{2}
D'_2 ...	21444·45	21444·41	21444·77	214·63	79·70	261·24	99·40	−0·56	−0·61	7·95 ,, ,,	6·78 ,, ,,
D'_3 ...	21580·70	21580·85	21580·90	180·05	53·16	223·40	70·89	−0·19	−0·29	7·02 ,, ,,	5·62 ,, ,,
D'_4 ...	21716·22	21715·96	21715·57	189·93	51·66	209·83	58·07	−0·06	−0·11	6·36 ,, ,,	5·59 ,, ,,
D'_5 ...	21885·13	21885·44	21885·77	197·76	53·32	236·24	68·68	−0·08	−0·17	5·99 ,, ,,	5·50 ,, ,,
D'_6 ...	22063·62	22063·53	22064·29	274·78	94·61	313·65	111·09	−0·42	−0·47	5·56 ,, ,,	5·17 ,, ,,
D'_7 ...	22261·70	22261·76	22262·14	394·16	159·62	436·14	180·24	−0·75	−0·80	5·07 ,, ,,	4·76 ,, ,,

are all assembled in Table VI. in the same order as was done in the previous paper. The values of F(2)'s and $f(1)$'s are given in that table to facilitate the work of checking the accuracy of the values.

The frequency of the null line is separately determined by using Q(1), P(2), and R(1) members of each band. Table IV. shows that the three values of ν_0 for each band obtained from three different sources are in perfect agreement with one another, and that ν_0 steadily increases from D'_1 to D'_7. The initial moment of inertia is larger than the final moment of inertia for each band, and the value of the moment of inertia steadily decreases from the first band to the last. The gradual decrease in the moment of inertia from band to band, and the systematic increase in the ν_0 values from set to set clearly indicate that these bands are related to each other.

A majority of band-lines in Table I. come up in the "first-type" discharge, which is known to favour the emission of spectrum by an excited molecule of hydrogen (H_2), and, looking to the values of the moment of inertia which are in the neighbourhood of the values given by Dieke* and by Richardson†, it appears that the emitter of the bands given in the present paper is an excited hydrogen molecule (H_2).

A group of bands similar to the yellow and the blue ones appears to be present in the violet region of the first-type spectrum. It is being investigated, and I hope to deal with it in another communication. A comparison of the moment of inertia values of the yellow and the blue bands seems to suggest that these two groups may be related to each other. However, at this stage it is rather difficult to express a definite view about this point. Perhaps the investigation in the violet region may give some clue in this direction.

Physics Department,
Lucknow University, India.

* Proc. Amsterdam Acad. Sci. xxvii. p. 490 (1924).
† Roy. Soc. Proc. A, cxiii. p. 410 (1926).

VI. *Illuminated Spacetime: Optical Effects of Isotropic Radiation Spread over Elliptic Space.* *By* LUDWIK SILBERSTEIN, *Ph.D.* (Communication No. 385.) *

THE solution of Einstein's amplified ("cosmological") equations of the gravitational field,

$$R_{ik} - \tfrac{1}{2}(R - 2\lambda)g_{ik} = -\kappa T_{ik}, \quad . \quad . \quad . \quad . \quad (1)$$

found by de Sitter, and represented by the line-element

$$ds^2 = \cos^2\sigma \cdot c^2\,dt^2 - [dr^2 + R^2 \sin^2\sigma(d\phi^2 + \sin^2\phi\, d\theta^2)], \quad (2)$$

$\sigma = r/R$, corresponds to an empty spacetime, *i. e.*, one devoid of matter proper and of energy as well, in fine for $T_{ik} = 0$.

Now, although stray particles of (palpable) matter, as molecules, atoms, protons, or electrons, are very scarce † in interstellar, and—no doubt—still more so in intergalactic regions, *radiant energy*, or plainly "light," visible and invisible, emitted by stars and nebulæ, can, without exaggeration, be said to be omnipresent, spread all over the space. Nay, its total mass-equivalent (E/c^2) amounts to an astounding figure. To realize this it is enough to recall that our own sun alone radiates at the very least (*i. e.*, not counting ultra-violet and X-rays) $3{\cdot}8 \,.\, 10^{33}$ ergs per second, or $1{\cdot}33.10^{2}$ grams per year, and since it is pretty certain that it has done this, and even more lavishly, at least during the last two thousand million years, and since but very little of this radiation has been intercepted, it is certain that the mass-equivalent of solar radiation now abroad in space is not less than

$$2{\cdot}66.10^{29} \text{ grams},$$

which, though only $5{\cdot}4.10^{-4}$ suns (mass unit), is in itself an imposing mass. Our galaxy consists of, say, $1{\cdot}5.10^{9}$ stars, of which many are more lavish than the sun. Thus the mass of radiant energy originally emitted during that time by all these stars and now abroad, partly within the galaxy and partly outside, in intergalactic regions, has the prodigious mass of 800,000 suns. And then there are certainly a good many millions of such, and perhaps bigger, galaxies. It is true that all this "radiant mass" (to have a brief name for

* Communicated by the Author. From the Kodak Research Laboratories.

† *Cf.*, for instance, A. S. Eddington's 'Internal Constitution of the Stars' (Cambridge University Press, 1926).

E/c^2) is distributed over a huge volume, viz., $V=\pi^2R^3$, so that its mean density does not amount to very much *. Yet it would be unwise, and somewhat repugnant, to neglect it.

It has, therefore, seemed by all means worth the trouble to take account of this stray light, so to speak. In other words, while de Sitter himself, and other writers, considered an empty, *dark* spacetime or world, we propose here to investigate an *illuminated* world. And as this "illumination" is actually provided by myriads of celestial bodies distributed more or less haphazardly, it is reasonable to treat it as *isotropic radiation*, in the generally accepted sense of the word.

Now such a radiation has the capital property that the light pressure, a hydrostatic pressure, associated with it is just *one-third* of the energy-density, say,

$$p = \tfrac{1}{3}\rho. \quad . \quad . \quad . \quad . \quad . \quad . \quad . \quad . \quad (3)$$

The corresponding energy-tension is, therefore, in orthogonal coordinates,

$$T_{ii} = \tfrac{1}{3}\rho g_{ii}, \qquad T_{44} = \rho g_{44}, \qquad i = 1, 2, 3, \quad . \quad . \quad (4)$$

and has the remarkable property that its scalar, or invariant, $T=\rho-3p$, *vanishes*. (This, by the way, is also the property of every electromagnetic energy-tensor.) Thus the field-equations (1), which give without trouble

$$\lambda = \tfrac{1}{4}R = \tfrac{1}{4}g^{\iota\kappa}R_{\iota\kappa},$$

become

$$\left.\begin{aligned} R_{ii} &= \left(\tfrac{1}{4}R + \frac{\kappa\rho}{3}\right)g_{ii}, \\ R_{44} &= (\tfrac{1}{4}R - \kappa\rho)g_{44}. \end{aligned}\right\} \quad . \quad . \quad . \quad . \quad (5)$$

Let us try to solve this system of equations by the radially-symmetrical form of the line-element,

$$ds^2 = g_{11}\,dx^2 - x^2(d\phi^2 + \sin^2\phi\,d\theta^2) + g_{44}c^2\,dt^2, \quad . \quad (6)$$

assuming, that is, ρ as function of x alone, and thus a *globe*, of any radius, filled with isotropic radiation. (This radius may, if we like, be made equal to $\frac{\pi}{2}R$, when *the whole*

* According to Eddington's quotation (*loc. cit.*) the total density of radiation "received *by us* from the stars" is $7{\cdot}7.10^{-13}$ erg/cm.^{3}, whence the corresponding mass-density, $\rho=8{\cdot}6.10^{-34}$ gr./cm.^{3}. The italicized words imply, of course, that this density holds in interstellar regions, within our galaxy. Somewhere half-way between the Milky Way and the nebula in Andromeda, say, the density ρ may be a good deal smaller.

elliptic space will be full of radiation, as very likely it is.) The problem consists in finding g_{11}, g_{44}, and ρ as functions of x.

Now, putting $h_1 = \log g_{11}$, $h_4 = \log g_{44}$, and denoting derivations with respect to x by dashes, we can write the second of equations (5)

$$-R_{22} = 1 + \frac{1}{g_{11}}\left[1 + \frac{x}{2}(h_4' - h_1')\right] = -\left(\frac{R}{4} + \frac{\kappa\rho}{3}\right)x^2. \quad (7)$$

The third says the same thing (for $R_{33} = R_{22}\sin^2\phi$); the fourth is

$$R_{44} = \frac{g_{44}}{g_{11}}\left[R_{11} + \frac{1}{x}(h_1' + h_4')\right]$$
$$= (\tfrac{1}{4}R - \kappa\rho)g_{44},$$

or, replacing R_{11} by its value given in (5),

$$h_1' + h_4' = -\tfrac{4}{3}\kappa\rho x g_{11} \quad . \quad . \quad . \quad . \quad . \quad (8)$$

Instead of the first of (5) it is more convenient to apply the first of the so-called equations of matter, which are known to be but a consequence of the gravitational field-equations, and this gives, without trouble, $\rho\sqrt{g_{44}} = \text{const.}$ Since, without any loss to generality, we can put $g_{44}(0) = 1$, we have

$$\rho = \frac{\rho_0}{\sqrt{g_{44}}},$$

where ρ_0 is the value of ρ (*system density* of radiant mass) at the origin O of the coordinates.

It remains to substitute this expression in the differential equations (7) and (8), and to solve them for g_{11}, g_{44} as functions of x.

Subtracting (8) from (7), one finds

$$\frac{d}{dx}\left(1 + \frac{1}{g_{11}}\right) + \frac{1}{x}\left(1 + \frac{1}{g_{11}}\right) = (\tfrac{1}{4}R + \kappa\rho)x,$$

whence, in absence of a singularity (mass-centre) at O,

$$-\frac{1}{g_{11}} = 1 - x^2/\mathrm{R}^2, \quad \mathrm{R}^2 = \frac{3}{\lambda + \kappa\rho}. \quad . \quad . \quad . \quad (9)$$

It remains to find g_{44} from (8). Now, this equation can be written

$$\frac{d\sqrt{g_{44}}}{dx} + \left(\frac{d}{dx}\log\sqrt{-g_{11}}\right)\cdot\sqrt{g_{44}} = -\tfrac{2}{3}\kappa\rho_0 x g_{11},$$

which is Euler's linear equation. Its complete solution is

$$\sqrt{g_{44}} = e^{-\int d\log\sqrt{-g_{11}}} \cdot \{C - \tfrac{2}{3}\kappa\rho_0 \int x g_{11} e^{\int d\log\sqrt{-g_{11}}}\, dx\},$$

where C is an arbitrary constant, or

$$\sqrt{g_{44}} = \frac{1}{\sqrt{-g_{11}}}\left\{C - \frac{2i}{3}\kappa\rho_0 \int x g_1^{3/2}\, dx\right\}, \qquad (10)$$

where $i = \sqrt{-1}$, while g_{11} is given by (9) and $\rho = \rho_0/\sqrt{g_{44}}$. Thus, however, R, which contains ρ and $\lambda = \frac{1}{4}R = \frac{1}{4}g^{\iota\kappa}R_{\iota\kappa}$, might depend on g_{44} and directly on x, and the actual evaluation of g_{44} from (10) would be a highly complicated affair, possibly a hopeless task.

Fortunately, however, the combination $\lambda + \kappa\rho$ is a constant. In fact, we may write

$$R = \frac{1}{g_{11}}R_{11} + \frac{2}{g_{22}}R_{22} + \frac{1}{g_{44}}R_{44}$$

$$= \frac{2}{g_{11}}R_{11} - \frac{2}{x^2}R_{22} + \frac{h_1' + h_4'}{x g_{11}},$$

$$\lambda = \tfrac{1}{4}R = \frac{1}{x^2 g_{11}}\left\{1 + \frac{x}{2}(h_4' - h_1')\right\} + \frac{1}{x^2} + \frac{h_1' + h_4'}{2x g_{11}} + \tfrac{1}{3}\kappa\rho,$$

or, after some simple reductions,

$$\lambda = \kappa\rho + \frac{3}{2}\frac{g_{44}'}{x g_{11} g_{44}},$$

and, eliminating g_{44}' with the aid of (8),

$$\lambda = -\kappa\rho + \frac{3}{2x}\frac{d}{dx}\left(\frac{1}{g_{11}}\right)$$

$$= -\kappa\rho + \frac{3}{\mathrm{R}^2}\left[1 - \frac{x}{\mathrm{R}}\frac{d\mathrm{R}}{dx}\right],$$

the latter by (9). Thus

$$\frac{1}{\mathrm{R}^2} = \tfrac{1}{3}(\lambda + \kappa\rho) = \frac{1}{\mathrm{R}^2}\left[1 - \frac{x}{\mathrm{R}}\frac{d\mathrm{R}}{dx}\right],$$

from which we see two things: first, that $d\mathrm{R}/dx = 0$, *i. e.*, that R is *constant* throughout the space; and second, that *its numerical value remains free*, that is to say, is not determined by the density ρ or ρ_0 of the radiant energy. The value of R (the curvature radius of spacetime) is thus to be explored independently, by means of observations (viz., the Doppler effect of stars).

Under these circumstances (R=const.) the evaluation of the integral in formula (10) becomes a perfectly easy matter. In fact, put

$$x = \mathrm{R}\sin\sigma, \qquad \sigma = r/\mathrm{R}.$$

Then, by (8),

$$g_{11} = -\sec^2\sigma, \qquad \frac{1}{\sqrt{g_{11}}} = i\cos\sigma,$$

so that

$$\int x g_{11}^{3/2}\,dx = i\mathrm{R}^2\int \frac{\sin\sigma}{\cos^2\sigma}d\sigma = i\mathrm{R}^2\sec\sigma,$$

and (10) gives

$$\sqrt{g_{44}} = \mathrm{C}.\cos\sigma + \tfrac{2}{3}\kappa\rho_0\mathrm{R}^2;$$

or, since $g_{44}(0) = 1$,

$$\sqrt{g_{44}} = \cos\sigma + \tfrac{2}{3}\kappa\rho_0\mathrm{R}^2(1-\cos\sigma). \quad . \quad . \quad (11)$$

Again,

$$dx = \mathrm{R}\cos\sigma.d\sigma = \cos\sigma\,dr,$$

so that

$$g_{11}\,dx^2 = -dr^2,$$

and the required solution, of form (6), ultimately becomes

$$ds^2 = g_{44}c^2\,dt^2 - dl^2, \quad . \quad . \quad . \quad . \quad (12)$$

where g_{44} is as in (11) and

$$dl^2 = dr^2 + \mathrm{R}^2\sin^2\sigma(d\phi^2 + \sin^2\phi\,d\theta^2),$$

i. e., the familiar line-element of an elliptic three-space of curvature radius R. As we have just seen, this radius is, exactly as in empty space, *constant*, while its value is in no way predetermined by the intensity of illumination.

Since $\kappa = 8\pi k/c^2$, where k is the gravitation constant, we have

$$\tfrac{2}{3}\kappa\rho_0 = \frac{16\pi}{3}\cdot\frac{k\rho_0}{c^2}.$$

The second factor, being the "gravitation radius" of the radiant mass per unit volume, has the dimensions of

$$\frac{\text{length}}{\text{volume}}$$

or of a reciprocal area. Thus, if λ_0 be a length and we put

$$\frac{k\rho_0}{c^2} = \frac{1}{\lambda_0^2},$$

the last expression becomes $\frac{16\pi}{3}\frac{R^2}{\lambda_0^2}$, and

$$\sqrt{g_{44}} = \cos\sigma + \frac{16\pi}{3}\left(\frac{R}{\lambda_0}\right)^2(1-\cos\sigma). \quad . \quad (11\,a)$$

Needless to say, all the optical and kinetical properties of the spacetime thus illuminated are fully determined by the line-element (12) with this value of g_{44}.

For $\rho_0=0$ ($\lambda_0=\infty$) our solution reduces to that found by de Sitter, viz., $g_{44}=\cos^2\sigma$, as it should.

With regard to the density of distribution of the radiant energy or its mass-equivalent, it is important to notice that ρ, for which we have found the value $\rho_0/\sqrt{g_{44}}$, is the system density. The *natural measure* of density can readily be shown to be $\rho\sqrt{g_{44}}$, and is, therefore, in our case *constant*, namely, ρ_0 itself.

All the physical consequences of the solution just obtained can readily be derived, remembering that $ds=0$ gives the propagation of light, and $\delta\int ds=0$ the motion of a free particle inserted in the illuminated world.

Here, however, it will be enough to consider the Doppler effect, for a star and an observer in relative free (inertial) motion, as influenced by the illumination.

By a reasoning given in the writer's 'Theory of Relativity' (1924, chap. XVI.), and in symbols there explained, the Doppler effect is

$$D \equiv \frac{\delta\lambda}{\lambda} = \frac{ds}{ds'} - 1,$$

and if the origin of coordinates is placed in the star,

$$c\,dt - ds' = \frac{1}{\sqrt{g_{44}}}dr$$

or

$$c\,dt\left[1-\frac{1}{\sqrt{g_{44}}}\frac{dr}{c\,dt}\right] = ds'.$$

Further, since the observing station (sun) is supposed to have a free, inertial motion,

$$g_{44}c\frac{dt}{ds} = k = \text{const.}$$

Thus

$$\frac{ds}{ds'} = \frac{g_{44}/k}{1-\frac{1}{\sqrt{g_{44}}}\frac{dr}{c\,dt}},$$

and ultimately, the required formula for the Doppler effect,

$$D+1 \equiv \frac{\delta\lambda}{\lambda}+1 = \frac{g_{44}}{k\left\{1-\frac{1}{\sqrt{g_{44}}}\frac{dr}{c\,dt}\right\}}, \quad . \quad . \quad (13)$$

where dr/dt is the radial velocity of the observer relatively to the star or *vice versa*. This follows readily from the developed form of $\delta\int ds=0$, which gives

$$\frac{1}{c}\frac{dr}{dt} = \sqrt{g_{44}}\cdot\sqrt{1-\frac{g_{44}}{k^2}-\frac{p^2 g_{44}}{k^2 R^2 \sin^2\sigma}}, \quad . \quad (14)$$

where $p=R^2\sin^2\sigma\, d\theta/ds=\text{const.}$ is (besides $g_{44}c\,dt/ds=k$) a first integral of the equations of free motion. Thus the Doppler effect is given, rigorously, by (13) and (14), where r and dr/dt refer to the instant of receiving the light.

For small values of $\sigma=r/R$, that is to say, neglecting σ^4 in presence of unity, also $\sigma^2 v_r^2/c^2$, the Doppler effect reduces to

$$D=\frac{v_r}{c}=\pm\sqrt{g_{44}}\cdot\sqrt{1-\frac{g_{44}}{k^2}-\frac{p^2 g_{44}}{k^2 R^2}}, \quad . \quad . \quad (15)$$

where

$$k=\frac{g_0}{\sqrt{g_0-\beta_0^2}}, \qquad p=\frac{\beta_0 R\sin\sigma_0}{\sqrt{g_0-\beta_0^2}}. \quad . \quad . \quad (16)$$

Here β_0, σ_0 refer to the perihelion of the star's orbit, g_0 is written for $g_{44}(\sigma_0)$, and β for v/c. The positive sign in (15) corresponds to a receding, and the negative to an approaching star.

Developing the rigorous expressions (16) to the said degree of approximation, one finds, after simple reductions,

$$D^2=\frac{v_r^2}{c^2}=\left(1-\frac{r_0^2}{r^2}\right)\{\beta_0^2+N\sigma^2\}, \quad . \quad . \quad . \quad (17)$$

where

$$N=1-\frac{16\pi}{3}\frac{R^2}{\lambda_0^2}.$$

The only difference, with the Doppler-effect formula for dark spacetime, is that σ^2 in the second factor is replaced by $N\sigma^2$, *i. e.*, r^2/R^2 by r^2N/R^2. In fine, R, as evaluated from radial velocities of celestial objects of known distance, is replaced by

$$R'=\frac{R}{\sqrt{N}}=\frac{R}{\sqrt{1-\frac{16\pi}{3}\frac{R^2}{\lambda_0^2}}}. \quad . \quad . \quad . \quad (18)$$

Thus what we have determined, say from the Cepheid Variables and the O-stars *, is R′. Having found R′, we can determine R (λ_0 being assumed to be known), viz. :

$$R = \frac{R'}{\sqrt{1 + \frac{16\pi}{3}\left(\frac{R'}{\lambda_0}\right)^2}}. \quad . \quad . \quad . \quad (18\,a)$$

While R′ is of the order of 10^{11} to 10^{12} astronomical units, λ_0 is some ten or hundred thousand times greater. In fact, according to Eddington's quotation (*loc. cit.*), the "total density of radiation received by us from the stars," *i. e.* valid for interstellar regions, is $7{\cdot}7.10^{-13}$ erg/cm.^{3}, whence

$$k\rho_0 = 5{\cdot}73.10^{-41} \text{ astr. mass units per cm.}^3,$$

and

$$\lambda_0 = \frac{c}{\sqrt{k\rho_0}} = 2{\cdot}65\,.\,10^{17} \text{ astr. units.}$$

Possibly, if ultra-violet and X-rays were taken into account, ρ_0 would be several times greater, and λ_0 might drop to the order of 10^{16} or even 10^{15} a.u. At any rate, however, formula (18 *a*) can be safely replaced by

$$R = R'\left\{1 - \frac{8\pi}{3}\left(\frac{R'}{\lambda_0}\right)^2\right\}.$$

Rochester, N.Y.
February 15, 1929.

VII. *The Calculation of Absorption in X-Ray Powder-Photographs and the Scattering Power of Tungsten. By* Dr. A. Claassen †.

1. Quantitative intensity measurements obtained from powder photographs have to be corrected for absorption in the powder rod. This correction has been made in special cases by Debye and Scherrer ‡ and Greenwood § by means of graphical integration. As this is a very tedious proceeding, it is probably worth while to

* *Cf.* 'The Size of the Universe,' now in the course of printing at the Oxford University Press.

† Communicated by the Author.

‡ P. Debye and P. Scherrer, *Phys. Zeitschr.* xix. p. 474 (1918).

§ G. Greenwood, Phil. Mag. i. p. 963 (1927).

give some data * with which it is possible to calculate the absorption-coefficient in any particular case. This will be done in the following, and the results will be applied to the determination of the scattering power of tungsten.

2. Let the circle of fig. 1 represent the cross-section of the rod of crystal powder, and let its centre be at C and its radius be equal to R.

The absorption-factor A, *i. e.* the ratio between the intensity of the diffracted beam and the intensity of the beam uninfluenced by absorption, is given by

$$A = \frac{1}{\pi R^2}\int\int e^{-\mu a} dO, \quad . \quad . \quad . \quad . \quad (1)$$

in which a = length of the path of the ray through the rod;

Fig. 1.

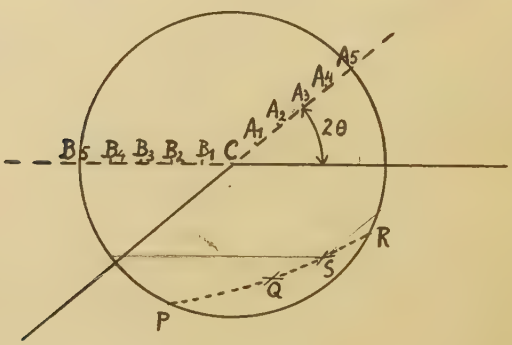

μ = absorption-coefficient of the crystal powder; dO = surface-element of C. The integration must be carried out all over C. The rod is supposed to be bathed in a parallel beam of X-rays.

It is impossible to evaluate this integral, but it can be solved graphically. To this purpose C is divided into strips of size ΔO, such that rays diffracted by points in ΔO traverse a distance between a and $a + \Delta a$ through the rod. We have then approximately

$$A = \frac{1}{\pi R^2}\Sigma e^{-\mu a}\Delta O. \quad . \quad . \quad . \quad . \quad . \quad (2)$$

This division into strips can easily be carried out geometrically. Let in fig. 1 the incident beam be parallel to BC and the reflected beam parallel to CA. Let, further, $MA_1 = A_1A_2 = \ldots$

* A. Claassen, Dissertation, Amsterdam, 1926.

$A_4A_5 = 1/5\,R$ and $MB_1 = B_1B_2 = \ldots = B_4B_5 = 1/5\,R$, and suppose that S is the point of intersection of two circles, each with radius R, erected in the points A_3 and B_1. Then the ray scattered in S has traversed a distance equal to $3/5\,R + 1/5\,R = 4/5\,R$ through the rod. In the same way the ray scattered in Q (circles erected in A_2 and B_2) has traversed also a distance 4/5 R. Thus the line PR is constructed as the locus of all points in which rays are scattered, which traverse a distance 4/5 R through the rod. Let us call these points for shortness "points 4/5 R," generally "points *a*."

By constructing the loci for several values of a, the size of the strips ΔO belonging to these values of a can be readily obtained by measuring their area with a planimeter.

When in (1) we put $x = \frac{a}{R}$, then the area Δs (expressed in the total area of C as unity) containing all points from x to $x + \Delta x$ is a function of x only. Hence (1) becomes

$$A = \Sigma e^{-\mu R x} \Delta s. \quad . \quad . \quad . \quad . \quad . \quad . \quad (3)$$

Table I. gives values of Δs for four different glancing-angles and with $\Delta x = 0{\cdot}2$.

TABLE I.

x.	$\Delta s \cdot 10^2$.				
	$\theta = 0°$.	$\theta = 22\frac{1}{2}°$.	$\theta = 45°$.	$\theta = 67\frac{1}{2}°$.	$\theta = 90°$.
0	0·04	0·78	2·64	4·94	6·22
0·2	0·32	1·41	3·36	4·86	6·47
0·4	0·84	2·04	4·05	5·80	6·43
0·6	1·90	2·72	4·65	6·04	6·18
0·8	2·68	3·58	5·38	6·50	6·38
1·0	4·58	4·61	6·10	6·44	6·18
1·2	7·10	5·95	6·88	6·40	6·18
1·4	11·10	7·95	7·52	6·64	5·98
1·6	17·84	15·35	8·46	6·30	5·44
1·8	53·60	22·20	9·60	6·40	5·44
2·0	—	33·30	10·20	6·34	5·44
2·2	—	—	11·00	6·20	5·04
2·4	—	—	9·90	5·90	5·04
2·6	—	—	8·88	5·36	4·86
2·8	—	—	1·30	4·88	4·20
3·0	—	—	—	4·44	4·12
3·2	—	—	—	3·22	3·50
3·4	—	—	—	2·70	3·22
3·6	—	—	—	0·60	2·47
3·8	—	—	—	—	1·24

Calculation of (3) from this table gives the absorption-factor for these glancing-angles. For other glancing-angles

the absorption-factors can be obtained with sufficient accuracy by graphical interpolation.

3. The calculation of A, according to (3), is not possible when μ becomes very large, because the factor $e^{-\mu Rx}$ changes so rapidly in one strip that it cannot be considered as a constant. This difficulty could be overcome by taking Δx much smaller than 0·2, but then the exact evaluation of Δs for small values of x (by which A is practically entirely determined) is very difficult. A better method is the following one :—

Let the area containing all points $< x$ be equal to $f(x)$. This $f(x)$ can be calculated from Table I. It appears that for values of x smaller than 1, $f(x)$ can be represented by the first three terms of a power-series:

$$f(x) = \alpha x + \beta x^2 + \gamma x^3 + \ldots \quad . \quad . \quad . \quad (4)$$

Now $ds = \frac{df}{dx} dx$, and substitution in (1) gives

$$A = \int e^{-\mu Rx} \frac{df}{dx} dx = \int e^{-\mu Rx} (\alpha + 2\beta x + 3\gamma x^2 + \ldots) dx. \quad (5)$$

If μ is large, we may integrate from $\mu = 0$ to $\mu = \infty$, and we get

$$A = \frac{1}{\mu R} \left\{ \alpha + \frac{2\beta}{\mu R} + \frac{6\gamma}{\mu^2 R^2} + \ldots \right\} \quad . \quad . \quad (6)$$

(R expressed in cm.)

Table II. gives the values of α, β, and γ.

Table II.

θ.	$\alpha . 10^2$.	$\beta . 10^2$.	$\gamma . 10^2$.
0°	0	3·0	5·0
$22\frac{1}{2}$°	3·1	4·0	4·0
45°	11·4	9·0	0
$67\frac{1}{2}$°	23·2	5·0	0
90°	31·1	0·7	0

For exceedingly heavy powders the terms containing β and γ in (6) may be neglected, and in this case the absorption-factor is simply proportional to α. For this limiting case of $\mu = \infty$ the absorption can also be calculated directly, which gives a check on the values of α derived from Table I.

For a plane powder surface the absorption-factor for very large μ is easily seen to be proportional to

$$\int_0^\infty \text{exp. } \mu x\left\{\frac{1}{\sin\phi}+\frac{1}{\sin(2\theta-\phi)}\right\}dx,$$

with ϕ = angle of incidence,

or
$$A_\phi^\theta \sim \frac{\sin\phi\sin(2\theta-\phi)}{\sin\phi+\sin(2\theta-\phi)}. \quad . \quad . \quad . \quad . \quad (7)$$

For a cylindrical rod of a very heavy powder it is evident that only the portion AB of the surface (see fig. 2) is effective in scattering.

Fig. 2.

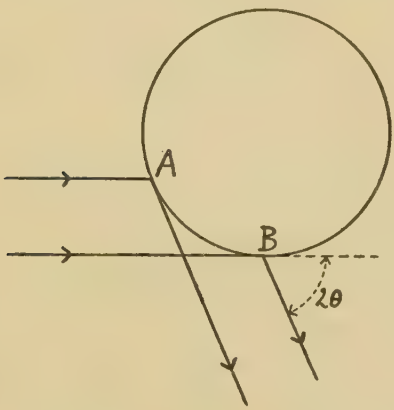

The angle of incidence for the surface elements of AB varies from $\phi = 0$ in B to $\phi = 2\theta$ in A. Thus the total absorption-factor for a glancing-angle θ becomes

$$A_\theta = \int_0^{2\theta} A_\phi^\theta \, d\phi = \int_0^{2\theta} \frac{\sin\phi\sin(2\theta-\phi)}{\sin\phi+\sin(2\theta-\phi)}\, d\phi. \quad . \quad (8)$$

This integral can be evaluated graphically or numerically. The values of α in Table II. are corrected by means of the values of A_θ calculated from (8).

All these absorption-factors have been calculated supposing a perfectly circular rod. In practice this often will not be the case, but if the rod is rotated during exposure these calculations are still valid.

4. The scattering power of tungsten.

The crystal structure of tungsten is cubic, body-centred with $a = 3{\cdot}158$ Å *. Powder photographs were made with CuK α-rays. The diameter of the rod was about 0·8 mm., while the tungsten powder was enclosed in a glass tube of $\pm 5\mu$ thickness. The rod was rotated continuously during exposure. The powder particles were smaller than $\pm 5\mu$, so that primary extinction may be assumed to be absent †.

The intensities of the reflexions were measured with a Moll self-registering photometer, applying the usual corrections. The blackening curve of the films used has been determined by van Arkel and Burgers ‡. The blackening of the strongest lines never exceeded 1.

Table III. gives the observed intensities (average from 5 films, accuracy from 5–10 per cent.).

The intensity of a line in a powder photograph is given by

$$I \sim \frac{A\nu F^2(1+\cos^2 2\theta)}{\sin^2\theta\cos\theta}\, e^{-2M}\ \S,$$

Table III.

Indices.	Sin θ.	$\frac{\nu(1+\cos^2 2\theta)}{\sin^2\theta\cos\theta}$.	A.	e^{-2M}.	$I_{obs.}$	$F_{rel.}$	$F_{abs.}$
110	0·346	170·4	2·5	1·00	108	51	61
200	0·489	36·2	5·0	0·95	37	46	55
211	0·599	91·0	7·8	0·93	118	42	50
220	0·690	34·9	10·9	0·91	57	41	48
310	0·772	65·8	14·3	0·89	125	39	46
222	0·845	25·0	18·3	0·86	50	35	42
321	0·912	202·1	22·2	0·85	420	33	40
400	0·975	50·9	28·3	0·82	136	31	37

in which A = absorption-factor, ν = plane-number factor, F = structure factor (in this case the scattering power of tungsten), and e^{-2M} the Debye ‖ temperature factor as

* A. E. van Arkel, *Zeitschr. für Krystall.* lxvii. p. 235 (1928).

† See J. Brentano, Phil. Mag. iv. p. 620 (1927).

‡ A. E. van Arkel and W. G. Burgers, *Zeitschr. für Phys.* xlviii. p. 690 (1928).

§ P. Debye and P. Scherrer, *Phys. Zeitschr.* xix. p. 474 (1918). G. C. Darwin, Phil. Mag. xliii. p. 800 (1922). J. M. Bijvoet, *Rec. Trav. Chim.* xlii. p. 886 (1924).

‖ P. Debye, *Ann. der Phys.* xliii. p. 49 (1914).

modified by Waller*. In this expression M is given by

$$M = \frac{6h^2}{\mu k \Theta}\left(\frac{\phi(x)}{x} + \frac{1}{4}\right)\frac{\sin^2\theta}{\lambda^2},$$

with μ the mass of the tungsten atom, h Planck's constant, k the gas constant per molecule, Θ the characteristic temperature of the crystal which occurs in the theory of specific heats; $x = \Theta/T$, where T is the absolute temperature and $\phi(x)$ is a certain function of x, which Debye evaluates. Zero-point energy is assumed according to Waller and James†.

The absorption-coefficient of tungsten for CuK α-rays amounts to about 3500, so that A in Table III. has been taken equal to α in Table I.

To evaluate M the approximate value $\Theta = 280°$ was calculated from Lindemann's‡ formula, giving $M = 0{,}10 \sin^2\theta$.

In the 7th column of Table III. the values of F calculated from (8) are given. As only relative intensities have been measured, these values are only relative ones. To arrive at the absolute F-values we have extrapolated the relative F-values to $\sin\theta = 0$, and assigned to the number so obtained the absolute value 74, *i. e.* the number of electrons in a tungsten atom. This extrapolation is, of course, rather uncertain, but in any case it will give an approximate idea of the decline of scattering power with increasing glancing-angle for a heavy atom. The F-curve obtained in this way is reproduced in fig. 3. Table IV. gives F-values for various values of $\frac{\sin\theta}{\lambda}$.

Table IV.

$\frac{\sin\theta}{\lambda}$	0	0·1	0·2	0·3	0·4	0·5	0·6
F_{exp}	74	70	63	57	51	45	39
F_{Thomas}	74	68	61	53	47	42	37

A theoretical F-curve can be calculated according to Bragg and West§ from an atomic model calculated by Thomas‖. In this model it is assumed that the effective

* I. Waller, Dissertation, Upsala, 1925; *Ann. der. Phys.* lxxxiii. p. 154 (1927).

† I. Waller and R. W. James, Proc. Roy. Soc. cxvii. p. 214 (1927).

‡ See, *e.g.*, M. Born, 'Atomtheorie des festen Zustandes,' p. 630, or 'Handbuch der Experimentalphysik,' viii. p. 250.

§ W. L. Bragg and J. West, *Zeitschr. für Krystall.* lxix. p. 118 (1928).

‖ L. Thomas, Proc. Cambridge Soc. xxiii. p. 542 (1927).

field in an atom is given by a potential V depending only on the distance r from the nucleus; that the electrons are distributed uniformly in the six-dimensional phase-space for the motion of an electron at the rate of two for each h^3 of six-dimensional volume; and that this potential V is itself determined by the nuclear charge and the distribution of electrons. With these assumptions Thomas solves numerically a differential equation in V which gives the density of electrons at a distance r from the nucleus as a function of the atomic number. Thomas calculated the electron distribution for

Fig. 3.

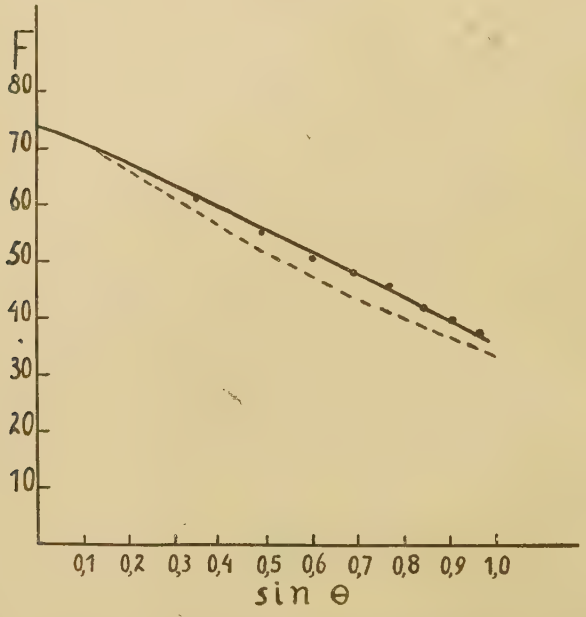

cæsium. From the form of Thomas's equation it follows that the electron distribution for any other atom can be simply calculated if it is known for a given atom (*in casu* cæsium). These theoretical F-curves should be quite accurate, especially for atoms of high atomic number; even in the case of light elements the difference with the experimental results is not great *.

The dotted line in fig. 3 gives the F-curve for tungsten calculated in this way from Thomas's figures. Table IV. compares the numerical values.

* W. L. Bragg and J. West, *Zeitschr. für Krystall.* lxix. p. 118 (1928).

It is seen that the agreement is rather satisfactory, considering the rough way in which the experimental F-values have been obtained.

On the other hand, this agreement proves to a certain extent the validity of our calculated absorption-coefficients.

Summary.

This paper describes the calculation of absorption in X-ray powder photographs. For heavy powders a simple formula is deduced. The results are applied to the reflexion intensities of tungsten. The experimental scattering power of tungsten agrees approximately with the F-curve calculated from the Thomas model of the atom.

I wish to thank Dr. W. G. Burgers for having the powder photographs made.

Natuurkundig Laboratorium der
N. V. Philips's Gloeilampenfabrieken,
Eindhoven, Aug. 1929.

VIII. *The Crystal Structures of the Elements of the B Sub-Groups and their Connexion with the Periodic Table and Atomic Structures.* *By* WILLIAM HUME-ROTHERY, *M.A., Ph.D.**

1. *Introductory.*

THE general factors affecting crystal structure are at present comparatively little understood except for simple ionized structures such as those of the halide salts, and correspondingly simple covalent structures such as that of the diamond. In a series of most interesting papers Goldschmidt† has recently examined the interatomic distances in a large number of crystals, and has used these in order to deduce a series of "atomic radii" which are characteristic of the different elements under similar conditions, but which may vary with the degree of "coordination," *i.e.*, the number of atoms which surround

* Communicated by Prof. W. L. Bragg, F.R.S.
† Goldschmidt, *Z. Phys. Chem.* cxxxiii. p. 397 (1928).

the particular atom considered. Goldschmidt has extended this work to metallic crystals, and has deduced a series of "atomic radii" characteristic of those structures in which each atom is surrounded by 12 others, namely, the hexagonal close-packed, and face-centred cubic structures. In the case of metals which do not crystallize in either of these structures, Goldschmidt deduces the appropriate atomic radius from the structures of alloys in which the coordination number is 12. In this way he shows that when the coordination number is less than 12, the atomic radius is diminished, the contractions being approximately as follows :—

[12]→[8] 3 per cent. contraction,

[12]→[6] 4 per cent. contraction,

[12]→[4] 12 per cent. contraction.

Goldschmidt then points out that these effects are of the same order as those in ionic compounds, and concludes that the binding forces in metals may well be of the same nature as those in salts.

The advance made here is very considerable, but it is open to the criticism that, in deducing the atomic radii for those elements which do not crystallize with coordination number 12, rather indiscriminate use is made of intermediate alloy phases, both solid solutions and intermetallic compounds being employed. Thus the radius of the antimony atom is deduced from the interatomic distances in the compound Ag_3Sb, which in many of its properties is different from a pure metal, and it appears rather arbitrary to use different phases in this way unless it is quite certain that the binding forces are always of the same kind.

In the present paper it is proposed to attack the problem from another angle, and to deal with the structures of the pure elements of the B sub-groups. It is hoped to show that these structures—at first apparently so different and confusing—are in reality the outcome of one general process, which can be readily understood from the Periodic Table of the Elements as interpreted by modern theories of atomic structure. For this purpose it is proposed first to describe the relations connecting the crystal structures, and later to discuss their theoretical interpretation.

2. *General Principles.*

The elements of the B sub-groups are as follows :—

Group.	I.	II.	III.	IV.	V.	VI.	VII.
1st Long Period	Cu	Zn	Ga	Ge	As	Se	Br
2nd „ „	Ag	Cd	In	Sn	Sb	Te	I
3rd „ „	Au	Hg	Tl	Pb	Bi	—	—

The crystal structures of these elements may then be regarded as the outcome of the two following processes :—

(*a*) On the one hand there is a tendency for an element to crystallize so that each atom is surrounded by (8-N) neighbours, where N is the number of the group to which the element belongs. This tendency is always found in Group II, although the structure of mercury (rhombohedral) is different from that of zinc and cadmium (close-packed prolate spheroids). In the other groups this tendency decreases with increasing atomic weights. In the first long period it is found as far back as Group III. (gallium) ; in the second long period it stops at Group IV. (grey tin), and even here there is a second allotropic form ; whilst in the third long period it stops at bismuth in Group V.

As will be shown later, there is reason to suppose that, where this kind of structure is found in Groups II. and III., the process is not quite the same as in Groups IV. to VII., but, considered empirically, the rule holds.

(*b*) Opposing this there is a tendency to form close-packed structures, corresponding actually or very nearly to those given by close-packed spheres. This tendency decreases with the number of the group to which the element belongs, and increases with increasing atomic weight. It is always found in Group I. In Group III. it is found in the second and third long periods, but not in the first, whilst in Group IV., it is found only in the third long period.

It is now proposed to show how these rules can be applied to the actual structures of the elements.

3.

(a) *The First Long Period.*

The crystal structure of bromine does not yet seem to have been determined, so it is necessary to begin with

selenium in Group VI. In this case the above rules require each atom to have $8-6=2$ neighbours. The actual structure is hexagonal with space-group D_3^4 or D_3^6 (enantiomorphous), the atoms being in spiral chains, in which each atom has two close neighbours at a distance of 2·35 Å. the remaining interatomic distances being considerably greater.

Turning now to arsenic in Group V., the above rules require each atom to have $8-5=3$ neighbours. Actually arsenic crystallizes in the rhombohedral hexagonal type, space-group D_{3d}^5, in which each atom has three close neighbours at a distance of 2·51 Å., the remaining distances being considerably greater. Germanium in Group IV. crystallizes in the tetrahedral diamond type of structure, in which each atom has four neighbours, in agreement with the above rules, the interatomic distance being 2·44 Å., which lies between those of selenium and arsenic.

In the case of gallium (Group III.), if the above rules be correct, the structure should be such that each atom is surrounded by $8-3=5$ neighbours, which at first sight appears improbable. In actual fact, however, the structure deduced by Jaegar, Terpstra, and Westenbrink* is precisely that which is required. Gallium crystallizes with di-tetragonal bi-pyramidal symmetry, and the structure deduced by X-ray measurements has space-group D_{4h}^{16}, and is a curious double-layer structure in which each atom is in close contact with one other in its own layer, and with four others in the next layer, the interatomic distances being 2·56 Å. If the atoms are assumed to be spherical (which is, of course, a pure assumption) the double layers are not in contact with one another, but would be so if the distance between the double layers were reduced by 0·14 Å. If this structure be correct, it is of the greatest interest, since the tendency for the atom to surround itself by (8-N) neighbours is still clear, whilst it can also be seen from the figure that the structure is beginning to resemble a much distorted close-packed arrangement. In a private communication, Professor Bragg has kindly told the present author that, while the structure deduced by Jaegar, Terpstra, and Westenbrink may well be correct, the evidence is not as completely conclusive as in the case

* Jaegar, Terpstra, and Westenbrink, *Proc. Akad. Amsterdam*, xxix. p. 1193 (1926).

of the structures in Groups IV. to VI. It will be noted that the closest distance of approach in gallium is the same as that in copper (2·56 Å). This is in contrast to the second and third long periods, in which the interatomic distances in the Group III. metals indium and thallium are considerably greater than those in the corresponding Group I. elements silver and gold (see p. 75).

Turning now to zinc, the structure is one of close-packed prolate spheroids, each atom being surrounded by six others in its own layer at a distance of 2·67 Å, and by six

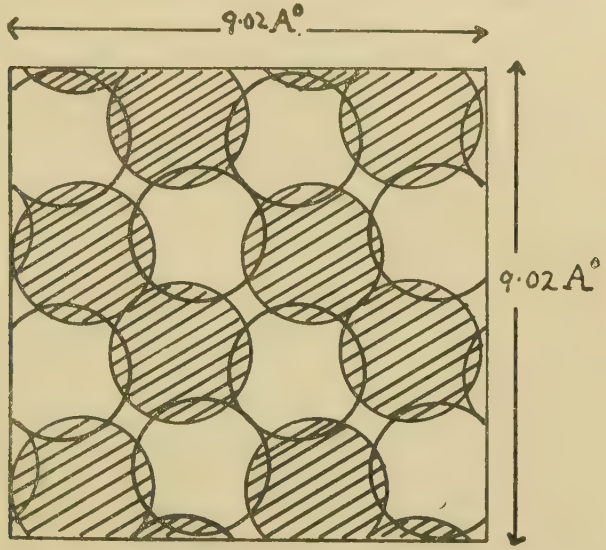

The figure shows one of the double layers in the structure deduced for gallium by Jaeger, Terpstra, and Westenbrink. The atoms in one layer are shaded, and those in the next are left white. Four atoms in one layer form a trapezium, in the centre of which fits the atom of the adjacent layer, whilst in its own layer each atom is in close contact with one other at a distance equal to that which separates it from the four in the adjacent layer. The next double layer has an identical structure except that it is turned through 90°. The interatomic distances between the double layers are greater than the closest distances of approach within the double layer, so that, if spherical atoms be assumed, the double layers are separated by gaps.

others (three in the layer above, and three in that below) at a distance of 2·92 Å. In sections 4–5 we shall discuss the question as to how far the presence of six neighbours

in zinc and of five in gallium is a real continuation of the (8-N) process which is so clear in the later groups. Finally, in copper the structure is one of simple close-packed spheres.

(b) *The Second Long Period.*

In this period the crystal structure of iodine has been determined, and the whole process from iodine to silver can be examined.

In Group VII., iodine, the structure deduced by Harris, Mack, and Blake * shows the unit cell to possess orthorhombic bi-pyramidal symmetry, space-group V_8^{16} case *f*, the atoms being arranged in pairs, which the above authors took to be I_2 molecules, the closest distance of approach being 2·70 Å. Each atom, therefore, has one neighbour in accordance with the general principle.

In Groups VI. and V. tellurium and antimony crystallize with the same structures as selenium and arsenic respectively, the atoms having two neighbours in Group VI. and three in Group V. The closest distances of approach are 2·87Å. for both tellurium and antimony.

In Group IV. grey tin has the tetrahedral structure, with four neighbours at a distance of 2·80 Å. In this period, however, the tendency to form the pure (8-N) type of structure has diminished, and the tetrahedral form is accompanied by another modification, white tin, in which each atom is still surrounded by four others, but the distance is considerably greater, 3·07 Å., as compared with 2·80 Å. in the grey modification. The tetrahedral arrangement is also much distorted, and besides the four near neighbours there are two others at a slightly greater distance, 3·16 Å.

The next metal, indium, possesses a very curious and interesting structure which is face-centred tetragonal, but the axial ratio is only 1·06, so that it is only a very slightly distorted form of the close-packed face-centred cubic arrangement. Each neighbour has four neighbours at a distance of 3·24 Å., and eight others at 3·33 Å., so that the structure is very nearly that of close-packed spheres, the distances being very much greater than in grey tin.

* Harris, Mack and Blake, J. Amer. Chem. Soc. l. p. 1583 (1928).

† Actually it is a possible close packing of spheroids with axes in the ratio 1·06 : 1.

In this period, therefore, the tendency to form an (8-N) structure has disappeared in Group III., and is replaced by the formation of a close-packed structure.

Cadmium and silver crystallize with the same structures as zinc and copper, and we shall discuss later the meaning of the six grouping in cadmium. The interatomic distance in silver is 2·88 Å., and is thus much less than in indium.

(c) *The Third Long Period.*

Here the tendency to form the pure (8-N) kind of structure has diminished so greatly that it is found only for bismuth, which has the same structure as arsenic and antimony, each atom being surrounded by three others at a distance of 3·10 Å. In this period the tendency to form close-packed structures is much greater, and thallium (Group III.) has the structure corresponding to the hexagonal close packing of spheres, and lead (Group IV) the face-centred cubic close packing of spheres, the interatomic distances being 3·40 Å. (Tl) and 3·48 Å (Pb), both of which are considerably greater than the closest distance of approach in bismuth (3·10 Å).

Mercury, like the other Group II. elements, crystallizes so that each atom is surrounded by $8-3=6$ others, but structure is here simple rhombohedral instead of that of the close-packed prolate spheroids characteristic of zinc and cadmium. Gold resembles copper and silver, and has the face-centred cubic close-packed structure, the closest distance of approach being 2·88 Å, which is much less than that in thallium.

From the above description it can be seen how all these apparently complex and different structures can be regarded as the outcome of two simple opposing tendencies. There is first the tendency to form structures in which each atom is surrounded by (8-N) others, and this diminishes as we pass from the first to the third long period. There is, secondly, the tendency to form close-packed structures, which diminishes as we proceed from Group I. to Group VIII., and increases as we pass from the first to the third long period.

In the remaining sections it is proposed to discuss the theoretical interpretations of these general principles, and later to compare the conclusions which are drawn with those of J. D. Bernal and other previous investigators.

4. *The Covalent, Molecular and Metallic Linkages.*

For Groups IV. to VII. the most obvious explanation of the (8-N) rule described above is that, just as in the covalent compounds of chemistry an atom of Group N immediately preceding an inert gas completes its octet of electrons by sharing one electron with each of (8-N) other atoms, so in the crystal of the elements the octet is completed by the atom taking (8-N) neighbours and sharing one electron with each. In this way the presence of one, two, three, and four neighbours to each atom in the crystals of the elements of Groups VII., VI., V., and IV. respectively is readily accounted for. Reference to the literature shows that in the original pioneer work of A. J. Bradley * this explanation was already realized, for this author states† : "... in the normal crystalline forms of ... germanium, grey tin, arsenic, antimony, bismuth, selenium, and tellurium, electron sharing takes place until the outer shell of each atom has its full quota of electrons. In this way each atom of these elements is in close contact with as many neighbours as it has negative valencies."

In Group IV. this conception accounts for the linkages throughout the crystal, since the tetrahedral arrangement throughout space enables the whole crystal to be bound together. But in the remaining groups this is not the case, and, while it seems clear that each atom is completing its octet by sharing with one, two, or three others, some additional forces must be postulated in order to account for the complete structure, and it seems probable that these are of a *molecular* nature. This suggestion is not in any way an *ad hoc* assumption, for it seems to be perfectly clear that in the case of iodine the pairs of atoms are I_2 molecules, and since it is a fact that these are held together in the solid crystal, it does not seem unreasonable to assume that similar forces are present in the case of Group VI. where there exist chains of atoms each with two neighbours, and Group V., where there are layers of atoms which give each atom three neighbours. The alternative view of J. D. Bernal, that the additional forces are metallic in nature, will be discussed later.

It is when we come to deal with the retention of the (8-N) rule in Groups III. and II. that difficulty arises, for

* A. J. Bradley, Phil. Mag. xlviii. p. 477 (1924).
† *Ibid.* p. 496.

here it seems clear that the presence of simple covalent linkages will not account for the fact that each atom has five or six neighbours. Since each gallium atom has only three valency electrons, it cannot share one electron with each of five others, because there are not enough electrons available. The position is rather like that met with in connexion with the hydrides of the elements of the first short period, where we can readily account for OH_2, NH_3, and CH_4, but where the hydride of boron, B_2H_6, presents difficulty. It is suggested that we have here the real underlying cause of the formation of the *metallic linkage* in the crystals of the solid elements. When there are not sufficient valency electrons per atom to enable the octet to be completed by each atom sharing one electron with each of its neighbours, the need arises for a new kind of bond, in which an electron can serve for more than two atoms, and so the metallic linkage comes into being, and is apparently favoured by three structures, the body-centred cubic, the face-centred cubic, and the hexagonal close-packed structures.

It is here that the structure of gallium is so particularly interesting, if the work of Jaegar, Terpstra, and Westenbrink be correct. For, in spite of the fact that the full number of electrons necessary to form an octet by simple covalent linkages is no longer available, the tendency to form the (8-N) type of structure is still found, and at the same time the tendency to form a distorted close-packed structure is so very apparent. It seems, however, to be almost certain that most of the linkages are covalent, because (1) the metal shows marked diamagnetism, contraction and fall in resistance on melting, etc., just as with bismuth and antimony, and (2) the closest distance of approach in gallium does not show the marked increase which is found when we pass from the covalent linkage in grey tin (2·80 Å.) and bismuth (3·10 Å.) to the preceding close-packed metallic structures in indium (3·24 Å.) and lead (3·48 Å.). Further, as we have already indicated, the closest distances of approach in indium and thallium are much greater than in the preceding univalent metals silver and gold, whereas in the case of gallium and copper the distances are almost the same (see p. 69). But whether the remaining linkages in gallium are metallic, as suggested by J. D. Bernal*, or molecular appears less certain. As

* J. D. Bernal, Trans. Faraday, Soc. (1929).

we have already indicated (p. 68), the structure of gallium is not yet absolutely certain, so that discussion of this point is not carried further.

The structures of the Group II. elements will be considered separately in the next section. In the case of the Group I. B-elements, we find typical close packed-structures which clearly correspond to the purely metallic linkages. It is considered unwise to attempt to give anything in the way of a mechanical picture of this kind of binding. in view of the fact that the whole tendency of modern atomic theory is to avoid the precise mechanical pictures of the older dynamics. The essential points are that the metallic linkage comes into being when the number of valency electrons in the atom is insufficient to allow the (8-N) type of structure to be produced by simple co-valency electron sharing, and that the characteristic of the linkage is that one electron can serve for more than two atoms. Alternative views are that of the electron lattice* of Lindemann, in which the electrons are conceived of as vibrating about fixed centres, so that they may be said to be shared by the surrounding atoms. As shown by the present author, this conception is in many ways attractive†, but it is sometimes considered too static in nature, and the new theories of Bloch ‡, in which the valency electrons are regarded as moving in a three-dimensional periodic field characteristic of the crystal as a whole, may perhaps be considered as an attempt to express our general idea in more precise terms.

From this point of view, therefore, the metallic bond is to be looked upon as of a homopolar nature, in which one electron may be associated with many atoms. In support of this conclusion we may note that the interatomic distances in copper, silver, and gold are of the same order as those of the covalent linkages in the same long period, the actual values being as follows :—

Copper ...	2·56 Å.	Covalent linkages	Ga–Se ...	2·56Å.–2·35 Å.
Silver ...	2·88 Å.	„	„ Sn–I	2·87 Å–2·70 Å.
Gold	2·88 Å.	„	„ Bi	3·10 Å.

* It should be noted that an electron lattice may be considered either as an ionic structure of electrons and ions, or as a homopolar structure in which the electrons on the lattice are shared by the surrounding atoms.

† Hume-Rothery, Phil. Mag. iv. p. 1017 (1927).

‡ Bloch, *Z. Physik*, lii. p. 555 (1928–29).

It is not to be expected that these distances will be exactly equal, because an allowance must presumably be made for the degree of coordination, and also for the effect of atomic number upon the dimensions of the electronic orbits. It is, however, noteworthy that in the case of gallium, where the covalent bonds are accompanied by what is nearly a close-packed structure, the closest distance of approach is the same as in the case of the purely metallic copper in Group I.

It remains now to account for the sudden expansion of the interatomic distances in indium, thallium, and lead, to which we have assigned metallic structures, and it is just here that the theory of atomic structure gives the necessary support. According to the generally accepted theory, the building up of a group of eight electrons takes place in steps of 2, 2, and 4 electrons respectively. The outer electron groupings in atoms *in the free state* of the Group III. and Group IV. metals are thus (18) (2) (1) and (18) (2) (2) respectively, and the whole of the facts of chemistry indicate that the relative stability of the underlying (18) (2) group increases as we go down the periods. Thus in aluminium only trivalent salts are stable, whilst with thallium the univalent $(18)(2)^{+}$ salts are stable, and the trivalent $(18)^{+++}$ salts relatively unstable. It is, therefore, quite to be expected that in indium, thallium, lead and, possibly, also in white tin we have in the metal crystal only one free electron per atom in Group III. and two in Group IV., in which case the remaining atomic cores which are responsible for the repulsive forces will be larger than in the case of silver and gold, where the cores contain only the group of (18). But, on the other hand, it is just this group of (18) which remains in the covalent structures, so that the difference is at once accounted for. The fact that in indium the structure is not quite that of close-packed spheres is not in contradiction to this point of view, since there is no reason to suppose that a group of (18) (2) electrons will retain spherical symmetry in the crystal structure, even though it may do so in the free state.

5. *The Structure of the Group II. Elements.*

We have already indicated that, although the Group II. elements obey the (8-N) rule, there is reason for thinking that the process is here different from that met with in

Groups IV. to VII. Bernal has suggested that in the B-Group elements we have purely metallic structures in Group I., purely homopolar structures in germanium and grey tin, and structures containing both metallic and homopolar bonds in most of the remaining elements. He also concludes that zinc and cadmium are not to be looked upon as possessing merely a distorted form of close-packed structure. At first it might be suggested that these are larger lattices in which the atoms in each layer are bound together by homopolar bonds, but if this be so, it is clear that the "homopolar bonds" must be different from the covalent bonds which we have suggested for Groups IV, to VII.*, since there are not enough electrons present to form these. The alternative view which is suggested here is that both zinc and cadmium are true metals in which the atoms are held together solely by metallic linkages, but that only one electron per atom is free to form the metallic bond. The fact that we have close-packed spheroids instead of spheres is, then, the result of there being one electron above the (18) group attached to the positive ions, which are thus readily polarizable in the structure, and so no longer correspond to spheres. In support of this rather unexpected conclusion the following points may be noted :—

(1) In the A groups, when we pass from the univalent alkalis to the divalent alkaline earths, the melting-points rise, and the interatomic distances diminish. In the B groups the reverse is the case.

(2) The electrode potentials change in opposite directions in the A and B groups when passing from Group I. to Group II.

(3) The photoelectric threshold frequencies of the alkaline earths are much higher than those of the alkalis, whilst in the B sub-groups the threshold frequencies are much the same for Groups I. and II.

These, and other abnormalities, are explained if zinc and cadmium are only singly ionized in the metallic state, the ions being larger than those of the preceding univalent metal, and in the crystal structure much less symmetrical.

* In Group IV. the "covalent linkages" of the present paper are identical with the "homopolar bonds" of Bernal. In the other groups Bernal's "homopolar bonds" are less clear.

The structure of mercury is quite abnormal, but the interatomic distances (2·99 Å.) are greater than those of gold (2·88 Å.), and here again it is suggested that the solid metal is univalent, giving one free electron per atom to form the metallic linkage.

6. *The Question of Electrical Conductivity.*

The most obvious objection to the above suggestions is that if the elements in Groups IV. to VII., to which we have assigned covalent and molecular structures, are really of this nature, they should be non-conductors, since all the valency electrons are required for the covalent bonds. In this connexion it is interesting to note that for germanium and grey tin, which possess the tetrahedral structure, it has already been concluded by Kapitza*, from work on the properties of metals in strong magnetic fields, that these metals (and also silicon) are really not normal metallic conductors at all, and this point of view was accepted by Bernal. It has, in fact, been suggested by Kapitza that if these metals could be obtained quite free from impurities they would, at any rate at low temperatures, be non-conductors, and that the actual conductivity observed is due to traces of impurities upsetting the regularity of the lattice, and so liberating some electrons, a process which is assisted by rise of temperature which increases the atomic vibrations. These metals have, in fact, very abnormal properties as regards the electrical conductivity. Thus silicon has a negative temperature coefficient of resistance up to a high temperature, at which polymorphic changes occur. Germanium shows the phenomenon of a minimum resistance at $-116°$ C., and Bidwell† has concluded that the same may be true for the elements of Groups V. and VI., and also that silicon would attain a minimum resistance at a high temperature if it were not for the polymorphic change. The phenomenon of a minimum resistance is, of course, quite in agreement with the above view, since on raising the temperature from the absolute zero we may expect the resistance first to diminish owing to the gradual liberation of electrons; but later the increasing amplitude of the atomic vibrations will interfere with the motion of the electrons in the

* Kapitza, Proc. Roy. Soc. cxxiii. p. 292 (1929).
† Bidwell, Physical Review, xix. p. 447 (1922).

ordinary way. From this point of view, since the covalent linkage becomes less stable as we pass from the first to the third long period, we should expect the minimum resistance to occur at a lower temperature, which is in agreement with the fact. The metals silicon, germanium, and grey tin may be said to form the critical test in this connexion. If once it be admitted that these are purely covalent (Bernal " purely homopolar "), in spite of their conductivity and other metallic properties, then the present theory cannot be attacked on this ground, whilst it is, of course, well known that other electrical properties, such as the Hall Effect, thermoelectric power, etc., are very abnormal for these elements, and for those of Groups V. and VI.

Once, however, we get the purely metallic bond, conductivity is obviously possible, since the electrons are no longer required to be bound to two particular atoms. It may be noted that supraconductivity is shown by none of the metals to which we have assigned covalent and molecular structures : it is white, and not grey, tin which is supraconducting.

7. *The Relation of the Present Work to that of Bernal.*

We have already discussed the suggestions of Bernal with reference to the structure of the Group II. elements, and we may now refer to other points in the most stimulating paper by this author. The chief point made by Bernal in connexion with the structure of the B-group elements was that we have here to deal with both homopolar and metallic bonds in the same crystal. In the structure of selenium, for example, the atoms are regarded as bound by homopolar bonds into the zigzag chains (each having two neighbours), and the chains themselves are regarded as held together by metallic bonds. A similar suggestion was made for Group V. It is suggested that the present view of covalent and molecular linkages is more probably correct for the following reasons :—

(1) If the " homopolar " bonds are the covalent bonds which have been suggested here, it seems impossible to provide the free electrons necessary to form the metallic linkage. Each selenium atom has completed its octet by

sharing with two others, and if it is to give further free electrons to provide a metallic linkage, the octet will be broken up. This might be overcome by assuming that the metallic linkage does not involve the conductivity electrons at all, but is the same as what has been called the "molecular linkage" in the present paper; but the properties as regards plasticity, etc., are not the same, and the evidence that the conductivity electrons are concerned in the metallic bond appears considerable.

(2) Alternatively, if it be assumed that the "homopolar bond" is not the covalent bond described above, we are at a loss to account for the (8-N) rule, which appears such a characteristic feature.

It is suggested, therefore, that the present view, which regards the metallic bond as never appearing in Groups V. and VI., and only in the second and third long periods in Group IV., is more probably correct, as well as the conclusions that zinc, cadmium, mercury, and indium are true metals, but with distorted ions. Apart from these points, Bernal's arguments concerning diamagnetism, etc., are fully accepted as indicating the presence of covalent bonds, and no claim is made that the suggestion of covalent bonds in these metals is a novel one, and, as we have already indicated, this suggestion was, in part at any rate, anticipated in the original work of Bradley.

8. *Conclusion.*

It is hoped that the above paper will assist in giving a general indication of the relations between the crystal structures of the B-group Elements, and the Periodic Table and Atomic structures. It must be emphasized, however, that we have dealt here solely with the pure elements, and that the principles described need not necessarily always apply in alloys. When, for example, we have suggested that zinc, cadmium, and indium are univalent in the pure metal, there is no suggestion that this necessarily applies in alloys. It is hoped to deal later with the regularities underlying the formation of solid solutions and intermetallic compounds, and particularly with the question as to the conditions under which an atom preserves a "constant radius."

9. *Acknowledgments.*

The author must express his thanks to Professor F. Soddy, F.R.S., for giving laboratory accommodation which enables him to work in Oxford, and to Professor W. L. Bragg, F.R.S., Dr. A. J. Bradley, and Dr. T. V. Barker for help and criticism. He must also thank the Armourers' and Brasiers' Company for election to a Research Fellowship.

The Old Chemistry Department,
The Museum, Oxford.

IX. *On the Distribution of Space Charge between a Plane Hot Cathode and a Parallel Anode.* *By* Hrishikesh Rakshit, *M.Sc., Khaira Research Scholar in Physics* *.

Introduction.

When a metal is heated, electrons are emitted from it according to Richardson's law. The emitted electrons are mostly concentrated near the surface of the hot metal, and thus an atmosphere of electrons is set up near it. The negative space charge thus created repels the electrons subsequently emitted and presses the slowly moving ones into the hot metal. After some time an equilibrium condition is reached when the number of electrons emitted in unit time is the same as the number pressed back into the hot metal by the space charge. In such an equilibrium condition the distribution of potential near the hot surface when it is plane and infinitely extended has been worked out by Richardson † and Laue ‡. Similar calculations have been made by Epstein §, Fry ‖, and Adams ¶ for the case when the potential distribution is altered, due to the presence of a parallel positively charged plate of infinite extent near the hot surface. The corresponding problem of determining the distribution of electron density near a heated surface has been solved only in the case of a plate of infinite extent

* Communicated by Prof. S. K. Mitra, D.Sc.
† Phil. Trans. A, cci. p. 516 (1903).
‡ *Jahrb. d. Radioakt. u. Elektronik*, xv. p. 205 (1918).
§ *Ber. d. Deut. Phys. Ges.* xxi. p. 85 (1919).
‖ Phys. Rev., April 1921.
¶ Not published; *cf.* Langmuir, Phys. Rev., April 1923.

without any external field*. The case of altered distribution of electron density when a current flows between the cathode and the anode, though often met with in practice, has not received adequate attention from workers in this field. It is proposed in this paper to determine this altered distribution of electron density in the simple case of two parallel infinite plates, and to give quantitative results for a few typical cases.

Mathematical Discussion.

In any case of thermionic emission, when the current between the cathode and anode is less than the saturation current, there is a region of negative potential gradient near the cathode. The general nature of potential distribution is

Fig. 1

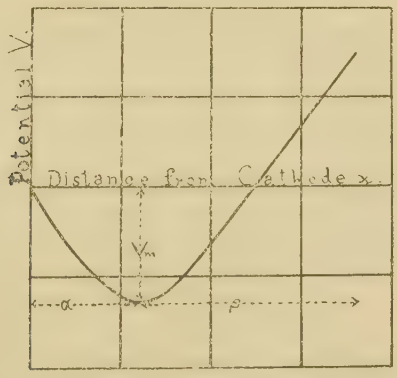

shown in fig. 1. The potential becomes more and more negative as the distance from the cathode increases; it attains a certain minimum value V_m and then increases, being ultimately positive at greater distances from the cathode. With Fry let us denote the region between the cathode and the surface of minimum potential as the region α, and the rest of the region to the anode as region β.

Let dN be the number of electrons emitted per unit time per unit area, having emission velocities normal to the cathode between the limits v_0 and $v_0 + dv_0$. Then, in accordance with Maxwell's law,

$$dN = N \cdot \frac{mv_0}{kT} \cdot \epsilon^{-\frac{mv_0^2}{2kT}} \cdot dv_0,$$

* Langmuir, Phys. Rev., April 1923.

where N is the total number of electrons emitted per unit time per unit area from the cathode at temperature T° K. The emitted electrons have velocities ranging from zero to infinity, and it is therefore evident that the slowly moving ones will go only a certain distance from the cathode and then be stopped and turned back to the cathode by the retarding field in region α. Thus in this region there are two groups of electrons, those going away from the cathode and those returning back to the cathode; but in region β the electrons are only moving away from the cathode. Let us consider a point in region α whose distance from the cathode is x. If V is the potential of this point (with respect to the cathode), the electrons that are emitted with velocities, normal to the cathode, lower than $\sqrt{\frac{2Ve}{m}}$ do not reach x; those with emission velocities lying between $\sqrt{\frac{2Ve}{m}}$ and $\sqrt{\frac{2V_m e}{m}}$ reach and pass x, but are stopped before reaching the surface of minimum potential and turned back by the retarding field; the electrons with emission velocities higher than $\sqrt{\frac{2V_m e}{m}}$ pass x, but do not return after passing, V_m being the minimum potential between cathode and anode. If, now, v is the actual velocity of the electrons dN, the contribution of these to the space-charge density ρ is given by

$$d\rho = \frac{dN}{v} \cdot e.$$

This takes into account only the absolute value of v, and not its direction. Thus each of the two equally dense streams of electrons in region α, with emission velocities lying between $\sqrt{\frac{2Ve}{m}}$ and $\sqrt{\frac{2V_m e}{m}}$, but moving in opposite directions, contributes to the space charge ρ_α, which can thus be expressed in the form

$$\rho_\alpha = 2e\int_{\sqrt{\frac{2Ve}{m}}}^{\sqrt{\frac{2V_m e}{m}}} \frac{N}{v} \cdot \frac{mv_0}{kT} \cdot \epsilon^{-\frac{mv_0^2}{2kT}} \cdot dv_0$$

$$+ e\int_{\sqrt{\frac{2V_m e}{m}}}^{\infty} \frac{N}{v} \cdot \frac{mv_0}{kT} \cdot \epsilon^{-\frac{mv_0^2}{2kT}} \cdot dv_0, \quad . \quad . \quad (1)$$

where v is the velocity of an electron at a point whose potential with respect to the cathode is V, and v_0 is the emission velocity of this electron.

Let us now put A for Nem/kT, which is equal to $i_0 m/kT$, i_0 being the saturation current per sq. cm. of the cathode, and θ for $\frac{m}{2kT}$; then eqn. (1) becomes

$$\rho_\alpha = 2A\int_{\sqrt{\frac{2Ve}{m}}}^{\infty} \frac{v_0 \cdot \epsilon^{-\theta v_0^2}}{v} \cdot dv_0 - A\int_{\sqrt{\frac{2V_m e}{m}}}^{\infty} \frac{v_0 \cdot \epsilon^{-\theta v_0^2}}{v} \cdot dv_0. \quad (2)$$

Now

$$v^2 = v_0^2 + \frac{2Ve}{m},$$

the numerical value of e being taken;

$$\therefore \quad vdv = v_0 dv_0. \quad . \quad . \quad . \quad . \quad . \quad (3)$$

Substituting (3) in (2), changing the variable, and remembering that, in region α, V is negative, we get

$$\rho_\alpha = 2A \cdot \epsilon^{\frac{2\theta Ve}{m}} \int_0^\infty \epsilon^{-\theta v^2} dv - A \cdot \epsilon^{\frac{2\theta Ve}{m}} \int_{\sqrt{\frac{2e}{m}(V_m+V)}}^{\infty} \epsilon^{-\theta v^2} dv,$$

where the numerical value of V_m is to be taken.

Putting $\sqrt{\theta} \cdot v = z$, this further reduces to the form

$$\rho_\alpha = \frac{2A}{\sqrt{\theta}} \cdot \epsilon^{\frac{2\theta Ve}{m}} \int_0^\infty \epsilon^{-z^2} dz - \frac{A}{\sqrt{\theta}} \cdot \epsilon^{\frac{2\theta Ve}{m}} \int_{\sqrt{\frac{2e}{m}(V_m+V)}}^{\infty} \epsilon^{-z^2} dz. \quad (4)$$

In region β only those electrons are present which have emission velocities greater than or at least equal to $\sqrt{\frac{2V_m e}{m}}$. Hence

$$\rho_\beta = e\int_{\sqrt{\frac{2V_m e}{m}}}^{\infty} \frac{N}{v} \cdot \frac{mv_0}{kT} \cdot \epsilon^{-\frac{mv_0^2}{2kT}} \cdot dv_0. \quad . \quad . \quad (5)$$

Proceeding as above, this reduces to the form

$$\rho_\beta = \frac{A}{\sqrt{\theta}} \cdot \epsilon^{\frac{2\theta Ve}{m}} \int_{\sqrt{\frac{2e}{m}(V_m+V)}}^{\infty} \epsilon^{-z^2} dz. \quad . \quad . \quad . \quad (6)$$

The integrals involved in equations (4) and (6) are of well-known type, and can be evaluated by means of tables of Probability Integrals when the limits are known. To determine the limits it is necessary to find the potential distribution between the plates.

Suppose that the cathode is a large flat surface at a known temperature and the anode is a parallel surface at a certain distance from the cathode. With this position of the plates, when a steady current flows between the two, the potential distribution can be found, after some laborious calculations, according to the method indicated by Langmuir *. This will give the values of V_m and V, the latter being different for different distances from the cathode. The next step is to find the distance x_m of the surface of minimum potential from the cathode, by which we can know whether any chosen point is in region α or β. To find the density of space charge at this point, formula (4) or (6) is applied, according as the case may be.

Numerical Results for a Typical Case.

Suppose that the cathode is a flat tungsten surface at temperature 2400° K., and the anode is a parallel surface at a distance of 0·5 cm. With Fry we assume that the saturation current i_0 per sq. cm. of the cathode is 0·16 ampere at 2400° K. Let us consider the case in which the current i between the plates is 0·00016 ampere per sq. cm. of the cathode. Proceeding, as indicated by Langmuir, we get, for this case

$$x_m = 0{\cdot}074 \text{ cm.},$$
$$V_m = -1{\cdot}4292 \text{ volts}.$$

The distribution of potential is also worked out for this case. Knowing the potential V at any point, the value of

$$z = \sqrt{\frac{2\theta e}{m}(V_m + V)} = \sqrt{4{\cdot}833(1{\cdot}4292 + V)}$$

is found out, and from the tables of probability integrals the value of $\int_z^\infty \epsilon^{-z^2}\,dz$ is obtained by interpolation. When z is large, the value of $\int_z^\infty \epsilon^{-z^2}\,dz$ is obtained from the equation

$$\int_z^\infty \epsilon^{-z^2}\,dz = \frac{\epsilon^{-z^2}}{2z}\left[1 - \frac{1}{2z^2} + \frac{1{\cdot}3}{(2z^2)^2} - \ldots\right].$$

* Langmuir, Phys. Rev., April 1923.

Next the value of $\epsilon^{\frac{2\theta e}{m} \times V} = \epsilon^{4\cdot833 \times V}$ is found, and the density ρ of space charge at the point under consideration is obtained from formula (4) or (6), according as $x <$ or $> x_m$. The distribution of electron density for different values of the current i is given in the following tables, together with the distribution when there is no external field.

Curves in fig. 2 show the distribution of electron density

Fig. 2.

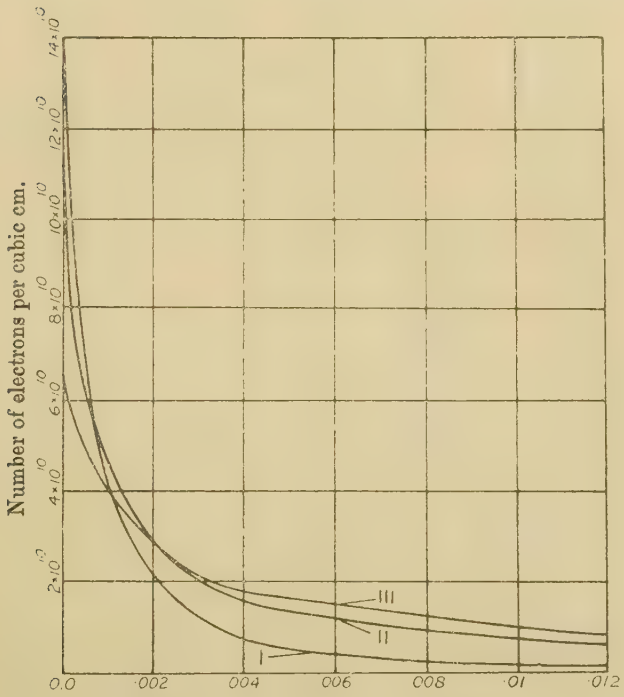

between the cathode and the anode for different values of thermionic current between the plates. It will be seen that immediately near the surface of the cathode the electron density diminishes as the current increases, but at greater distances it increases with the current. Also, the steepness of the curves immediately near the cathode diminishes with increase of current, but at greater distances the curves are very nearly parallel to the axis of x (distance from the cathode) for all values of the current—the effect of increasing

the current being merely to raise this portion of the curve higher.

In fig. 2, curve I. shows the distribution when there is no external field, *i.e.*, when the current is zero ; curve II. shows the distribution when the current is 0·08 ampere per sq. cm. of the cathode, *i.e.*, half the saturation current; and curve III. when the current is saturated. The curves for the cases when the current is 0·00016, 0·0016, and 0·016 respectively have not been drawn, for they follow curve I. very closely.

Case I.

$i = 0$. (No external field.)

x (cm.).	V (volts).	ρ (e. s. u.).	Number of electrons/c.c.
0	0	62·938	$13·18\times10^{10}$
0·0001	−0·03026	54·388	$11·39\times10^{10}$
0·001	−0·23330	20·380	$4·27\times10^{10}$
0·003	−0·49060	5·878	$1·23\times10^{10}$
0·005	−0·64790	2·747	$5·75\times10^{9}$
0·007	−0·76190	1·585	$3·32\times10^{9}$
0·01	−0·88920	0·856	$1·79\times10^{9}$
0·1	−1·79600	0·011	$2·24\times10^{7}$
0·2	−2·08100	0·003	$5·67\times10^{6}$

Case II.

$i = 0·08$ amp. per sq. cm. ; $x_m = 0·0018347$ cm. ; $V_m = -0·1434$ volt.

x (cm.).	V (volts).	ρ (e. s. u.).	Number of electrons/c.c.
0	0	55·405	$11·605\times10^{10}$
0·0001	−0·01872	49·670	$10·400\times10^{10}$
0·001	−0·12663	22·400	$4·691\times10^{10}$
0·003	−0·10860	10·462	$2·192\times10^{10}$
0·005	+0·07050	6·651	$1·393\times10^{10}$
0·007	+0·35230	4·952	$1·037\times10^{10}$
0·01	+0·91177	3·630	$7·603\times10^{9}$
0·1	+42·82900	0·691	$1·447\times10^{9}$
0·2	+113·78400	0·505	$1·058\times10^{9}$

Tables showing the electron density and the potential at various distances from the cathode are given for curves I., II., and III.

Case III.

$i = 0{\cdot}16$ amp. per sq. cm. ; $x_m = 0$ cm. ; $V_m = 0$ volt.

x (cm.).	V (volts).	ρ (e. s. u.).	Number of electrons/c.c.
0	0	31·464	$6{\cdot}590\times10^{10}$
0·0001	+0·00058	29·646	$6{\cdot}210\times10^{10}$
0·001	+0·05028	19·487	$4{\cdot}083\times10^{10}$
0·003	+0·35520	11·193	$2{\cdot}344\times10^{10}$
0·005	+0·83480	8·022	$1{\cdot}681\times10^{10}$
0·007	+1·43720	6·348	$1{\cdot}329\times10^{10}$
0·01	+2·51624	4·907	$1{\cdot}028\times10^{10}$
0·1	+71·56550	1·231	$2{\cdot}579\times10^{9}$

Conclusion.

The distribution of electron density between a plane-heated cathode and a parallel anode has been calculated when a thermionic current flows between the two. Numerical results for a few typical cases are given. It is found that when a current flows the electron density diminishes immediately near the hot surface, but increases at a greater distance from it. Curves showing the variation of electron density are given for various values of electronic current flowing between the cathode and the anode.

My best thanks are due to Prof. S. K. Mitra, D.Sc., for having suggested the problem to me and for taking keen and helpful interest during the progress of the work.

Wireless Laboratory,
University College of Science,
92 Upper Circular Boad,
Calcutta, India.

May 21, 1929.

X. *On the Generation of Pulses in Vibrating Strings.* *By* D. Banerji, *M.Sc., Lecturer in Physics, Calcutta University, and* R. Ganguli, *Lecturer in Physics, Serampore College, Bengal* *.

[Plate I.]

Introduction.

THE vibrations of long strings, stretched between their ends and excited by vibrations of shorter segments of their own, present many acoustical peculiarities which do not appear to have received any attention from workers in this field.

The experiment is suggested by an art of finger-playing (known as "Abataran Ash") on the strings of the Indian musical instrument "Vina" †. This is a sudden drop of the tone-frequency from a high to a low value by a brisk movement of the finger-tip from one position to another, which increases the vibrating length of the string. The other form of "Ash," namely, the "Arohan Ash," is the converse of "Abataran Ash" just described, inasmuch as here the length of the vibrating string is suddenly diminished instead of increased, as in the former case. The latter form of "Ash" is easier to comprehend from the known acoustical principles of vibrating strings, but the effect of the former cannot be estimated *a priori* without a detailed examination of the mode of vibration of the string immediately after release of the finger-tip. Although such an art is recognized by Indian musicians to be unique in its musical effect, and is, therefore, very often resorted to for the adornment of instrumental music, yet no scientific study has been made of the exact nature of the transition of the mode of vibration from one of higher frequency to another of lower frequency or *vice versa*. It is proposed to give in the following lines the results of an investigation to bring out the characteristics of the vibrations of a stretched string clamped at different points on its length by a mechanical device which can suddenly be released after excitation of one of the segments of division by gentle plucking. Although such an arrangement differs in details from an actual "Vina," inasmuch as the points of clamping are not those where the frets are actually placed, yet the sudden release of the clamp, while one segment of the string is

* Communicated by Prof. S. K. Mitra, D.Sc.

† For description of "Vina," see an article by C. V. Raman, Proc. Ind. Assoc. Cult. of Science, vii. pp. 29–33 (1921).

executing its natural vibration, is a sufficient imitation of the process of "Abataran Ash," previously described. It is also expected that the investigation will throw light on the main issue of the problem, namely, how the form of the string-vibration changes suddenly from one of higher frequency to another of lower frequency.

Experiment.

With the above object in view, a steel wire was tied at one end to a rigid support, and from the other end, which passed over a pulley, weights were hung to put it under proper tension. A scissor-like clamp, specially designed for the purpose, and shown in the adjoining figure, could be adjusted

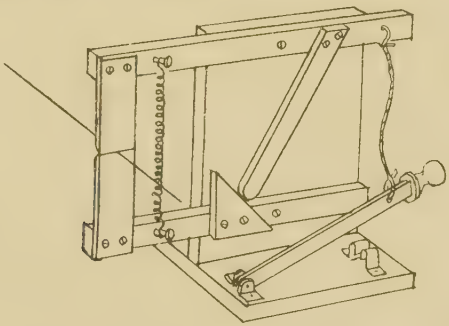

to clamp the string in any desired position, and by the application of a lever-hammer attached to its framework the blades of the clamp could be suddenly separated without disturbing the string. The form of vibration of one segment of the string when it is plucked with the finger-tips over a finite length, so as to elicit only the fundamental of the segment, together with the complex tone on transition to the lower frequency of the complete length just after release of the clamp, can thus both be depicted photographically on a sensitive paper moving uniformly at the focus of a point of the segment of the string.

Results and Discussion.

In fig. 1 (Pl. I.) the clamp was at a point $>1/2$.

„ 2 „ „ „ the mid-point.
„ 3 (*a*) & (*b*) „ „ between 1/2 and 1/3.
„ 4 „ „ at 1/3.
„ 5 „ „ „ 1/5.
„ 6 „ „ „ 1/7.

The main results of observations are stated below :—

(*a*) When the clamp is applied so as to divide the string into two segments in the ratios of 1 : 1, 1 : 2, 1 : 3, and so on, and the shorter segment is made to vibrate by plucking over a finite length, the unexcited part takes up a less intense vibration from the excited part, and is divided into segments of lengths equal to that of the excited part. Care is taken to pluck the string gently over a finite length to elicit only the gravest component of the Fourier Series. This phenomenon of leakage of oscillation, which is due to the effect of resonance, is particularly noticeable when the clamped point is exactly in the position of nodal division of the string, and is completely minimized on shifting the clamp on either side of this position. The clamp takes up the oscillation of the shorter segment and communicates it to the other segment of commensurable period.

(*b*) The time-displacement curve of the complete length immediately after the clamp is removed presents peculiarities in that, whenever the excited shorter segment is an aliquot fraction of its total length, its total amplitude is equal to the amplitude of the exciting oscillation. There is one important exception, namely, when the position of the clamp is near 1/7 the amplitude is increased. This anomalous increase of amplitude near 1/7 may have some bearing with similarly observed phenomena in struck strings, of which no satisfactory explanation has been offered. The time-displacement curves, especially at smaller ratios of division, make it clear that the original exciting vibration tends to persist in the final motion, and seems, though slightly modified by the presence of very weak upper partials, to repeat after intervals of rest-positions of the string equal to its fundamental period.

(*c*) The transition from the original oscillation of higher frequency to the graver fundamental of the string is as sudden as the release of the clamp, and may take effect at any phase of the former. The number of partials excited by the transition appears to be limited by the fundamental of the shorter segment. The relative intensities of the partials which are sufficiently strong at 1/2 and 1/3 do not seem to be altered appreciably by slightly shifting the position of the clamp on either side of the nodal points. If the total energy content of the string before the release of the clamp is distributed without loss over the partials generated by the release of the clamp, then, according to a well-known energy principle, the relation between the

amplitudes of the vibrations before and after the release of the clamp will be as below :

$$\frac{\Sigma A_i^2}{a^2} = \frac{m}{M} \frac{\Sigma T_i^2}{t^2}$$

(where m and M are the respective masses of the shorter segment and of the whole string, t and T_i the respective periods of the shorter segment and of the whole string vibrating in its ith harmonic component, and a and A_i the corresponding amp itudes). Such a relation, however, fails to correspond with facts, and the calculated and observed values of the final amplitudes differ considerably for all cases. The amplitude of the original simple vibration is nucleated in pulses of equal amplitude repeating at intervals of the period of the fundamental of the total length of the string. The effect can be explained if we remember that the clamp, in communicating the vibration from one side to the other, is itself thrown in a state of vibration. The result of the sudden removal of the clamp is on the one hand the disappearance of a certain amount of energy which was in the clamp, and on the other hand the cessation of communication of energy from the excited to the unexcited segment. The consequence is that the displaced form of the shorter segment at the moment of release of the clamp is propagated along the length of the string in the form of a pulse which travels to and fro between the two ends of the string. This can easily be verified by the measurements of the distances between the pulses in the plate.

This probably explains the use of the " Abataran Ash " by musicians in India. The sudden change of length of the vibrating string produces pulses which bring in a peculiar richness in the tonal quality which is not otherwise possible.

Summary and Conclusion.

Experiments are made to imitate the common practice (technically known as " Abataran Ash ") of exciting the string of the Indian musical instrument " Vina." This consists of a sudden drop of the tone-frequency from a higher to a lower val ue by suddenly removing the finger tip so as to increase t he length of the vibrating string. A string stretched between its ends is clamped at points of aliquot division of the string, and the shorter segment is excited by plucking. On releasing the clamp suddenly the original high-frequency oscillation appears to be nucleated in pulses which move to and fro between the ends of the

string. It seems, therefore, that "Abataran Ash" is only a technique of exciting pulses in the vibrating string of the "Vina." The pulses, which are well known to be rich in harmonics, help to produce the peculiar musical effect.

In conclusion, we desire to express our best thanks to Prof. S. K. Mitra for his kind interest in our work and much useful help.

University College of Science,
92 Upper Circular Road, Calcutta, India.
29th May, 1929.

XI. *The Mutual Action of a Pair of Rational Current Elements.* *By* G. F. C. Searle, *Sc.D., F.R.S., University Lecturer in Experimental Physics, Cambridge* *.

THE "rational current element" devised by Oliver Heaviside consists of an elementary line of length ds conveying an electric current i, the current flowing out at the positive end of the element into an infinite medium, as from a point-source, and flowing in at the negative end. The current density in the medium is that due to the two radial currents. Two rational elements, $i_1 ds_1$ and $i_2 ds_2$, in any given positions will give rise to a magnetic field, and T, the magnetic energy of the field, will be a homogeneous quadratic function of i_1 and i_2. Heaviside calculated the part of T which depends upon the product $i_1 i_2$, and has termed it the "mutual action" of the two elements. He stated the results in his 'Electrical Papers,' vol. ii. pp. 501, 502, but he did not give a proof. An indication of the method is given in vol. ii. p. 506. A recent inquiry leads me to give an elementary account of the calculation.

If H be the magnetic force and μ the magnetic permeability, we have

$$\mathrm{T} = \frac{1}{8\pi} \iiint \mu \mathrm{H}^2 \, dx \, dy \, dz, \quad . \quad . \quad . \quad . \quad (1)$$

where the integration extends through all space. We can replace (1) by

$$\mathrm{T} = \tfrac{1}{2} \iiint \mathbf{SAC} \, dx \, dy \, dz, \quad . \quad . \quad . \quad . \quad . \quad (2)$$

where SAC is the scalar product of the vector potential **A** and the current density **C**, and the integration again extends through all space. We have $\mathbf{SAC} = \mathrm{AC} \cos \psi$, where A, C

* Communicated by the Author.

are the magnitudes of $\mathbf{A}$, $\mathbf{C}$, and ψ is the angle between their forward directions. Vector symbols are printed in **Clarendon** type.

We may write $\mathbf{A}=\mathbf{A}_1+\mathbf{A}_2$, $\mathbf{C}=\mathbf{C}_1+\mathbf{C}_2$, where $\mathbf{A}_1$, $\mathbf{C}_1$ are the vector potential and the current density due to the element $i_1 ds_1$ and $\mathbf{A}_2$, $\mathbf{C}_2$ are due to $i_2 ds_2$. If T_{12} be the part of T which depends upon the product $i_1 i_2$, we have

$$T_{12}=\tfrac{1}{2}I_1+\tfrac{1}{2}I_2, \quad . \quad . \quad . \quad . \quad . \quad . \quad (3)$$

where

$$I_1=\iiint S\mathbf{A}_1\mathbf{C}_2\,dx\,dy\,dz, \qquad I_2=\iiint S\mathbf{A}_2\mathbf{C}_1\,dx\,dy\,dz. \quad . \quad (4)$$

The vector potential due to the vector element $i_1 d\mathbf{s}_1$ at a point at a distance r from the element is $\mathbf{A}_1=\mu i_1 d\mathbf{s}_1/r$, the two vectors being parallel and having the same positive direction. Similarly $\mathbf{A}_2=\mu i_2 d\mathbf{s}_2/r$.

If α_2 be the cross-section of the element $i_2 ds_2$, and if $\mathbf{C}_2$ be the current density in the element, $i_2=C_2\alpha_2$, and thus, if dv_2 be the infinitesimal volume occupied by ds_2, we have $\mathbf{C}_2 dv_2=i_2 d\mathbf{s}_2$. Throughout dv_2 we may treat $\mathbf{A}_1$ as constant, and thus the contribution of dv_2 to the integral I_1 is

$$\mu i_1 i_2 ds_1 ds_2 \cos\epsilon/r, \quad . \quad . \quad . \quad . \quad . \quad . \quad (5)$$

where r is the distance between the two elements and ϵ is the angle between the positive directions of the elements.

The evaluation of the integrals in (4) will be found to depend on the integral

$$\int (R^2/\rho)\cos\psi\, d\omega$$

taken over the surface of a sphere of centre O_2 and radius R. Here $d\omega$ is an elementary solid angle, ρ is the distance from the surface element $R^2 d\omega$ at Q on the sphere to a fixed point O_1, and ψ is the angle between O_2Q and a straight line O_2F_2, which is parallel to and has the same forward direction as a fixed straight line O_1F_1. The value of the integral depends upon whether R is less or greater than r, where $r=O_1O_2$. We shall write

$$G=\int (R^2/\rho)\cos\psi\, d\omega, \quad \text{when } R<r, \quad . \quad . \quad (6)$$

$$J=\int (R^2/\rho)\cos\psi\, d\omega, \quad \text{when } R>r. \quad . \quad . \quad (7)$$

If a sphere of radius R and density k^{-1} be centred at O_2, and a second sphere of radius R and density $-k^{-1}$ be centred at O_2' on O_2F_2, where $O_2'O_2=k$ and $O_2'O_2$ has the same forward direction as O_2F_2, the spheres neutralize each other except in those parts where they do not overlap. When k is very small, the radial thickness at Q of the un-neutralized part

is $k\cos\psi$. The "surface density" is thus $k^{-1}.k\cos\psi$ or $\cos\psi$. Hence G (or J), the potential at O_1 of the layer of surface density $\cos\psi$, is also the potential at O_1 of the system of the two spheres. We note that, when k is infinitesimal,

$$O_1O_2 - O_1O_2' = k\cos O_2O_1F_1. \quad . \quad . \quad . \quad . \quad (8)$$

If we take the positive direction of O_1F_1 to coincide with the positive direction of the element ds_1, we have

$$\cos O_2O_1F_1 = -dr/ds_1. \quad . \quad . \quad . \quad . \quad . \quad (9)$$

At distance r from the centre of a sphere of radius R and density k^{-1}, the potential is $4\pi R^3/3kr$, when $R<r$. Hence, when $R < r$, we have, by (8) and (9),

$$G = \frac{4\pi R^3}{3k}\left(\frac{1}{O_1O_2} - \frac{1}{O_1O_2'}\right) = \frac{4\pi R^3}{3r^2}\cdot\frac{dr}{ds_1}. \quad . \quad (10)$$

When $R > r$, O_1 lies inside the sphere centred at O_2. The potential at O_1 of that part of the sphere which lies within a distance r from O_2 is $4\pi r^3/(3kr)$ or $4\pi r^2/3k$. The potential within the sphere of radius r and centre O_2 due to the shell of radii R and r is constant and equal to the potential at O_2, and thus equals

$$\int_r^R \frac{4\pi R^2 dR}{kR} = \frac{4\pi}{k}\cdot\frac{R^2 - r^2}{2}.$$

Thus the potential at O_1 of the sphere of radius R centred at O_2 is

$$\frac{4\pi}{k}\left(\frac{r^2}{3} + \frac{R^2 - r^2}{2}\right) = \frac{2\pi}{k}\left(R^2 - \frac{r^2}{3}\right).$$

Hence J, the potential at O_1 of the layer of surface density $\cos\psi$, when $R > r$, is given, through (8) and (9), by

$$J = -\frac{2\pi}{3k}(O_1O_2^2 - O_1O_2'^2) = \frac{2\pi}{3k}(O_1O_2 + O_1O_2')k\frac{dr}{ds_1}$$
$$= \frac{4\pi r}{3}\cdot\frac{dr}{ds_1}. \quad . \quad . \quad . \quad . \quad . \quad (11$$

The values of G and J agree when $R = r$.

We will now return to the electrical problem and, using the values of G and J, will find the part of the integral I_1 arising from the radial current flowing out of P_2, the positive end of ds_2; we suppose P_2 to be at O_2. The element i_1ds_1 is at O_1, and, as in (9), we take O_1F_1 to coincide with the forward direction of ds_1. The current density, C_2, due to

i_2 is $i_2/4\pi R^2$ at Q at the distance R from P_2, and thus, since $O_1Q=\rho$,

$$SA_1C_2 . R^2 d\omega = \frac{\mu i_1 ds_1}{\rho} . \frac{i_2}{4\pi R^2} \cos\psi . R^2 d\omega$$

$$= \frac{\mu i_1 i_2 ds_1}{4\pi R^2} . \frac{R^2 \cos\psi d\omega}{\rho} .$$

The contribution of the shell of radii R and $R+dR$ to the integral I_1 is

$$dR . \int SA_1C_2 . R^2 d\omega = \frac{\mu i_1 i_2 ds_1}{4\pi R^2} G dR, \quad \text{when } R<r, \quad (12)$$

$$dR . \int SA_1C_2 . R^2 d\omega = \frac{\mu i_1 i_2 ds_1}{4\pi R^2} J dR, \quad \text{when } R>r. \quad (13)$$

Hence the part of I_1 due to the current flowing out at P_2 is

$$\frac{\mu i_1 i_2 ds_1}{4\pi} \left\{ \int_0^r \frac{G dR}{R^2} + \int_r^\infty \frac{J dR}{R^2} \right\} = \tfrac{1}{2}\mu i_1 i_2 ds_1 . \frac{dr}{ds_1} . \quad (14)$$

At N_2, the negative end of ds_2, the arc of which ds_2 is a part is less than at P_2 by ds_2. Hence the part of I_1 due to the current flowing in at N_2 is

$$-\tfrac{1}{2}\mu i_1 i_2 ds_1 \left\{ \frac{dr}{ds_1} - \frac{d}{ds_2}\frac{dr}{ds_1} . ds_2 \right\} . \quad . \quad . \quad . \quad (15)$$

Adding the two expressions (14) and (15), we find that the part of I_1 due to the two radial currents is

$$\tfrac{1}{2}\mu i_1 i_2 ds_1 ds_2 . d^2r/ds_2 ds_1 . \quad . \quad . \quad . \quad . \quad (16)$$

Adding the expression (5), we find

$$I_1 = \left(\frac{\cos\epsilon}{r} + \frac{1}{2}\frac{d^2r}{ds_2 ds_1} \right) \mu i_1 i_2 ds_1 ds_2 . \quad . \quad . \quad . \quad (17)$$

Since $d^2r/ds_1 ds_2 = d^2r/ds_2 ds_1$, $I_2 = I_1$, and thus, by (3), we obtain Heaviside's result *,

$$T_{12} = \mu i_1 i_2 \left(\frac{\cos\epsilon}{r} + \frac{1}{2}\frac{d^2r}{ds_1 ds_2} \right) ds_1 ds_2 . \quad . \quad . \quad . \quad (18)$$

We can express $d^2r/ds_1 ds_2$ in another form. Let the coordinates of O_1, O_2, the centres of the elements, be x_1, y_1, z_1 and x_2, y_2, z_2, and let ξ_1, η_1, ζ_1 and ξ_2, η_2, ζ_2 be the coordinates of points on the elements relative to O_1, O_2. Then $r^2 = a^2 + b^2 + c^2$, where

$$a = x_2 + \xi_2 - x_1 - \xi_1, \quad b = y_2 + \eta_2 - y_1 - \eta_1, \quad c = z_2 + \zeta_2 - z_1 - \zeta_1 .$$

* 'Electrical Papers,' vol. ii. p. 501.

Since ξ_1, η_1, ζ_1 and $d\xi_1/ds_1$, $d\eta_1/ds_1$, $d\zeta_1/ds_1$ are independent of s_2, we have

$$r\frac{dr}{ds_2} = a\frac{d\xi_2}{ds_2} + b\frac{d\eta_2}{ds_2} + c\frac{d\zeta_2}{ds_2},$$

$$r\frac{dr}{ds_1} = -\left(a\frac{d\xi_1}{ds_1} + b\frac{d\eta_1}{ds_1} + c\frac{d\zeta_1}{ds_1}\right),$$

$$r\frac{d^2r}{ds_1 ds_2} = -\left(\frac{d\xi_1}{ds_1}\frac{d\xi_2}{ds_2} + \frac{d\eta_1}{ds_1}\frac{d\eta_2}{ds_2} + \frac{d\zeta_1}{ds_1}\frac{d\zeta_2}{ds_2}\right) - \frac{dr}{ds_1}\frac{dr}{ds_2}.$$

We now evaluate the differential coefficients when

$$\xi_1 = \eta_1 = \zeta_1 = 0 \quad \text{and} \quad \xi_2 = \eta_2 = \zeta_2 = 0.$$

The direction cosines of the vector O_1O_2 are a/r, b/r, c/r, those of the vector ds_1 are $d\xi_1/ds_1$, etc., and those of the vector ds_2 are $d\xi_2/ds_2$, etc. Then

$$rd^2r/ds_1 ds_2 = -\cos\epsilon + \cos\phi_1\cos\phi_2,$$

where ϕ_1 and ϕ_2 are the angles between the vector O_1O_2 and the vectors ds_1 and ds_2 respectively. Hence, by (18),

$$T_{12} = \tfrac{1}{2}\mu i_1 i_2 r^{-1}(\cos\epsilon + \cos\phi_1\cos\phi_2)ds_1 ds_2. \quad . \quad (19)$$

Following Heaviside, we now take the axis of x along O_1O_2. If the direction cosines of the elements be l_1, m_1, n_1 and l_2, m_2, n_2, we have

$$\cos\phi_1 = l_1, \quad \cos\phi_2 = l_2, \quad \cos\epsilon = l_1l_2 + m_1m_2 + n_1n_2,$$

and then we obtain Heaviside's result *,

$$T_{12} = \tfrac{1}{2}\mu i_1 i_2 r^{-1}(2l_1l_2 + m_1m_2 + n_1n_2)ds_1 ds_2. \quad . \quad (20)$$

If the currents i_1, i_2, instead of flowing in two elements, flow in two finite unclosed arcs N_1P_1, N_2P_2, we integrate with respect to ds_1 and also with respect to ds_2. We obtain

$$\iint \frac{d^2r}{ds_1 ds_2} ds_1 ds_2 = \int\left(\frac{dr}{ds_2}\text{ at } P_1 - \frac{dr}{ds_2}\text{ at } N_1\right)ds_2$$
$$= P_1P_2 - P_1N_2 - P_2N_1 + N_2N_1,$$

and thus, by (18), as Heaviside found †,

$$T_{12} = \mu i_1 i_2\{\iint r^{-1}\cos\epsilon\, ds_1 ds_2 + \tfrac{1}{2}(P_1P_2 + N_1N_2 - P_1N_2 - P_2N_1)\}.$$
$$. \quad . \quad . \quad (21)$$

If the second circuit be closed, N_2 is identical with P_2, and then, whether the first circuit be closed or unclosed, (21) becomes

$$T_{12} = \mu i_1 i_2 \iint r^{-1}\cos\epsilon\, ds_1 ds_2. \quad . \quad . \quad . \quad (22)$$

* 'Electrical Papers,' vol. ii. p. 501.

† 'Electrical Papers,' vol. ii. p. 502.

XII. *Determination of the Variation with Pressure of the Force between Two Plates at Different Temperatures at Low Pressures, with a View to the Determination of Molecular Mean Free Paths.* By A. E. Martin, *Ph.D.**

1. *Introduction.*

THE object of the work to be described was to measure the force between two small, plane, parallel plates, due to difference of temperature between them at low pressures, and to study the variation of the force with the pressure and nature of the gas, the temperature difference, and the distance between the plates. Simple considerations show that at pressures so low that the mean free path of the gas molecules is large compared with the distance between the plates, other factors remaining constant, the force between the plates is proportional to the pressure, and this, indeed, is the basis of the Knudsen low-pressure gauge ; but at higher pressures, when the distance between the plates and the mean free path are comparable, this linear relation is no longer followed, and an attempt has been made to determine the mean free path from the observed deviations. Measurements of the heat conducted from a heated surface at low pressures are also given, and here again the deviations from a linear relation could be used to determine the mean free path, although this has not yet been attempted.

2. *Description of Apparatus.*

The apparatus is shown diagrammatically in fig. 1, and consisted of a glass bulb containing heater and suspended system, a modified McLeod pressure-gauge, vacuum-pumps, and an arrangement for admitting the gas to be investigated into the apparatus to any desired pressure not less than ·001 mm. Hg.

The glass bulb B (fig. 1) was about 10 cm. diameter, and to it was sealed a wide glass tube, fitted with a ground-glass stopper. Just below the stopper was placed a short length of glass tubing, kept in place by dents in the outer tube, and between the two tubes was wedged a piece of copper strip C, bent as shown in fig. 2. To this strip was

* Communicated by Prof. J. R. Partington, D.Sc.

attached a piece of copper wire D, from which was suspended a quartz fibre F, about 20 cm. long, the attachment being effected by means of a minute quantity of Faraday wax. The bulb also contained the heater, the platinum leads to which were sealed into a glass tube passing into the bulb.

Fig. 1.

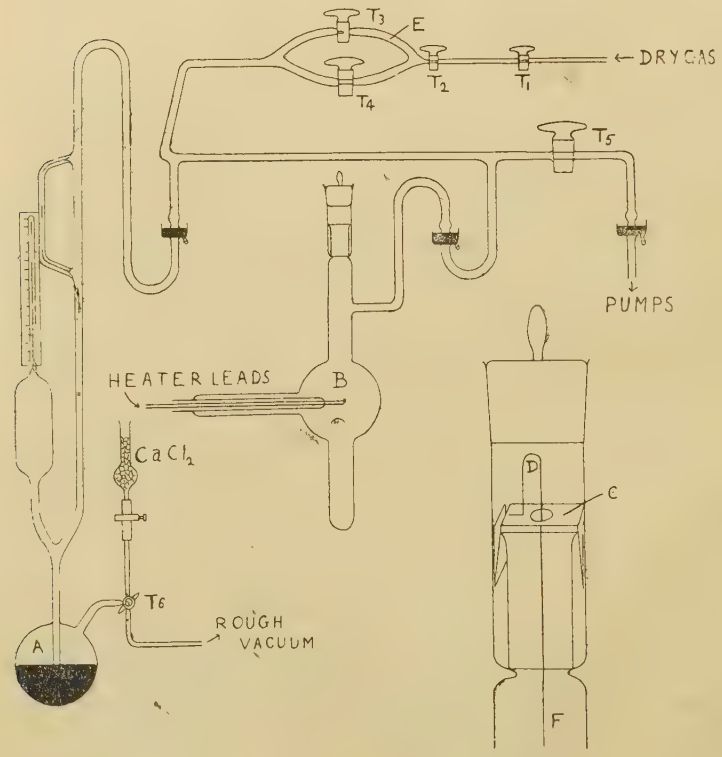

Fig. 2.

The heater (fig. 3 *a*) consisted of a copper bobbin on which was wound, as non-inductively as possible, about 1 yard of No. 47 gauge enamelled copper wire, the ends of which were attached to the platinum leads.

One of the leads supported the bobbin, the free face of which, a copper plate 2 mm. square, formed the heated surface from which gas molecules were reflected. The temperature of this plate was taken as being the same as

that of the heating coil, which was used as a resistance thermometer. This coil was made one arm of a resistance bridge, and resistance measurements were made in the usual way except that a valve amplifier and telephones were used instead of a galvanometer.

The bulb containing the heater was almost completely surrounded by a water-jacket, and the temperature of the water was taken at frequent intervals during each experiment.

The target (fig. 3*b*) was a copper plate 2 mm. square, similar to that forming part of the heater, and was attached to an arm of thin copper wire, which was in turn attached to the quartz-fibre suspension by means of a trace of Faraday wax. The target was counterbalanced by a small

Fig. 3.

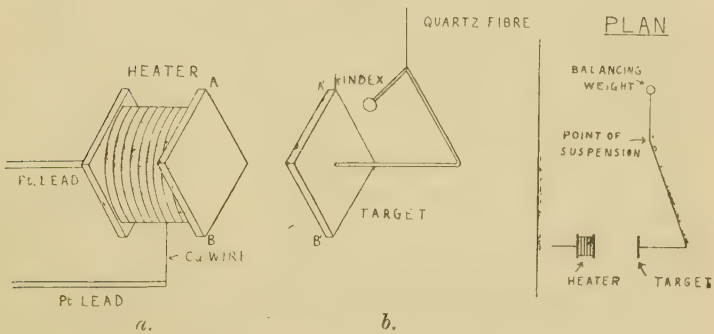

blob of solder. The upper end of the quartz fibre was attached to a kind of torsion head, already described, by means of which the position of rest of the target could be altered. Before any particular experiment the target was arranged so that when deflected during the experiment it would be directly opposite and parallel to the heater surface. It was desired to carry out experiments under such conditions that all molecules which travelled direct from heater surface to target traversed the same distance, and to this end the heater surface and target were made as small as possible. The distance between the heater surface and target was varied from 3 to 8 mm. during the course of the work, but could not be altered outside these limits. To enable the deflexions of the target to be accurately measured an index of phosphor-bronze strip

(0·1 × 0·01 mm.) was attached to the target, so that when viewed through a microscope the thin edge was visible. The heater surface and target were mounted, each having a diagonal vertical, so that when the microscope was in position any one of the diagonal corners could be focussed by moving the microscope up and down or from side to side. In this way both the distance between the two upper corners, A and A′, and between the lower corners, B and B′ (figs. 3 *a* and 3 *b*) could be measured. The mean of these two measurements is given as *s* in the tables of measurements. All deflexions and distances were determined to ·01 mm.

In order to prevent any shift of the suspended system during experiments the whole apparatus was securely clamped at a number of places; also, as the suspended system was very susceptible to vibration, it was necessary to avoid any disturbance in the neighbourhood of the apparatus while readings were being taken. All readings were taken late at night, when vibration was at a minimum, and as the apparatus was unavoidably disturbed to some extent when pressure and other readings were taken, it was necessary to leave the apparatus entirely alone for some minutes after any adjustment before the position of the image of the target index on the eyepiece-scale could be determined. All pumps were shut off while measurements were being taken, except when it was necessary to use the filter-pump for a few seconds partially to exhaust the reservoir, which, besides being employed in conjunction with the filter-pump to provide a rough vacuum for the first stage of the two diffusion-pumps used to evacuate the apparatus, served to operate the pressure-gauge. This gauge was provided with a mercury reservoir A (fig. 1), which communicated with the rough vacuum while the apparatus was being evacuated. In order to take a pressure reading, the tap T_6 was turned so as to cut off A from the rough vacuum, and air was admitted through a drying-tube, its rate of entry being controlled by means of a screw clip and pressure tubing. When the surface of the mercury in the open capillary was level with the top of the closed capillary the air was shut off and the length of the gas column in the closed capillary read off on a mirror scale. The pressure in the apparatus was calculated in the usual way, the capillary having been calibrated by means of a mercury thread during the construction of the

gauge, and the volume of the bulb being known from the weight of water required to fill it at a known temperature.

The gas pressure in the apparatus during an experiment was altered by means of tap T_3 (fig. 1). The plug of this tap had a hole bored halfway through, the volume of the hole being about 10 cu. mm.; gas filled the cavity at atmospheric pressure when the tap was turned so that the bore communicated with the tube E, and this gas was discharged into the apparatus by turning the tap through 180°, the pressure being thereby increased by ·01mm. The pressure could also be increased by ·001 mm. at a time by admitting gas at atmospheric pressure from the tube connecting T_1 and T_2 to the tubes connecting T_2 to T_3 and T_4, previously evacuated, and then admitting this gas into the apparatus as before by tap T_3. The tubes mentioned were exhausted at the commencement of each experiment through tap T_4; this tap was then turned off, and gas, free from moisture and carbon dioxide, admitted through T_1. The gases investigated were air and hydrogen. The various pieces of apparatus were connected by means of ground joints, fitted with mercury seals.

3. *Mode of Experiment.*

The apparatus at the commencement of each experiment was exhausted to a pressure certainly below 10^{-4} mm. The pressure-gauge indicated 10^{-5} mm. ignoring any vapours present, and a similar value is obtained from considerations involving the speed of the pumps and rate of formation of mercury and other vapours in the apparatus.

The apparatus having been exhausted and flushed out with dry gas, the pumping was continued for about twenty minutes, the pumps then being shut off from the apparatus by means of T_5 and stopped. Gas was immediately admitted into the apparatus to a pressure of ·01 mm. in the case of air and ·02 mm. in the case of hydrogen, it being found impossible to take readings at lower pressures owing to the small amount of damping of the oscillating target. Devices for increasing the damping were tried, but were unsatisfactory and were discarded. After admitting the gas the temperature of the heater was adjusted to a suitable value, and a pressure reading was taken. The position of the image of the target index on the eyepiece-scale was read off as soon as possible

(about fifteen minutes after shutting off the pumps), and this reading was repeated at intervals of some minutes, so that subsequently a correction could be applied for mercury and other vapours in the apparatus, the drift of the target being a measure of the amount of vapour formed.

Readings were then taken at higher pressures, the pressure being increased by ·01 mm. at a time, and the temperature of the heater being suitably adjusted so as to keep the deflexion of the target, and hence the distance between the target and heater, practically constant. It was not found advisable to attempt to keep the deflexion absolutely constant, as after each change of heating current an appreciable time elapsed before equilibrium was attained. Readings were taken up to a pressure of ·11 mm., the limit of the gauge.

The force acting on the target at any time was proportional to the deflexion, and the torsional constant of the fibre being known, the moment of the force could be calculated, and hence the force itself. The torsional constant of the fibre was obtained by determining the period of torsional oscillation *in vacuo* of a body, of which the moment of inertia could be calculated from its mass and dimensions, attached to the fibre in place of the target. In the Tables absolute values of the force on the target are only given when there is an object in doing so. In the case of fibre 1 the force required to cause a deflexion of 1 mm. was ·001208 dyne ; with fibre 2 a force of ·00114 dyne produced the same deflexion. The two fibres were actually identical, except that the target became detached from fibre 1 and had to be replaced.

4. *Variation of Deflecting Force with Temperature Difference between Target and Heater.*

Measurements of the resistance of the heating coil were made at 0° C. and at 100° C. both before the heater was sealed into the bulb and after the apparatus was dismantled. These two sets of measurements agreed so well that no serious change in the heater could have occurred during the course of the work. For the determination of temperatures from resistance measurements it was assumed that the temperature coefficient of the heating coil was constant between 0° C. and 100° C. Allowance was made for the leads attached to the heating coil.

The temperature of the target could not be directly measured, but was taken as being equal to that of the water jacket. This is not quite correct, as the target was at a temperature slightly higher than that of its surroundings owing to the heat received from the heater during the course of an experiment; but this difference is so small that it can be safely neglected. If the temperature of the heater is θ_2 and the resistance of the heating coil is R_2,

Fig. 4.

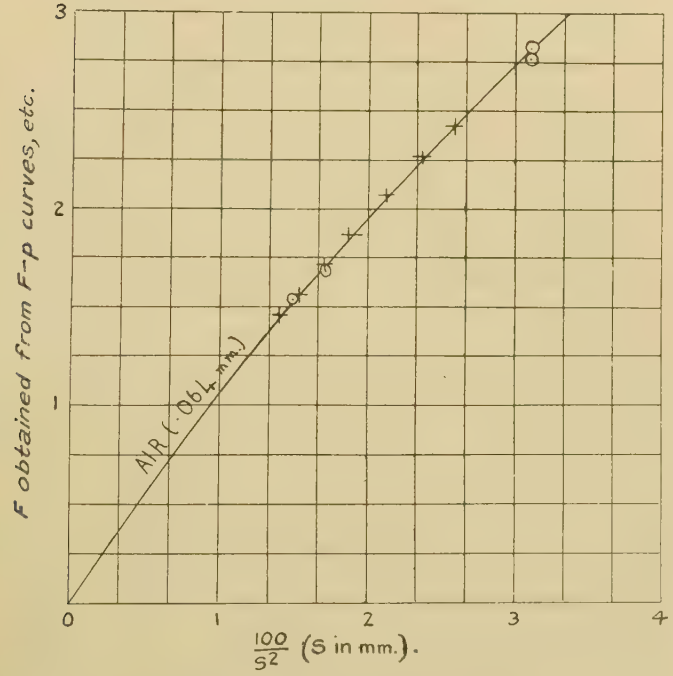

and if the temperature of the water jacket is θ_1 and the resistance of the heating coil at this temperature is R_1, then

$$\theta_2 - \theta_1 = 36{\cdot}61(R_2 - R_1),$$

θ_2 and θ_1 being in °C. and the resistances in ohms. In the tables of figures and in the curves given values of $R_2 - R_1$ are used rather than the corresponding values of $\theta_2 - \theta_1$, needless calculation being thus avoided.

It is of interest to determine how the deflecting force varies with $\theta_2 - \theta_1$ when the gas pressure and distance

between the heater and target are kept constant. This variation cannot be directly determined, since the deflecting force is measured by means of changes in the distance s, but an indirect method can be used. Values of the quantity $\frac{\text{Deflexion (mm.)}}{R_2 - R_1}$, denoted by F, are plotted

TABLE I.

Quartz fibre 1. *Air.*

No. of Expt.	F.	s. mm.	$\frac{100}{s^2}$.
3	2·76	5·68	3·10
4	2·81	5·68	3·10
5	3·03	5·46	3·36
6	1·68	7·64	1·714
7	1·54	8·20	1·488

Points plotted from above values are marked ⊙ in fig. 4.

Quartz fibre 2. *Air.*

$R_2 - R_1$. ohms.	Deflexion. mm.	$\frac{\text{Deflexion}}{R_2 - R_1} = F$.	$\frac{F}{1·060}$.	Distance s. mm.	$\frac{100}{s^2}$.
·866	1·71	1·974	1·863	7·32	1·866
·569	1·25	2·197	2·072	6·86	2·126
·376	0·88	2·395	2·259	6·51	2·360
·226	0·58	2·566	2·421	6·21	2·592
1·507	2·49	1·652	1·559	8·08	1·533
1·842	2·84	1·542	1·454	8·43	1·406
1·129	2·05	1·816	1·713	7·66	1·706

Points plotted from above values are marked + in fig. 4.

Since the force required for 1 mm. deflexion is different for the two fibres, it is necessary to divide the values of F in the second series by 1·060 to make them comparable with those in the first series.

against the pressure, small corrections having been applied for small variations in s, and from the curves obtained values of F are read off for some particular pressure, and a curve showing the relation between F and s at constant pressure is obtained.

The temperature differences corresponding to the values of F plotted did not greatly differ throughout the series. A

series of readings had previously been taken at the same pressure, but with widely different temperature differences; and it will be seen that the corresponding values of F, when plotted against s, fall on the curve previously obtained (fig. 4). This shows, within the limit of experimental error, that, for given values of pressure and distance s, $\frac{\text{Deflexion}}{\theta_2-\theta_1}$ is constant; *i. e.*, the deflexion is proportional to the temperature difference. These measurements are given in Table I.

5. *Variation of Deflecting Force with Pressure, other Factors remaining constant.*

Assuming that F is independent of temperature difference, it is only necessary to correct the values of F, obtained from any series of readings, for small variations in the value of s, and for mercury and other vapours in the apparatus, after which curves showing the variation of deflecting force with pressure can be drawn. The former correction is given later, but the latter will be discussed at this point.

As previously stated, the pressure inside the apparatus at the instant when the pumps were shut off was between 10^{-5} and 10^{-4} mm. This amount can be safely neglected, since the lowest pressure at which readings were taken was 10^{-2} mm. The rate of external leakage under average conditions was measured by exhausting the apparatus and leaving overnight, and was found to be quite negligible. The sole pressure correction arises through the formation of mercury and other vapours in the apparatus after the pumps were shut off. These vapours were, of course, ignored by the McLeod gauge. Experiments were made to find how the rate of formation of vapour varied with the time, and it was found that it fell off almost exponentially, and was, as far as could be ascertained, independent of gas in the apparatus at pressures up to ·1 mm. Theoretical considerations lead to a similar result.

Let the amount of mercury, grease, etc. adsorbed on the walls of the apparatus at the instant when the pumps were shut off be a. Suppose that after time t this amount has decreased by x, the vapour formed being proportional to x; then the rate at which molecules in the vapour phase strike the walls of the apparatus will also be proportional to x,

and, if it is assumed that a constant proportion of such molecules is readsorbed, the rate at which x is decreasing from this cause will be proportional to x itself. At the same time x will be increasing, due to evaporation from the walls of the apparatus, at a rate proportional to the amount of volatile material remaining. Thus we have

$$\frac{dx}{dt} = k_1(a-x) - k_2x = k_1a - kx,$$

where k_1 and k_2 are constants and $k_1+k_2=k$.

$$\therefore \quad dt = \frac{dx}{k_1a-kx} \quad \text{and} \quad kt = \mathrm{C} - \ln(k_1a - kx),$$

C being the integration constant. When $t=0$, $x=0$;

$$\therefore \qquad kt = \ln\left(\frac{k_1a}{k_1a-kx}\right)$$

$$\text{and} \qquad x = \frac{ak_1}{k}(1-e^{-kt}). \quad . \quad . \quad . \quad . \quad . \quad (1)$$

a will vary from one experiment to another, but k should remain reasonably constant, since neither the composition of the adsorbed volatile material nor the temperature of the apparatus varied very much during the course of the work. It was found from experiment that the vapour formed during the first hour was double that formed during the second hour, which was in turn double that formed during the third hour, in agreement with equation (1) when $e^{-k}=\frac{1}{2}$, t being measured in hours.

The corrections for vapour pressure are obtained by plotting F against time, using the measurements taken at the commencement of each experiment, before admitting a second quantity of gas into the apparatus. The curve obtained is completed by making use of the observation that the vapour formed during the first hour is double that formed during the second hour, as previously explained. Over the small pressure range applying to the values of F obtained from measurements taken at the commencement of an experiment, $\frac{\delta \mathrm{F}}{\delta p}$ is practically constant and can be obtained from the appropriate $\mathrm{F}-p$ curve; the F scale in the F-time curve can be directly converted to pressure, and the vapour formed in the apparatus at any given time can be read off from the curve. This pressure is

added to the gauge pressure, and the total taken as the actual pressure in the apparatus at this particular time. The pressure correction is not, of course, the actual vapour pressure, but the pressure of air or hydrogen to which it is equivalent in these experiments. Figs. 5 and 6 show the variation of the deflecting force with the pressure, other factors remaining constant. These curves are referred to as F —p curves for convenience.

Fig. 5.

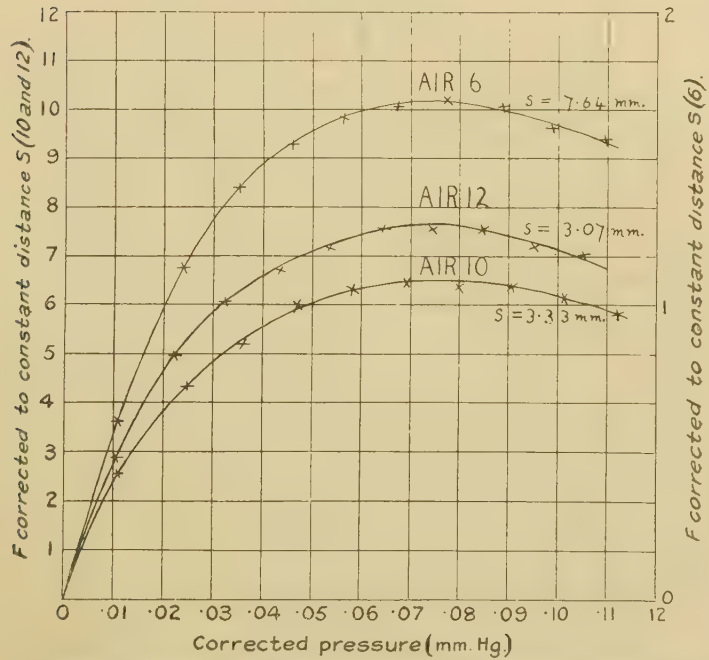
AIR 6
s = 7·64 mm.
AIR 12
s = 3·07 mm.
AIR 10
s = 3·33 mm.
F corrected to constant distance s (10 and 12).
F corrected to constant distance s (6).
Corrected pressure (mm. Hg)
0 ·01 ·02 ·03 ·04 ·05 ·06 ·07 ·08 ·09 ·10 ·11 12
1 2 3 4 5 6 7 8 9 10 11 12
0 1 2

To convert values of F to dynes multiply by ·001208 for (6) and (10), and by ·00114 for (12).

6. *Relation between F and s at Constant Pressure.*

From the F —p curves for air and hydrogen values of F and s at constant pressure were obtained, and curves were drawn showing the relation between F and s (fig. 7). These curves were used to correct the values of F $\left(\frac{\text{Deflexion}}{R_2 - R_1}\right)$ for small variations in s as follows :—

Suppose that in a given experiment F and s have the

values F_1 and s_1 at a pressure p, and that it is required to find the change in F, δF_1, due to a change in s of δs_1 at the same pressure.

Assuming the relation between F_1, s_1, and p to be of the form

$$F_1 = f(p)f(s_1),$$

we have

$$\frac{\delta F_1}{\delta s_1} = f(p)f'(s_1) = F_1 \cdot \frac{f'(s_1)}{f(s_1)}.$$

Fig. 6.

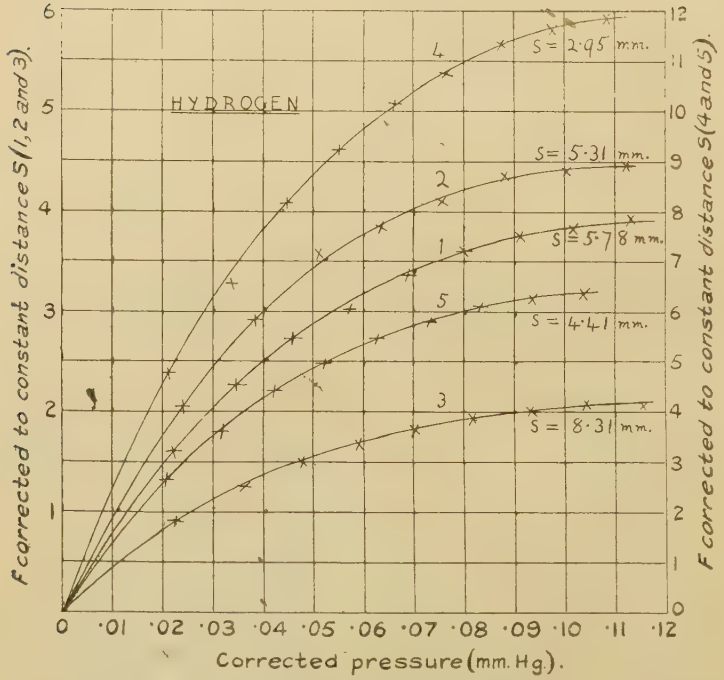
HYDROGEN
S = 2·95 mm.
S = 5·31 mm.
S = 5·78 mm.
S = 4·41 mm.
S = 8·31 mm.
1
2
3
4
5
F corrected to constant distance S(1, 2 and 3).
F corrected to constant distance S(4 and 5).
Corrected pressure (mm. Hg).
0 ·01 ·02 ·03 ·04 ·05 ·06 ·07 ·08 ·09 ·10 ·11 ·12

To convert values of F to dynes multiply by ·001208 for (1), (2), and (3), and by ·00114 for (4) and (5).

But the slope of the appropriate curve in fig. 7 at any point is

$$\frac{\delta F}{\delta s} = F\frac{f'(s)}{f(s)}$$

$$= F_2\frac{f'(s_1)}{f(s_1)}$$

at the point where $s = s_1$, F_2 being the corresponding value of F,

$$\therefore \quad \frac{\delta F_1}{\delta s_1} = \frac{F_1}{F_2}\frac{\delta F}{\delta s},$$

and since $\frac{\delta F}{\delta s}$ can be found from the curve, $\frac{\delta F_1}{\delta s_1}$ can be obtained.

Fig. 7.

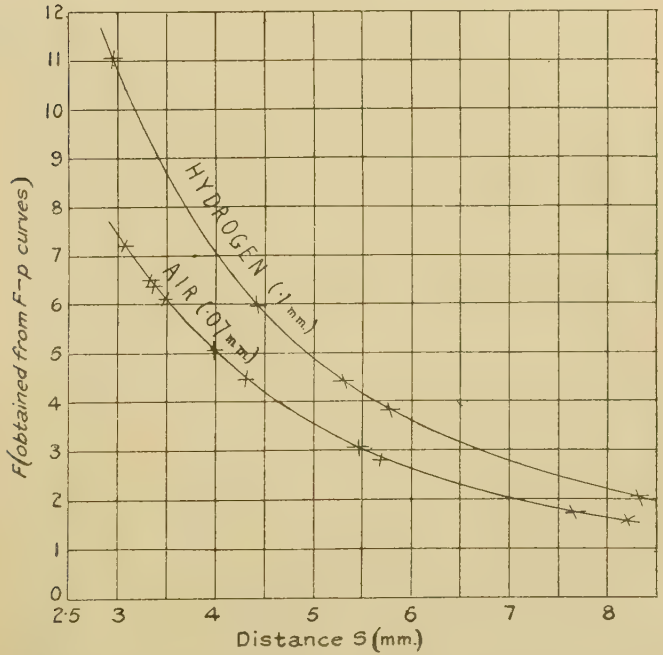

The relation between F and s at constant pressure is shown better by plotting F against $\frac{100}{s^2}$ (fig. 8).

7. *Discussion of Results.*

Both for air and hydrogen it is seen that the curves obtained by plotting F against p, s constant, pass through the origin. It might be supposed that the deflecting force acting on the target is not solely due to the bombarding molecules, and in order to explore this possibility various

forces which might conceivably deflect the target are enumerated below and, as will be seen, finally disregarded.

The possible forces are as follows :—

(1) Gravitational attraction between heater and target. Approximate calculation shows that this force would be less than 10^{-7} dyne, which can be safely neglected, since the smallest readable deflexion was equivalent to 10^{-5} dyne.

Fig. 8.

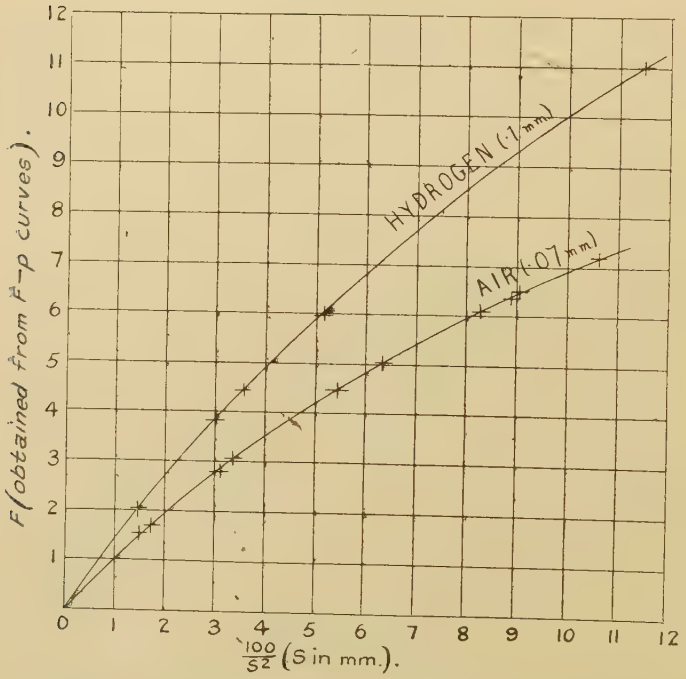

(2) Deflecting force due to heat radiation falling on target. The rate at which heat was generated in the heater was measured in some experiments, and using these values for approximate calculation, it is found that in no case would the force due to heat radiation exceed 10^{-6} dyne, and this is negligible.

(3) The energy received by the target would cause the face nearer the heater to be at a higher temperature than the other surface. This alone would cause the forces acting

on the two sides to be unequal, so that a deflecting force would be produced. Rough calculation shows that the difference of temperature between the two sides during an experiment would never be greater than $\frac{1}{10{,}000}$° C., and this is quite incapable of causing any readable deflexion.

(4) Any slight magnetic field due to current circulating in the heating coil might deflect the target, especially if the latter contained any magnetic impurities. A force of this nature can be dismissed, since a powerful electromagnet when brought near to the target produced no observable deflexion.

The fact that the F $-p$ curves pass through the origin is in agreement with the conclusion that the only deflecting force is due to molecular bombardment.

From the F $-p$ curves for air it is seen that F reaches a maximum value at about ·07 mm. pressure, this pressure being independent of s.

In the case of hydrogen no maxima of F are obtained, but there is little doubt that such maxima would have been exhibited at about ·13 mm.

The curves obtained for air and hydrogen by plotting F against $\frac{100}{s^2}$ at constant pressure (fig. 8) are almost straight lines passing through the origin, which latter would be obtained if F were proportional to $\frac{1}{s^2}$. Thus the inverse square law is obeyed, provided that s is large compared with the dimensions of heater surface and target.

The above observations admit of quite simple theoretical explanation and are of interest in connexion with the working of the radiometer. In explaining these results, use will be made of some theoretical work due to Einstein * and Hettner †.

In the case of a vane, the dimensions of which are small compared with the mean free path L, situated in a gas, pressure p, in which exists a temperature gradient $\frac{\delta T}{\delta s}$, normal to the surface of the vane, area σ, a force given by

* A. Einstein, *Zeitschr. f. Phys.* xxvii. p. 1 (1924).
† G. Hettner, *loc. cit.* xxvii. p. 12 (1924).

equation (2) will act on the vane, tending to move it in the direction of decreasing temperature.

$$K = \frac{\sigma f}{u} = -\frac{1}{2} p \frac{L}{T} \frac{\delta T}{\delta s} \sigma, \quad . \quad . \quad . \quad . \quad (2)$$

where K is the force, f the heat flow across unit area of the plane containing the vane, u the mean velocity of the molecules striking the vane, and T the temperature of the vane. This equation is due to Einstein. In fig. 9, if E is the heat energy conducted from the heater per second by gas molecules, then

$$E = 4\pi s^2 f,$$

Fig. 9.

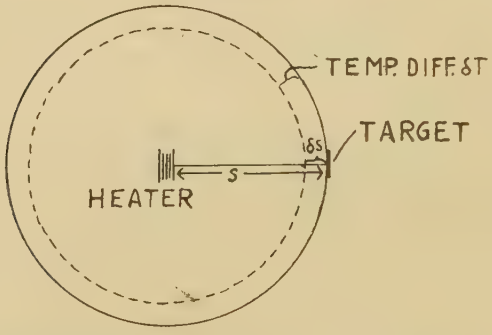

and substituting for f in equation (2) we obtain

$$K = \frac{\sigma E}{4\pi s^2 u}. \quad . \quad . \quad . \quad . \quad . \quad . \quad (3)$$

This equation agrees with results obtained at low pressures, since E is proportional to the pressure and to the temperature difference between the heater and surroundings. If E in equation (3) is replaced by E_1, the heat conducted at any pressure for a temperature difference of 36·6° C., then K can be replaced by F, in conformity with previous practice. Equation (3) then becomes

$$F = \frac{\sigma E_1}{4\pi s^2 u}. \quad . \quad . \quad . \quad . \quad . \quad . \quad (3\,a)$$

Measurements of the heat conducted from the heater by the gas at various pressures are given later, and from them values of E_1 have been found and used to calculate values of F from equation (3 *a*).

The calculated values of F are found to be about five times greater than the observed values in the case of air, and about three times greater in the case of hydrogen. These differences are explained by the fact that Einstein in deriving equation (2) only considered the translational velocities of the molecules, and did not allow for the accommodation coefficient. A further cause for discrepancy lies in the fact that heat is not conducted from the heater equally in all directions as assumed above. The whole question of the force on the target at low pressures is discussed more fully at a later point.

Einstein extends equation (2) to cover the case of a vane of dimensions great compared with the mean free path. Equation (2) applies in this case only to the extreme edges of the vane, over a region of the order of a mean free path wide. Over the remainder of the vane the pressure is the same on both sides. This leads to the equation

$$K = \frac{fL}{u} = -\frac{1}{2} p \frac{L^2}{T} \frac{\delta T}{\delta s}, \quad . \quad . \quad . \quad . \quad . \quad (4)$$

where K is now the force per unit-length of edge of the vane. Proceeding as before we obtain

$$K = \frac{EL}{4\pi s^2 u}, \quad . \quad . \quad . \quad . \quad . \quad . \quad (5)$$

where E is the energy conducted by the gas molecules. If the pressure is sufficiently high, then E will be proportional to temperature difference but independent of pressure.

Equation (5) can then be modified as follows :—

$$F = \frac{E_2 L l}{4\pi s^2 u}, \quad . \quad . \quad . \quad . \quad . \quad . \quad (5\,a)$$

where E_2 is the energy conducted for a temperature difference of 36·6° C., and F is the force for the entire length of edge (l) of the vane. It is thus seen that at high pressures

$$F \propto \frac{1}{p}.$$

Hettner derives an equation to cover all pressures as follows :—

At high pressures put $F = \frac{a}{p}$, and at low pressures put

$F=bp$, a and b being constants. At any pressure we have approximately

$$\frac{1}{F}=\frac{p}{a}+\frac{1}{bp}, \quad \ldots\ldots\ldots \quad (6)$$

or

$$\frac{p}{F}=\frac{p^2}{a}+\frac{1}{b}. \quad \ldots\ldots\ldots \quad (6\,a)$$

If equation (6 a) holds good, then a straight line should be obtained by plotting p^2 along the x axis and $\frac{p}{F}$ along the y axis.

Further, from equation (6) F is a maximum when

$$p=\sqrt{\frac{a}{b}}=p_0 \text{ (say)}.$$

But from equation (6 a)

$$p^2=-\frac{a}{b}, \text{ when } \frac{p}{F}=0,$$

so that the intercept on the x axis is

$$-\frac{a}{b}=-p_0^2.$$

Equation (6 a) was tested for air and hydrogen in the manner indicated, and it is found that the points plotted lie almost exactly on two straight lines (fig. 10). From these straight lines the following values for p_0 are obtained :—

Air, $p_0=\cdot 07$ mm. ; hydrogen, $p_0=\cdot 11$ mm.

The value for air is identical with that obtained from the corresponding $F-p$ curve. The $F-p$ curve for hydrogen does not actually show a maximum, although a value for p_0 in the neighbourhood of ·13 mm. is indicated.

The value of p_0 for any case can be calculated purely theoretically as follows :—

By comparison of equations (3 a) and (5 a) with equation (6) we obtain

$$a=\frac{E_2 L l p}{4\pi s^2 u} \quad \text{and} \quad b=\frac{\sigma E_1}{4\pi s^2 u p},$$

whence

$$\frac{a}{b}=\frac{E_2 L l p^2}{\sigma E_1}$$

and

$$p_0=p\sqrt{\frac{L l E_2}{\sigma E_1}}. \quad \ldots\ldots \quad (7)$$

Equation (7) shows that p_0 is independent of s, which is in accord with experimental results. E_1 and E_2 were found for air and hydrogen from measurements of heat conduction, and by substituting these values together with the values for L, usually given, in equation (7), the values of p_0 for air and hydrogen are found to be ·09 mm. and ·16 mm., respectively. These values agree quite well with the observed values, and this agreement proves the correctness of equation (4), at least as regards order of magnitude.

Fig. 10.

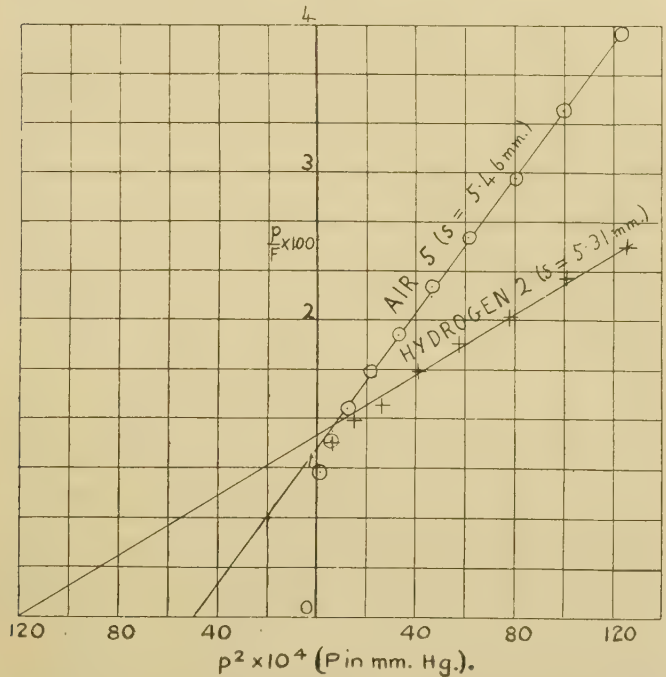

It should be noted that equations (2) and (4) are subject to the same errors, since equation (4) was derived from equation (2); these errors cancel each other in the calculation of p_0.

8. *Relation between the Heat conducted from the Heater by Gas Molecules for a Constant Temperature Difference, and the Gas Pressure.*

In some experiments measurements were made of the current flowing through the heater coil, from which the

rate at which energy was generated in the heater could be found. In order to determine that portion of the heat conducted away by the surrounding gas measurements were made to find the heat lost by radiation and conduction through the leads for various temperature differences between the heater and its surrounding at the lowest pressure obtainable.

The method adopted was to exhaust the apparatus to as low a pressure as possible, shut off the pumps and take resistance, current, temperature, and time readings. The heat generated in the heater per unit-time at the instant when the pumps were cut off was obtained by extrapolation, and was, of course, equal to the heat lost by radiation and conduction through the leads. The rate of energy loss from the heater *in vacuo* was taken to be C^2R, C being the current and R the resistance of the heating coil—*i. e.*, R_2 less the resistance of the leads. A curve was drawn showing the relation between C^2R and R_2-R_1, and it was found to be very nearly a straight line, as might be expected. To determine the heat conducted by gas under any given conditions the heat lost by radiation and conduction through the leads in absence of gas was obtained from the curve and subtracted from the total heat lost.

The heat conducted by the gas at various pressures having been found for air and hydrogen, the values were reduced to a common temperature difference, and curves were drawn showing the relation between the heat conducted by the gas and the pressure (fig. 11). In this calculation it is assumed that the heat conducted by the gas at a given pressure is proportional to the temperature difference. The pressure readings were corrected for the presence of vapours in the apparatus in a manner similar to that already described.

The number of molecules striking the heater per unit-area per second is $\frac{NC}{\sqrt{6\pi}}$, where N is the number of molecules per c.c. and C is the R.M.S. speed. The mass of gas striking unit-area per second is $\frac{mNC}{\sqrt{6\pi}}$, m being the mass of a single molecule. But the pressure of the gas, p, is $\frac{1}{3}NmC^2$, and therefore the mass of gas striking unit-

area per second is $\frac{3p}{\sqrt{6\pi C}}$. At very low pressures the impinging molecules will be "cold" and will take from the heater energy proportional to $\theta_2 - \theta_1$, but at higher pressures the impinging molecules will be "warmed" by previous collisions with "hot" molecules rebounding from the heater, and the average amount of heat taken from the heater by each molecule striking it will be reduced.

Fig. 11.

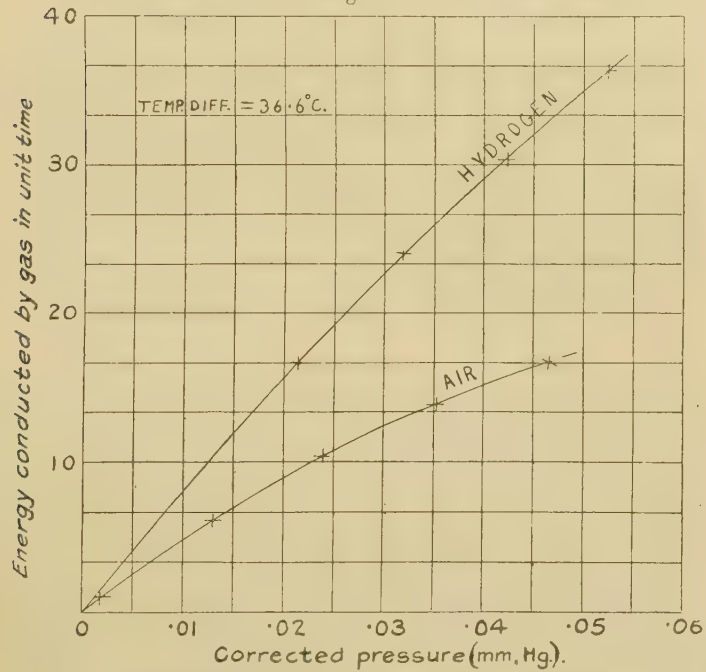

To convert energy conducted in unit time to ergs per sec., multiply by $5{\cdot}37 \times 10^3$.

At low pressures, therefore, the heat conducted is proportional to the pressure, as can be seen from fig. 11, whilst at higher pressures the heat conducted increases more and more slowly with pressure until it becomes practically constant. The slope of each of the curves of fig. 11 as it passes through the origin has been determined, the values being as follows :—

Gas.	*Rate at which energy is conducted by gas.*	*Temp. of surroundings.*
Air.....	$2{\cdot}73 \times 10^3$ ergs per second per ·001 mm. Hg.	17·5° C.
Hydrogen	4·40 „ „ „ „ „ „	16·4° C.

These values correspond to a temperature difference between heater and surroundings of 36·6° C.

$$\cdot 001 \text{ mm. Hg.} = \frac{13{\cdot}6 \times 981}{10^4} \text{ dynes per cm.}^2$$

C (mean for O_2 and N_2 in air at 17·5° C.). $5{\cdot}02 \times 10^4$ cm./sec.

C (for H_2 at 16·4° C.) . . . . . $18{\cdot}9 \times 10^4$ cm./sec.

Specific heat of air at constant volume. 0·170.

Specific heat of hydrogen at constant volume . . . . . 2·360.

Knowing that the mass of gas striking unit-area in unit-time is $\frac{3p}{\sqrt{6\pi C}}$, and assuming that the air molecules have the same temperature as the heater on leaving, we find by making use of the above values that the energy taken from unit-area of the heater per second is $4{\cdot}78 \times 10^3$ ergs for a pressure of ·001 mm. Hg,

$$\therefore \text{ the effective area of the heater} = \frac{2{\cdot}73 \times 10^3}{4{\cdot}78 \times 10^3} \text{ sq. cm.}$$

$$= 57{\cdot}2 \text{ sq. mm.}$$

This value is considerably greater than that obtained by measurement (21·0 sq. mm.), and this is probably due to irregularities on the surface of the heater enabling more impacts to take place than is indicated by the simple theory used. The area of the heater available for molecular impacts is difficult to measure at all accurately, owing to the presence of the wire.

In the case of hydrogen it cannot be assumed that the molecules rebounding have the same temperature as the heater, but if θ is the average temperature of the molecules striking the surface, θ_1 the temperature of the surface, and θ_2 the average temperature of the molecules leaving, then

$$\theta_2 - \theta = a(\theta_1 - \theta),$$

where a is the accommodation constant of Knudsen.

Using the value for the effective area of the heater already obtained, a can be found as follows :—

In a similar manner to that used for air, but using the appropriate values for hydrogen, the energy conducted per second from the heater for a pressure of ·001 mm. is found to be $10{\cdot}08 \times 10^3 \times a$ ergs.

But the heat conducted per second was found by measurement to be $4{\cdot}40 \times 10^3$ ergs.

$$\therefore \quad a = {\cdot}437.$$

This value for a is intermediate between the values obtained with hydrogen by Knudsen for polished platinum and platinum slightly coated with platinum black.

9. *Determination of the Force between two Small, Parallel Plates, due to a Temperature-Difference between them at Very Low Pressures.*

Assuming that the molecules are specularly reflected from the heater surface (fig. 12), the number of molecules reflected per second at an angle between θ and $\theta + d\theta$ with the normal to the surface is

$$dn = \frac{2\mathrm{NAC}_1}{\sqrt{6\pi}} \sin\theta \cos\theta \, d\theta,$$

where N is the number of molecules per c.c. and C_1 the R.M.S. speed of the molecules striking the heater.

Fig. 12.

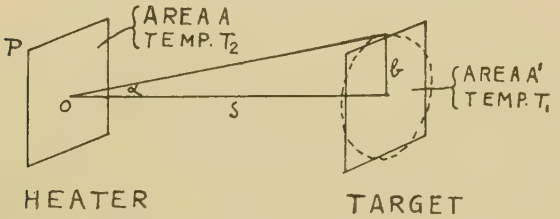

The total number of molecules from the heater surface striking the target per second, supposing the pressure to be so low that none of these molecules collide with " cold " molecules on their way to the target, is

$$n = \frac{2\mathrm{NAC}_1}{\sqrt{6\pi}} \int_0^{\alpha} \sin\theta \cos\theta \, d\theta$$

$$= \frac{\mathrm{NAC}_1}{\sqrt{6\pi}} \sin^2\alpha = \frac{\mathrm{NAC}_1}{\sqrt{6\pi}} \cdot \frac{b^2}{s^2},$$

if b is small compared with s (b is the radius of a circle having an area equal to that of target),

$$\therefore \quad n = \frac{\mathrm{NAC}_1}{\sqrt{6\pi}} \cdot \frac{\mathrm{A}'}{\pi s^2}.$$

If these molecules have a mean speed $\bar{c}_2$, appropriate to the temperature of the heater, T_2, then, since they all strike the target nearly normally, the force on the target due to their impact is

$$\frac{NAA'C_1}{\sqrt{6\pi}.\pi s^2}.m\bar{c}_2=\frac{mNAA'C_1C_2}{\sqrt{6\pi}.\pi s^2}.\sqrt{\frac{8}{3\pi}}$$

$$=\frac{2}{3}\frac{mNAA'C_1C_2}{\pi^2 s^2},$$

and the deflecting force on the target, due to the extra energy imparted to the molecules by the heater, is

$$\frac{2}{3}\frac{AA'mNC_1^2}{\pi^2 s^2}\left(\frac{C_2-C_1}{C_1}\right),$$

provided that the "hot" molecules give up all excess energy to the target on impact—*i. e.*, the temperature of these molecules on leaving the target is T_1.

Now $$\frac{C_2-C_1}{C_1}=\frac{T_2-T_1}{2T_1}$$

approximately, if T_2-T_1 is small compared with T_1, so that the deflecting force acting on the target is

$$K=\frac{pAA'}{\pi^2 s^2}\left(\frac{T_2-T_1}{T_1}\right), \quad . \quad . \quad . \quad . \quad (8)$$

p being the gas pressure in the apparatus.

Equation (8) is approximately correct for air, but in the case of hydrogen allowance must be made for the fact that in general hydrogen molecules rebounding from a surface have a mean temperature different from that of the surface. Thus, hydrogen molecules rebounding from the heater will have a mean velocity corresponding to a temperature less than T_2 (say T_2'), and the "hot" molecules rebounding from the target will have a mean velocity corresponding to a temperature higher than T_1 (say T_1'),

where $$T_2'-T_1=a(T_2-T_1)$$

and $$T_2'-T_1'=a(T_2'-T_1),$$

a being the coefficient of accommodation of Knudsen,

$$\therefore \quad T_1'-T_1=a(T_2-T_2')$$

$$=a\{T_2-T_1-a(T_2-T_1)\}$$

$$=a(1-a)\,(T_2-T_1).$$

If the "hot" molecules rebound normally from the target, then the deflecting force due to this rebound is

$$\frac{NAA'C_1'}{\sqrt{6\pi}.\pi s^2}.m(\bar{c}_1'-\bar{c}_1),$$

where $\bar{c}_1'$ and $\bar{c}_1$ are the mean speeds corresponding to the temperatures T_1' and T_1.

This force

$$=\frac{NAA'C_1^2}{\sqrt{6\pi}.\pi s^2}.m\left(\frac{C_1'-C_1}{C_1}\right)\sqrt{\frac{8}{3\pi}}$$

$$=\frac{pAA'}{\pi^2 s^2}.\left(\frac{T_1'-T_1}{T_1}\right)=a(1-a).\frac{pAA'}{\pi^2 s^2}\left(\frac{T_2-T_1}{T_1}\right).$$

The deflecting force due to impact is

$$\frac{pAA'}{\pi^2 s^2}.\left(\frac{T_2'-T_1}{T_1}\right)=a.\frac{pAA'}{\pi^2 s^2}.\left(\frac{T_2-T_1}{T_1}\right);$$

therefore the total deflecting force is

$$K=a(2-a).\frac{pAA'}{\pi^2 s^2}\left(\frac{T_2-T_1}{T_1}\right). \quad . \quad . \quad . \quad (9)$$

Under the conditions of these experiments a has been found to be ·437 for hydrogen from measurements of energy conducted from heater by bombarding molecules, and substituting this value we obtain from (9)

$$K=\cdot 683\frac{pAA'}{\pi^2 s^2}\left(\frac{T_2-T_1}{T_1}\right). \quad . \quad . \quad . \quad (9\,a)$$

This work will now be repeated assuming the molecules to be reflected from the heater surface according to the cosine law.

The number of molecules reflected from the heater surface (fig. 12), at an angle between θ and $\theta+d\theta$ with the normal to the surface, is

$$\frac{NAC_1}{\sqrt{6\pi}}\cos\theta\, d\theta.$$

The total number reflected between 0 and α is

$$\frac{NAC_1}{\sqrt{6\pi}}\int_0^{\alpha}\cos\theta\, d\theta=\frac{NAC_1}{\sqrt{6\pi}}\sin\alpha$$

$$=\frac{NAC_1}{\sqrt{6\pi}}.\frac{b}{s},$$

b being the radius of a circle equal in area to the target and being small compared with s. This number would be correct if the molecules rebounding from the heater surface left the surface only from O ; if, however, all the molecules left from one corner of the heater surface (assumed to be a perfect square, roughly equal in area to the target), such as P (fig. 13), then the number of molecules intercepted by the target would be

$$\frac{1}{4}\frac{NAC_1}{\sqrt{6\pi}}\int_0^{\beta}\cos\theta\,d\theta=\frac{1}{4}\frac{NAC_1}{\sqrt{6\pi}}\sin\beta=\frac{NAC_1}{\sqrt{6\pi}}\cdot\frac{b}{2s}.$$

Fig. 13.

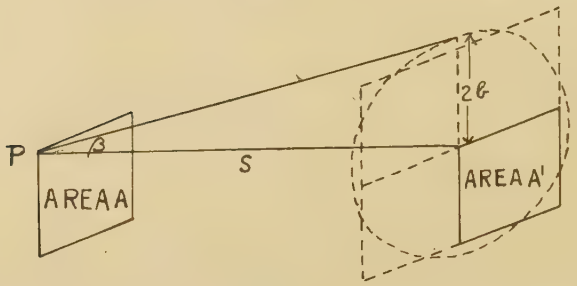

Taking the mean of these extreme values, we have approximately that the number of molecules from the heater surface intercepted by the target is

$$\frac{3}{4}\cdot\frac{NAC_1}{\sqrt{6\pi}}\cdot\frac{b}{s}.$$

Proceeding as before, the deflecting force due to the impact of these molecules is found to be

$$K=\frac{3}{4}\cdot\frac{pAb}{\pi s}\cdot\left(\frac{T_2-T_1}{T_1}\right) \quad . \quad . \quad . \quad . \quad (10)$$

In the case of hydrogen the accommodation coefficient must be introduced as before. If we have gas at a uniform temperature contained in a vessel (N molecules per c.c. and R.M.S. speed C), then molecules will be leaving unit-area of the surface at the rate of $\frac{NC}{\sqrt{6\pi}}$ per second, and the pressure produced normal to the surface, due to their departure, will be $\frac{NmC^2}{6}$, m being the mass of a molecule.

The mean force due to the departure (or impact) of a single molecule, therefore, is $\sqrt{\frac{\pi}{6}}\,m\mathrm{C}$.

Assuming this relation to hold for the "hot" molecules rebounding from the target, the deflecting force produced is

$$\frac{3}{4}\frac{\mathrm{NAC}_1}{\sqrt{6\pi}}\cdot\frac{b}{s}\sqrt{\frac{\pi}{6}}\cdot m(\mathrm{C}_1'-\mathrm{C}_1)=\frac{3}{16}\frac{p\mathrm{A}b}{s}\cdot\left(\frac{\mathrm{T}_1'-\mathrm{T}_1}{\mathrm{T}_1}\right)$$

$$=\frac{3}{16}a(1-a)\frac{p\mathrm{A}b}{s}\cdot\left(\frac{\mathrm{T}_2-\mathrm{T}_1}{\mathrm{T}_1}\right).$$

TABLE II.

$p=1$ dyne per sq. cm. $\quad \mathrm{T}_2-\mathrm{T}_1=36°{\cdot}6$ C.

No. of Expt.	s. cm.	T_1 °K.	Deflecting force in dynes. Observed.	Calculated from equations (8) & (10). Specular reflexion.	Cosine law.
Air.					
3.....	·568	291	$9{\cdot}87\times10^{-5}$	$7{\cdot}61\times10^{-5}$	$25{\cdot}8\times10^{-5}$
4.....	·568	291	$9{\cdot}87\times10^{-5}$	$7{\cdot}61\times10^{-5}$	$25{\cdot}8\times10^{-5}$
5.....	·546	291	$10{\cdot}6\times10^{-5}$	$8{\cdot}23\times10^{-5}$	$26{\cdot}8\times10^{-5}$
6.....	·764	291	$5{\cdot}75\times10^{-5}$	$4{\cdot}20\times10^{-5}$	$19{\cdot}2\times10^{-5}$
7.....	·820	290	$5{\cdot}79\times10^{-5}$	$3{\cdot}66\times10^{-5}$	$17{\cdot}8\times10^{-5}$
Hydrogen.				Calculated from equations (9a) & (11).	
1.....	·578	292	$7{\cdot}61\times10^{-5}$	$5{\cdot}00\times10^{-5}$	$15{\cdot}9\times10^{-5}$
2.....	·531	291	$9{\cdot}05\times10^{-5}$	$5{\cdot}94\times10^{-5}$	$17{\cdot}4\times10^{-5}$
3.....	·831	291	$4{\cdot}53\times10^{-5}$	$2{\cdot}43\times10^{-5}$	$11{\cdot}1\times10^{-5}$

The deflecting force due to impact is from (10)

$$\mathrm{K}=\frac{3}{4}\cdot\frac{p\mathrm{A}b}{\pi s}\left(\frac{\mathrm{T}_2-\mathrm{T}_1}{\mathrm{T}_1}\right)\times a,$$

and the total deflecting force, after putting $a=·437$, is

$$\mathrm{K}=·630\times\frac{3}{4}\cdot\frac{p\mathrm{A}b}{\pi s}\cdot\left(\frac{\mathrm{T}_2-\mathrm{T}_1}{\mathrm{T}_1}\right).\quad .\quad .\quad .\quad .\quad (11)$$

A comparison between the observed and calculated values of the deflecting force for air and hydrogen is given in Table II. Each observed value is obtained from the slope of the appropriate F$-p$ curve at the origin. It will be seen that the assumption of specular reflexion gives

results which are too low, whereas, assuming that the molecules are reflected according to the cosine law, we obtain values which are too high. It would seem probable that reflexion is mainly specular, the low results being due to the underestimation of the number of molecules striking the heater surface per second. This effect was commented on when the heat conducted from the heater by gas molecules at low pressures was calculated.

10. *Calculation of Mean Free Paths.*

Measurements of the force between heater and target at very low pressures give no idea of the molecular mean free path, since collisions between molecules are rare in comparison with collisions between molecules and the target or heater. At higher pressures collisions between molecules become more frequent, and the deflecting force can be considered as the resultant of two forces :—

(1) a direct force due to molecules travelling direct from heater surface to target ;

(2) an indirect force due to the communication of extra energy to "cold" molecules, which subsequently reach the target by collision with "hot" molecules.

Whatever the law of reflexion obeyed by the molecules reflected from the heater surface, the direct deflecting force is proportional to $pe^{-\frac{s}{L}}$, where L is the mean free path of the gas molecules. At very low pressures $e^{-\frac{s}{L}}=1$, and the deflecting force is proportional to the pressure, as already shown. Now $pe^{-\frac{s}{L}}$ has a maximum value when $L=s$, and if the indirect force could be made negligible it would only be necessary to find the pressure for which the deflecting force had a maximal value, to determine the mean free path at this pressure. It was on these lines that experiments were started, but it was not found possible to realise the desired conditions. It is therefore necessary to attempt to calculate the indirect force under various conditions, although an exact analysis is not possible. It will be assumed that the molecules rebounding from the heater surface are specularly reflected, as this assumption was found to agree fairly well with results obtained at

low pressures. Only molecules from the heater A (fig. 14) which collide with other molecules at a distance from A less than s, and their partners in these collisions, will be considered, as conditions are deliberately chosen so that the effect on A′ of molecules colliding at a distance greater than s will be small. Molecules from A colliding with other molecules more than once before reaching A′ and their partners in these collisions will also be ignored, as their effect will be insignificant.

Fig. 14.

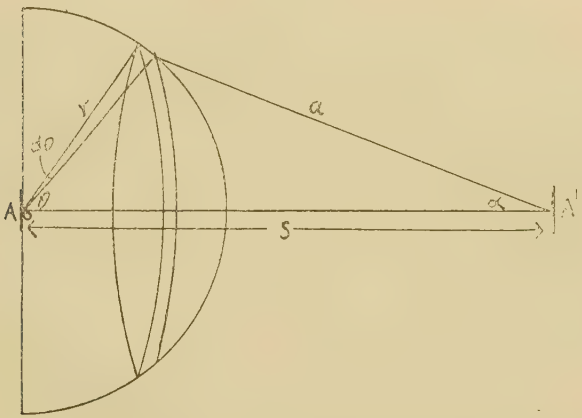

The number of molecules reflected from A per second, making an angle between θ and $\theta+d\theta$ with a normal to the surface, is

$$\frac{2NAC_1}{\sqrt{6\pi}} \cdot \sin\theta\cos\theta\, d\theta,$$

C_1 being the R.M.S. speed of the molecules striking A. To simplify matters the molecules leaving A are regarded as leaving O, the geometrical centre of A.

The number of these molecules which collide with other molecules at a distance between r and $r+dr$ from A per second is

$$\frac{2NAC_1}{\sqrt{6\pi}} \cdot \sin\theta\cos\theta\, d\theta\, e^{-\frac{r}{L}} \cdot \frac{dr}{L},$$

L being the mean free path. (In the case of air the oxygen and nitrogen molecules are assumed to have equal mean free paths.)

The majority of molecules leaving A will collide with molecules moving in the opposite direction, and we may assume, with no great error, that after collision all directions of motion are equally likely for the colliding molecules, so that, owing to the molecules leaving A at an angle between θ and $\theta+d\theta$ with the normal, which collide at a distance between r and $r+dr$,

$$\frac{4NAC_1}{\sqrt{6\pi}}\sin\theta\cos\theta\,d\theta\,e^{-\frac{r}{L}}\frac{dr}{L}\cdot\frac{A'\cos\alpha}{4\pi a^2}$$

molecules with a R.M.S. speed $\frac{C_1+C_2}{2}$ will strike A′ per second, C_2 being the R.M.S. speed of the molecules leaving A, and it being assumed that on the average a "hot" molecule colliding with a "cold" molecule gives half of its excess energy to the latter. As previously stated, it is assumed that few of these molecules (partners in the first collision) will again collide on their way to the target, and this will be the case provided that L is not less than $\frac{s}{2}$.

If the average force on the target due to the impact of a molecule with R.M.S. speed

$$\frac{C_1+C_2}{2}\text{ is taken to be }\frac{m(C_1+C_2)}{2}\cdot\sqrt{\frac{\pi}{6}},$$

as previously explained, the force on the target due to the molecules striking with this speed is

$$\frac{NAA'C_1\cos\alpha}{\sqrt{6\pi}\,\pi a^2 L}\cdot\sin\theta\cos\theta\,d\theta\,e^{-\frac{r}{L}}dr\cdot m\left(\frac{C_1+C_2}{2}\right)\sqrt{\frac{\pi}{6}}$$

$$=\frac{pAA'\cos\alpha}{4\pi a^2 L}\cdot\sin\theta\cos\theta\,d\theta\,e^{-\frac{r}{L}}dr\left(\frac{C_1+C_2}{C_1}\right),$$

and the deflecting force is

$$\frac{pAA'\cos\alpha}{4\pi a^2 L}\sin\theta\cos\theta\,d\theta\,e^{-\frac{r}{L}}dr\left(\frac{C_2-C_1}{C_1}\right)$$

$$=\frac{pAA'\cos\alpha}{8\pi a^2 L}\sin\theta\cos\theta\,d\theta\,e^{-\frac{r}{L}}dr\left(\frac{T_2-T_1}{T_1}\right).$$

The impulse due to the recoil of these molecules will not contribute to the deflecting force, provided that the

impinging molecules acquire the temperature of the target before leaving. In the case of hydrogen an extra deflecting force must be allowed for, but with air this force is small and will be neglected.

The total deflecting force due to all the molecules which leave the heater surface and collide at a distance from O between r and $r+dr$ is

$$dK = \frac{pAA'}{8\pi L} e^{-\frac{r}{L}} dr \left(\frac{T_2 - T_1}{T_1}\right) \int_0^{\frac{\pi}{2}} \sin\theta \cos\theta \cdot \frac{\cos\alpha}{a^2} d\theta.$$

But $$\cos\alpha = \frac{s - r\cos\theta}{a} \quad \text{and} \quad a^2 = s^2 + r^2 - 2sr\cos\theta,$$

$$\therefore \quad s - r\cos\theta = \frac{s^2 - (r^2 - a^2)}{2s} \quad \text{and} \quad a\,da = sr\sin\theta\, d\theta.$$

Hence

$$\int_0^{\frac{\pi}{2}} \sin\theta\cos\theta \cdot \frac{\cos\alpha}{a^2} d\theta = \int_{s-r}^{\sqrt{s^2+r^2}} \left\{ \frac{a\,da}{sr} \cdot \frac{(s^2 + r^2 - a^2)}{2sr} \cdot \frac{(s^2 - r^2 + a^2)}{2sa^3} \right\}$$

$$= \frac{1}{4s^3r^2} \int_{s-r}^{\sqrt{s^2+r^2}} \left(\frac{s^4 - r^4 - a^4 + 2a^2r^2}{a^2}\right) da$$

$$= \frac{1}{4s^3r^2} \left[\left(\frac{r^4 - s^4}{a}\right) - \frac{1}{3}a^3 + 2r^2 a \right]_{s-r}^{\sqrt{s^2+r^2}}.$$

If we put $r = sx$, we obtain

$$\frac{1}{4x^2s^2}\left[(1-x)^4 \left\{\frac{1}{(1-x)} - \frac{1}{\sqrt{1+x^2}}\right\} - \frac{1}{3}\left\{(1+x^2)^{\frac{3}{2}} - (1-x)^3\right\} + 2x^2\left\{\sqrt{1+x^2} - (1-x)\right\}\right]$$

$$= \frac{1}{3x^2s^2}\left[(1+2x^3) + \sqrt{1+x^2}(2x^2-1)\right].$$

$$dK = \frac{pAA'}{24\pi Ls} e^{-\frac{sx}{L}} \left(\frac{T_2 - T_1}{T_1}\right)\left[\left(2x + \frac{1}{x^2}\right) + \sqrt{1+x^2}\left(2 - \frac{1}{x^2}\right)\right] dx.$$

The expression

$$\left(2x+\frac{1}{x^2}\right)+\sqrt{1+x^2}\left(2-\frac{1}{x^2}\right)$$

can be replaced by $(\frac{4}{3}+3x)$ with very little error, and making this substitution we have

$$\mathrm{K}=\frac{p\mathrm{A}\mathrm{A}'}{24\pi \mathrm{L}s}\left(\frac{\mathrm{T}_2-\mathrm{T}_1}{\mathrm{T}_1}\right)\int_0^1\left(\frac{4}{3}+3x\right)e^{-\frac{s}{\mathrm{L}}x}\,dx$$

$$=\frac{p\mathrm{A}\mathrm{A}'}{72\pi s^2}\left(\frac{\mathrm{T}_2-\mathrm{T}_1}{\mathrm{T}_1}\right)\left[\frac{9\mathrm{L}}{s}\left(1-e^{-\frac{s}{\mathrm{L}}}\right)+4-13e^{-\frac{s}{\mathrm{L}}}\right]. \quad (12)$$

Equation (12) will probably give values of K lower than those observed, since from measurements of heat conducted from the heater it was found that the number of impacts per unit-area of the heater was greater than simple theory indicated. To allow for this we may put

$$\mathrm{K}=kp\left(\frac{\mathrm{T}_2-\mathrm{T}_1}{\mathrm{T}_1}\right)\left[\frac{9\mathrm{L}}{s}\left(1-e^{-\frac{s}{\mathrm{L}}}\right)+4-13e^{-\frac{s}{\mathrm{L}}}\right],$$

k being constant for any given experiment.

Similarly we can put for the direct force

$$k_1p\left(\frac{\mathrm{T}_2-\mathrm{T}_1}{\mathrm{T}_1}\right)e^{-\frac{s}{\mathrm{L}}},$$

k_1 also being constant, so that the total deflecting force is

$$\mathrm{K}=kp\left(\frac{\mathrm{T}_2-\mathrm{T}_1}{\mathrm{T}_1}\right)\left[\frac{9\mathrm{L}}{s}\left(1-e^{-\frac{s}{\mathrm{L}}}\right)+4-e^{-\frac{s}{\mathrm{L}}}\left(13-\frac{k_1}{k}\right)\right]. \quad (13)$$

Equation (13) is found to agree with the experimentally determined F$-p$ curves when $\frac{k_1}{k}=9$. The equation then becomes

$$\mathrm{K}=kp\left(\frac{\mathrm{T}_2-\mathrm{T}_1}{\mathrm{T}_1}\right)\left(1-e^{-\frac{s}{\mathrm{L}}}\right)\left(\frac{9\mathrm{L}}{s}+4\right).$$

If, now, the pressure is doubled, L will be halved, and if K_1 is the new value of the deflecting force, then

$$\mathrm{K}_1=2kp\left(\frac{\mathrm{T}_2-\mathrm{T}_1}{\mathrm{T}_1}\right)\left(1-e^{-\frac{2s}{\mathrm{L}}}\right)\left(\frac{9\mathrm{L}}{2s}+4\right).$$

$$\therefore\quad \frac{\mathrm{K}_1}{\mathrm{K}}=\frac{\left(1+e^{-\frac{s}{\mathrm{L}}}\right)\left(\frac{9\mathrm{L}}{s}+8\right)}{\left(\frac{9\mathrm{L}}{s}+4\right)}=\frac{\mathrm{F}_1}{\mathrm{F}},$$

F_1 and F being obtained from the appropriate F$-p$ curve.

If $L=s$ at the pressure p, we have

$$\frac{F_1}{F}=\frac{(1+e^{-1})\times 17}{13}=1\cdot 79.$$

The value of p satisfying this condition can be found from the F—p curve.

If $L=\frac{s}{2}$ at the pressure p,

$$\frac{F_1}{F}=\frac{(1+e^{-2})\times 12\cdot 5}{8\cdot 5}=1\cdot 67.$$

TABLE III.

Air.

No. of Expt.	F.	F_1.	$\frac{F_1}{F}$.	p.	s.	L at ·01 mm.
				mm.	mm.	mm.
3.....	·775	1·39	1·79	·0075	5·68	4·26
3.....	1·15	1·92	1·67	·012	5·68	3·41
6.....	·415	·742	1·79	·0070	7·64	5·35
6.....	·742	1·24	1·67	·014	7·64	5·35
7.....	·54	·90	1·67	·010	8·20	4·10
			Hydrogen.			
1.....	1·065	1·91	1·79	·014	5·78	8·09
2.....	1·36	2·43	1·79	·015	5·31	7·97
3.....	·696	1·16	1·67	·016	8·31	6·65
3.....	·464	·830	1·79	·010	8·31	8·31

The value of p satisfying this equation can similarly be found.

The value of L being known at one pressure, it can be found at any other, since $p\times L$ is constant.

Values of L calculated in the manner indicated are given in Table III.

The variation in the values obtained for L is partly due to limitations of the theory, and partly due to the fact that small errors in the determination of F lead to large errors in the values of L.

In the case of hydrogen, both direct and indirect forces have to be multiplied by $a(2-a)$, a being the accommodation coefficient, but the method used for air to determine L can be used without alteration.

11. *Summary.*

An apparatus for measuring the force between two small, plane, parallel plates, due to a difference of temperature between them at low pressures, is described. It is found that the force is proportional to the temperature difference, other factors remaining constant, and inversely proportional to the square of the distance between the plates, provided that the distance is large compared with the linear dimensions of the plates. Both with air and hydrogen the force is found to increase linearly with the pressure at low pressures, other factors remaining constant, and under these conditions the calculated values of the deflecting force are found to agree with the observed values, allowing for some uncertainty as to the manner in which impinging molecules are reflected from the two plates. At higher pressures the deflecting force increases less rapidly than the linear relation requires, and exhibits a maximum value at about ·07 mm. in the case of air, thereafter slowly declining with increasing pressure. With hydrogen no maximum is obtained, although had measurements been continued at still higher pressures there is no doubt that the deflecting force would have reached a maximum value at about ·13 mm. From the deviations from a linear relation the mean free paths of air and hydrogen molecules at a given pressure have been calculated, and the values obtained agree with the values obtained by other methods as well as can be expected, considering the uncertainties involved in the calculation. Theoretical reasoning is adduced to explain the observed variation of the deflecting force with pressure.

The material of this publication is largely taken from a Thesis approved for the Degree of Doctor of Philosophy in the University of London.

In conclusion, the author would like to thank Professor J. R. Partington for his interest in the work.

Chemistry Department,
East London College,
University of London.

XIII. *Studies in Coordination.* Part I.—*Ion Hydrates.*

By F. J. Garrick *.

1. *Introduction.*

THERE are at present two distinct theories of the formation of such molecular compounds as ammino- and hydrato-complex ions. On the one hand, there is Sidgwick's Coordination Covalency Theory, which is remarkably successful as representing a vast number of chemical phenomena, but which cannot well be applied quantitatively, since nothing is known about the mechanism of this coordinate electron-sharing link. Thus this theory affords little indication as to why the coordination number should have the values actually observed

On the other hand, it is held by many that the mechanism of this type of complex formation is purely electrostatic, depending on the dipole moment and polarizability of the water or ammonia molecule. This view has the advantage of introducing no new concepts, and of being readily susceptible to quantitative investigation. In the present paper an attempt is made by means of such quantitative investigation to show that the theory affords an adequate representation of the observed phenomena.

A qualitative consideration shows that, as is observed, the coordination number should be larger for large ions, but the complex less stable. For, if we consider a number of dipoles, each having its axis radial to a central charge, it is clear that, while all are attracted by the latter, they repel one another, and this repulsion increases with the number of dipoles present. At a particular distance from the central ion it may happen that with six dipoles the attractive force is greater than the repulsive, while with eight the reverse is the case. On increasing the distance, however, the attraction falls off as the inverse cube, the repulsion as the inverse fourth power of the distance, so that at a sufficient distance, even with eight dipoles, the attractive force will exceed the repulsive. Also, if the water or ammonia molecules are considered as impenetrable spheres of fixed radius, for any given coordination number there exists a lower limit to the distance from the centre, when the molecules touch one another but not the central ion. Thus for a small ion when six water molecules are present, they can approach the central ion more closely than when eight are present, and

* Communicated by the Author.

thus the smaller number may correspond to a greater energy of formation. Both these effects can be seen on the figure, which represents the electrostatic energy of a univalent hydrato-complex ion (calculated according to the method to be described) for various coordination numbers and distances from the central ion. This figure shows how, if the complex having the maximum formation energy is assumed to be

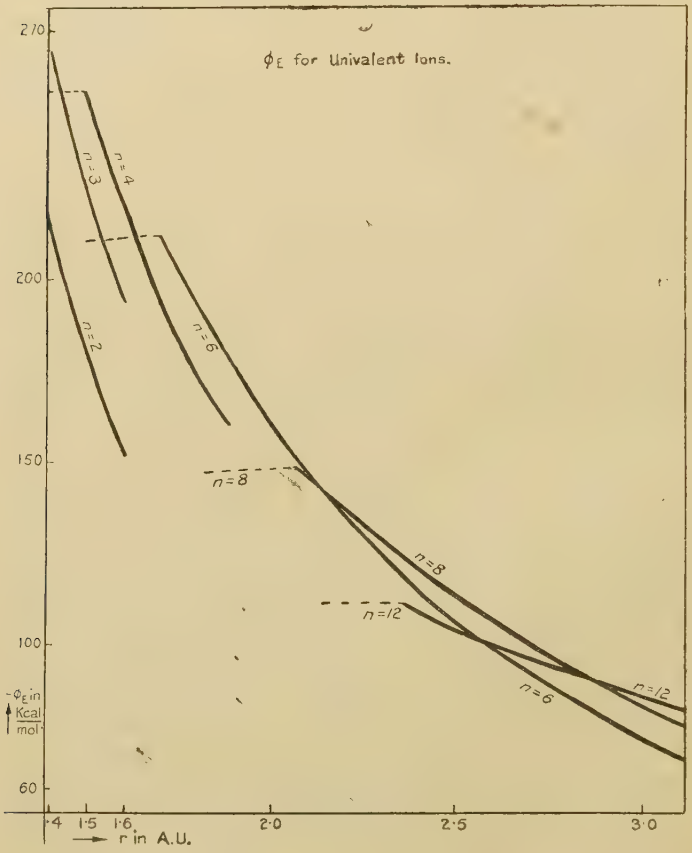

most stable, the coordination number increases with the size of the central ion. A number of other factors must also be considered. First, the molecules are not impenetrable spheres but exert repulsive forces falling off inversely as a high power of the distance. Then, as the above-mentioned lower limits are approached, the potential energy corresponding to these repulsive forces increases rapidly. Also,

the molecules are held in an equilibrium position by the electrostatic forces and the intrinsic repulsive forces between ion and molecules and between the molecules themselves. Thus for a given ion the equilibrium distance is greater, the more molecules are present. All these factors work in the same direction, namely, in favour of a smaller coordination number.

This line of argument will now be treated quantitatively by calculating the energy of formation of various complex ions.

2. *The Electrostatic Energy.*

This may be written

$$\phi_E = \phi_A + \phi_{ER} + \phi_P.$$

Here ϕ_A refers to the attraction between charge and dipoles, ϕ_{ER} to the mutual repulsions of the dipoles, and ϕ_P to the quasi-elastic energy of polarization.

If z be the valency of the ion, and ze its charge, and if there be n molecules, each having the electric moment p, and each having its axis radial to the ion, and at a distance r, we have

$$\phi_A = -npzer^{-2}. \quad . \quad . \quad . \quad . \quad . \quad . \quad (1)$$

Again, if p' be the induced part of the dipole moment of each molecule (so that $p = p' + P$, where P is the permanent dipole moment), and if α be the polarizability, we have

$$p' = \alpha E,$$

where E is the field strength, and thus

$$\phi_P = np'^2/2\alpha. \quad . \quad . \quad . \quad . \quad . \quad . \quad (2)$$

ϕ_{ER} is the sum of a number of terms of the form

$$\frac{p^2}{s^3}(\sin\theta_1 \sin\theta_2 - 2\cos\theta_1 \cos\theta_2).$$

This is the mutual potential energy of two dipoles at a distance s making angles θ_1 and θ_2 with their axes. We only consider cases where the dipoles are arranged radially and symmetrically, so that

$$\theta_1 = 180° - \theta_2.$$

We may write

$$\phi_{ER} = \sum_{k=1}^{k=\frac{n(n-1)}{2}} \frac{p^2}{s_k^3}(1 + \cos^2\theta_k). \quad . \quad . \quad . \quad (3)$$

The following cases are considered:—

1. $n=2$. Here $s=2r$; $\theta=0°$.

2. $n=3$ (equilateral triangle).

$$s_1=s_2=s_3=r\sqrt{3}\ ;\ \theta_1=\theta_2=\theta_3=30°.$$

3. $n=4$ (regular tetrahedron).

$$s_1=s_2=\ldots=s_6=2r\frac{\sqrt{2}}{\sqrt{3}}\ ;\ \theta_1=\theta_2=\ldots=\theta_6=35°{\cdot}77.$$

4. $n=6$ (regular octahedron).

$$s_1=s_2=\ldots=s_{12}=r\sqrt{2}\ ;\ \theta_1=\theta_2=\ldots=\theta_{12}=45°.$$
$$s_{13}=s_{14}=s_{15}=2r\ ;\qquad \theta_{13}=\theta_{14}=\theta_{15}=0°.$$

5. $n=8$ (cube).

$$s_1=s_2=\ldots=s_{12}=\frac{2r}{\sqrt{3}}\ ;\qquad \theta_1=\theta_2=\ldots=\theta_{12}=\cos^{-1}\frac{1}{\sqrt{3}};$$
$$s_{13}=s_{14}=\ldots=s_{24}=\frac{2\sqrt{2}}{\sqrt{3}}.r\ ;\ \theta_{13}=\theta_{14}=\ldots=\theta_{24}=\cos^{-1}\frac{\sqrt{2}}{\sqrt{3}};$$
$$s_{25}=s_{26}=s_{27}=s_{28}=2r\ ;\qquad \theta_{25}=\theta_{26}=\theta_{27}=\theta_{28}=0°.$$

6. $n=12$ (regular icosahedron).

$$s_1=s_2=\ldots=s_{30}=1{\cdot}052\,r\ ;\ \theta_1=\theta_2=\ldots=\theta_{30}=\cos^{-1}0{\cdot}526;$$
$$s_{31}=s_{32}=\ldots=s_{60}=1{\cdot}702\,r\ ;\ \theta_{31}=\theta_{32}=\ldots=\theta_{60}=\cos^{-1}0{\cdot}851;$$
$$s_{61}=s_{62}=\ldots=s_{66}=2r\ ;\qquad \theta_{61}=\theta_{62}=\ldots=\theta_{66}=0°.$$

In these equations p depends on z, r, and n, as follows. We have, as above,

$$p'=\alpha\mathrm{E}. \quad . \quad . \quad . \quad . \quad . \quad . \quad . \quad . \quad (5)$$

The field strength E at a point representing the position of one of the molecules is the vector sum of components due to the central ion and to the other dipoles. We need only consider the components along the line joining the molecule in question to the central ion, since from symmetry the components at right angles to this neutralize one another. The component of the field strength due to the central ion is ze/r^2. That due to the other dipoles is

$$-\mathrm{E}_d=\frac{d\mathrm{V}_d}{dr},$$

where V_d is the potential at the point in question due to the other dipoles.

We have

$$V_d = \sum_{k=1}^{k=(n-1)} \frac{p}{s_k^2} \cos\theta_k ;$$

$$d\theta_k = \frac{dr}{s_k} \sin\theta_k ; \quad ds_k = dr . \cos\theta_k .$$

$$\therefore \quad E_d = -\frac{dV_d}{dr} = \sum_{k=1}^{k=(n-1)} \frac{p}{s_k^3}(1+\cos^2\theta_k). \quad . \quad . \quad (6)$$

Then

$$E = \frac{ze}{r^2} - E_d, \quad \text{and} \quad p = p' + P.$$

$$\therefore \quad p = P + \alpha E = \frac{P + \frac{\alpha ze}{r^2}}{1 + \sum_{k=1}^{k=(n-1)} \frac{\alpha}{s_k^3}(1+\cos^2\theta_k)}. \quad (7)$$

In equations (6) and (7), s_k and θ_k are as given below.

When $n=2$, $s=2r$; $\theta = 0°$.

„ $n=3$, $s_1=s_2=r\sqrt{3}$; $\theta_1=\theta_2=30°$.

„ $n=4$, $s_1=s_2=s_3=\frac{2\sqrt{2}}{\sqrt{3}}r$;

$\theta_1=\theta_2=\theta_3=35^{\circ}\cdot 77$.

„ $n=6$, $s_1=s_2=\ldots=s_4=r\sqrt{2}$;

$\theta_1=\theta_2=\ldots=\theta_4=45°$;

$s_5=2r$; $\theta_5=0°$.

„ $n=8$, $s_1=s_2=s_3=\frac{2r}{\sqrt{3}}$;

$\theta_1=\theta_2=\theta_3=\cos^{-1}\frac{1}{\sqrt{3}}$;

$s_4=s_5=s_6=\frac{2\sqrt{2}}{\sqrt{3}}r$;

$\theta_4=\theta_5=\theta_6=\cos^{-1}\frac{\sqrt{2}}{\sqrt{3}}$;

$s_7=2r$; $\theta_7=0°$.

„ $n=12$, $s_1=s_2=\ldots=s_5=1\cdot 052\,r$;

$\theta_1=\theta_2=\ldots=\theta_5=\cos^{-1}0\cdot 526$;

$s_6=s_7=\ldots=s_{10}=1\cdot 702\,r$;

$\theta_6=\theta_7=\ldots=\theta_{10}=\cos^{-1}0\cdot 851$;

$s_{11}=2r$; $\theta_{11}=0°$.

In applying these equations we consider the case of a hydrato-complex. Then P is $1{\cdot}75\times10^{-18}$ E.S.U., this being the mean of the two latest determinations—1·70 (Williams, *Z. Phys.* xxix. p. 683, 1928) and 1·79 (Stuart, *Z. Phys.* li. p 490, 1928) ; while α is given by $\alpha=3R/4\pi N$, where R is the Lorentz refraction constant for water (=3·71), and N is the Avogadro number ($=6{\cdot}06\times10^{23}$). This gives $\alpha=1{\cdot}46\times10^{-24}$. e, the electronic charge, is taken as $4{\cdot}774\times^{-10}$.

By means of the equations given above the electrostatic part ϕ_E of the energy of a complex ion of given valency and coordination number can be calculated for various values of r, and the results for univalent ions are shown in the figure, where the ordinates represent $-\phi_E$ in k. cal./mol., and the abscissæ r in A.U. The horizontal dotted lines show the energies corresponding to the lower limits of r in various cases, when the water molecule is regarded as an impenetrable sphere of radius about 1·2 A.U. These energies are therefore maxima for the corresponding coordination numbers.

The curves for divalent complexes are not shown, as the relations are closely similar, except that the energies are much greater. From these results alone, and neglecting the other factors mentioned above, it is possible to draw some interesting conclusions, since the other energy terms are for the most part not more than about 15 per cent. of ϕ_E, as will appear later.

First, $-\phi_E$ is less for $n=2$ or 3 than for $n=4$, when r is greater than 1·4. Since the effective radius of a water molecule is about 1·2 A.U., and assuming that the stable complex is that having the maximum energy of formation, this means that for all ordinary ions the maximum coordination number is 4 or more. Then for r greater than 1·65, $-\phi_E$ is greater for $n=6$ than for $n=4$. Thus for ions of radius greater than about 0·5 A.U. the coordination number is 6 or more. The only ordinary ions smaller than this are H^+, Be^{2+}, and possibly Li^+. For the other ions, then, it is enough to consider only $n=6$, 8, or 12 (*cp.* data for Na^+ in Table III.).

The H^+ ion is probably incapable of free existence and in solution is thought to be present as H_3O^+. For Be^{2+} (radius 0·3 A.U.) and possibly Li^+ (radius 0·6 A.U.) the consideration of ϕ_E alone implies that the coordination number is probably 4, but no more definite conclusions than this can be reached, since in the absence of information as to their force constants the more detailed treatment to be described for the other ions cannot be applied to them.

3. *The Determination of the Total Energy in Particular Cases.*

To determine the total energy it is necessary first to find the equilibrium distance for each ion (for, as was pointed out above, this will in general be different for different hydrates of the same ion), and second to estimate the non-electrostatic energy corresponding to the intrinsic repulsive fields. To attain these ends it is necessary to estimate the force laws of the ions and the water molecules. No direct information is available as to the applicability of spherically symmetric fields to a water molecule, nor as to the values of the force constants. But it is at least reasonable to suppose that the force law can be approximately represented by an expression of the type $\lambda r^{-\nu}$, and in the absence of any more definite data the values of λ and ν will be deduced by means of certain more or less plausible assumptions.

The repulsive force fields of a number of ions of inert-gas type have been investigated by Lennard-Jones*. In determining the force constants it is assumed that the "generalized diameters" are proportional to the radii of the outer electron orbits, and it seems reasonable to suppose that they are proportional to the effective radii as measured by any one appropriate method. Now the water molecule may be regarded as a pseudo-atom of the Ne type; that is, the protons are buried inside the electron shell of the oxide ion†. It will be assumed that the resulting electron structure is sufficiently like that of the ions of the Ne type that the same force index (namely, 11) may be applied, and that the generalized diameter of the water molecule is to that of a Ne atom in the ratio of their kinetic theory diameters, that is, according to Landolt-Börnstein, as 1·3 to 1·15.

Then using the notation of Lennard-Jones (except that ν is written instead of n for the index), we have

$$\sigma^{(\nu)}_{H_2O} = \sigma^{(\nu)}_{Ne} \cdot \frac{1{\cdot}3}{1{\cdot}15}, \quad . \quad . \quad . \quad . \quad . \quad (8)$$

$\sigma^{(\nu)}$ is, of course, a function of ν. For the values of ν we use those given by Lennard-Jones for the Ne group, namely 11 for two ions of this type or one of this type and one of Xe type, or 10 for an ion of this type and one of Ar or Kr type.

* Lennard-Jones, Proc. Roy. Soc. A, cix. p. 584 (1925); Lennard, Jones and Taylor, *ibid.* p. 476.

† Knorr, *Z. Anorg. Chem.* cxxix. p. 109 (1923); Paneth and Rabinowitsch, *Ber. d. D. Chem. Ges.* lviii. p. 1138 (1925); Grimm, *Z. Elektrochem.* xxxi. p. 476 (1925). See also Garrick, Phil. Mag. 1929, p. 102.

(The term ion in this connexion, of course, includes neutral atoms, and is here extended to the pseudo-atom H_2O.) Table I. shows the values of $\sigma^{(\nu)}_{H_2O}$ for $\nu=10$ and $\nu=11$. Here the values of $\sigma^{(\nu)}_{Ne}$ are taken from Lennard-Jones (*loc. cit.*), and those of $\sigma^{(\nu)}_{H_2O}$ are derived from them by equation (8).

Table I.

ν.	$\sigma^{(\nu)}_{Ne}$.	$\sigma^{(\nu)}_{H_2O}$.
10	4·63	5·24
11	4·30	4·86

Then to calculate the force constant for an ion and a water molecule, we use the relations

$$\sigma^{(\nu)}_{12}=\frac{(\sigma^{(\nu)}_{11}+\sigma^{(\nu)}_{22})}{2} \quad \text{and} \quad \sigma^{(\nu)}=\left(\frac{\lambda^{(\nu)}}{2{\cdot}06\times10^{-16}.(\nu-1)}\right)^{\frac{1}{\nu-1}}$$

Table II.

Ion.	ν.	$10^8.\sigma^{(\nu)}_{ion}$.	$\frac{1}{2}.10^8.\left(\sigma^{(\nu)}_{ion}+\sigma^{(\nu)}_{H_2O}\right)$.	$\lambda^{(\nu)}_{ion-H_2O}$.
Na^+	11	4·03	4·44	0·612
K^+	10	5·93	5·58	0·972
Rb^+	10	6·41	5·82	1·42
Cs^+	11	6·50	5·68	7·20
Mg^{++}	11	3·51	4·19	0·344
Ca^{++}	10	5·45	5·34	0·655
Sr^{++}	10	5·98	5·61	1·02
Ba^{++}	11	6·01	5·43	4·59

(Lennard-Jones and Taylor, *loc. cit.* pp. 482 and 483). The force constants so obtained are shown in Table II. λ is given in such units that when r is in A.U. the force is in dynes. The values of $\sigma^{(\nu)}_{ion}$ are taken from Lennard-Jones, *loc. cit.* tab. viii.

These constants when substituted in the expression $\lambda r^{-\nu}$ give as a function of r the repulsive force between the above ions and a water molecule. For an ion of known valency and for a particular number of water molecules the net electrostatic force on each water molecule can also be plotted as a function of r, and hence by graphical solution the equilibrium distances for the various systems in question can be obtained. The electrostatic attraction on each molecule, in the line joining it to the central ion, is

$$F_E = p \cdot \frac{dE}{dr}.$$

But

$$E = \frac{ze}{r^2} - \sum_{k=1}^{k=(n-1)} \frac{p}{s_k^3}(1+\cos^2\theta_k). \quad . \quad . \quad . \quad (6)$$

Whence

$$F_E = p \cdot \frac{dE}{dr} = -\frac{2zep}{r^3} + \sum_{k=1}^{k=(n-1)} \frac{p^2}{s_k^4}(5+\cos^2\theta_k)\cos\theta_k.$$

In these equations s_k and θ_k have the values given above for equation (7). In many cases, when the lower limits mentioned above are approached, the mutual intrinsic repulsions of the water molecules must be allowed for. Only the nearest neighbours of each molecule exert an appreciable repulsion. If x be the number of such neighbours, and s and θ the appropriate values of s_k and θ_k, the repulsion due to them is $x.1{\cdot}515\, s^{-11}\cos\theta$. Here 1·515 is, of course, the force constant for two water molecules. All the necessary data are now available for the calculation of the equilibrium distances. By substitution of these and the appropriate values of p (from (7)) in (1), (2), and (3), the electrostatic energy ϕ_E is determined. The total energy ϕ includes two other terms due to the intrinsic repulsions between ion and molecules and between the molecules themselves. These are

$$\phi_{R_1} = \frac{n\lambda}{\nu-1} r^{-(\nu-1)} \quad \text{and} \quad \phi_{R_2} = \frac{nx}{2} \cdot \frac{1{\cdot}515}{10} s^{-10}.$$

Then

$$\phi = \phi_E + \phi_{R_1} + \phi_{R_2}.$$

The results are shown in Table III. $-\phi_{(n=12)}$ is only given for the two largest ions, Cs^+ and Ba^{2+}. It is always less than $-\phi_{(n=8)}$, and, of course, the difference is greater for the smaller ions. The numbers for $Na^+{}_{(n=4)}$ are given in order to illustrate the conclusions of Sect. 2. In the table r is in A.U., and $-\phi$ in k. cal./mol.

TABLE III.

Ion.	n.	r.	$-\phi_E$.	ϕ_{R_1}.	ϕ_{R_2}.	$-\phi$.
Na^+	4	2·05	132	26	4	102
	6	2·22	135	18	3	114
	8	2·53	112	7	8	97
K^+	6	2·58	102	18	1	83
	8	2·83	95	11	3	81
Rb^+	6	2·71	93	15	0	78
	8	2·92	90	10	2	78
Cs^+	6	2·92	81	14	0	67
	8	3·09	82	10	1	71
	12	3·6	70	3	1	66
Mg^{++}	6	1·81	586	75	22	489
	8	2·08	473	14	42	417
Ca^{++}	6	2·08	441	99	5	340
	8	2·28	400	51	17	332
Sr^{++}	6	2·20	390	86	3	301
	8	2·38	369	54	11	304
Ba^{++}	6	2·37	332	66	1	265
	8	2·53	320	33	6	290
	12	2·8	313	19	13	281

4. *Discussion of Results.*

As regards the accuracy of the results the actual values of ϕ are very doubtful, since P is far from certainly known, while it is highly improbable that α remains constant for extreme polarizations. Moreover, the procedure used to determine the force constants may be very unsound, but this does not make much difference since large changes in λ only affect r slightly, while ϕ_{R_1} and ϕ_{R_2} are small terms.

On the other hand, it seems likely that for the same ion with different values of n, the relative magnitudes of ϕ are not far from the truth, since the errors should produce much the same effect in both cases. Since for our present purpose of determining the coordination numbers we need only the relative magnitudes of ϕ for various hydrates of the same ion, it seems that the numbers may be used with fair confidence. Assuming, then, that the most stable hydrate is that for which $-\phi$ is a maximum, we find :—

The coordination number is *six* for

Na^+, K^+, Mg^{++}, and Ca^{++}.

The coordination number is *eight* for

Cs^+, Sr^{++}, and Ba^{++}

(for Rb^+ the hexa- and octo-hydrates are about equally stable).

The coordination number is *four or six* for

Li^+ and Be^{++}.

The coordination number *twelve* is never found.

These results may be compared with Sidgwick's covalency rule ('The Electronic Theory of Valency,' p. 152 : Oxford, 1927), "The maximum covalency (coordination number) is .... for the elements of the first short period 4, for the second short and first long periods 6, and for the heavier elements (Rb to U) 8."

It appears, then, that the electrostatic mechanism agrees satisfactorily with observation in the case of hydrates. It is hoped in later papers to apply the theory to other types of complex, and it may become possible to test it more stringently by direct comparison of theoretical and experimental energy quantities.

The author's thanks are due to Professor Lennard-Jones for kindly criticism and advice.

Inorganic Chemistry Dept.,
The University,
Leeds.

XIV. *The Kirchhoff Formula extended to a Moving Surface.* *By* W. R. Morgans, *M.Sc., late Garrod Thomas Fellow of the University College of Wales, Aberystwyth ; Commonwealth Fellow, California Institute of Technology, Pasadena* *.

1. *The Kirchhoff Formula*

IT is well known that if ϕ be a function which satisfies the wave equation

$$\nabla^2\phi = \frac{1}{c^2}\frac{\partial^2\phi}{\partial t^2}$$

within a volume Ω, bounded by a fixed surface σ, and if ϕ and its first derivatives are continuous and finite within that

* Communicated by Prof. G. A. Schott, F.R.S.

volume, while the second derivatives exist and are finite, then the value of the function ϕ at time t_0 at a point P $(\xi\,\eta\,\zeta)$ within the volume is given by a surface integral extended to the fixed surface σ of the form

$$\phi_P(t_0) = \frac{1}{4\pi}\int_\sigma \left\{ \frac{1}{r}\left[\frac{\partial\phi}{\partial n}\right] - [\phi]\frac{\partial}{\partial n}\left(\frac{1}{r}\right) + \frac{1}{cr}\frac{\partial r}{\partial n}\left[\frac{\partial\phi}{\partial t}\right] \right\} d\sigma. \quad . \; . \; . \quad (1)$$

The square brackets mean that the enclosed functions of the time are to be taken for a time t given in terms of the the time t_0 by the equation

$$t = t_0 - r/c,$$

where r is the distance from the field point P $(\xi\,\eta\,\zeta)$ to an element $d\sigma$ of the surface, and n is the outward normal.

To assume that the surface σ is fixed is an unnecessary limitation on the generality of the solution, and it has been noticed that in a number of physical problems a similar type of solution is required, but one which is applicable to a moving surface S. In such cases the formula given by Kirchhoff for a fixed surface is not applicable. We shall, therefore, present a solution of the wave equation in the form of a surface integral extended to a moving surface S bounding a volume Ω, in which the function ϕ and its derivatives satisfy the conditions of finiteness and continuity as mentioned above. The method followed will be that of Kirchhoff, and the final result will show that the Kirchhoff formula is a particular case of the extended formula when the normal velocity of the surface is equated to zero.

In the following discussion we shall denote a fixed surface by σ, a moving surface by S, a volume integral by $\int_\Omega d\Omega$, a surface integral by $\int_\Omega dS$, and the outward normal to the surface by n.

2. *The Kirchhoff Formula extended to a Moving Surface.*

Let ϕ and χ be two functions which satisfy the equations

$$\nabla^2\phi = \frac{1}{c^2}\frac{\partial^2\phi}{\partial t^2}; \quad \nabla^2\chi = \frac{1}{c^2}\frac{\partial^2\chi}{\partial t^2} \quad . \; . \; . \quad (2)$$

within a volume Ω and such that they and their first derivatives are finite and continuous, while the second derivatives

exist and are finite within Ω. Then Green's Theorem gives for a volume bounded by a surface, moving or fixed, the expression

$$\int_\Omega (\phi \nabla^2 \chi - \chi \nabla^2 \phi)\, d\Omega = \int_S \left(\phi \frac{\partial \chi}{\partial n} - \chi \frac{\partial \phi}{\partial n}\right) dS.$$

If the point P, $r=0$, within the volume Ω be surrounded by a fixed infinitesimal sphere σ, and if we notice that

$$\phi \nabla^2 \chi - \chi \nabla^2 \phi = \frac{1}{c^2} \frac{\partial}{\partial t}\left(\phi \frac{\partial \chi}{\partial t} - \chi \frac{\partial \phi}{\partial t}\right),$$

the above becomes

$$\frac{1}{c^2}\int_\Omega \frac{\partial}{\partial t}\left(\phi \frac{\partial \chi}{\partial t} - \chi \frac{\partial \phi}{\partial t}\right) d\Omega$$

$$= \int_S \left(\phi \frac{\partial \chi}{\partial n} - \chi \frac{\partial \phi}{\partial n}\right) dS + \int_\sigma \left(\phi \frac{\partial \chi}{\partial n} - \chi \frac{\partial \phi}{\partial n}\right) d\sigma. \quad (3)$$

It is known that if the volume Ω, bounded by a surface S with normal velocity v, is a function of the time, the following expression holds :

$$\frac{\partial}{\partial t}\int_\Omega f\, d\Omega = \int_\Omega \frac{\partial f}{\partial t} d\Omega + \int_S v f\, dS,$$

where f is any function of x, y, z, t.

Applying this to (3) we obtain

$$\frac{1}{c^2}\frac{\partial}{\partial t}\int_\Omega \left(\phi \frac{\partial \chi}{\partial t} - \chi \frac{\partial \phi}{\partial t}\right) d\Omega$$

$$= \frac{1}{c^2}\int_S v\left(\phi \frac{\partial \chi}{\partial t} - \chi \frac{\partial \phi}{\partial t}\right) dS + \int_S \left(\phi \frac{\partial \chi}{\partial n} - \chi \frac{\partial \phi}{\partial n}\right) dS$$

$$+ \int_\sigma \left(\phi \frac{\partial \chi}{\partial n} - \chi \frac{\partial \phi}{\partial n}\right) d\sigma. \quad (4)$$

No other surface integral arises from σ due to its having zero normal velocity. If (2) holds for all values of t, we may integrate between two values of t, $-t_1$ and t_2, where t_1 and t_2 are both positive and such that for the most distant parts of S,

$$-t_1 - t_0 + r/c < 0, \quad t_2 - t_0 + r/c > 0.$$

We obtain

$$\frac{1}{c^2}\int_{-t_1}^{t_2} dt \int_S v\left(\phi\frac{\partial\chi}{\partial t}-\chi\frac{\partial\phi}{\partial t}\right)dS+\int_{-t_1}^{t_2} dt\int_S\left(\phi\frac{\partial\chi}{\partial n}-\chi\frac{\partial\phi}{\partial n}\right)dS$$

$$=\frac{1}{c^2}\left|\int_\Omega\left(\phi\frac{\partial\chi}{\partial t}-\chi\frac{\partial\phi}{\partial t}\right)d\Omega\right|_{-t_1}^{t}$$

$$-\int_{-t_1}^{t_2} dt\int_\sigma\left(\phi\frac{\partial\chi}{\partial n}-\chi\frac{\partial\phi}{\partial n}\right)d\sigma. \quad . \quad (5)$$

We are going to particularize the function χ from being any solution of the wave equation to one of the form $F(ct-ct_0+r)/r$, where $F(\zeta)$ vanishes for $\zeta=\pm\infty$, is appreciable only for $\zeta=0$, and is such that

$$\int_{-\infty}^{\infty} F(\zeta)\,d\zeta = 1.$$

That such a function exists may be seen by taking

$$F(\zeta) = \operatorname*{Lt}_{a\to 0}\frac{a}{\pi(\zeta^2+a^2)}.$$

In fact, $F(\zeta)$ can be made to differ from zero outside the arbitrary small interval $+\delta, -\delta, (\delta>0)$ by as small a quantity as we please. By such a choice of $F(\zeta)$ it is seen that χ and $\dfrac{\partial\chi}{\partial t}$ vanish at both limits $-t_1$ and t_2, so that the volume integral in (5) vanishes at both limits. Moreover, as σ is a fixed surface independent of t, the limits of the surface integral are independent of t, so that the order of integration can be changed. Therefore

$$c\int_{-t_1}^{t_2} dt\int_\sigma\left(\phi\frac{\partial\chi}{\partial n}-\chi\frac{\partial\phi}{\partial n}\right)d\sigma$$

$$=\int_\sigma d\sigma\int_{-t_1}^{t_2}\left(\phi\frac{\partial\chi}{\partial n}-\chi\frac{\partial\phi}{\partial n}\right)c\,dt.$$

Due to the change of order of integration and the choice of the function χ, the integral can be evaluated. With Kirchhoff*, its value as the sphere σ tends to zero becomes

* Kirchhoff, 'Zur Theorie der Lichtstrahlen,' 1882.

$4\pi\phi_P(t_0)$. Then a rearrangement of (5) gives, after multiplication by c,

$$4\pi\phi_P(t_0) = \int_{-t_1}^{t_2} c\,dt \int_S \left\{ \chi\left(\frac{\partial\phi}{\partial n} + \frac{v}{c}\frac{\partial\phi}{c\,\partial t}\right) - \phi\left(\frac{\partial\chi}{\partial n} + \frac{v}{c}\frac{\partial\chi}{c\,\partial t}\right)\right\} dS. \quad (6)$$

Here, however, the change of order of integration is not permissible owing to the fact that the limits of the surface integration are functions of the time. To overcome the difficulty of the time integration we shall introduce three curvilinear coordinates u, v, w. The regular surface S * can be represented by equations of the form

$$x = f(uv), \quad y = p(uv), \quad z = q(uv),$$

where we shall assume that the variables u, v are independent of ct and that w alone is a function of ct. The element of area will become in the new system of coordinates

$$dS = \sqrt{EG - F^2}.du\,dv = H\,du\,dv, \quad . \quad . \quad . \quad (7)$$

where

$$E = \left(\frac{\partial x}{\partial u}\right)^2 + \left(\frac{\partial y}{\partial u}\right)^2 + \left(\frac{\partial z}{\partial u}\right)^2,$$

$$F = \frac{\partial x}{\partial u}\frac{\partial x}{\partial v} + \frac{\partial y}{\partial u}\frac{\partial y}{\partial v} + \frac{\partial z}{\partial u}\frac{\partial z}{\partial v},$$

$$G = \left(\frac{\partial x}{\partial v}\right)^2 + \left(\frac{\partial y}{\partial v}\right)^2 + \left(\frac{\partial z}{\partial v}\right)^2.$$

As u and v are both independent of t, the limits of integration in the surface integral, after replacing dS by $H\,du\,dv$, will also be independent of t. Consequently, a change in the order of integration is permissible. From (6) we have

$$4\pi\phi_P(t_0) = \int_S du\,dv \int_{-t_1}^{t_2} \left\{ \chi\left(\frac{\partial\phi}{\partial n} + \frac{v}{c}\frac{\partial\phi}{c\,\partial t}\right) - \phi\left(\frac{\partial\chi}{\partial n} + \frac{v}{c}\frac{\partial\chi}{c\,\partial t}\right)\right\} H\,c\,dt, \quad (8)$$

a form capable of integration.

* We shall assume the conditions given in Goursat-Hedrick, 'Mathematical Analysis,' § 131, to hold.

Again,

$$\chi = \mathrm{F}(ct - ct_0 + r)/r,$$

$$\frac{\partial \chi}{c\,\partial t} = \mathrm{F}'/r\,; \quad \mathrm{F}' = \left[\frac{d}{d\zeta}\mathrm{F}(\zeta)\right]_{\zeta = ct - ct_0 + r},$$

$$\frac{\partial \chi}{\partial n} = \left(-\frac{\chi}{r} + \frac{\partial \chi}{c\,\partial t}\right)\frac{\partial r}{\partial n},$$

$$\frac{d\chi}{c\,dt} = \frac{\partial \chi}{c\,\partial t} + \frac{\partial \chi}{\partial r}\frac{\partial r}{c\,\partial t}$$

$$= \left(1 + \frac{\dot r}{c}\right)\frac{\partial \chi}{c\,\partial t} - \frac{\chi \dot r}{cr},$$

whence

$$\frac{\partial \chi}{c\,\partial t} = \left(\frac{d\chi}{c\,dt} + \frac{\chi \dot r}{cr}\right)\Big/ 1 + \dot r/c,$$

$$\frac{\partial \chi}{\partial n} = \left(\frac{d\chi}{c\,dt} - \frac{\chi}{r}\right)\frac{\partial r}{\partial n}\Big/ 1 + \dot r/c,$$

$$\frac{\partial \chi}{\partial n} + \frac{v}{c}\frac{\partial \chi}{c\,\partial t} = \frac{\dfrac{\partial r}{\partial n} + \dfrac{v}{c}}{1 + \dot r/c}\frac{d\chi}{c\,dt} - \frac{\dfrac{\partial r}{\partial n} - \dfrac{\dot r v}{c^2}}{1 + \dot r/c}\frac{\chi}{r}.$$

The integral (8) becomes

$$4\pi\phi_{\mathrm{P}}(t_0) = \int_{\mathrm{S}} du\,dv \int_{-t_1}^{t} \left\{ \chi\left(\frac{\partial \phi}{\partial n} + \frac{v}{c}\frac{\partial \phi}{c\,\partial t} + \frac{\dfrac{\partial r}{\partial n} - \dfrac{\dot r v}{c^2}}{1 + \dot r/c}\frac{\phi}{r}\right) - \frac{\dfrac{\partial r}{\partial n} + \dfrac{v}{c}}{1 + \dot r/c}\phi\frac{d\chi}{c\,dt}\right\} \mathrm{H}\,c\,dt. \quad (9)$$

Let us consider any integral of the form $\int_{-t_1}^{t_2} \chi\mu c\,dt$, where μ is any function of x, y, z, ct denoted by $\mu(ct)$. With

$$\zeta = ct - ct_0 + r, \qquad d\zeta = dt(c + \dot r),$$

the integral transforms into

$$\int_{-t_1}^{t_2} \chi\mu c\,dt = \int_{-t_1}^{t_2} \frac{\mathrm{F}(ct - ct_0 + r)}{r}\,\mu(ct)\,c\,dt$$

$$= \int_{-\zeta_1}^{\zeta_2} \frac{\mathrm{F}\cdot\zeta)}{r}\,\frac{\mu(\zeta + ct_0 - r)}{(1 + \dot r/c)}\,d\zeta \qquad \zeta_1 > 0,\ \zeta_2 > 0.$$

Due to the choice of $F(\zeta)$ the contribution is obtained only in the neighbourhood of $\zeta=0$, which leads to the value given by

$$\int_{-t_1}^{t_2} \chi \mu c \, dt = \frac{\mu(ct_0 - r)}{r(1+\dot{r}/c)},$$

where μ must be taken at time $t_0 - r/c$.

The first part of the integral (9) will give the contribution

$$\int_S du\,dv \left\{ \frac{H}{r(1+\dot{r}/c)} \left(\frac{\partial \phi}{\partial n} + \frac{v}{c} \frac{1}{c} \frac{\partial \phi}{\partial t} + \frac{\dfrac{\partial r}{\partial n} - \dfrac{\dot{r}v}{c^2}}{1+\dot{r}/c} \frac{\phi}{r} \right) \right\}_{t=t_0-r/c}.$$

Let us consider an integral of the form

$$\int_{-t_1}^{t_2} \mu \frac{d\chi}{c\,dt} \, c\,dt.$$

We have

$$\int_{-t_1}^{t_2} \mu \frac{d\chi}{c\,dt} \, c\,dt = \mu\chi \Big|_{-t_1}^{t_2} - \int_{-t_1}^{t_2} \chi \frac{d\mu}{c\,dt} \, c\,dt.$$

The former portion vanishes by the choice of χ; the latter is in the previous integrable form. The remaining part of the integral (9) will therefore give a contribution

$$\int_S du\,dv \frac{1}{r(1+\dot{r}/c)} \frac{d}{c\,dt} \left(\frac{\dfrac{\partial r}{\partial n} + \dfrac{v}{c}}{1+\dot{r}/c} \phi H \right)_{t=t_0-r/c}.$$

The complete expression for (9) can be written as

$$4\pi\phi_P(t_0) = \int_S \frac{du\,dv}{r(1+\dot{r}/c)} \left[\left(\frac{\partial \phi}{\partial n} + \frac{v}{c} \frac{1}{c} \frac{\partial \phi}{\partial t} + \frac{\dfrac{\partial r}{\partial n} - \dfrac{\dot{r}v}{c^2}}{1+\dot{r}/c} \frac{\phi}{r} \right) H + \frac{d}{c\,dt} \left(\frac{\dfrac{\partial r}{\partial n} + \dfrac{v}{c}}{1+\dot{r}/c} \phi H \right) \right]_{t=t_0-r/c}$$

$$= \int_S \frac{dS}{r(1+\dot{r}/c)} \left[\frac{\partial \phi}{\partial n} + \frac{v}{c} \frac{1}{c} \frac{\partial \phi}{\partial t} + \frac{\dfrac{\partial r}{\partial n} - \dfrac{\dot{r}v}{c^2}}{1+\dot{r}/c} \frac{\phi}{r} + \frac{1}{H} \frac{d}{c\,dt} \left(\frac{\dfrac{\partial r}{\partial n} + \dfrac{v}{c}}{1+\dot{r}/c} \phi H \right) \right]_{t=t_0-r/c},$$

which gives the value of ϕ at time t_0 at a point P. For any time t the expression can be written as

$$4\pi\phi_P(t) = \int_S \frac{dS}{r(1+\dot{r}/c)}\left[\frac{\partial\phi}{\partial n} + \frac{v}{c}\frac{\partial\phi}{c\,\partial t} + \frac{\frac{\partial r}{\partial n} - \frac{\dot{r}v}{c^2}}{1+\dot{r}/c}\frac{\phi}{r} + \frac{1}{H}\frac{d}{c\,dt}\left(\frac{\frac{\partial r}{\partial n}+\frac{v}{c}}{1+\dot{r}/c}\phi H\right)\right]_{r=t-r/c}.$$

In this it must be noticed that dS denotes the element of the moving surface whose velocity in the direction of the outward normal is v.

3. *Verification of the Solution.*

a. Its reduction to the Kirchhoff Form.

When the surface is fixed, $\dot{r}=0$, $v=0$, H and $\frac{\partial r}{\partial n}$ are both independent of the time, and $\frac{d}{dt}=\frac{\partial}{\partial t}$. With these values the integral becomes

$$4\pi\phi_P(t_0) = \int_S \frac{dS}{r}\left[\frac{\partial\phi}{\partial n} + \frac{\partial r}{\partial n}\frac{\phi}{r} + \frac{1}{c}\frac{\partial r}{\partial n}\frac{\partial\phi}{\partial t}\right]_{t=t_0-r/c}$$

$$= \int_S \left\{\frac{1}{r}\left[\frac{\partial\phi}{\partial n}\right] - [\phi]\frac{\partial}{\partial n}\left(\frac{1}{r}\right) + \frac{1}{cr}\frac{\partial r}{\partial n}\left[\frac{\partial\phi}{\partial t}\right]\right\},$$

which on comparison with (1) is seen to be the Kirchhoff form.

b. Its reduction to the Poisson Formula.

As the Poisson formula is only a particular case of the Kirchhoff formula when the surface S is a sphere, centre the point P, the more general solution will reduce to the Poisson form in the same particular case.

4. *The Form taken by the Extended Formula when the Surface* S *is a Sphere of Radius* $\rho=ct$.

When the surface S is a sphere expanding with a radial velocity equal to that of light, the expression takes a comparatively simple form. In this case the following curvilinear coordinates may be used :—

$u=\mu=\cos\theta$; $v=\psi$; $w=\rho=ct$;

θ=angle between x-axis and the vector R ;

ψ=angle between the plane PQO and the xy-plane (see fig. 1).

Fig. 1.

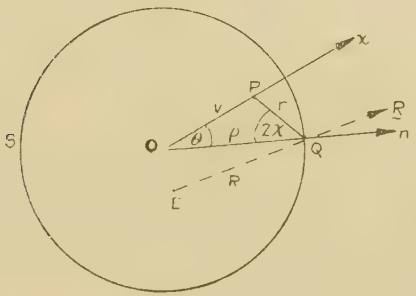

Then

$$du\,dv=d\mu\,d\psi\,;\quad \mathrm{H}=\rho^2\,;\quad d\mathrm{S}=\rho^2\,d\mu\,d\psi\,;\quad v=\dot\rho=c\,;$$

$$\frac{\partial r}{\partial n}=\frac{\partial r}{\partial\rho}=\cos 2\chi\,;\quad \dot r=\dot\rho\cos 2\chi=c\cos 2\chi\,;$$

$$\frac{\partial r}{\partial n}+\frac{v}{c}=1+\cos 2\chi=1+\dot r/c\,;$$

$$\frac{\partial r}{\partial u}-\frac{\dot r v}{c^2}=\cos 2\chi-\cos 2\chi=0.$$

Substituting these values the extended formula becomes

$$4\pi\phi_{\mathrm{P}}(t_0)$$

$$=\int_{\mathrm{S}}\frac{d\mu\,d\psi}{r(1+\cos 2\chi)}\left[\rho^2\left(\frac{\partial\phi}{\partial\rho}+\frac{\partial\phi}{c\,\partial t}\right)+\frac{d}{c\,dt}\,(\rho^2\phi)\right]_{t=t_0-r/c}$$

$$=\int_{\mathrm{S}}\frac{2\rho\,d\mu\,d\psi}{r(1+\cos 2\chi)}\left[\rho\left(\frac{\partial\phi}{\partial\rho}+\frac{\partial\phi}{c\,\partial t}\right)+\phi\right]_{t=t_0-r/c}$$

$$=\int_{\mathrm{S}}\frac{2\rho\,d\mu\,d\psi}{r(1+\cos 2\chi)}\left[\frac{d}{c\,dt}(\rho\phi)\right]_{t=t_0-r/c}.\quad\ldots\quad(10)$$

As remarked previously, the function ϕ is continuous within the surface S. If ϕ has, within S, a number of singularities,

they must be surrounded by surfaces σ, moving or fixed, to each of which the extended integral must be applied. Should these surfaces be chosen as fixed, then, according to $3a$, the extended form reduces to the Kirchhoff form. In the peripharactic region, bounded within by the surfaces surrounding the singularities and on the outside by the sphere S, the function is continuous. Consequently, the value of ϕ at the point P at time t_0 will be given by the modified Kirchhoff formula extended to the expanding sphere together with the integrals extended to the boundaries surrounding the singularities, due precaution being taken to the sign of the outward normal.

In the succeeding case this expanding sphere can be conveniently taken as a boundary, and the only singularity will be a simple one to be excluded by a fixed sphere. Hence two integrals will occur: the integral (10) applied to the expanding sphere, and a Kirchhoff integral extended to this fixed sphere surrounding the singularity.

5. *A Wave Function ϕ which has a Singularity moving along a Curve.*

If we take for ϕ * the expression

$$\phi = f(\tau)/\mathrm{KR},$$

where

$$\mathrm{R}^2 = [x-\xi(\tau)]^2+[y-\eta(\tau)]^2+[z-\zeta(\tau)]^2 = c^2(t-\tau)^2, \quad (11)$$

$$\mathrm{K} = 1-\frac{[x-\xi(\tau)]\dot{\xi}(\tau)+[y-\eta(\tau)]\dot{\eta}(\tau)+[z-\zeta(\tau)]\dot{\zeta}(\tau)}{c\mathrm{R}},$$

and $f(\tau)$ is any function of the variable τ which is a solution of (11), then ϕ will be a solution of the wave equation which has a singularity moving along a curve Γ given by

$$x = \xi(\tau), \quad y = \eta(\tau), \quad z = \zeta(\tau).$$

Here the function ϕ is a function of τ as well as of x, y, z explicitly. We shall also denote by ρ the quantity

$$\rho^2 = x^2+y^2+z^2.$$

If this singularity be taken as an electron, the variable τ will denote the proper time, $\xi(\tau)$, $\eta(\tau)$, $\zeta(\tau)$ its coordinates, x, y, z a field-point, and ϕ a retarded potential. If, further, we

* Proc. Lond. Math. Soc. [2] i. p. 154 (1903).

suppose that this electron be at rest at the origin O, $\rho=0$, prior to the time $\tau=0$, and if at the instant $\tau=0$ it be set in motion along the curve Γ, then electromagnetic waves emanate from the electron into the surrounding medium with velocity c, the wave boundary being an expanding sphere of radius $\rho=ct$. The electron at time τ will occupy a position E given by $\mathrm{R}=0$ and the wave boundary will correspond to the sphere $\rho=ct$ mentioned in § 4.

6. *Application of the Formula to the Wave Function* $\phi=f(\tau)/\mathrm{KR}$.

In order to apply the extended formula to the function ϕ and thus obtain a further verification of the formula by identifying the value $\phi_{\mathrm{P}}(t_0)$ with the value obtained from the integral, we shall take as the expanding surface S the wave boundary $\rho=ct$, and as the boundary surrounding the electron a fixed sphere σ, centre at the origin $\rho=0$. Between the two spheres the function ϕ is continuous. Therefore we have

$$\begin{aligned}4\pi\phi_{\mathrm{P}}(t_0) &= \int_{\mathrm{S}}\frac{2\rho\,d\mu\,d\psi}{r(1+\cos 2\chi)}\left[\left[\rho\left(\frac{\partial\phi}{\partial\rho}+\frac{\partial\phi}{c\,\partial t}\right)+\phi\right]_{\tau=t-\mathrm{R}/c}\right]_{t=t_0-r/c}\\ &\quad+\int_{\sigma}\frac{d\sigma}{r}\left[\left[\frac{\partial\phi}{\partial n}+\frac{\partial\phi}{c\,\partial t}\frac{\partial r}{\partial n}+\frac{\phi}{r}\frac{\partial r}{\partial n}\right]_{\tau=t-\mathrm{R}/c}\right]_{t=t_0-r/c}. \qquad (12)\\ &=\mathrm{I}_1+\mathrm{I}_2.\end{aligned}$$

The inner square brackets mean that the enclosed functions of the time must be calculated before τ is given the value $t-\mathrm{R}/c$. After performing the differentiations in the enclosed functions, τ is set equal to $t-\mathrm{R}/c$. The function then becomes a function of t in which we must set $t=t_0-r/c$.

For the evaluation of these integrals a number of relations are required. They can be easily evaluated and are as follows*:—

$$1/\mathrm{K}=\frac{\partial\tau}{\partial t}, \qquad (13)$$

$$\mathrm{K}=\frac{\partial t}{\partial\tau}=1+\frac{1}{c}\frac{\partial\mathrm{R}}{\partial\tau}=1-\frac{(\mathbf{v}\mathbf{R}_1)}{c}, \qquad (14)$$

* Schott, 'Electromagnetic Radiation,' chap. III.

where $\mathbf{R}_1$ is the unit vector in the direction of the vector $\mathbf{R}$, and $(\mathbf{vR}_1)$ is a scalar product.

$$\frac{\partial\tau}{\partial x}=-\frac{x-\xi}{c\mathrm{RK}},$$

$$\frac{\partial\tau}{\partial\rho}=\sum_{x,y,z}\frac{x}{\rho}\frac{\partial\tau}{\partial x}=-\frac{1}{c\mathrm{K}}\sum_{x,y,z}\frac{x-\xi}{\mathrm{R}}\frac{x}{\rho}, \quad . \quad (15)$$

$$\frac{\partial}{\partial x}(\mathrm{KR})_{\tau=\text{const.}}=\frac{x-\xi}{\mathrm{R}}-\frac{\dot{\xi}}{c},$$

$$\sum_{x,y,z}\frac{x}{\rho}\frac{\partial}{\partial x}(\mathrm{KR})_{\tau=\text{const.}}=\sum_{xyz}\left(\frac{x}{\rho}\frac{x-\xi}{\mathrm{R}}-\frac{x}{\rho}\frac{\dot{\xi}}{c}\right), \quad (16)$$

$$\frac{\partial}{c\,\partial\tau}(\mathrm{KR})=\mathrm{K}-k^2-\frac{(\mathbf{vR})}{c^2}, \quad . \quad . \quad (17)$$

$$k^2=1-\frac{v^2}{c^2}=1-\beta^2.$$

7. *The Integral* I_1 *extended to the Expanding Sphere* $\rho=ct$ *vanishes.*

It is known that $\tau=t-\mathrm{R}/c$ always, and as the wave boundary corresponds to the proper time $\tau=0$, we find that $\mathrm{R}=ct$. But as $\rho=ct$, then $\mathrm{R}=\rho$. It has been stated, however, that we cannot put $\tau=0$ and the consequent values $\mathrm{R}=\rho$, $\xi=\eta=\zeta=0$ before differentiation, but rather we must differentiate first and afterwards set $\mathrm{R}=\rho$, and $\xi=\eta=\zeta=0$ (see fig. 1).

Now as ρ is the outward normal, we have

$$\frac{\partial\phi}{\partial n}=\frac{\partial\phi}{\partial\rho}=\sum_{xyz}\frac{x}{\rho}\left(\frac{\partial\phi}{\partial x}\right)_{\tau=\text{const.}}+\left(\frac{\partial\phi}{\partial\tau}\frac{\partial\tau}{\partial\rho}\right)_{t=\text{const.}}$$

$$=-\frac{f(\tau)}{\mathrm{K}^2\mathrm{R}^2}\sum_{xyz}\frac{x}{\rho}\frac{\partial}{\partial x}(\mathrm{KR})_{\tau=\text{const.}}+\frac{\partial\phi}{\partial\tau}\sum\frac{x}{\rho}\frac{\partial\tau}{\partial x}.$$

Using expressions (15) and (16) it becomes

$$=-\frac{f(\tau)}{\mathrm{K}^2\mathrm{R}^2}\sum_{xyz}\left(\frac{x}{\rho}\frac{x-\xi}{\mathrm{R}}-\frac{x}{\rho}\frac{\dot{\xi}}{c}\right)-\frac{1}{c\mathrm{K}}\frac{\partial\phi}{\partial\tau}\sum_{xyz}\frac{x-\xi}{\mathrm{R}}\frac{x}{\rho}.$$

Again,

$$\frac{\partial\phi}{c\,\partial t}=\frac{\partial\phi}{c\,\partial\tau}\frac{\partial\tau}{\partial t}.$$

Using (13) we obtain

$$\frac{\partial \phi}{c\,\partial t} = \frac{1}{c\mathrm{K}} \frac{\partial \phi}{\partial \tau}.$$

Consequently,

$$\rho\left(\frac{\partial \phi}{\partial \rho} + \frac{\partial \phi}{c\,\partial t}\right) + \phi = \frac{f(\tau)}{\mathrm{KR}}\left[1 - \frac{\rho}{\mathrm{KR}} \sum_{xyz}\left(\frac{x}{\rho}\frac{x-\xi}{\mathrm{R}} - \frac{x}{\rho}\frac{\dot{\xi}}{c}\right)\right]$$

$$+ \frac{\rho}{\mathrm{K}} \frac{\partial \phi}{c\,\partial \tau}\left[1 - \sum_{xyz} \frac{x-\xi}{\mathrm{R}} \frac{x}{\rho}\right].$$

We may now put $\mathrm{R}=\rho$, $\xi=\eta=\zeta=0$, and the expression, if we take account of (14), is seen to vanish.

Thus we have the result that when the expanding surface S is a sphere whose radial velocity is equal to that of light and when the function ϕ is a solution of the wave equation corresponding to an isotropic wave expanding outwards from the origin, the extended formula applied to this surface vanishes. The value of ϕ will depend solely upon the singularities of ϕ within S.

In this particular case it is a simple singularity and we are left to determine the integral I_2.

8. *The Kirchhoff Integral* I_2.

To effect this latter integration we shall suppose that P is a point within the expanding sphere S such that it tends towards the surface $\mathrm{R}=ct_0$. As P tends towards this sphere we can then assume that the fixed sphere σ, of radius ρ, tends simultaneously towards a limiting sphere at the origin O. For this purpose it is necessary that $ct_0=\nu+2\rho$, where ν is the distance from the origin O to the field-point P. Then as $\nu \rightarrow ct_0$, $\rho \rightarrow$ zero.

Again, every element $d\sigma$, though contributing towards the integral, corresponds to different times t. Various elements lying at different distances r from P will correspond to different times $t=t_0-r/c$, which can equally well be represented by $t=\tau+\mathrm{R}/c$, i. e., to different times τ of the electron. Therefore the electron has, for an element $d\sigma$ of the surface, a position E at time τ such that the contribution taken in the integral at time t comes from the electron at E at time τ. The outward normal has the direction of the inward drawn radius $-\rho$ (see fig. 2).

In this case we have

$$\frac{\partial\phi}{\partial n}=-\frac{\partial\phi}{\partial\rho}=-\sum_{xyz}\frac{x}{\rho}\frac{\partial\phi}{\partial x}_{\tau=\text{const.}}-\frac{\partial\phi}{\partial\tau}\frac{\partial\tau}{\partial\rho}_{t=\text{const.}}$$

$$=\frac{f(\tau)}{\mathrm{K}^2\mathrm{R}^2}\sum_{xyz}\frac{x}{\rho}\frac{\partial}{\partial x}(\mathrm{KR})_{\tau=\text{const.}}-\frac{\partial\tau}{\partial\rho}\frac{\partial\phi}{\partial\tau}_{t=\text{const.}}. \quad (18)$$

$$\frac{\partial\phi}{\partial\tau}_{t=\text{const.}}=\frac{f'(\tau)}{\mathrm{KR}}-\frac{f(\tau)}{\mathrm{K}^2\mathrm{R}^2}\frac{\partial}{\partial\tau}(\mathrm{KR}). \quad (19)$$

Fig. 2.

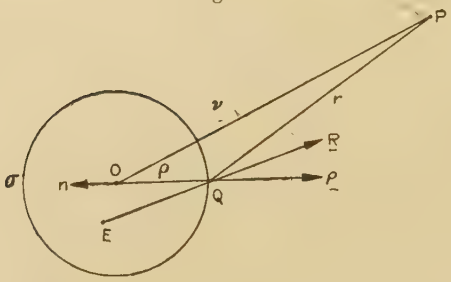

Using the relations (19), (15), (16), $\frac{\partial\phi}{\partial n}$ becomes

$$\frac{\partial\phi}{\partial n}=\frac{f(\tau)}{\mathrm{K}^2\mathrm{R}^2}\sum_{xyz}\left(\frac{x}{\rho}\frac{x-\xi}{\mathrm{R}}-\frac{x}{\rho}\frac{\dot{\xi}}{c}\right)+\frac{f'(\tau)}{c\,\mathrm{K}^2\mathrm{R}}\sum_{xyz}\frac{x-\xi}{\mathrm{R}}\frac{x}{\rho}$$

$$-\frac{f(\tau)}{c\,\mathrm{K}^3\mathrm{R}^2}\frac{\partial(\mathrm{KR})}{\partial\tau}\sum_{xyz}\frac{x-\xi}{\mathrm{R}}\frac{x}{\rho}. \quad (20)$$

Also

$$\frac{\partial\phi}{c\,\partial t}=\frac{\partial\phi}{c\,\partial\tau}\frac{\partial\tau}{\partial t}=\frac{1}{c\mathrm{K}}\frac{\partial\phi}{\partial\tau}=\frac{f'(\tau)}{c\,\mathrm{K}^2\mathrm{R}}-\frac{f(\tau)}{\mathrm{K}^3\mathrm{R}^2}\frac{\partial}{c\,\partial\tau}(\mathrm{KR})$$

$$\frac{\partial r}{\partial n}=-\frac{\partial r}{\partial\rho}=-\sum_{xyz}\frac{x}{\rho}\frac{\partial r}{\partial x}=-\cos(r\rho).$$

Hence

$$\frac{\partial\phi}{c\,\partial t}\frac{\partial r}{\partial n}=-\frac{f'(\tau)\cos(r\rho)}{c\,\mathrm{K}^2\mathrm{R}}+\frac{f(\tau)}{\mathrm{K}^3\mathrm{R}^2}\frac{\partial}{c\,\partial\tau}(\mathrm{KR})\cos(r\rho), \quad (21)$$

$$\frac{\phi}{r}\frac{\partial r}{\partial n}=-\frac{f(\tau)}{\mathrm{KR}r}\cos(r\rho). \quad (22)$$

From (20), (21), (22) we find that

$$\frac{\partial\phi}{\partial n}+\frac{\partial\phi}{c\,\partial t}\frac{\partial r}{\partial n}+\frac{\phi}{r}\frac{\partial r}{\partial n}$$

$$=\frac{f(\tau)}{\mathrm{K}^2\mathrm{R}^2}[\cos(\rho\mathrm{R})-\beta\cos(v\rho)]$$

$$-\frac{f(\tau)}{\mathrm{K}^3\mathrm{R}^2}[\cos(\rho\mathrm{R})-\cos(r\rho)]\frac{\partial}{c\,\partial\tau}(\mathrm{KR})$$

$$-\frac{f(\tau)}{\mathrm{KR}r}\cos(r\rho)+\frac{f'(\tau)}{c\,\mathrm{K}^2\mathrm{R}}[\cos(\rho\mathrm{R})-\cos(r\rho)], \quad (23)$$

where we have used the simplified notation

$$\cos(\rho\mathrm{R})=\sum_{xyz}\frac{x}{\rho}\frac{x-\xi}{\mathrm{R}}, \text{ etc.}$$

Substituting (17) in this expression, the integral becomes

$$\mathrm{I}_2=\int_\sigma\frac{d\sigma}{r}\Big[\frac{f(\tau)}{\mathrm{K}^2\mathrm{R}^2}\{\cos(r\rho)-\beta\cos(v\rho)\}$$

$$+\frac{k^2f(\tau)}{\mathrm{K}^3\mathrm{R}^2}\{\cos(\rho\mathrm{R})-\cos(r\rho)\}$$

$$+\frac{f(\tau)}{\mathrm{K}^3\mathrm{R}^2}\frac{(\dot{\mathrm{v}}\mathrm{R})}{c^2}\{\cos(\rho\mathrm{R})-\cos(r\rho)\}$$

$$-\frac{f(\tau)}{\mathrm{KR}r}\cos(r\rho)+\frac{f'(\tau)}{c\,\mathrm{K}^2\mathrm{R}}\{\cos(\rho\mathrm{R})-\cos(r\rho)\}\Big].$$

Neglecting higher powers of ρ and $c\tau$ than squares and products, we have

$$r=(v^2+\rho^2-2v\rho\mu)^{1/2} \qquad \mu=\cos\theta$$

$$=v-\rho\mu,$$

$$ct_0=v+2\rho \qquad \text{or} \qquad c\tau=(2+\mu)\rho-\mathrm{R}.$$

Hence

$$\mathrm{R}^2=\{c\tau-(2+\mu)\rho\}^2$$

$$=\rho^2-2\rho(\xi\cos\theta+\eta\sin\theta\cos\psi+\zeta\sin\theta\sin\psi)$$

$$+\xi^2+\eta^2+\zeta^2, \quad (24)$$

$\cos\theta$, $\sin\theta\cos\psi$, $\sin\theta\sin\psi$ being the direction cosines of OQ, and $\mathrm{R}=\mathrm{EQ}$.

By the choice of axes we may write

$$\begin{aligned}\xi(\tau) &= \dot{\xi}_0\tau + \tfrac{1}{2}\ddot{\xi}_0\tau^2 + \ldots,\\ \eta(\tau) &= \dot{\eta}_0\tau + \tfrac{1}{2}\ddot{\eta}_0\tau^2 + \ldots,\\ \zeta(\tau) &= \tfrac{1}{2}\ddot{\zeta}_0\tau^2 + \ldots \qquad \dot{\zeta}_0 = 0,\\ f(\tau) &= f(0) + f'(0)\tau + \ldots.\end{aligned}$$

To the same order of approximation we find

$$\left.\begin{aligned}&\xi\cos\theta + \eta\sin\theta\cos\psi + \zeta\sin\theta\sin\psi\\ &\quad = (\dot{\xi}_0\cos\theta + \dot{\eta}_0\sin\theta\cos\psi)\tau\\ &\quad = c\tau\beta\cos(v\rho)\\ &\quad = c\tau\beta\cos\chi\\ &\quad = c\tau(1-\mathrm{K}).\end{aligned}\right\} \qquad (25)$$

If we substitute these values in (24), by a rearrangement we see that

$$k^2c^2\tau^2 - 2c\tau\rho(1+\mu+\mathrm{K}) + \rho^2[(2+\mu)^2-1] = 0.$$

Both roots are positive for $|\mu| < 1$ and $|\mathrm{K}| < 1$ and are given by

$$k^2c\tau = \rho(1+\mu+\mathrm{K} \mp \mathrm{S}), \qquad (26)$$

where

$$\begin{aligned}\mathrm{S}^2 &= (1+\mu+\mathrm{K})^2 - k^2[(2+\mu)^2-1]\\ &= [(2+\mu)\beta - \cos\chi]^2 + k^2\sin^2\chi > 0.\end{aligned}$$

Assuming the square root to have the positive sign, the negative sign must be taken in the expression (26) in order to make R positive, for

$$\begin{aligned}k^2\mathrm{R} &= k^2[(2+\mu)\rho - c\tau]\\ &= \rho[\mathrm{S} + \beta\cos\chi - \beta^2(2+\mu)]\end{aligned}$$

by the equations (25), (26).

Again by the equations (25) and (26),

$$\begin{aligned}\mathrm{KR} &= \mathrm{R} - [(x-\xi)\dot{\xi} + (y-\eta)\dot{\eta} + (z-\zeta)\dot{\zeta}]/c\\ &\to \mathrm{R} - \rho\beta\cos\chi + \beta^2c\tau.\end{aligned}$$

As $\rho \to$ zero, $\cos(r\rho) \to -\mu$, $\mathrm{R}\cos(\mathrm{R}\rho) = \rho - c\tau\beta\cos\chi$.

Therefore that part of the integrand

$$f(\tau)\left[\frac{\cos(r\rho)-\beta\cos(v\rho)}{\mathrm{K}^2\mathrm{R}^2}+k^2\frac{\cos(\rho\mathrm{R})-\cos(r\rho)}{\mathrm{K}^3\mathrm{R}^2}\right]$$

will tend to the value

$$f(0)\left[-\frac{\mu+\beta\cos\chi}{\rho^2\mathrm{S}^2}+\frac{k^2(\rho-c\tau\beta\cos\chi)+k^2\mu\mathrm{R}}{\rho^3\mathrm{S}^3}\right]$$

$$=f(0)\left[-\frac{\mu+\beta\cos\chi}{\rho^2\mathrm{S}^2}+\frac{k^2+(\mu+\beta\cos\chi)\mathrm{S}-\beta^2\mu(2+\mu)-\beta\cos\chi(2-\beta\cos\chi)}{\rho^2\mathrm{S}^3}\right]$$

$$=f(0)\frac{\mathrm{K}^2-\beta^2(1+\mu)^2}{\rho^2\mathrm{S}^3}. \quad . \quad . \quad . \quad . \quad . \quad . \quad . \quad . \quad . \quad . \quad (27)$$

Moreover, the remaining terms of the integrand, when taken in conjunction with the element $d\sigma$, are going to give terms of the order ρ which will vanish as ρ tends to zero. The principal part of the integral may be written, therefore, as

$$\mathrm{I}_2=\frac{f(0)}{\nu}\int_{\mu=-1}^{+1}\int_{\psi=0}^{2\pi}\frac{\mathrm{K}^2-\beta^2(1+\mu)^2}{\mathrm{S}^3}d\mu\,d\psi. \quad . \quad (28)$$

Let

$$s=1+\mu=1+\cos\theta\,; \qquad \beta=\cos j,$$

$$\nu=\cos\theta\cos\alpha+\sin\theta\sin\alpha\cos\psi=\cos\omega.$$

We know that

$$\mathrm{K}=1-\beta\cos\theta\cos\alpha-\beta\sin\theta\sin\alpha\cos\psi$$

$$=1-\beta\cos\omega$$

$$=1-\nu\cos j,$$

$\alpha=$ angle which electron makes with OP,

$$\mathrm{S}^2=\cos^2 j\,[(\sec j-\nu)^2+2s(1-\nu\sec j)+s^2].$$

We have

$$\sin\omega\,d\omega=\sin\theta\sin\alpha\sin\psi\,d\psi \quad \text{when } \theta \text{ is kept constant.}$$

Also

$$\sin^2\theta\sin^2\alpha\sin^2\psi$$

$$=\sin^2\theta\sin^2\alpha-(\cos\omega-\cos\theta\cos\alpha)^2$$

$$=1-\cos^2\theta-\cos^2\omega-\cos^2\alpha+2\cos\theta\cos\omega\cos\alpha.$$

The integral to be evaluated is

$$I_2 = \frac{f(0)}{\nu}\int_0^{\pi}\sin\theta\,d\theta\int_0^{2\pi}d\psi\,\frac{K^2-\beta^2s^2}{S^3}$$

$$= \frac{2f(0)}{\nu}\int_0^{\pi}\sin\theta\,d\theta\int_{|\theta-\alpha|}^{\theta+\alpha}\frac{K^2-\beta^2s^2}{S^3}$$

$$\times\frac{\sin\omega\,d\omega}{\sqrt{1-\cos^2\theta-\cos^2\omega-\cos^2\alpha+2\cos\theta\cos\omega\cos\alpha}}.$$

Now

$$\frac{\pi}{2}\sum_0^{\infty}(2n+1)P_n(\cos\alpha)\,P_n(\cos\theta)\,P_n(\cos\omega)$$

$$= 1/\sqrt{1-\cos^2\theta-\cos^2\omega-\cos^2\alpha+2\cos\theta\cos\omega\cos\alpha},$$

if the quantity under the square root is positive, and is zero when the quantity under the square root is negative.

Hence

$$I_2 = \frac{\pi f(0)}{\nu}\int_0^{\pi}\sin\theta\,d\theta\int_0^{\pi}\sin\omega\,d\omega\,\frac{K^2-\beta^2s^2}{S^3}$$

$$\sum_{n=0}^{\infty}(2n+1)P_n(\cos\alpha)\,P_n(\cos\theta)\,P_n(\cos\omega)$$

$$= \frac{\pi f(0)}{\nu\beta}\int_{-1}^{1}\int_{-1}^{1}d\mu\,d\nu\,(\sec j-\nu)^{-1}\frac{(1-x^2)}{(1-2x\cos\chi+x^2)^{3/2}}$$

$$\times\Sigma(2n+1)P_n(\cos\alpha)\,P_n(\cos\theta)\,P_n(\cos\omega),$$

where

$$\cos\chi = \frac{\nu\sec j-1}{\sec j-\nu}\,;\qquad x = \frac{s}{\sec j-\nu}.$$

Now

$$\frac{1-x^2}{(1-2x\cos\chi+x^2)^{3/2}} = \sum_{m=0}^{\infty}(2m+1)x^mP_m(\cos\chi)$$

and

$$\int_{-1}^{1}x^mP_n(\mu)\,d\mu = \frac{1}{(\tau-\nu)^m}\int_{-1}^{1}(1+\mu)^mP_n(\mu)\,d\mu,$$

where

$$\tau = \sec j.$$

But

$$\int_{-1}^{1}(1+\mu)^mP_n(\mu)\,d\mu = \frac{2^{m+1}\,\underline{|m}\,\underline{|n}}{\underline{|m-n}\,\underline{|m+n+1}}\qquad m\geq n,$$

so that

$$I_2 = \frac{\pi f(0)}{\nu\beta}\int_{-1}^{+1} d\nu \sum_{n=0}^{\infty}\sum_{m=n}^{\infty} \frac{1}{(\tau-\nu)^{m+1}} P_m\left(\frac{\nu\tau-1}{\tau-\nu}\right)$$
$$\times 2^{m+1}\frac{(2n+1)(2m+1)\ \lfloor m\ \lfloor n}{\lfloor m-n\ \lfloor m+n+1} P_n(\cos\alpha)\, P_n(\nu).$$

Now we also have the equation

$$\frac{1}{(\tau-\nu)^{m+1}} P_m\left(\frac{\nu\tau-1}{\tau-\nu}\right) = \sum_{p=m}^{\infty} \frac{\lfloor p+m\ \ (2p+1)}{2^m \lfloor p-m\ \lfloor m\ \lfloor m} Q_p(\tau) P_p(\nu),$$

where

$$Q_n(\tau) = \frac{1}{2^{n+1}}\int_{-1}^{+1} (1-t^2)^n (\tau-t)^{-n-1}\, dt,$$

and we have $p \geqslant m \geqslant n$, while

$$\int_{-1}^{+1} P_n(\nu) P_p(\nu)\, d\nu = 0 \qquad p > n.$$

The only terms which survive are those for which $p=m=n$. Thus we obtain, finally,

$$I_2 = \frac{4\pi f(0)}{\nu\beta}\sum_{n=0}^{\infty} \frac{(2n+1)^2\ \lfloor 2n}{\lfloor 2n+1} Q_n(\tau) P_n(\cos\alpha)$$
$$= \frac{4\pi f(0)}{\nu\beta}\sum_{n=0}^{\infty} (2n+1) Q_n\left(\frac{1}{\beta}\right) P_n(\cos\alpha)$$
$$= \frac{4\pi f(0)}{\nu(1-\beta\cos\alpha)}.$$

This, moreover, is the expression for the complete integral. It is identified immediately with the value of $4\pi\phi_P(t_0)$, if we put for the field-point P, $R=\nu$ and $\theta=0$ in the expresssion

$$K = 1-\beta\cos\theta\cos\alpha-\sin\theta\sin\alpha\cos\psi.$$

We must also take the value $\tau=0$ to correspond to the time t_0.

9. *Particular Cases of the Function* $\phi = f(\tau)/KR$.

a. If we denote by $f(\tau)$ the component velocities of the electron, the functions obtained give the components of the retarded vector potential

$$\mathfrak{a} = \frac{v}{[KR]}.$$

b. If we set $f(\tau)=1$, the function

$$\phi = 1/[\mathrm{KR}]$$

gives the scalar retarded potential.

c. If we assume that the electron is static, at rest at the origin $\rho=0$, so that

$$\xi=\eta=\zeta=0, \quad \dot{\xi}=\dot{\eta}=\dot{\zeta}=0, \quad \text{and} \quad \rho=\mathrm{R},$$

then

$$\mathrm{K}=1,$$
$$\mathrm{R}^2=x^2+y^2+z^2,$$
$$f(\tau)=f(t-\mathrm{R}/c),$$

and the function ϕ becomes

$$\phi=\frac{(t-\mathrm{R}/c)}{\mathrm{R}}.$$

If this form of the function ϕ is used in the extended formula, it is noticed that an easy verification is obtained.

10. *Summary.*

It has been shown that if ϕ be a function which satisfies the wave equation within a volume Ω bounded by a moving surface S and is subject to the conditions of continuity as mentioned in § 2, then the value of ϕ determined at an internal point P at a time t is given by the expression

$$4\pi\phi_{\mathrm{P}}(t)=\int_{\mathrm{S}}\frac{d\mathrm{S}}{r(1+\dot{r}/c)}\left[\frac{\partial\phi}{\partial n}+\frac{v}{c}\frac{\partial\phi}{c\,\partial t}+\frac{\frac{\partial r}{\partial n}-\frac{\dot{r}v}{c^2}}{1+\dot{r}/c}\frac{\phi}{r}\right.$$
$$\left.+\frac{1}{\mathrm{H}}\frac{d}{c\,dt}\left(\frac{\frac{\partial r}{\partial n}+\frac{v}{c}}{1+\dot{r}/c}\phi\mathrm{H}\right)\right]_{r=t-r/c},$$

where v is the velocity of the element $d\mathrm{S}$ in the direction of the outward normal.

When the outward normal velocity of the surface is zero the extended formula reduces to the Kirchhoff form.

When the moving surface S is an expanding sphere, centre the origin $\rho=0$, whose outward normal velocity is equal to that of light, and when the function ϕ corresponds to an isotropic wave expanding outwards from the origin, the integral extended to S vanishes, so that the value of ϕ

at P is due entirely to the singularities of ϕ within the sphere S.

Use is made of this expanding sphere to obtain further verifications of the extended Formula by identifying the value of ϕ at a point P at time t_0 with that obtained from the surface integrals in which the boundary values of ϕ and its derivatives are inserted. Its application to the function $f(\tau)/[\mathrm{KR}]$, which includes, as particular cases, the scalar and vector retarded potentials and the function $f(ct-\mathrm{R})/\mathrm{R}$, gives the desired values, which afford strong evidence that the formula deduced can be taken as the Kirchhoff formula extended to a moving surface.

In conclusion, I wish to express my thanks to Prof. G. A. Schott, F.R.S., Head of the Mathematics Department in the University College of Wales, Aberystwyth, for suggesting this problem, and for his assistance and advice while the work was in progress, and to H. Bateman, F.R.S., Professor of Mathematics, Theoretical Physics and Aeronautics at the California Institute of Technology, Pasadena, for the evaluation of integral (28).

Norman Bridge Laboratory of Physics,
California Institute,
Pasadena, California,
April 8, 1929.

XV. *Some Hydrodynamical Inertia Coefficients.* *By* J. Lockwood Taylor, *D.Sc., Munitions Committee Research Fellow, University of Liverpool* *.

THE question of the "virtual inertia" of a body immersed in fluid has acquired some additional interest from the influence which it appears to have on the natural frequency of vibration of a ship †, and most of the results which follow have been obtained with this problem in view. Part I. gives solutions for motion in two dimensions due to the translation of cylinders having various cross-sections, and discusses the application of the results to the ship problem. The results can be applied immediately to the case of vertical

* Communicated by the Author.

† Nicholls, Trans. Inst. of Naval Architects, p. 141 (1924); Moullin, Proc. Cambridge Phil. Soc. xxiv. p. 400 (1927–28).

vibrations, since the special boundary condition appropriate to the free surface is automatically fulfilled at an axis of symmetry perpendicular to the direction of motion. The free surface condition for the case of horizontal vibration requires special consideration (Part II.). Part III. deals with the effect of rigid boundaries, *e.g.*, as in shallow water or canals, and Part IV. the effect of the abandonment of the restriction to two-dimensional motion, and of compressibility of the fluid in a particular case—that of the circular cylinder. The inertia is generally less, in the two-dimensional case, for motion parallel to the free surface than for motion in a perpendicular direction, when the breadth of the cylinder is greater than the depth; a rigid boundary increases the inertia, as also does compressibility to a small extent, but freedom of the fluid to move in three dimensions naturally has the effect of reducing the energy.

Part I.

The problem of fluid motion due to the translation in a direction perpendicular to the generators of cylinders having the following sections is considered.

Sections symmetrical about two perpendicular axes, bounded by :—

(1) Two circular arcs intersecting at any angle.
(2) Two parabolic arcs intersecting orthogonally.
(3) Four equal straight lines.
(4) Four semicircles.
(5) A circle with projecting laminæ.
(6) A square with rounded corners.

(1) *Section bounded by Circular Arcs.*

In terms of complex variables, z, w, and an intermediate variable, t, the equations

$$z = \cot t,$$
$$w_1 = in \cot nt,$$
$$w_2 = n \operatorname{cosec} nt,$$

represent a uniform stream of unit velocity flowing past a section as described, in a direction parallel and perpendicular to the common chord, respectively. The correspondence of the various planes is as in fig. 1, the exterior angle of intersection of the arcs being $2\pi/n$, n being positive and greater than unity but not necessarily integral (the case of n integral

can be solved by the method of images). Expanding the trigonometrical functions, we have, when z, w are large,

$$w = iz + \frac{1}{iz}\frac{(n^2-1)}{3} + \dots,$$

and

$$w = z + \frac{1}{z}\frac{(n^2+2)}{6} + \dots.$$

Fig. 1.

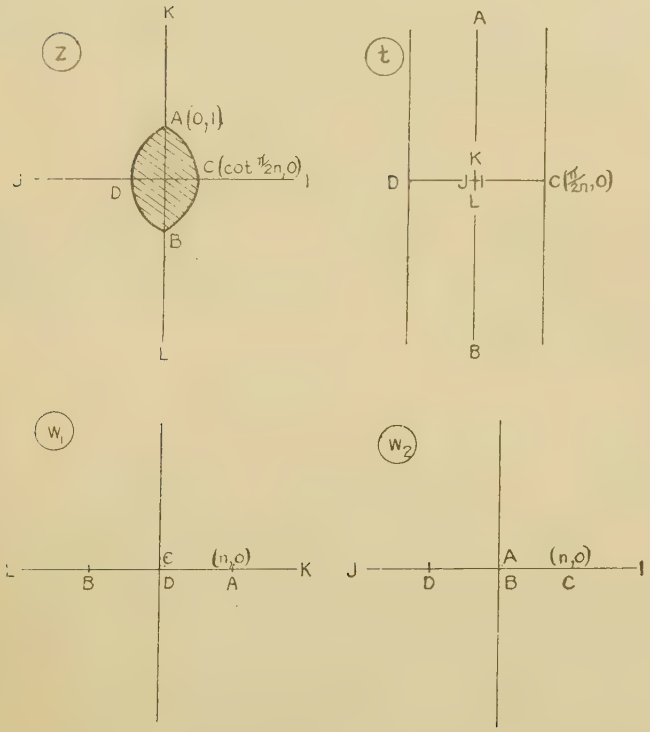

If A is the area of the section, and C the "entrained area," corresponding to the kinetic energy of the fluid ($1/2\,\rho\,C\,.\,U^2$ for density ρ, and velocity U) when the uniform stream is annulled,

$$(A + C_1) = \frac{2\pi}{3}(n^2-1),$$

$$(A + C_2) = \frac{\pi}{3}(n^2+2),$$

by a result of Leathem's *. Also

$$A = 2\left\{\left(\pi - \frac{\pi}{n}\right)\cdot \operatorname{cosec}^2\frac{\pi}{n} + \cot\frac{\pi}{n}\right\},$$

so that C_1, C_2 may be found by subtraction. The table shows the values of C, b (the width of the section measured perpendicular to the direction of motion), and C/b^2. It is seen that the latter coefficient does not vary very greatly, the extreme values being $2/\pi$ and $\pi/2(\pi^2/6-1)$, or 0·636 and 1·013 respectively. The latter value corresponds to the limiting case of w_2 when n is large, *i. e.*, for two circles in contact, moving perpendicular to the common tangent. The solution for this case may be written alternatively

$$w_2 = \pi \operatorname{cosec} \pi/z.$$

Similarly,
$$w_1 = i\pi \cot \pi/z,$$
$$C/b^2 = \pi/8(\pi^2/3-1) = \cdot 900$$

represents motion parallel to the common tangent, or may be regarded as the solution for a single circle, of unit radius, in contact with a plane boundary. The cases $n=1$, 2 correspond to the known solutions for the lamina and circle respectively.

n	1	6/3	4/3	3/2	2	3	4	5	6
$2\pi/n$	360°	300	270	240	180	120	90	60	0
Radius	∞	2	1·41	1·15	1	1·15	1·41	2	∞
Width, b_1...	0	·536	·828	1·15	2	3·46	4·83	7·46	∞
,, b_2...	2	2	2	2	2	2·31	2·83	4	∞
C_1	0	·197	·488	·980	3·14	10·0	20·0	48·9	∞
C_2	3·14	2·88	2·82	2·81	3·14	4·78	7·42	15·4	∞
C_1/b_1^2	(·636)	·685	·709	·735	·785	·835	·857	·878	(·900)
C_2/b_2^2	·785	·719	·704	·703	·785	·896	·928	·962	(1·01)

(2) *Section bounded by Parabolic Arcs.*

For motion parallel to the chord (fig. 2),

$$z = \left(\frac{t}{2}\right)^2, \qquad t = \int^w (w^2-1)^{-\frac{1}{2}}\,.\,dw.$$

When w, z are large, this gives

$$z = w - 1/6\,w + \ldots,$$
$$(A + C) = \pi/3.$$

* Leathem, Phil. Trans. A, ccxv. p. 453 (1915).

The length of the chord is

$$1/4\left\{\int_{-1}^{1}(1-w^2)^{-\frac{1}{2}}.\,dw\right\}^2=\pi^2/2\,.\,\mathrm{K}^2,$$

K being the complete elliptic integral of modulus $1/\sqrt{2}$.

Fig. 2.

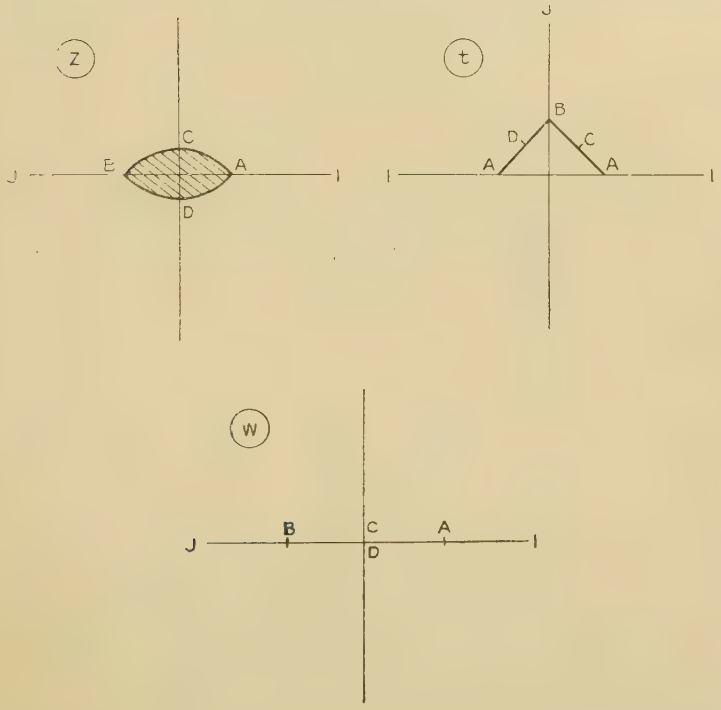

Hence

$$\mathrm{A}=\left(\frac{\pi^2}{2\mathrm{K}^2}\times\frac{\pi^2}{4\mathrm{K}^2}\times\frac{2}{3}\right)=\pi^4/12\,.\,\mathrm{K}^4=0{\cdot}687,$$

$$\mathrm{C}=\pi/3-0{\cdot}687=0{\cdot}360.$$

$$\mathrm{C}/b^2=0{\cdot}360\div0{\cdot}515=0{\cdot}698.$$

For motion perpendicular to the chord (fig. 3),

$$z=\left(\frac{t}{2}\right)^2,\quad t=\int^{w}\left(\frac{w}{w^2-1}\right)^{\frac{1}{2}}.\,dw,$$

giving

$$z = w - 1/3 \cdot w + \ldots,$$

$$(A + C) = 2\pi/3,$$

$$C = 2\pi/3 - 0{\cdot}687 = 1{\cdot}407,$$

$$C/b^2 = 1{\cdot}407 \div 2{\cdot}061 = 0{\cdot}683.$$

The coefficients C/b^2 agree fairly closely with those for the section consisting of orthogonally intersecting circular

Fig. 3.

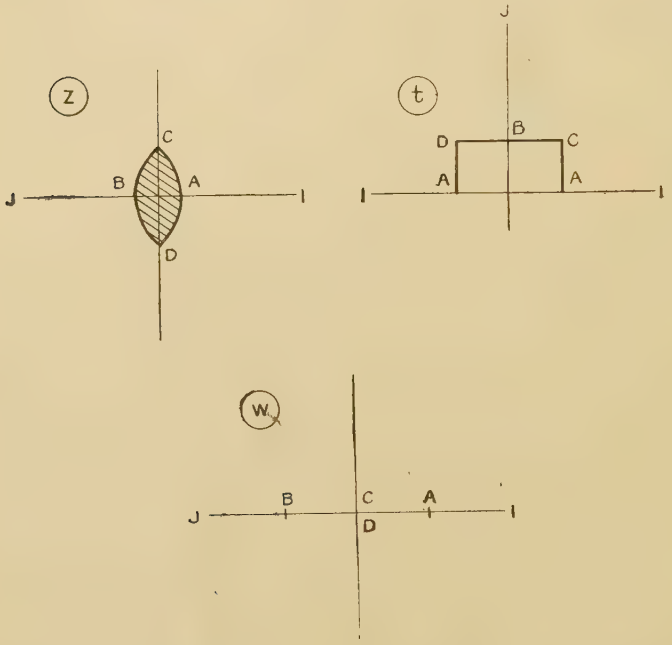

arcs, viz. 0·709 and 0·704 respectively, as would be anticipated.

(3) *Quadrilateral with equal sides.*

The angle between the side and the diagonal parallel to the direction of motion being $n \cdot \pi$, Schwarz's method gives (fig. 4)

$$z = \int^{w} \left(\frac{w^2}{w^2 - 1}\right)^n \cdot dw,$$

whence

$$z = w - n/w + \ldots$$

when z, w are large, so that

$$(A+C)=2\,.\,\pi\,.\,n.$$

The length of a side of the quadrilateral is given by

$$s=\int_0^1\left(\frac{w^2}{1-w^2}\right)^n.\,dw=\frac{\Gamma(1/2+n)\,.\,\Gamma(1-n)}{2\Gamma(3/2)},$$

and $$A=s^2\,.\,\sin 2\,.\,n\pi,$$

so that $$C=2\,.\,n\pi-s^2\,.\,\sin 2\,.\,n\pi.$$

Fig. 4.

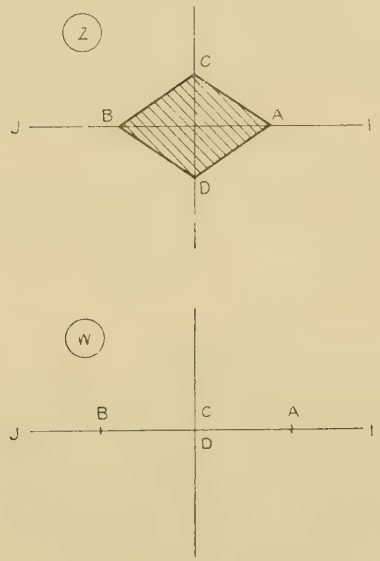

The values of the coefficient C/b^2 are tabulated below for several values of the angle $n\,.\,\pi$:—

$n\pi$	90°	60	45	30	$\rightarrow 0$
C/b^2	·785	·650	·594	·543	·441

The value for $n\rightarrow 0$ is obtained as follows :

$$\Gamma(1/2+n)=\sqrt{\pi}(1-n(\gamma+\log 4)),$$

$$\Gamma(1-n)=(1+n\,.\,\gamma),$$

to the first order, when n is small, γ being Euler's constant.

Hence

$$s=(1-n\,.\log 4),$$
$$A=2\,.\,n\pi(1-2\,.\,n\log 4),$$
$$C=4\,.\,n^2\pi\log 4.$$

Also

$$b=2\,.\,n\pi,$$
$$C/b^2=\frac{1}{\pi}\,.\log 4=0{\cdot}441.$$

For the particular case of the square ($n=1/4$), the entrained area is obviously the same for two directions at right angles and is therefore the same for motion in any direction. The present result is therefore directly comparable with the particular case of Riabouchinsky's solution * for a rectangle moving parallel to a side, viz.,

$$C=\frac{\pi}{2}-(2\,.\,E-K)^2=\frac{\pi}{2}-\frac{\pi^2}{4\,.\,K^2}$$

by Legendre's relation E, K being complete elliptic integrals of modulus $1/\sqrt{2}$. This is to be compared with

$$C=\frac{\pi}{2}-\left\{\frac{[\Gamma(3/4)]^2}{2\Gamma(3/2)}\right\},$$

giving

$$K=\frac{\pi^{\frac{1}{2}}\Gamma(3/2)}{\{\Gamma(3/4)\}^2}.$$

a known relation.

(4) *Section bounded by Four Semicircles.*

The solution is derived from the representation of the interior of a square on that of a circle, viz.,

$$\zeta=\int_0^t\frac{dt}{(1-t^4)^{\frac{1}{2}}},$$

by putting

$$z=1/\zeta,$$
$$w=t+1/t. \qquad \text{(fig. 5.)}$$

Hence, when w, z are large and ζ, t small,

$$\zeta=t+(t^3)+\ldots,$$
$$z=1/t-(1/t^3)+\ldots,$$
$$w=z+1/z+\ldots,$$
$$(A+C)=2\,.\,\pi.$$

* Internat. Congress of Math., Strasbourg, p. 568 (1920).

In the plane of ζ,

$$\mathrm{IA} = \int_0^1 \frac{dt}{(1-t^4)^{\frac{1}{2}}} = \mathrm{K}/\sqrt{2},$$

so that the half-diagonal of the square ABCD in the

Fig. 5.

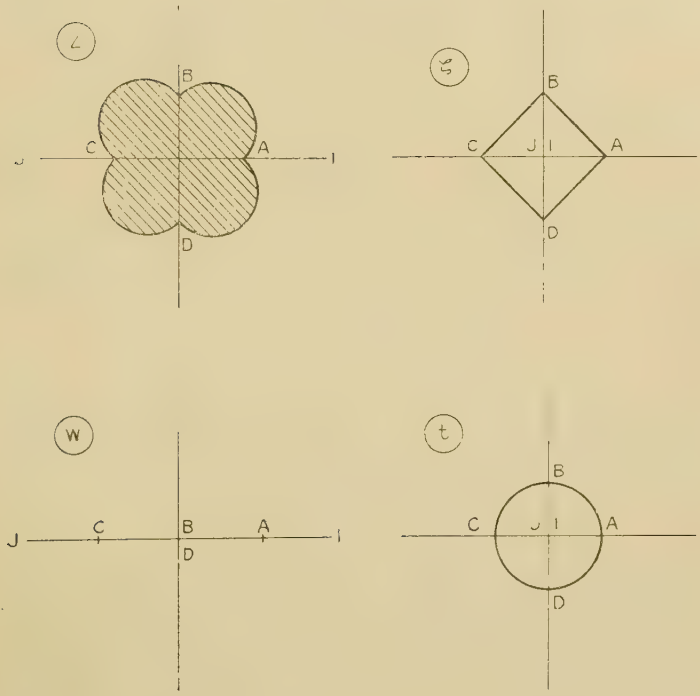

z-plane is $\sqrt{2}/\mathrm{K}$. This gives as the total area of the section $(1+\pi/2) \cdot 4/\mathrm{K}^2 = 2{\cdot}99$, so that

$$\mathrm{C} = 2 \cdot \pi - 2{\cdot}99 = 3{\cdot}29 = 0{\cdot}968 b^2,$$

where b is the extreme width of the section $\frac{2+\sqrt{2}}{\mathrm{K}}$. Since the entrained area, C, is the same for motion in the perpendicular direction, it may also be expressed in terms of the diagonal $4/\mathrm{K} = b$ say, viz., $\mathrm{C} = 0{\cdot}707\, b^2$, corresponding to the case of motion at 45° to the axes.

(5) *Circle with Projecting Laminæ.*

The solution is derived from that for a single lamina,

$$z = \sqrt{(w^2 - c^2)},$$

by adding a second similar term, so that

$$z = 1/2\,(\sqrt{(w^2 - c^2)} + \sqrt{(w^2 - 4 - c^2)})$$

represents the flow past a circle of unit radius with a lamina projecting at either extremity of the diameter perpendicular to the direction of flow, the total width $2b$ being given by

$$c = (b^2 - 1)/b.$$

When w is large, expansion gives

$$z = w - \frac{(1 + c^2/2)}{w} + \ldots .$$

Hence

$$(\mathrm{A} + \mathrm{C}) = \pi(2 + c^2),$$

$$\mathrm{C} = \pi(1 + c^2) = \pi\,\frac{(b^4 - b^2 + 1)}{b^2},$$

$$\mathrm{C}/4b^2 = \pi/4(1 - 1/b^2 + 1/b^4).$$

The coefficient is equal to $\pi/4$ when $b = 1$, and also when b is large, as would be anticipated, since the influence of the circle of unit radius is then negligible. The minimum value, for $b = \sqrt{2}$, is $3\pi/16$ or 0·589.

(6) *Square with rounded corners.*

By adding, in a similar manner to the above, two terms corresponding to the flow past rectangles of different proportions, the resulting section is a rectangle with the corners rounded off. Riabouchinsky * has given the solution for a single rectangle, which may be somewhat more simply expressed as

$$z = \int \sqrt{\frac{w^2 - \cos^2\alpha}{w^2 - 1}}\,.\,dw.$$

This gives

$$(\mathrm{A} + \mathrm{C}) = \pi \sin^2\alpha,$$

$$\mathrm{A} = b \times d,$$

$$= 4(\mathrm{E} - \cos^2\alpha\,.\,\mathrm{K})(\mathrm{E}' - \sin^2\alpha\,.\,\mathrm{K}'),$$

E, K being the elliptic integrals of modulus $\sin\alpha$, and E′, K′ those of the complementary modulus $\cos\alpha$. The

* *Loc. cit.*

effect of writing $\sin\alpha$ for $\cos\alpha$ is to interchange the breadth and depth of the rectangle so that the addition of two terms

$$2z = \int \frac{\{(\sqrt{w^2-\cos^2\alpha}) + (\sqrt{w^2-\sin^2\alpha})\}\,.\,dw}{\sqrt{w^2-1}}$$

gives a square of side $1/2(b+d)$, the sides being connected by an arc of length

$$\int ds = \int_{\sin\alpha}^{\cos\alpha} \left\{ \left(\frac{dx}{dw}\right)^2 + \left(\frac{dy}{dw}\right)^2 \right\}^{\frac{1}{2}} . dw$$

$$= \frac{1}{2} \int_{\sin\alpha}^{\cos\alpha} \frac{(\cos^2\alpha - w^2 + w^2 - \sin^2\alpha)^{\frac{1}{2}}}{(1-w^2)^{\frac{1}{2}}} . dw.$$

This gives

$$s = \tfrac{1}{2}\sqrt{\cos 2\alpha}(\pi/2 - 2\alpha).$$

The exact area of the section may be calculated by quadrature, but if α is not less than say $\pi/6$, it is given very nearly by

$$\mathrm{A} = \frac{(b+d)^2}{4} - 16/30\,.\,s^2.$$

Also $$(\mathrm{A}+\mathrm{C}) = \pi/2(\sin^2\alpha + \cos^2\alpha) = \pi/2.$$

For $\alpha = \pi/6$,

$$b = 2(1{\cdot}468 - 0{\cdot}75 \times 1{\cdot}686) = 0{\cdot}2035 \times 2,$$
$$d = 2(1{\cdot}211 - 0{\cdot}25 \times 2{\cdot}157) = 0{\cdot}672 \times 2,$$
$$s = 1/2\sqrt{2} \times \pi/6 = 0{\cdot}185,$$
$$\mathrm{A} = (0{\cdot}8755)^2 - 0{\cdot}018 = 0{\cdot}749,$$
$$\mathrm{C} = \pi/2 - 0{\cdot}749 = 0{\cdot}822 = 1{\cdot}07\,b^2,$$

b being the width of the section, *i.e.*, the side of the square. Comparing this with the corresponding figure for a complete square, 1·188, it appears that the reduction of the area, by rounding off the corners, by about $2\frac{1}{2}$ per cent. has reduced the entrained area by 10 per cent.

Application of the above results.

If $\phi\cos\sigma t$ is the velocity potential of a fluid motion due to the simple-harmonic vibrations of an immersed body, the usual condition at a free surface is

$$\sigma^2\phi = g\,.\,\frac{\partial\phi}{\partial n}.$$

If the frequency is sufficiently large, $\frac{g}{\sigma^2} \cdot \frac{\partial \phi}{\partial n}$ is evidently small, and the condition reduces to $\phi = 0$ *. The order of the neglected term is $g \cdot v/\sigma^2$, where v is the maximum velocity of the vibration, while ϕ in the vicinity of the section is of the order $(b \cdot v)$, b being one of the dimensions of the vibrating body. The ratio, $g/b\sigma^2$ or $g \cdot T^2/4\pi^2 \cdot b$, is very small for periods (T) of less than one second, as in practice, b being of the order of, say, 50 feet.

The condition $\phi = 0$ is evidently fulfilled at an axis of symmetry perpendicular to the direction of motion, *e.g.*, the y-axis in all the foregoing examples, which may therefore be regarded as a free surface. Conversely, for any given section partly immersed, the section is to be completed by adding its reflexion in the free surface, and the problem solved for the section so formed. When the boundary of the section cuts the free surface at an acute angle the velocity becomes infinite at the corner, so that the approximation to the fulfilment of the surface condition is locally inadequate, but the effect on the motion as a whole is probably small. The fact that the theoretically infinite velocity at a sharp corner does not affect the practical applicability of the results appears to have been established by Moullin † in the case of a totally submerged section. He finds that for a rectangular section of breadth twice the depth, an approximation to the entrained area is that of the circumscribing circle, *i. e.*, $5\pi/16 \cdot b^2$ or $0{\cdot}98\, b^2$, while interpolation between Riabouchinsky's results ‡ gives $1{\cdot}05\, b^2$ in fair agreement. For deeper sections the approximation does not hold; thus for a square (corresponding to a partly immersed section of depth equal to half the breadth) the respective figures are $1{\cdot}57\, b^2$ and $1{\cdot}188\, b^2$.

It appears more reasonable to base the approximation on the maximum width, making some allowance for the shape of section, and while no empirical formula is likely to give very accurate results for a great variety of sections, the expression $(b^2 \times A/b \cdot d)$ or $(A \times b/d)$ is reasonably accurate for sections (1), (2), (4), and (6), and is exact for an ellipse. The area for a partly immersed section, vibrating vertically, becomes $(A' \times b/2d')$ where A' and d' are the actual area and depth respectively, but this makes no allowance for any departure from two-dimensional motion (Part IV.).

* *Cf.* Rayleigh, 'Collected Papers,' ii. p. 208.
† *Loc. cit.* ‡ *Loc. cit.*

Part II.

When the free surface is parallel to the direction of motion the fulfilment of the condition $\phi=0$ is not quite so easy, but a solution can be obtained for a semi-elliptical section with the axis in the free surface.

Putting

$$x+iy=\sinh(\xi+i\eta),$$

the boundary condition,

$$\psi-c=y=\cosh\xi\sin\eta \qquad \xi=\xi_0,$$

can be fulfilled for values of η between 0 and π by

$$\psi=\cosh\xi_0\sum_1^\infty A_n\,.\,e^{-2n(\xi-\xi_0)}\cos 2n\eta,$$

where

$$A=\frac{4}{\pi(4n^2-1)}.$$

The corresponding value of ϕ is

$$\phi=\cosh\xi_0\sum_1^\infty A_n\,.\,e^{-2n(\xi-\xi_0)}\,.\sin 2n\eta,$$

and when $\xi=\xi_0$,

$$\phi=\phi_0=\cosh\xi_0\sum_1^\infty A_n\,.\sin 2n\eta.$$

The entrained area is given by

$$\begin{aligned}\int_0^\pi \phi_0\left(\frac{dy}{d\eta}\right)_0 d\eta &= \cosh^2\xi_0\sum_1^\infty A_n\int_0^\pi \sin 2n\eta\,.\cos\eta\,d\eta\\ &=\cosh^2\xi_0\sum_1^\infty\frac{16\,.\,n}{\pi(4n^2-1)^2}\\ &=(2/\pi)\cosh^2\xi_0\\ &=(2/\pi)b^2,\end{aligned}$$

since $\cosh\xi_0=b$, the major semi-axis, perpendicular to the direction of motion and to the free surface. The result is the same when motion takes place parallel to the major axis, and the semicircle and lamina are particular cases. The comparative figure for the semicircle moving perpendicularly to the surface is $(\pi/2)b^2$, so that the virtual inertia for horizontal motion is only $(4/\pi^2)$ times that for vertical motion. For other sections the ratio depends, of course, on the ratio of the axes.

Moullin * carried out experiments on a flat bar, the most direct comparison possible being that for the bar $\frac{1}{4}$ in. thick

* *Loc. cit.*

with its edge submerged $2\frac{3}{4}$ in. From the ratio of the frequency in this condition to that in air, it is possible to calculate that the added mass of water is about $0{\cdot}58\,b^2$ per unit length as against $0{\cdot}636$, as calculated for a lamina.

A solution can also be obtained for the case of a circular cylinder, with horizontal axis, submerged to any depth below the surface. Employing the coordinates

$$z = x+iy = \cot 1/2(\xi+i\eta) = \frac{\sin\xi - i.\sinh\eta}{\cosh\eta-\cos\xi},$$

we may take $y=\eta=0$ as the free surface and $\eta=\alpha$ as the boundary of the circular section, of radius $\operatorname{cosech}\alpha$, the centre being at a depth $\coth\alpha$ below the surface.

The boundary condition $\psi=-y+\text{constant}$, for $\eta=\alpha$, can be satisfied by

$$\psi = 2\sum_1^\infty \frac{e^{-n\alpha}}{\cosh n\alpha}\cos n\xi.\cosh n\eta,$$

which makes

$$\phi = 2\sum_1^\infty \frac{e^{-n\alpha}}{\cosh n\alpha}\sin n\xi.\sinh n\eta,$$

and this vanishes at the free surface $\eta=0$.

The kinetic energy integral

$$-\int\phi\frac{d\phi}{dn}ds = \int_{-\pi}^{\pi}\phi\frac{dy}{d\xi}.d\xi \qquad (\eta=\alpha)$$

$$= 2\sum_1^\infty e^{-n\alpha}.\tanh n\alpha.\sinh\alpha\int_{-\pi}^{\pi}\frac{\sin n\xi.\sin\xi\,d\xi}{(\cosh\alpha-\cos\xi)^2}$$

$$= 4\pi\sum_1^\infty n.e^{-2n\alpha}.\tanh n\alpha.$$

When α is large the series converges rapidly, and expansion of the first three terms gives

$$4\pi\{e^{-2\alpha}+(e^{-6\alpha})+\ldots\}.$$

Expressing this in terms of

$$r = \operatorname{cosech}\alpha = 2e^{-\alpha}(1+e^{-2\alpha}\ldots),$$

we have

$$\pi r^2(1-2e^{-2\alpha}+\ldots)$$
$$= \pi r^2(1-r^2/2c^2)$$

to this order, putting $c=\coth\alpha=1$ nearly, for the depth of immersion to the centre of the circle. The factor $(1-r^2/2c^2)$ shows the reduction in the kinetic energy due to the free surface, when the ratio r/c is fairly small.

When α is small we have the integral

$$\int_0^\infty n \,.\, e^{-2n\alpha} \,.\, \tanh n\alpha \,.\, dn$$

whose value is $1/4\alpha^2(\pi^2/6-1)$, so that the entrained area is $\pi/\alpha^2(\pi^2/6-1)$ or $\pi r^2(\pi^2/6-1)$, r being equal to $1/\alpha$. This result, corresponding to the case of relatively small immersion, agrees with the result of Part I. (1) for motion *perpendicular* to the surface ($y=0$), *i.e.*, the common tangent to the two circles in the example quoted. The solution just given can in fact be adapted to this case, the expression for the entrained area being identical, which shows that the direction of motion is immaterial.

Part III.—Effect of Rigid Boundaries.

(1) *Circle with Plane Boundary.*

With the same coordinates as in the last example, the expression

$$\psi = 2\sum_1^\infty \frac{e^{-n\alpha}}{\sinh n\alpha} \cos n\xi \sinh n\eta$$

satisfies the boundary condition $\psi = -y + \text{constant}$ for $\eta=\alpha$, and also makes $\psi=0$ for $\eta=0$, as is required for a boundary at $y=\eta=0$. The expression for the entrained area

$$\begin{aligned} -\int \phi \frac{d\phi}{dn} \,.\, ds &= -\int_{-\pi}^{\pi} \phi \frac{d\phi}{d\eta} \,.\, d\xi \\ &= 2\sum_1^\infty e^{-n\alpha} \coth n\alpha \int_{-\pi}^{\pi} \frac{\sin n\xi \sin \xi \sinh \alpha}{(\cosh \alpha - \cos \xi)^2} \,.\, d\xi \\ &= 4\pi \sum_1^\infty n \,.\, e^{-2n\alpha} \,.\, \coth n\alpha. \end{aligned}$$

In the same way as before this gives, for α large,

$$-\int \phi \frac{d\phi}{dn} \,.\, ds = \pi r^2 \left(1 + \frac{r^2}{2c^2}\right),$$

indicating the effect of a distant boundary, and for α small,

$$-\int \phi \frac{d\phi}{dn} \,.\, ds = \pi r^2 \left(\frac{\pi^2}{3} - 1\right),$$

which again agrees with the example (1) of Part I. It can be shown that the direction of motion is immaterial in this case also.

(2) *Semicircle with Boundary and Free Surface.*

The example just considered, while of interest as giving a comparison with the results in Part II., does not satisfy the condition $\phi=0$ at a plane through the axis of the cylinder, parallel to the fixed boundary, as would be required for a cylinder of semicircular section in a limited depth of water.

Putting
$$w = \mathrm{C}.\operatorname{cosec} z/2,$$
$$\phi = 2\mathrm{C}.\frac{\sin x/2\,.\cosh y/2}{\cosh y-\cos x},$$
$$\psi = 2\mathrm{C}.\frac{\cos x/2\,.\sinh y/2}{\cosh y-\cos x}$$

represents a doublet at the origin, with axis Ox, with boundaries $\psi=0$ at $x=\pm\pi$, and may also be regarded as representing the motion due to a small circle at the origin, moving in the direction Ox. If the velocity is unity, the condition
$$y=0, \qquad \frac{d\phi}{dx} = \mathrm{C}.\frac{\cos x/2}{1-\cos x} = 1$$
gives
$$\mathrm{C} = \frac{1-\cos x}{\cos x/2} = x^2/2 + x^4/48 + \ldots,$$
x being small, which expresses C in terms of the radius of the circle a on putting $x=a$. Similarly,
$$x=0, \quad \psi = \mathrm{C}/\sinh y/2 = y, \quad \mathrm{C} = y^2/2 + y^4/48 + \ldots$$
verifies, on putting $y=a$, that to this order the circular shape holds.

In the vicinity of the origin, more generally, on expanding
$$\phi = 2\mathrm{C}\left\{\frac{(x/2-x^3/48+\ldots)(1+y^2/8\ldots)}{y^2/2+x^2/2+y^4/384-x^4/384+\ldots}\right\}$$
$$= 2\mathrm{C}.x/r^2(1+\text{terms in } r^2),$$
$$\frac{d\phi}{dr} = -2\mathrm{C}.\frac{\cos\theta}{r}(1+\text{terms in } r^2).$$

Hence
$$-\int\phi\frac{d\phi}{dr}.r.d\theta = 4\mathrm{C}.\left(\frac{\pi}{r^2}+\text{terms in } r^2\right)$$
$$= \frac{\pi}{r^2}(r^4+r^6/12)$$
to this order.

When $r=a$, this is the kinetic energy integral, the value being $\pi a^2(1+a^2/12)$. This applies to the case of a boundary at distance π from the centre of the circle, and generalization for any distance of boundary c (large in relation to a) gives $\pi a^2(1+a^2\pi^2/12c^2)$.

In a very similar manner $w=C.\coth z/2$ * represents a small circle midway between two plane boundaries at distance $\pm\pi$, moving parallel to the boundaries, the entrained area being $\pi a^2(1+a^2\pi^2/6c^2)$. In each case the plane through the centre perpendicular to the direction of motion may be regarded as a free surface, the entrained area for the semicircle being, of course, half the above.

(3) *Lamina between two Plane Boundaries.*

Applying Lamb's solution †, $\cosh w=\mu\cosh z$, which applies to the motion of a lamina of width $2.\cos^{-1}(1/\mu)$ midway between two plane boundaries distance π apart, and moving in a direction parallel to the boundaries. At the surface of the lamina,

$$x=0, \quad y<\cos^{-1}(1/\mu), \quad \psi=0,$$

and

$$\phi=\cosh^{-1}(\mu\cos y), \qquad \frac{d\phi}{dn}=-1,$$

so that

$$-\int\phi\frac{d\phi}{dn}\,ds=4\int_0^{\sec^{-1}\mu}\cosh^{-1}(\mu\cos y)\,dy$$
$$=2\pi\log\mu$$
$$=2\pi\log\sec b,$$

if $b=\cos^{-1}(1/\mu)$ is the half width of the lamina. This gives, on expansion,

$$-\int\phi\frac{d\phi}{dn}\,ds=2\pi(b^2/2+b^4/12+\ldots)$$
$$=\pi b^2(1+b^2/6\ldots).$$

This applies to the case when the width of the lamina is moderately small in relation to the distance between the boundaries, and may be generalized for boundaries at a distance c from the centre of the lamina as $\pi b^2\left(1+\frac{\pi^2b^2}{24c^2}\right)$.

* Lamb, 'Hydrodynamics,' p. 68 (5th ed.).
† *Loc. cit.* p. 508.

The factor may be compared with that for a circle of radius b in the corresponding case considered in (2) above.

(4) *Circle completely surrounded by Rigid Boundary.*

The first order correction to the inertia coefficient for a circle enclosed by a rigid boundary, corresponding to the three-dimensional problem of an infinite circular cylinder enclosed by a fixed cylinder of any cross-section, can be readily obtained, provided a solution is known for the fluid motion due to the translation of a cylinder whose section is the inverse of that of the fixed cylinder, with respect to an internal point, namely the centre of the circle.

Taking this point as the origin, and superposing a uniform stream on the known solution, inversion gives a doublet at the origin, which may therefore be supposed to be the centre of a small circle, moving inside the fixed boundary.

In terms of z', which is equal to $1/z$, we have, when z' is large, a solution of form

$$w = z' + a/z' + \ldots,$$

and, accordingly, when z is small,

$$w = 1/z + az + \ldots$$

$$\phi = \cos\theta/r + ar\cos\theta + \ldots,$$

$$\frac{d\phi}{dr} = -\cos\theta/r^2 + a\cos\theta + \ldots,$$

neglecting terms of higher degree in r.

Putting $r=b$, this corresponds to the case of a small circle of radius b moving in the direction Ox with velocity $(1/b^2 - a)$.

$$-\int \phi \frac{d\phi}{dn} ds = -\int_0^{2\pi} \phi \frac{d\phi}{dr} b \, d\theta \qquad (r=b)$$

$$= \pi(1/b^2 - a^2 b^2).$$

Correcting this for unit velocity, since the kinetic energy varies as the square of the velocity, the entrained area is

$$\pi \frac{(1/b^2 - a^2 b^2)}{(1/b^2 - a)^2}$$

$$= \pi b^2 (1 + 2ab^2)$$

to this order in b.

Thus, it is only necessary to know the coefficient a in the original solution in order to determine the first order

correction to the inertia. If the boundary is a circle of unit radius which inverts into itself, $a=1$, giving $\pi b^2(1+2b^2)$ or more generally when the radius of the outer circle is c, $\pi b^2(1+2b^2/c^2)$ in agreement, for the case of (b/c) small, with the exact solution, which in this case may readily be shown to be $\pi b^2\left(\frac{c^2+b^2}{c^2-b^2}\right)$.

When the outer boundary is a squsre the solution of Part I. (4) may be applied. $a=1$, giving $\pi b^2(1+2b^2/c^2)$ in this case also, the side of the square being $K=1{\cdot}854$. Generalizing the solution for a square of side $2c$ gives $\pi b^2(1+K^2b^2/2c^2)$ or $\pi b^2(1+1{\cdot}72b^2/c^2)$, slightly less, as would be anticipated, than for a circle of radius c.

Part IV.—Motions in Three Dimensions.

(1) *Infinite Circular Cylinder.*

If a cylinder of radius a be supposed to execute flexural vibrations of small amplitude, the velocity being given by $b.\cos kz$, z being measured along the axis, the appropriate solution for the motion of the external fluid is

$$\phi = C.K_1(kr).\cos\theta.\cos kz$$

with a suitable time-factor, K_1 being Bessel's function of order unity of the second kind (and "of imaginary argument"), which is selected so as to make the motion vanish at infinity. The motion is parallel to the plane zx, and the constant C is determined by the boundary condition

$$\frac{d\phi}{dr} = -b.\cos kz.\cos\theta \qquad (r=a)$$

$$= C.k.K_1'(ka)\cos\theta.\cos kz,$$

$$C = b/\{k.K_1'(ka)\},$$

$$-\int_0^{2\pi}\phi\frac{d\phi}{dr}.a.d\theta$$

$$= -C^2.(ka)\cos^2 kz.K_1(ka).K_1'(ka)\int_0^{2\pi}\cos^2\theta\,d\theta$$

$$= \pi a^2\left(\frac{-K_1(ka)}{ka.K_1'(ka)}\right).b^2\cos^2 kz.$$

If the fluid were constrained by a series of planes perpendicular to Oz, so that the motion took place in two dimensions only, the corresponding expression would be $\pi.b^2.a^2.\cos^2 kz$.

so that the expression in brackets, which is always less than unity, indicates the ratio in which the energy is reduced, as compared with the two-dimensional case. Its value R in terms of a/λ or $ka/2\pi$, λ being the wave-length of the vibration, is given below:—

a/λ.....	$1/4\pi$	$1/2\pi$	$3/4\pi$	$1/\pi$
R	0·781	0·588	0·464	0·380

If, instead of seeking a solution of Laplace's equation, we had used the equation $(\nabla^2+k_1^2)\phi=0$, appropriate to a compressible fluid, $2\pi/k_1$ being the length of the compression wave of the same frequency as the vibration, the same form of solution would have applied, provided $k>k_1$, $(k^2-k_1^2)^{\frac{1}{2}}$ being substituted for k. This has the effect of increasing slightly the kinetic energy.

(2) *Ellipsoid.*

A solution can be obtained which fulfils the boundary condition for what is practically a two-node flexural vibration of a prolate ellipsoid of revolution.

In terms of the usual coordinates *

$$x=k\mu\zeta\,;\quad y=k(1-\mu^2)^{\frac{1}{2}}(\zeta^2-1)^{\frac{1}{2}}\cos\omega\,;$$
$$z=k(1-\mu^2)^{\frac{1}{2}}(\zeta^2-1)^{\frac{1}{2}}\sin\omega$$

appropriate to a prolate ellipsoid, the foci of the meridian being the points $(\pm k, 0, 0)$,

$$\phi=\mathrm{C}\,.\,\mathrm{P}_3'(\mu)\,.\,\mathrm{Q}_3'(\zeta)\,.\cos\omega$$

is a known solution of Laplace's equation:

$$\mathrm{P}_3'(\mu)=(1-\mu^2)^{\frac{1}{2}}\,.\,1/2\,.\,(15\mu^2-3),$$

$$\mathrm{Q}_3'(\zeta)=(\zeta^2-1)^{\frac{1}{2}}\,.\left\{\frac{1}{4}(15\zeta^2-3)\log\frac{\zeta+1}{\zeta-1}-\frac{1}{2}\left(15\zeta+\frac{2\zeta}{\zeta^2-1}\right)\right\},$$

$$\frac{\partial\mathrm{Q}_3'(\zeta)}{\partial\zeta}=(\zeta^2-1)^{-\frac{1}{2}}\,.\left\{\left(\frac{45}{4}\zeta^3-\frac{33}{4}\zeta\right)\log\frac{\zeta+1}{\zeta-1}\right.$$
$$\left.-\frac{45}{2}\zeta^2+9+\frac{1}{\zeta^2-1}\right\}.$$

* Lamb, p 130.

The velocity potential can be made to satisfy the boundary condition

$$\frac{\partial \phi}{\partial \zeta} = (a^2 - x^2)\frac{\partial y}{\partial \zeta} + 2\,.\,xy\frac{\partial x}{\partial \zeta} \qquad (\zeta = \zeta_0)$$

by adjusting suitably the values of C and a. Since

$$(a^2 - x^2)\frac{\partial y}{\partial \zeta} + 2\,.\,xy\frac{\partial x}{\partial \zeta}$$
$$= \{k\zeta(a^2 - k^2\mu^2\zeta^2) + 2k^3\mu^2\zeta(\zeta^2 - 1)\}(\zeta^2 - 1)^{-\frac{1}{2}}\,.\,(1-\mu^2)^{\frac{1}{2}}\,.\cos\omega,$$

this gives

$$a^2 = \frac{k^2(2-\zeta_0^2)}{5},$$

$$C = k\,.\,a^2\zeta_0 \div \left\{ 3/2(\zeta_0^2 - 1)^{\frac{1}{2}}\,.\,\frac{\partial Q_3'(\zeta)}{\partial \zeta} \right\} \qquad (\zeta = \zeta_0),$$

$$2T = -\iint \phi \frac{d\phi}{dn}\,.\,dS$$

$$= -\int_{-1}^{1} d\mu\,.\frac{\delta s}{\delta \mu}\int_0^{2\pi} \phi\,.\frac{\partial \phi}{\partial \zeta}\,.\frac{\delta \zeta}{\delta n}\,.\,k(1-\mu^2)^{\frac{1}{2}}(\zeta^2-1)^{\frac{1}{2}}\,.\,d\omega$$

$$= -\int_{-1}^{1} d\mu\,.\int_0^{2\pi} \phi\,.\frac{\partial \phi}{\partial \zeta}\,.\,k\left(\frac{\zeta^2-\mu^2}{1-\mu^2}\right)^{\frac{1}{2}}$$
$$\cdot\frac{1}{k}\left(\frac{\zeta^2-1}{\zeta^2-\mu^2}\right)^{\frac{1}{2}}\,.\,k(1-\mu^2)^{\frac{1}{2}}\,.\,(\zeta^2-1)^{\frac{1}{2}}\,d\omega$$

$$= -k\int_{-1}^{1} d\mu(\zeta^2-1)\int_0^{2\pi} \phi\frac{\partial \phi}{\partial \zeta}\,d\omega$$

$$= -\pi k\,.\,(\zeta^2-1)\,.\,C^2\,.\,Q_3'(\zeta)$$
$$\cdot\left\{\frac{\partial Q_3'(\zeta)}{\partial \zeta}\right\}\int_{-1}^{1}(1-\mu^2)\left(\frac{15\mu^2-3}{2}\right)^2 d\mu$$

$$= \frac{32\pi k^3}{21_{\frac{1}{2}}}\,.\,a^4\,.\,\zeta^2\left\{\frac{-Q_3'(\zeta)}{\partial Q_3'(\zeta)/\partial \zeta}\right\} \qquad (\zeta = \zeta_0).$$

The assumed boundary condition (1) above corresponds to an approximate type of flexural vibration in which the amplitude is proportional to $(a^2 - x^2)$, the positions of the "nodes" being given by

$$x = \pm a = \pm k\frac{\sqrt{2-\zeta_0^2}}{\sqrt{5}}.$$

For a slender ellipsoid, ζ_0 is very little different from unity, so that the nodes are approximately $\pm\sqrt{1/5}$ of the major semi-axis ($k\zeta_0$) from the centre of the ellipsoid. This agrees fairly closely with the actual positions for a beam having the same mass distribution as an ellipsoid of uniform density. The effect of the departure of the actual amplitude curve from the parabolic shape is probably unimportant, but as the primary object of the investigation is to compare the inertia of the water with that of the ellipsoid itself, this may be allowed for by calculating the kinetic energy of the ellipsoid for a hypothetical vibration in which the amplitude is proportional to (a^2-x^2) as the basis of comparison.

The area of the circular section of the ellipsoid being

$$\pi k^2(1-\mu^2)(\zeta_0^2-1) \quad \text{or} \quad \frac{\pi(\zeta_0^2-1)}{\zeta_0^2}(k^2\zeta_0^2-x^2),$$

the kinetic energy, assuming unity density, and velocity proportional to (a^2-x^2) is given by

$$2T_1 = \frac{\pi(\zeta_0^2-1)}{\zeta_0^2}\int_{-k\zeta_0}^{k\zeta_0}(a^2-x^2)^2.(k^2\zeta_0^2-x^2)\,.\,dx$$

$$= \frac{16\pi}{525}k^7\zeta_0(\zeta_0^2-1)(7-14\zeta_0^2+2\zeta_0^4).$$

The ratio

$$T/T_1 = \frac{2(2-\zeta_0^2)^2}{(7-14\zeta_0^2+2\zeta_0^4)} \cdot \left\{ \begin{array}{l} 30\zeta_0^2+4+4/(\zeta_0^2-1)-\zeta_0(15\zeta_0^2-3)\log\dfrac{\zeta_0+1}{\zeta_0-1} \\ -90\zeta_0^2+36+4/(\zeta_0^2-1)+3\zeta_0(15\zeta_0^2-11)\log\dfrac{\zeta_0+1}{\zeta_0-1} \end{array} \right\}.$$

This tends to the value unity as ζ_0 tends to unity, *i. e.*, as the ellipsoid becomes indefinitely small in diameter, the length remaining constant. The fluid motion is then practically two-dimensional. The value for various ratios of the axes c/b is given below, the value of ζ_0 being $1\sqrt{1-c^2/b^2}$:—

c/b	0·045	0·10	0·141	0·201
T/T_1	0·946	0·825	0·729	0·615

The rotatory inertia of the ellipsoid has been neglected, since in any practical application of the results the effect of this factor would be separately estimated, if it were necessary to take it into account. It can readily be shown

that for an ellipsoid of uniform density the rotatory inertia is given by

$$R = 8/5 \frac{(\zeta_0^2 - 1)}{\zeta_0^2} \cdot \left(\frac{2}{7 - 14\zeta_0^2 + 9\zeta_0^4} \right) \cdot T_1,$$

from which the corrected ratio $T/(T_1 + R)$ may be obtained.

The results given above, both for the ellipsoid and for the infinite cylinder, show that, even when the diameter is moderately small in relation to the wave-length of the vibration, the three-dimensional character of the fluid motion cannot be ignored. In the case of the cylinder, the *distribution* of the pressure due to the fluid inertia is, however, identical with that when the motion is confined to two dimensions, being proportional to $\cos\theta \cdot \cos kz$. A similar result holds in the case of the ellipsoid as regards the amount of the normal pressure on the surface, but a small correction has to be applied to the component in the direction of motion towards the ends of the ellipsoid on account of the inclination of the surface to the axis.

In applying the results obtained to bodies of other forms—for instance, the hull of a ship,—reasonable accuracy should be obtained by assuming a distribution of the "added mass" of water according to the empirical formula given at the end of Part I. above, and correcting the total amount in accordance with the ratio found for an ellipsoid of similar proportions. This applies to vibrations in a vertical plane, but for horizontal motion the correction factor will be much nearer unity, since the fluid motion, as indicated in the examples of Part II., is more local in the two-dimensional case.

The author is indebted to Professor J. Proudman for some valuable suggestions in the preparation of this paper.

Author's note.—While this paper has been in the press, Prof. H. M. Lewis has published (Amer. Soc. of Nav. Arch., Nov. 1929) a solution corresponding to Part I., example (3). He also treats the case of an ellipsoid (Part IV. (2)), but neglects the term in $\frac{\partial x}{\partial \zeta}$ in the boundary conditions, and arrives at different results in consequence.]

XVI. *On some Closed Algebraic Curves and their Application to Dynamical Problems.*—Part I. *By* SEIICHI HIGUCHI*.

§ 1. *Introduction.*

THOUGH the conception of "Closed curve of the higher order" is not new for mathematicians, so far as the

Fig. 1, *a*.

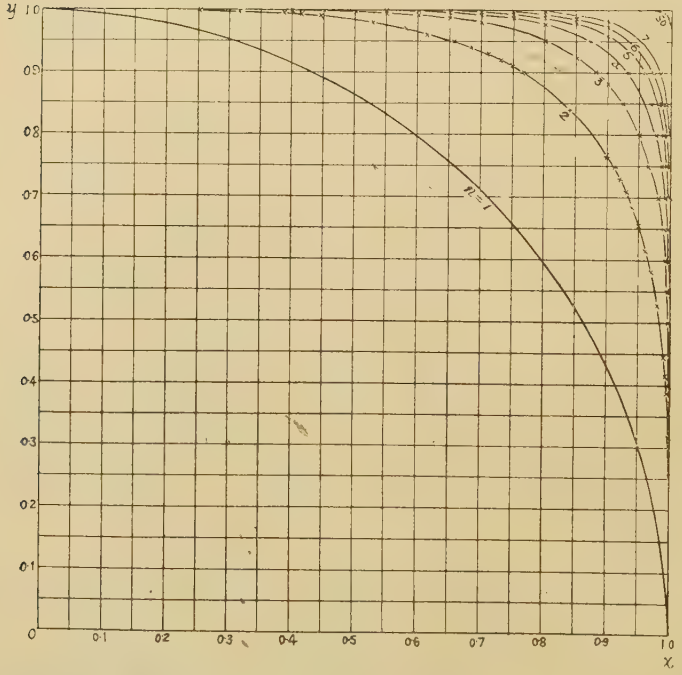

author is aware, no study with reference to its physical application has yet been published.

In this paper it is proposed first to deal with some closed algebraic curves, say circles of the higher order, their main properties being mentioned, omitting the proofs, and figures of groups of them are calculated and graphed; and, secondly, a few applications to the dynamical problems, *i. e.*, the area included by the curve, volume of revolution, and radius of gyration about an axis are calculated and tabulated.

* Communicated by the Author.

However, the most important and useful application of the proposition would be no other than the discovery of the family of equipotential curves of the above ; but, unfortunately, the present writer did not obtain any satisfactory results in regard to this subject.

Further applications to the physical problems will be published in the second part of this paper.

Fig. 1, *b*.

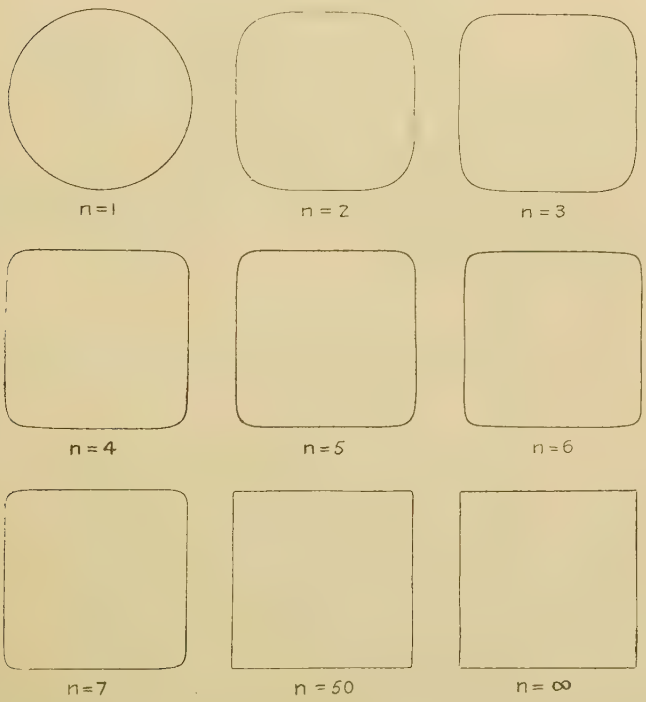

§ 2. *Proposition of the Curve and its Characteristic Properties.*

Let us consider the following system of closed algebraic curves * :

$$x^{2n} + y^{2n} = c, \quad . \quad . \quad . \quad . \quad . \quad . \quad . \quad . \quad (1)$$

* The orthogonal trajectories of the curves are easily found, as

$$x^{-(2n-2)} - y^{-(2n-2)} = b,$$

where b is a real number.

where n is a positive integer, c a real number, and x and y lie in the interval $(-c, +c)$.

Then we obtain a group of curves by changing the value of n, i. e., $n=1, 2, 3, 4, 5, \ldots$, including the circle for the special case when $n=1$.

Now we shall first study the characteristic properties of the curve, taking c as unity for the sake of simplicity.

(1) For the case where n is finite, the equation

$$y = f(x) = (1-x^{2n})^{\frac{1}{2n}}$$

is continuous in the interval of x $(-1 \leqq x \leqq +1)$, but when n is infinite, it is discontinuous at the upper and lower limits of x, i. e., $x=\pm 1$.

(2) The given curve is symmetrical with respect to the axes x, y, and also to the bisecting line $y=x$.

(3) The distance between the origin and the intersecting point of the curve and the bisecting line $y=x$ is the maximum radial distance.

TABLE I.

Relation between the above Maximum Radial Distance r and the Power n in the equation (1).

n.	x or y.	r.
1	0·7071	1
2	0·8409	1·1892
3	0·8909	1·2599
4	0·9170	1·2968
... .	.....	.....
50	0·9931	1·4044
... .	.....	.....
∞	1·0000	$\sqrt{2}=1·4142$

Now, based on the above proposition, we wish to propose the next expression for groups of an ellipse of a higher order, of a sphere of a higher order, of an ellipsoid of a higher order, respectively, but the discussion of these groups is here omitted,

$$\left.\begin{aligned} \left(\frac{x}{a}\right)^{2n} + \left(\frac{y}{b}\right)^{2n} &= 1, \\ x^{2n} + y^{2n} + z^{2n} &= \mathrm{C}, \\ \left(\frac{x}{a}\right)^{2n} + \left(\frac{y}{b}\right)^{2n} + \left(\frac{z}{c}\right)^{2n} &= 1. \end{aligned}\right\}$$

§ 3. *Graphical Representation of the given Curve*

$$x^{2n}+y^{2n}=1.$$

In fig. 1 (pp. 184, 185) the curves are graphed, taking the values of n as $n=1, 2, 3, 4, 5, 6, 7, 50$ respectively, and these

TABLE II.

The Numerical Values of the Solution of $x^{2n}+y^{2n}=1$.

y.	x.				y.	x.		
	$n=2$.	$n=3$.	$n=4$.	$n=5$.		$n=6$.	$n=7$.	$n=50$.
0·8409	0·8409				0·9438	0·9438		
0·8908	...	0·8908			0·95	0·9372		
0·90	0·7657	0·8814			0·9517	...	0·9517	
0·91	0·7487	0·8695			0·96	0·9239	0·9423	
0·9170	...	...	0·9170		0·97	0·9060	0·9272	
0·92	0·7297	0·8561	0·9139		0·98	0·8798	...	
0·93	0·7085	0·8407	0·9025		0·99	0·8342	0·8656	
0·9330	...	...	...	0·9930	0·992	0·8196	0·8521	
0·94	0·6843	0·8227	0·8891	0·9255	0·9931	...	...	0·9931
0·95	0·6563	0·8014	0·8725	0·9127	0·994	0·8009	0·8355	0·9921
0·96	0·6145	0·7753	0·8524	0·8964	0·996	0·7750	0·8124	0·9890
0·97	0·5820	0·7421	0·8275	0·8748	0·998	0·7322	0·7739	0·9831
0·98	0·5278	0·6966	0·7884	0·8438	0·999	0·6915	0·7368	
0·99	0·4455	0·6231	0·7261	0·7909	0·9992	0·6788	0·7253	0·9747
0·992	0·4217	0·6008	0·7065	0·7740	0·9994	0·6627	0·7106	0·9720
0·994	...	0·5731	0·6824	0·7529	0·9996	0·6407	0·6932	0·9681
0·998	0·2988	...	0·5959	0·6757	0·9998	0·6049	0·6571	0·9615
0·999	0·2527	0·4261	...	0·6307	0·9999	0·5713	0·6232	0·9549
0·9998	...	...	0·4500		0·99992	...	0·6158	0·9528
0·9999	...	...	...	0·5000	0·99994	...	0·6030	0·9501
					0·99996	...	0·5860	0·9465
					0·99998	...	0·5575	0·9397
1·0000	0·0	·0	0·0	0·0	1·00000	0·0	0·0	0·0

numerical values are tabulated in Table II., where these calculations are made in the range of x and y covering one octant by § 2 (2).

§ 4. *Applications of our Proposition to Dynamical Problems.*

A few applications to dynamical problems are obtained as follows :—

1. Area included by the curve $x^{2n}+y^{2n}=1$.

The expression of the area is

$$A = 4\int_0^1 (1-x^{2n})^{\frac{1}{2n}} dx,$$

and this integral is reducible to Euler's integral as :

For $n=1$, $A=4\int_0^1 (1-x^2)^{\frac{1}{2}} dx$

$$=4\left[\frac{x^2}{2}(1-x^2)^{\frac{1}{2}}+\frac{1}{2}\sin^{-1}x\right]_0^1,$$

or $A=2\mathrm{B}(\frac{1}{2},\frac{3}{2})=2\Gamma(\frac{1}{2}).\Gamma(\frac{3}{2}) \quad =4\Pi^2(\frac{1}{2})$,

$n=2$, $A=4\int_0^1 (1-x^4)^{\frac{1}{4}} dx=\mathrm{B}(\frac{1}{4},\frac{5}{4}) \quad =4\dfrac{\Pi^2(\frac{1}{4})}{\Pi(\frac{1}{2})}$,

$n=3$, $A=4\int_0^1 (1-x^6)^{\frac{1}{6}} dx=\frac{2}{3}\mathrm{B}(\frac{1}{6},\frac{7}{6}) \quad =4\dfrac{\Pi^2(\frac{1}{6})}{\Pi(\frac{1}{3})}$,

$n=4$, $A=4\int_0^1 (1-x^8)^{\frac{1}{8}} dx=\frac{1}{2}\mathrm{B}(\frac{1}{8},\frac{9}{8}) \quad =4\dfrac{\Pi^2(\frac{1}{8})}{\Pi(\frac{1}{4})}$,

$n=5$, $A=4\int_0^1 (1-x^{10})^{\frac{1}{10}} dx=\frac{2}{5}\mathrm{B}(\frac{1}{10},\frac{11}{10})=4\dfrac{\Pi^2(\frac{1}{10})}{\Pi(\frac{1}{5})}$,

. . . . . .

$n=50$, $A=4\int_0^1 (1-x^{100})^{\frac{1}{100}} dx=\frac{1}{25}\mathrm{B}(\frac{1}{100},\frac{101}{100})$

$$=4\frac{\Pi^2(\frac{1}{100})}{\Pi(\frac{1}{50})},$$

. . . . . .

$n=\infty$, $A=4$,

where B, Γ, Π denote Beta, Gamma, and Gauss functions respectively.

These numerical values are tabulated in Table III.

TABLE III *.

A, Q, and R^2.

n.	A.	Q.	R^2.
1	π	$\frac{1}{3}\pi$	$\frac{1}{4}$
2	0·92703 73×4	0·87401 92×2π	0·89860 52×$\frac{1}{8}$
3	0·96382 72×4	0·93481 32×2π	0·94492 99×$\frac{1}{8}$
4	0·97849 48×4	0·96027 50×2π	0·96538 73×$\frac{1}{8}$
5	0·98573 20×4	0·97329 14×2π	0·97622 59×$\frac{1}{8}$
6	0·98987 68×4	0·98085 31×2π	0·98264 18×$\frac{1}{8}$
7	0·99242 85×4	0·98557 39×2π	0·98679 04×$\frac{1}{8}$
... .	.....	.....	.....
50	0·99983 79×4	0·99967 81×2π	0·99968 27×$\frac{1}{8}$
... .	.....	.....	....
∞	4	2π	$\frac{1}{3}$

2. Volume of revolution about the axis x or y.

The general expression is

$$Q = 2\pi \int_0^1 (1-x^{2n})^n \, ax,$$

and these integrals are also reducible to Euler's integral, as shown below:

For $n=1$, $Q = 2\pi \int_0^1 (1-x^2)\,dx = 2\pi \left| x - \frac{x^3}{3} \right|_0^1$,

or $Q = \pi\, B(\frac{1}{2}, 2) = 2\pi \frac{\Pi(\frac{1}{2})}{\Pi(\frac{3}{2})}$,

$n=2$, $Q = 2\pi \int_0^1 (1-x^4)^{\frac{1}{2}}\,dx = 2\pi \frac{\Pi(\frac{1}{4})\Pi(\frac{1}{2})}{\Pi(\frac{3}{4})}$,

$n=3$, $Q = 2\pi \int_0^1 (1-x^6)\,dx = 2\pi \frac{\Pi(\frac{1}{6})\Pi(\frac{1}{3})}{\Pi(\frac{1}{2})}$,

$n=4$, $Q = 2\pi \int_0^1 (1-x^8)^{\frac{1}{4}}\,dx = 2\pi \frac{\Pi(\frac{1}{8})\Pi(\frac{1}{4})}{\Pi(\frac{3}{8})}$,

$n=5$, $Q = 2\pi \int_0^1 (1-x^{10})^{\frac{1}{5}}\,dx = 2\pi \frac{\Pi(\frac{1}{10})\Pi(\frac{1}{5})}{\Pi(\frac{3}{10})}$,

....

* These calculations are performed by using "The logarithmic table of Gamma function" (Gauss, *Ges. W.* iii. S. 161).

$$n=50, \quad Q=2\pi\int_0^1(1-x^{100})^{\frac{1}{500}}dx=2\pi\frac{\Pi(\frac{1}{100})\Pi(\frac{1}{500})}{\Pi(\frac{3}{100})},$$

. . . . . .

$$n=\infty, \quad Q=2\pi.$$

3. Radius of gyration about the axis x or y.

The value as generally expressed is

$$R^2=\frac{1}{3}\frac{\int(1-x^{2n})^{\frac{3}{2n}}dx}{\int(1-x^{2n})^{\frac{1}{2n}}dx},$$

and the calculations are shown below:

For $n=1$,
$$R^2=\frac{1}{3}\frac{\int_0^1(1-x^2)^{\frac{3}{2}}dx}{\int_0^1(1-x^2)^{\frac{1}{2}}dx}$$
$$=\frac{1}{3}\frac{\left|\frac{5-2x^2}{8}x\sqrt{1-x^2}+\frac{3}{8}\sin^{-1}x\right|_0^1}{\left|\frac{x}{2}(1-x^2)^{\frac{1}{2}}+\frac{1}{2}\sin^{-1}x\right|_0^1},$$

or
$$R^2=\frac{1}{3}\frac{B(\frac{1}{2},\frac{5}{2})}{B(\frac{1}{2},\frac{3}{2})}=\frac{1}{3}\frac{\Pi(\frac{3}{2})}{\Pi(2)\Pi(\frac{1}{2})},$$

$n=2$,
$$R^2=\frac{1}{3}\frac{B(\frac{1}{4},\frac{7}{4})}{B(\frac{1}{4},\frac{5}{4})}=\frac{1}{3}\frac{\Pi(\frac{3}{4})\Pi(\frac{1}{2})}{\Pi(\frac{1}{4})},$$

$n=3$,
$$R^2=\frac{1}{3}\frac{B(\frac{1}{6},\frac{3}{2})}{B(\frac{1}{6},\frac{7}{6})}=\frac{1}{3}\frac{\Pi(\frac{3}{6})\Pi(\frac{1}{3})}{\Pi(\frac{2}{3})\Pi(\frac{1}{6})},$$

$n=4$,
$$R^2=\frac{1}{3}\frac{B(\frac{1}{8},\frac{1}{8})}{B(\frac{1}{8},\frac{9}{8})}=\frac{1}{3}\frac{\Pi(\frac{3}{8})\Pi(\frac{1}{4})}{\Pi(\frac{7}{4})\Pi(\frac{1}{8})},$$

$n=5$,
$$R^2=\frac{1}{3}\frac{B(\frac{1}{10},\frac{13}{10})}{B(\frac{3}{10},\frac{11}{10})}=\frac{1}{3}\frac{\Pi(\frac{3}{10})\Pi(\frac{1}{5})}{\Pi(\frac{2}{5})\Pi(\frac{1}{10})},$$

. . . . . .

$n=50$,
$$R^2=\frac{1}{3}\frac{B(\frac{1}{100},\frac{3}{100})}{B(\frac{1}{100},\frac{101}{100})}=\frac{1}{3}\frac{\Pi(\frac{3}{100})\Pi(\frac{1}{50})}{\Pi(\frac{2}{50})\Pi(\frac{1}{100})}$$

. . . . . .

$n=\infty$ $R^2=\frac{1}{3}$.

XVII. *Notices respecting New Books*

Operational Circuit Analysis. By V. Bush, Eng.D. (Chapman & Hall, Ltd., 11 Henrietta St., Covent Garden, W.C.2. Price 22*s.* 6*d.* net.)

AFTER many years of neglect and lack of appreciation, renewed interest has been taken in the operational calculus introduced by Heaviside. Numerous contributions are being made towards the extension and development of this branch of mathematics, the operational method of solving the differential equations arising in physical problems, chiefly in connexion with electrical networks. By the application of the theory of functions of a complex variable, Bromwich established the validity of the method for systems with a finite number of degrees of freedom and also developed a method for continuous systems.

The author has here brought together all the important results, and, for the first time, has set them out in systematic form. Whilst recognizing that too much attention can be paid to questions of rigour, the author gives an introductory account of contour integration, the evaluation of residues, and the derivation of the expansion theorem—the "partial fraction rule"—by contour integrals. This symbolic method has been extended by Carson and Bromwich: recently B. B. Baker has generalized the theorem, and has given a formula which includes the foregoing as particular cases. Prof. N. Wiener contributes a chapter on Fourier analysis and Asymptotic series and a useful table of operational formulæ is given in an appendix.

"The monumental nature of Heaviside's work has not always and everywhere been appreciated," but Dr. Bush and others, "by insisting upon a due measure of appreciation of his genius, have done much to make his work used, as well as useful."

La Nouvelle Mécanique de Quanta. Par G. Birtwistle. Traduit par MM. Y. Rocard et M. Ponte. (Paris: Librairie Scientifique Albert Blanchard, 3 et 3 bis, Place de la Sorbonne. 1929.)

The New Quantum Mechanics of the late G. Birtwistle, published only two years after his Quantum Theory of the Atom, presents a clear and comprehensive summary of the theories of Heisenberg, Dirac and Schrödinger. This book has the further merit of rousing the interest of the student in modern problems of atomic structure, and with this additional equipment enabling him to keep abreast with the developments of the recent past and to undertake the study of researches which are following one another in quick succession. It is for these reasons that the New Quantum

Mechanics has been translated by MM. Rocard and Ponte. Although it is little more than a year since the Cambridge University Press issued this book, many notable memoirs have appeared during this short period: the translators have endeavoured to incorporate the latest results by summarizing a number of contributions which have been made since the publication of the English edition. These include papers by P. Ehrenfest on the validity of the classical mechanics in wave mechanics, F. Madelung on the quantum theory in hydrodynamic form, further papers by P. Dirac and C. G. Darwin, and the work of Kretschmann, Sommerfeld, and Houston on the electron theory of metals.

It would have been an advantage if the author index had been retained, even if this required revision.

Vorlesungen über Theoretische Physik. Band IV. *Die Relativitäts Theorie für gleichförmige Translationen.* Von Prof. H. A. Lorentz. 1929. Geb. R.M. 13.80. (Akademische Verlagsgesellschaft, m.b.H., Leipzig.)

The lectures on the Special Relativity theory given by Prof. H. A. Lorentz during the years 1910–12 have been revised by Dr. A. D. Fokker. Lorentz made many important contributions to the development of the principle, and provided the basis of the theory by the enunciation of the well-known Lorentz transformation. To him, in large measure, the restricted theory of relativity owes its origin. Nevertheless, his name does not appear in the text—only in one or two footnotes and in the bibliography. The chapter describing the researches on the variation of mass of an electron with velocity has been enlarged by the addition of later experimental results. These include the researches of Neumann, who, following Bucherer, used β-rays from radium as the source of cathode rays: the data gave a reliable value of the electron charge and confirmed the relation of dependence of mass upon velocity. A detailed account is also given of the work of Guye and Lavanchy on the experimental verification of the Lorentz formula for high-velocity cathode rays. References to original memoirs dealing with the topics in the various chapters are collected together in the Bibliography.

[*The Editors do not hold themselves responsible for the views expressed by their correspondents.*]

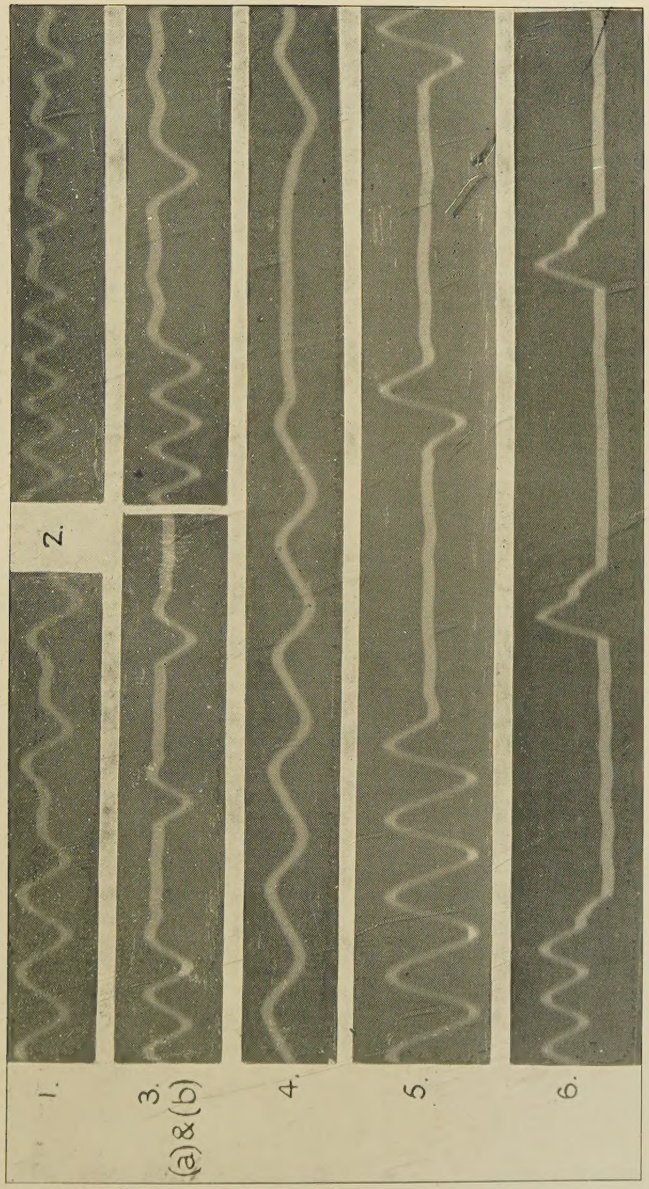
1.
2.
3.
(a) & (b)
4.
5.
6.